

**Gas Permeation Studies In Polyarylates
and Dispersed Polymeric systems**

BHALCHANDRA V. BHAGWAT

₹ | January 2000 | ₹

DECLARATION

Certified that the work incorporated in the thesis **“Gas Permeation Studies In Polyarylates and Dispersed Polymeric systems”** submitted by Mr. Bhalchandra V. Bhagwat was carried out by the candidate under my supervision. Such material as has been obtained from other sources has been duly acknowledged in the thesis.



Dr. S. G. Joshi.
Research Guide
National Chemical Laboratory .
Pune 411 008

ACKNOWLEDGEMENT

I would like to express my deep sense of gratitude to my research guide, Dr. S. G. Joshi, for his guidance and constant encouragement during the course of this work.

I take this opportunity to express my gratitude to Dr. S. S. Kulkarni, Dr. A. P. Joshi, Dr. M. G. Kulkarni, Dr. M. V. Paradkar, and Late Dr. Bodhe for their support during various stages of the investigation.

I specially take this opportunity to express my deep gratitude to Dr. J. Gadgil and Dr. C. R. Rajan for their valuable suggestions during preparation of the thesis.

Support from Dr. Ponrathnam, Ms. Mule, Ms. Bulakh, Mr. Sathe, Mr. Samuel, Mr. Sahu, Mr. Kapur, Ms. Kale, Ms. Violet, Dr. Pradhan, Dr. Sinekar, Ms. Sangeeta, Dr. Jog and Dr. Sathe for assistance during various stages are gratefully acknowledged.

I would like to express my sincere thanks to Dr. Ulhas Kharul, Dr. Sandeep Karode, Dr. Bhagyashree Gadgil, Dr. Milind Sathe, Dr. Arun Dixit, Dr. Deepak Musale, Dr. Jayarani, Dr. Mohan, Madhuri Shinde, Mahendra, Ajit Phadke, Ajit Kulkarni, Rohit Joshi, Ms. Mrunaleeni, Ms. Shubhangi, Ms. Savita, Ms. Yogita, Alankar, Mahesh, Naren, Omprakash, Trushar, Hajara, Manas, Debasis, Dr. Gadre and many others.

I am greatly indebted to my parents, family and relatives. Without their encouragement, full moral support and God's blessings, this work would have been impossible.

Finally, I would like to thank CSIR for awarding fellowship, Dr. B. D. Kulkarni, for permitting me to work in CE division, and Director, N. C. L. for providing the necessary facilities and permitting to submit this work in the form of a thesis to University of Pune.

B. V. Bhagwat

Bhalchandra V. Bhagwat

Contents
Chapter 1
Introduction

	Page no.	
1.1	Introduction	1
1.1.1	Separations using membranes	1
1.1.2	Methods of Gas Separation	2
1.1.3	Gas separation through polymeric membrane	3
1.1.4	Types of gas separation membranes	5
1.1.5	Typical vocabulary related to membrane processes	7
1.2	Present Work	8
1.2.1	Classification of Additive dispersed polymeric membranes	10

Chapter 2
Literature Survey on Polyarylate System

2	Theory of permeation	11
2.1	Introduction	11
2.2	Transport in Glassy polymers	12
2.2.1	Dual-Mode Sorption Model	13
2.3	Structural correlation with gas permeability in glassy polymers	16
2.3.1	Polysulfone (PSF)	16
2.3.1.1	Structural modifications in PSF	17
2.3.2	Polycarbonates (PC)	18
2.3.2.1	Structural modification in PC	18
2.3.3	Polyarylates (PAr)	21
2.3.4	Polyimides	24
2.3.5	Polyphenylene oxides	25

Chapter 3
Experimental (Polyarylate)

3.1	Materials	26
3.1.1	Materials used for the preparation of monomers and polymers	26
3.1.2	Synthesis of monomers	28
3.1.2.1	Tetrabromobisphenol-A (TBrbisA)	28

3.1.2.2	Dimethylbisphenol-A (DMbis-A)	29
3.1.2.3	Synthesis of 2-Trifluoromethyl-1,4-terephthalic acid chloride	32
3.1.2.3(i)	Preparation of 2-trifluoromethyl-1,4-xylene	32
3.1.2.3(ii)	Synthesis of 2-trifluoromethyl-1,4-terephthalic acid : (CF ₃ T)	35
3.1.2.3(iii)	Synthesis of 2-Trifluoromethyl-1,4-terephthalic acid chloride:(CF ₃ TCl)	39
3.1.3	Polymer synthesis	39
3.1.3.1	Solution polymerization	39
3.1.3.2	Interfacial polymerization	42
3.1.4	Polymer purification	49
3.2	Permeation studies	49
3.2.1	Casting of membrane	49
3.2.2	Gas permeation studies	49
3.2.2.1	Apparatus	49
3.2.2.2	Permeability measurements	51
3.3	Polymer characterization	52
3.3.1	Viscosity measurements	52
3.3.2	Density measurements	52
3.3.3	Glass transition temperature, T _g	52
3.3.4	Determination of d _{sp}	52
3.3.5	Thermogravimetric analysis (TGA)	53

Chapter 4

Results and Discussion of Polyarylate System

4.1	Results	54
4.1.1	Physical properties	55
4.1.2	Permeation properties	56
4.2	Discussion	56
4.2.1	Physical properties	56
4.2.2	Permeation properties	61
4.3	Effect of CF ₃ substitution in combination with the bisphenol substitution	63
4.4	Conclusions	64

Chapter 5

Literature Survey on Dispersed Polymer Systems

5.1	Role / Action of additive in dispersed polymer system	66
5.1.1	Plasticization	66
5.1.2	Antiplasticization	68
5.1.3	Filler	69
5.2	Theory of permeation in dispersed polymer systems	70
5.3	Mechanism of transport in dispersed polymeric systems	73
5.3.1	Permeation through polymer matrix having impermeable additives	73
5.3.2	Two phase systems with both phases permeable to different extents	75
5.4	Transport of penetrant in dispersed polymer systems	75
5.4.1	Organic low molecular weight compounds as an additive	76
5.4.2	An inorganic compound as an additive	78
5.4.3	Organometallic compounds as an additive	79
5.4.4	Low molecular weight polymer as an additive	82

Chapter 6

(Experimental : Additive Dispersed Polymeric System)

6.1	LC-Dispersed polymeric membranes	84
6.1.1	Materials	84
6.1.1.1	Polymers	84
6.1.1.2	Liquid crystalline compounds: LC1 and LC2	84
6.1.2	Film preparation	85
6.1.2.2	Measurement of gas permeability	92
6.1.3	Membrane Characterization	92
6.2	Experimental : Metal complex dispersed polymeric systems	92
6.2.1	Preparation of Metal Complexes	93
6.2.1.1	Synthesis of Tris(2,4-pentanediono)iron(III),	93
6.2.1.2	Synthesis of Tris(2,4-pentanediono)cobalt(III)	96
6.2.2	Casting of Membrane (Film)	96
6.2.3	Membrane / polymer characterization	99

Chapter 7
Results and Discussion on LC- Dispersed Polymer System

7.1	LC-dispersed polymeric systems	100
7.1.1	Results	100
7.1.2	Discussion	130
7.1.2.1	SL1 series : Discussion	130
7.1.2.2	SL1, CL1 and CL2 series : Discussion	132
7.1.3	Investigation of permeation of LC-dispersed polymeric system	133
7.1.4	LC compounds as the membrane materials in PSF and PC matrices.	134
7.2	Metal Complex -Dispersed Polymeric Membranes	136
7.2.1	Results	136
7.2.2	Discussion	152
7.2.2.1	Correlation between physical and permeation properties	152
7.2.2.2	Possible mechanism for permeability Reduction	154
7.2.3	MX_n compounds as the additive in PSF and PC matrices	156
7.3	Conclusions (Additive dispersed polymer system)	156

LIST OF FIGURES

Figure 1.1	Model of gas separation with a polymer membrane.	4
Figure 2.1	Polymer specific volume as a function of temperature.	13
Figure 2.2	Illustration of the dual-sorption model for glassy polymers	15
Figure 3.1	IR spectrum of TBrbisA	30
Figure 3.2	NMR spectrum of TBrbis-A monomer	31
Figure 3.3	IR spectrum of DMbisA	33
Figure 3.4	NMR spectrum of DMbisA monomer	34
Figure 3.5	IR spectrum of 2-Trifluoromethyl-1,4-xylene	36
Figure 3.6	NMR spectrum of 2-Trifluoromethyl-1,4-xylene.	37
Figure 3.7	Mass spectrum of 2-Trifluoromethyl-1,4-xylene	38
Figure 3.8	NMR spectrum of Trifluoromethyl terephthalic acid	40
Figure 3.9	Mass spectrum of Trifluoromethyl terephthalic acid	41
Figure 3.10	IR spectrum of PA1 polymer	43
Figure 3.11	IR spectrum of PA2 polymer	43
Figure 3.12	IR spectrum of PA3 polymer	44
Figure 3.13	IR spectrum of PA4 polymer	44
Figure 3.14	NMR spectrum of PA1 polymer	45
Figure 3.15	NMR spectrum of PA2 polymer	46
Figure 3.16	NMR spectrum of PA3 polymer	47
Figure 3.17	NMR spectrum of PA4 polymer	48
Figure 3.18	Schematic of permeability measurement apparatus.	50
Figure 4.1	WAXD spectra of polyarylates, a) PA1, b) PA2	57
Figure 4.2	WAXD spectra of polyarylates, a) PA3, b) PA4	58
Figure 4.3	TGA of PA4 and PA2 polymers in nitrogen	60
Figure 5.1	Modified Co- and Fe-porphyrin complexes and tetrakis (alkylamidophenyl) porphinatometals	80
Figure 6.1	IR spectrum of LC1	86
Figure 6.2	IR spectrum of LC2	86
Figure 6.3	NMR spectrum of LC1	87
Figure 6.4	NMR spectrum of LC2	88
Figure 6.5	Mass spectrum of LC1	89
Figure 6.6	Mass spectrum of LC2	90
Figure 6.7	IR spectrum of Fe(acac) ₃	94
Figure 6.8	IR spectrum of Co(acac) ₃	94
Figure 6.9	NMR spectrum of Fe(acac) ₃	95
Figure 6.10	NMR spectrum of Co(acac) ₃	97
Figure 7.1	WAXD spectra of SL1 series polymers, a) LC1, b) 0% (PSF), c) 1%, d) 3%, e) 6%, f) 9%, g) 12% series polymer.	101

Figure 7.2	WAXD spectra of SL2 series polymers, a) LC2, b) 0% (PSF), c)1%, d)12% series polymer.	102
Figure 7.3	WAXD spectra of CL1 series polymers, a) LC1, b) 0% (PC), c)1%, d) 6%, e) 9%, f) 12% series polymer.	103
Figure 7.4	WAXD spectra of CL2 series polymers, a) LC2, b) 0% (PC), c)1%, d) 6%, e) 9%, f) 12% series polymer.	104
Figure 7.5	DSC of 12% and PSF polymers	107
Figure 7.6	DSC of 1% and 3% SL1 series polymers	108
Figure 7.7	DSC of 9% SL1 and 1% CL1 series polymers	109
Figure 7.8	DSC of LC1 and LC2 show transitions	110
Figure 7.9	TGA of LC1 and LC2 compounds in air	115
Figure 7.10	TGA of 6%CL2 and PC polymers in air	116
Figure 7.11	TGA of 12% SL2 and 12% CL1 series polymers	117
Figure 7.12	TGA of 12% SL1 series polymer in air	118
Figure 7.13	Permeability for He, CO ₂ , N ₂ and O ₂ as a function of % LC1 loading in SL1 series membranes.	122
Figure 7.14	Permeability for He, CO ₂ , N ₂ and O ₂ as a function of % LC2 loading in SL2 series membranes.	124
Figure 7.15	Permeability for He, CO ₂ , N ₂ and O ₂ as a function of % LC1 loading in CL1 series membranes.	127
Figure 7.16	Permeability for He, CO ₂ , N ₂ and O ₂ as a function of % LC2 loading in CL2 series membranes.	129
Figure 7.17	WAXD spectra of SCo series polymers, a) Co(acac) ₃ , b) 0% (PSF), c)5%, d) 10%, e) 20%, f) 30% series polymer.	137
Figure 7.18	WAXD spectra of SFe series polymers, a) Fe(acac) ₃ , b) 0% (PSF), c)5%, d) 10%, e) 20%, f) 30% series polymer.	138
Figure 7.19	WAXD spectra of CFe series polymers, a) Fe(acac) ₃ , b) 0% (PC), c)5%, d) 10%, e) 20%, f) 30% series polymer.	139
Figure 7.20	TGA of 20% SCo and 20% CFe series polymers in air	142
Figure 7.21	TGA of 20% SFe and PSF polymer in air	143
Figure 7.22	Permeability for He, CO ₂ , N ₂ and O ₂ as a function of % Fe(acac) ₃ loading in SFe series membranes.	147
Figure 7.23	Permeability for He, CO ₂ , N ₂ and O ₂ as a function of % Co(acac) ₃ loading in SCo series membranes.	148
Figure 7.24	Permeability for He, CO ₂ , N ₂ and O ₂ as a function of % Fe(acac) ₃ loading in CFe series membranes.	149

LIST OF TABLES

Table no.	Contains	Page no.
Table 1.1	Commercially important membrane separation processes	3
Table 3.1	Sources and purity of materials	26
Table 3.2	Structures and abbreviations of chemicals (monomers and polymers)	27
Table 3.3	IR, NMR spectral values for polymers PA1, PA2, PA3, & PA4.	42
Table 4.1	Physical properties of CF ₃ -polyarylates compared with parent polymers	54
Table 4.2	Permeation properties of CF ₃ -polyarylates compared with parent polymers.	55
Table 4.3	Thermal stability of -CF ₃ group substituted polyarylates with respective parent polymers in nitrogen atmosphere	59
Table 4.4	Permselectivity (α) of various polyarylates with CF ₃ group substitution .	62
Table 6.1	Composition of membranes belonging to CL1 series.	91
Table 6.2	Composition of membranes belonging to CL2 series.	91
Table 6.3	Composition of membranes belonging to SL1 series.	91
Table 6.4	Composition of membranes belonging to SL2 series.	92
Table 6.5	Composition of membranes belonging to CFe series.	98
Table 6.6	Composition of membranes belonging to SFe series.	98
Table 6.7	Composition of membranes belonging to SCo series.	98
Table 7.1	Inter-segmental spacing of SL1 series membranes	105
Table 7.2	Inter-segmental spacing of SL2 series membranes	105
Table 7.3	Inter-segmental spacing of CL1 series membranes	105
Table 7.4	Inter-segmental spacing of CL2 series membranes	106
Table 7.5	Glass transition temperatures of SL1 and SL2 series membranes as a function of LC	111
Table 7.6	Glass transition temperatures of CL1 and CL2 series membranes as a function of LC	111
Table 7.7	Transition temperatures of LC1 and LC2	111
Table 7.8	Thermogravimetric data for SL1 series polymers	112
Table 7.9	Thermogravimetric data for SL2 series polymers	113
Table 7.10	Thermogravimetric data for CL1 series polymers	113
Table 7.11	Thermogravimetric data for CL2 series polymers	114
Table 7.12	Thermogravimetric data for LC1 and LC2	119
Table 7.13	Permeability of SL1 series as a function of LC1 concentration	121
Table 7.14	Selectivity of SL1 series as a function of LC1 concentration	123

Table 7.15	Permeability of SL2 series as a function of LC2 concentration	125
Table 7.16	Selectivity of SL2 series as a function of LC2 concentration	125
Table 7.17	Permeability of CL1 series as a function of LC1 concentration	126
Table 7.18	Selectivity of CL1 series as a function of LC1 concentration	126
Table 7.19	Permeability of CL2 series as a function of LC2 concentration	128
Table 7.20	Selectivity of CL2 series as a function of LC2 concentration	130
Table 7.21	Intersegmental spacing for SCo series membranes	136
Table 7.22	Intersegmental spacing for SFe series membranes	136
Table 7.23	Intersegmental spacing for CFe series membranes	140
Table 7.24	Thermal degradation of SCo series as a function of temperature.	140
Table 7.25	Thermal degradation of some of SFe series as a function of temperature.	141
Table 7.26	Thermal degradation of some of CFe series as a function of temperature	141
Table 7.27	Thermogravimetric data for Fe(acac) ₃ and Co(acac) ₃ .	144
Table 7.28	Gas permeability of SCo series as a function of Co(acac) ₃ loading.	145
Table 7.29	Gas permeability of SFe series as a function of Fe(acac) ₃ loading.	146
Table 7.30	Gas permeability of CFe series as a function of Fe(acac) ₃ loading.	146
Table 7.31	Permselectivity of gases for SCo series as a function of Co(acac) ₃ loading.	150
Table 7.32	Permselectivity of gases for SFe series as a function of Fe(acac) ₃ loading.	150
Table 7.33	Permselectivity of gases for CFe series membranes as a function of Fe(acac) ₃ loading.	151

***** ABSTRACT *****

Abstract of the Thesis

Pure gases have been used for many years for various applications, both industrial and medico-technical. Well known examples of gas separation are Heber process for ammonia gas; separation of nitrogen and helium for inert blanketing; separation of hydrocarbon gases (ethylene, propylene) for the production of commodity plastics such as polyethylene and polypropylene; medical grade air in hospitals. The separation of gases has thus gained wide importance.

Conventionally, the gas separation is practiced mainly by cryogenic processes. In recent years, however, the gas separation using polymeric membranes has acquired an important role in newer technological developments. The advantages of using membrane based processes is its overall simplicity, modular nature and low energy consumption.

The gas separation by polymeric membrane depends on the intrinsic properties of the membrane material. The process would be economically viable if the membrane material has high permeability (P) and overall high selectivity (α) for the gas to be separated.

This has given impetus to research directed towards the invention of new materials having high permeability with good selectivity. However, a reverse trend is observed for the behavior of P and α , i.e. any attempt to increase permeability, generally reduces the selectivity. The design of the suitable membrane material therefore has to have a balance on these two parameters i.e. P and α .

There are two possible approaches to attain this goal: (i) Synthesis of new polymeric materials based on novel monomers and (ii) Dispersion of additives to known polymers. Both the approaches have been evaluated in our present investigations.

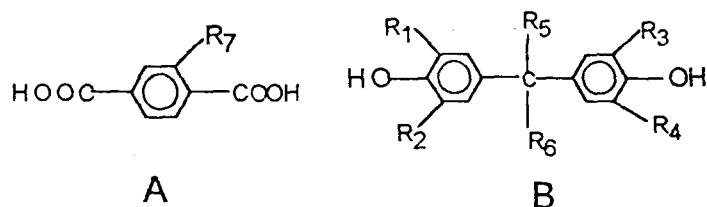
The thesis comprises of two parts. **Part I** deals with gas separation techniques using novel polyarylates and **Part II** comprises of use of additives to known polymers.

Part I

Polyarylates as Membrane Materials

Polyarylates in general, have good permeability and selectivity. Additionally they have good solubility in common organic solvents. This makes it easy to use them in desirable membrane form, i.e. as flat sheet in plate frame or spiral form or as hollow fibers modules.

Present study involves : (1) Synthesis and characterisation of novel polyarylates. (2) Evaluation of the polymers for gas separation. Novel polyarylates were synthesized from diacid and diols having general structures A and B respectively. The variation in structure and the polymers synthesized are given in Table.



	Name of Polyarylates	Code No.	Substituents						
			R1	R2	R3	R4	R5	R6	R7
1	(BisA-CF ₃ T)	PA1	H	H	H	H	Me	Me	CF ₃
2	(DMbisA-CF ₃ T) <i>Asymmetric</i>	PA2	Me	H	Me	H	Me	Me	CF ₃
3	(TBrbisA-CF ₃ T) <i>Symmetric</i>	PA3	Br	Br	Br	Br	Me	Me	CF ₃
4	(O-Cp-CF ₃ T) <i>Asymmetric</i>	PA4	Me	H	Me	H			CF ₃

The polymers were prepared by interfacial and solution condensation methodologies. The polyarylates obtained were characterized by wide angle X-ray diffraction (WAXD), density, differential scanning calorimetry (DSC), thermal gravimetric analysis (TGA) and intrinsic viscosity [η].

The membranes were prepared by solution casting. The permeation properties for pure gases viz. helium(He), argon(Ar), nitrogen(N₂), oxygen(O₂), methane(CH₄), and carbon dioxide(CO₂) were measured at 35°C and 10 atm. upstream pressure.

The comparison of the properties of CF₃ group substituted polyarylate was made with the known unsubstituted polyarylate by varying bisphenol moieties, as shown in the table.

All the polymers were soluble in chlorinated solvents. Viscosities of polymers were determined in 1,1,2,2-tetrachloroethane at 35°C. The viscosity values indicated formation of low molecular weight materials. Interchain spacing (dsp) of polymers PA1, PA2, PA3 were comparable, while it increased for PA4.

Gas permeation studies were evaluated by comparison with known unsubstituted polyarylate polymers. Polymer PA1 having CF₃ group showed marginal increase in helium permeability, while for polymer PA3 an increase in permeabilities for all gases were noted. In the case of polymer PA4, remarkable enhancement in selectivity for helium over methane was observed without loss of permeability.

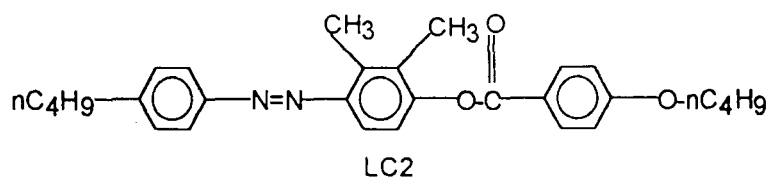
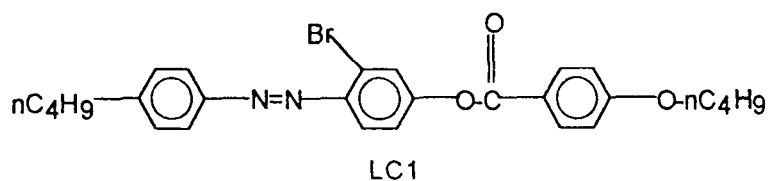
Part II

Dispersed Polymer membrane systems

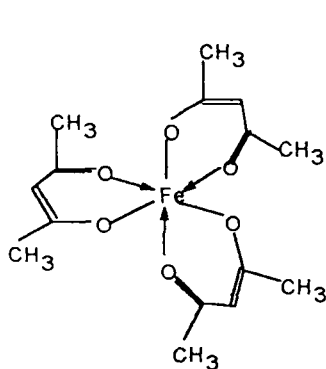
These comprised of low molecular weight compounds and organometallic complexes as additives. In the present study, liquid crystalline materials coded as LC1 and LC2 were used as low molecular weight compounds as structurally depicted below, while organometallic complexes were based on iron and cobalt as shown by structures MX1 and

MX2. The base polymers used in this investigations were polycarbonate (PC) and polysulfone (PSF).

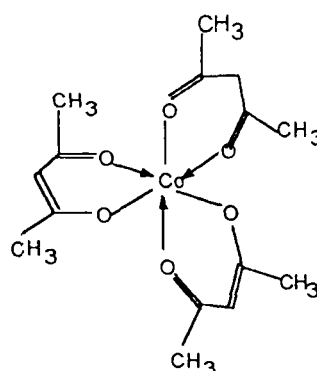
Structure of Liquid Crystalline compounds :



Structure of Metal complexes:



MX1 Iron-tris(acetyl acetone)



MX2 Cobalt-tris(acetyl acetone)

The incorporation of additives with varying concentrations into the polymers was carried out by their dissolution in dichloromethane and casting of membrane from resulting solutions.

The membrane systems are designated as,

- 1) (LC1-PSF) membranes : LC1 dispersed in PSF.
- 2) (LC2-PSF) membranes : LC2 dispersed in PSF.
- 3) (LC1-PC) membranes : LC1 dispersed in PC.
- 4) (LC2-PC) membranes : LC2 dispersed in PC.
- 5) (Co-PSF) membranes : $\text{Co}(\text{acac})_3$ dispersed in PSF.
- 6) (Fe-PSF) membranes : $\text{Fe}(\text{acac})_3$ dispersed in PSF.
- 7) (Fe-PC) membranes : $\text{Fe}(\text{acac})_3$ dispersed in PC.

The membrane materials thus prepared were characterized by DSC and TGA for their thermal behavior, while surface characteristics were studied by SEM and WAXD. The gas permeation studies were carried out at 35°C and 10 atm. using Helium (He), nitrogen (N₂), oxygen (O₂), and carbon dioxide (CO₂) gases.

DSC studies of LC incorporated systems showed single T_g peak. The permeability studies with liquid crystalline material systems revealed increased selectivity for helium, when PSF was used as the polymer matrix. However, reduction in permeability was noted. In the case of PC as the polymer matrix, no significant change was noted as compared to PSF.

In organometallic complex systems based on Fe and Co, it was noted that there was a reduction in gas permeability and increase in helium selectivity.

Chapter 1
Introduction

1.1 Introduction

Industrial separation processes consume a significant portion of resources. A survey carried out by the U.S. department of energy indicates that a very large quantum of energy is spent annually on separation processes like distillation, drying and evaporation. A systematic survey [The DOE Industrial Energy Program, (1987)] was carried out by the department of energy under "Industrial Energy Program". This survey also concluded that a significant portion of energy could be saved in petroleum, chemical and food industries; if these industries would adopt membrane separation systems. Membrane separation processes have significant advantages over existing separation processes like distillation, crystallization, evaporation etc. They not only consume less energy than the conventional processes but also are compact and modular, in addition to being easy to retrofit to the existing industrial process.

1.1.1 Separations using membranes

Membrane processes with extensive industrial applications are liquid filtration systems - microfiltration (MF), ultrafiltration (UF), reverse osmosis (RO), and electrodialysis (ED). These processes are reasonably well developed and understood technologies. Gas separation with polymeric membranes and pervaporation are regarded as developing processes.

MF / UF / RO are filtration techniques in which a solution containing dissolved or suspended solutes are forced through a membrane / filter device. The solvent passes through the membrane and solutes having higher size than membrane pore size are retained. The processes differ principally in the size of the particles to be separated by the membrane.

Microfiltration membranes have pore diameter between 0.1 μm (1000 \AA) to 10 μm . These membranes are used to filter suspended particulates, bacteria or large colloids from solutions. UF membranes have pore diameter in the range 20 - 1000 \AA and can be used to filter dissolved macromolecules such as proteins from solutions.

The pores of RO membranes are much smaller ($<10 \text{\AA}$) and are within the range of thermal motion of polymeric chains. They are used to separate dissolved solutes such as salts from water. The major application of RO is in the production of potable water from brackish ground water or the sea water.

In electrodialysis (ED), charged membranes are used to separate ions from aqueous solution under the driving force of electrical potential difference. The major application of ED is in desalting of brackish water.

In gas separation, a mixed gas, feed at elevated pressure is passed across the surface of the membrane which is selectively permeable to one component of the feed. The more permeable component was enriched in the permeate stream. Hydrogen (H_2) recovery was the first major application, followed quickly by acid gas separation, carbon dioxide / methane (CO_2/CH_4) and oxygen / nitrogen (O_2/N_2) separation.

Pervaporation is a relatively recent process. A liquid mixture is placed in contact with one side of membrane and permeate is swept away as a vapour from the other side. Currently the only industrial application of pervaporation is the dehydration of organic liquids. However, pervaporation processes are being developed for removal of dissolved organics from water and separation of organic solvent mixtures.

Facilitated transport is a developing process. It usually employs liquid membranes containing a complexing or carrier agent. The carrier agent reacts with one of the permeating component on the feed side of the membrane and then diffuses across the membrane to release the permeate on the product side of the membrane. The carrier agent thus selectively transports one component from the feed to the permeate side of the membrane. Various commercially important membrane separation processes are summarized in Table 1.1

This study deals with preparation of membranes and their utility for separation of gases and the survey of the methods used are listed below:

1.1.2 Methods of Gas Separation

The commonly used methods for gas separation are:

1) Cryogenic separation: In this process, the separation is carried out at low temperatures by the difference in the boiling point of the gases to be separated. The purity obtained by this process is high. However the process is not economical.

2) Pressure swing adsorption: Gas separation is achieved mainly by adsorption with the help of metal salts or metal-complexes. The gases are selectively adsorbed on the adsorbent surface. This method is used for the enrichment of one of the components in a mixture, to remove trace amount of unwanted/or harmful gases in industries, etc.

3) Membrane separation: Presently, polymeric as well as inorganic membranes are used for gas separation. The separation of gases in polymeric membranes is based on their solubility and diffusivity in the polymer matrix. The purity obtained is not as high as the cryogenic method, but the low energy consumption makes this technique an attractive proposition.

Table 1.1

Commercially important membrane separation processes

[Winston and Sirkar (1992).]

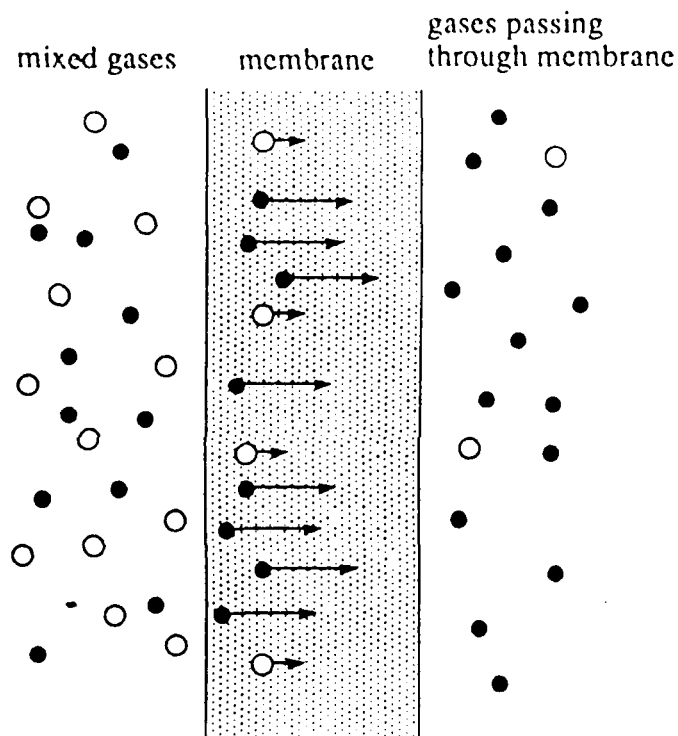
Separation process	Phase of feed and Permeate streams	Mechanism for Transport/ Selectivity	Driving Force
Gas separation	Gaseous	Solution-diffusion	Concentration gradient, (partial pressure difference)
Pervaporation	Liquid feed, gaseous permeate	Solution-diffusion	Vapour pressure gradient, temperature gradient
Dialysis	Liquid	Sieving, hindered diffusion in microporous membrane	Concentration gradient
Electrodialysis	Liquid	Counter-ion transport via ion exchange membranes	Electrical potential gradient, electro-osmosis
Reverse osmosis	Liquid	Preferential sorption/capillary flow	Hydrostatic pressure gradient vs osmotic pressure gradient
Ultrafiltration	Liquid	Sieving	Hydrostatic pressure gradient vs small osmotic pressure gradient
Microfiltration	Liquid or gas	Sieving	Hydrostatic pressure gradient
Emulsion liquid membrane	Generally liquid feed, emulsion containing permeate	Solution-diffusion, facilitated transport	Concentration gradient, pH gradient

1.1.3 Gas separation through polymeric membrane

The concept of separating gases using membrane is more than 100 years old [Grahams et al (1866)]. However, industrial gas separation using membrane technology started in the last four decades. In the membrane separation processes, the stream of gases to be separated is fed to the upstream of the membrane at an elevated pressure. The other

(permeate) side of the membrane is held at a lower (usually atmospheric) pressure. The separation of the mixture is achieved because of differential rate of transport of one component over others through the polymeric membrane. The transport rate of a gas through a polymeric membrane depends on its solubility and diffusivity in the polymer matrix and structural characteristics of the polymer. Typical mechanism for gas separation is shown in figure 1.1.

Figure 1.1 Model of gas separation with a polymer membrane.



If the membrane contains pores large enough to allow convective flow, separation does not take place [Zolandz, R. R. et. al. (1992)]. However, if the size of the pore is smaller than the mean free path of the gas molecules, then gas transport across the membrane takes place by Knudsen diffusion.

The mechanism of gas separation through dense membranes can be explained by the solution-diffusion mechanism. The gas molecules dissolve in the membrane surface, facing

the feed and then diffuse across it. Membrane performance is usually described in terms of its permeability (P) and selectivity (α). An ideal membrane should have high permeability coupled with high selectivity. However, in general, the effect of increased permeability is associated with decrease in selectivity.

Gas permeability can be expressed as the product of gas diffusivity (D) and its solubility (S) in the polymer matrix. Diffusivity (D) depends upon free volume of the polymer and size of the gas molecule; while solubility (S) depends on the condensibility of the gas in the polymer matrix and gas-polymer interactions. Permeation of gas molecules through dense membranes involves five steps, viz., 1) diffusion through the boundary layer of the membrane, 2) sorption into the membrane, 3) diffusion through the membrane, 4) desorption from bulk of the membrane, and 5) desorption from the boundary layer of the membrane. In the case of amorphous glassy polymers, diffusion through the membrane is the rate determining step [Vrentas J. S. et al. (1975)].

1.1.4 Types of gas separation membranes

In general, there are three basic types of gas transport mechanisms on which membranes are classified:

- (a) Knudsen diffusion membranes: Separation is proportional to the inverse square root of ratio of the molecular weights of gases being separated.
- (b) Ultramicroporous molecular sieve membranes: Increasing rates of diffusivity with decreasing molecular size brings about separation. For gas pairs of comparable size, differential sorptivity becomes important. A tortuous but continuous network of passage is characteristic of these types of membranes.
- (c) Solution-diffusion membranes: Solubility and diffusivity of the gas in the polymer matrix govern gas permeation.

Permeation of a gas through a polymeric membrane is controlled by diffusivity and solubility, hence selective mobility and selective solubility of a gas molecule through membrane results in selectivity of the gas molecule over other type of gas molecule.

By varying chemical nature of polymer, one can control size distribution of the randomly spaced gap, thereby reducing mobility of one gas and enhancing mobility of other type of gas molecule. Slight change (1.2 Å) in the pore dimension can change selectivity by 2000 folds [Kim T. H. et al (1988)]. This ability to regulate the distribution of transient-gap

size can be achieved using polymers with highly hindered segmental mobility and packing. This property requirement leads to the selection of noncrystalline or glassy polymers. However, at higher temperatures above their T_g , it begins to behave as a rubbery material and loses its selectivity.

Selective solubility can be explained by solubility parameters which depends on boiling points of the gases. Lower the boiling point lower the condensability of the gas, hence lower the sorption level of the gas in polymer matrix.

Selective mobility and solubility either complement or oppose each other resulting in net selectivity. At higher temperatures, selectivity is sacrificed at the expense of higher permeability in practice. [Toshima N., (1991a); Zolandz and Fleming, (1992b)].

Membrane separation of gases can be studied by determining permeation rates of individual pure components and mixture of both. However, at equivalent pressure differences between upstream and downstream faces of membrane, relative rates of permeation of the two components of a mixture, is within 10-15 % of the rate measured with pure individual gases. Hence studying permeation of pure gases through membrane enables us to predict selectivity of membrane for mixture of gases [Toshima N. chap. 4 (1991),].

Early attempts in developing technology failed to arouse commercial interest due to very low flux rates and multiple defects introduced during drying stage of asymmetric membranes. In 1970, discovery of extra-ordinarily high permeability of silicone homopolymer and copolymers with polycarbonate at General Electric, USA, stimulated development of ultrathin membranes [Ward et al (1976)]. Elimination of pinholes by laminating ultrathin multiple layer cellulose acetate lead to the development of composite membrane, using in 1970 but not pursued until 1977. Low flux rate of gas was overcome by increasing surface area using hollow fine fibers at Du Pont using melt spinning technology.

Glassy polymer materials with unusual high intrinsic permeabilities were identified, [Hoehn H. H. et al (1980)], which are attractive in asymmetric membrane form. Concurrently Monsanto introduced a concept of the resistance composite in which thin coating of silicone rubber was applied using reduced pressure on surface defects in asymmetric hollow fibers. The newly-formed layer eliminates Knudsen and viscous flow. The technology was commercialized using polysulfone membranes. Due to ready availability, adequate properties and easy processability, it was used in hydrogen recovery from ammonia.

Though most of the gas separation is carried out using polymeric and metallic alloys such as palladium - silver [Hunter J. B. et al (1966)] having high and withstanding temperatures as high as 400°C at elevated pressure are reported they are not used in large scale.

Current availability and identification of advanced material having potential performance better than presently available commercial membrane has given impetus to study further by substituting functional groups on different polymers and to correlate their physical and permeation properties. However, general observation suggests that structural modifications to inhibit chain packing and torsional mobility around flexible linkages tend to cause an increase in permeability and selectivity or increase in permeability with marginal loss in selectivity. Further modification like reducing population of the most flexible linkages in a polymer backbone tend to increase selectivity without compromise in permeability if modification does not significantly reduce intersegmental d-spacing. Use of exotic polymeric skin for high temperature and reactive chemical environments is likely to be of increasing interest. Glassy polymers at elevated temperatures may be used in membrane reactor hybrid process.

Historical outline of gas separation using polymeric membrane dates back to 1831 A. D. When Mitchell studied mixture of H₂ and CO₂ [Mitchell J. K. (1831)] demonstrated enrichment of oxygen in atmospheric air from 21 to 41% and postulated solution-diffusion mechanism of permeation.

1.1.5 Typical vocabulary related to membrane processes

The permeation of a gas through a polymeric membrane is controlled by the diffusivity and solubility. Hence, selective diffusivity, selective solubility or both, control the separation across the membrane.

Selective solubility is governed by solubility parameters that depend on the condensability of the gas in the polymer matrix. If the condensability of the gas is lower, the sorption level in polymer matrix also will be lower. In this case, decreased selectivity is due to decreased solubility selectivity. If selectivity is increased due to diffusivity, then it is because of increased diffusivity selectivity.

Permeability and selectivity of gases could therefore, in principle, be manipulated by suitable modification of the membrane material. The properties such as free volume, chain rigidity and gas-polymer interactions affect the permeation process. Structural modifications

on the monomer level was found to be capable of altering permeation characteristics of the membrane material for various types of polymers [Robeson L. M. et. al. (1997).; Pixton and Paul (1995b)]. A wide range of polymeric materials such as polysulfone, polycarbonate, polyamide, polyarylate, etc. are being studied for gas permeability.

The desired polymer properties can be obtained by modifying the monomer structure and / or by dispersing or blending one or more additives in the polymer matrix. Various additives such as low molecular weight organic / inorganic compounds, polymers, organometallic compounds, metal salts, zeolites are usually physically dispersed in polymer matrices to improve performance. Additive used may be dissolved completely or partly in polymer matrix, are known as homogeneous or heterogeneous blend respectively.

A prediction technique for gas permeability from polymer structure has been developed on the basis of a specific free volume diffusion theory. In this theory, the free volume available per unit mass in a polymer structure controls the rate of gas diffusion and hence, its rate of permeation. The smaller the specific free volume (SFV), the more difficult the gas diffusion. The reciprocal of SFV depends on the density and can be considered as a measure of the 'tightness' of the polymer structure. The larger its value, the tighter the structure becomes, thus restricting the permeation of the gas penetrant. The SFV can be obtained from group contribution calculations, which in turn varies with its molecular structure. This theory is useful for selecting barrier materials for packaging application. Gas solubility in the polymer is equally important while predicting the permeability.

1.2 Present Work

There are very few reports in the literature about substitution on acid moiety of polyarylates. The $-CF_3$ group on the bisphenol moiety is known to increase permeation [Kharul and Kulkarni (1994)]. Introduction of $-CF_3$ group on terephthalic acid and investigation of permeation properties in comparison to its substitution on bisphenol was carried out in the present investigations.

A new range of polyarylates were synthesized by modifying the acid moiety. Trifluoromethyl group was substituted on the terephthalic acid to obtain trifluoromethyl terephthalic acid (CF_3T). This acid was polymerized with different bisphenols (DMbis-A, TBrbis-A, and *o*-cresolphthalein). Physico-chemical characterization of resulting polymers were evaluated and correlated with gas permeation properties.

Permeability and selectivity depend on the substituents of bisphenol moiety [Moe et al (1988); Hellums et al; McHattie et al (1991b), Kharul et al (1998)]. Polarity, flexibility and bulk of the substituent governs the permeation properties of the resulting polyarylate. The position of substitution on bisphenol moiety also plays an important role.

Two different type of additives were dispersed in two commercial polymers (PC and PSF) as a second approach to tailor permeability and selectivity. These were:

[A] Liquid crystalline compound dispersed in polymers identified as LC- dispersed polymer systems and [B] Metal complex dispersed in polymers identified as MX_n - dispersed polymer systems.

In LC-dispersed polymer system, two liquid crystalline compounds LC1 and LC2 were dispersed in two commercial polymers: PC and PSF. In the metal complex systems, $Fe(acac)_3$ and $Co(acac)_3$ were used and the polymer matrices used were PC and PSF. These are shown in chart 1.2.1.

Physical properties like glass transition temperature (T_g), inter-chain distance (d_{sp}), density and thermal stability were determined for all dispersed polymeric membranes of both the systems. The permeation properties of all these membranes were compared with their parent polymer membrane (PC \ PSF without additive). The effects of the nature of additive and its concentration in the polymer on the permeation properties were investigated.

The thesis is divided into the following chapters:

Chapter 1 deals with introduction.

Chapter 2 deals with literature related to polyarylate.

Chapter 3 deals with experimental part of polyarylate.

Chapter 4 deals with results and discussion on polyarylate.

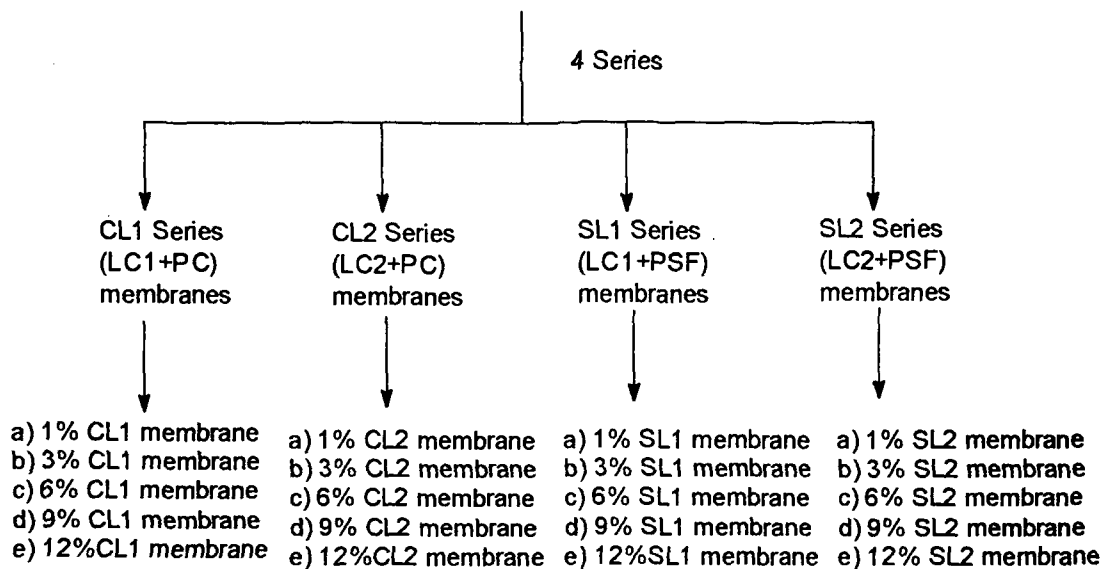
Chapter 5 deals with literature related to additive dispersed polymeric systems.

Chapter 6 deals with experimental part of dispersed systems.

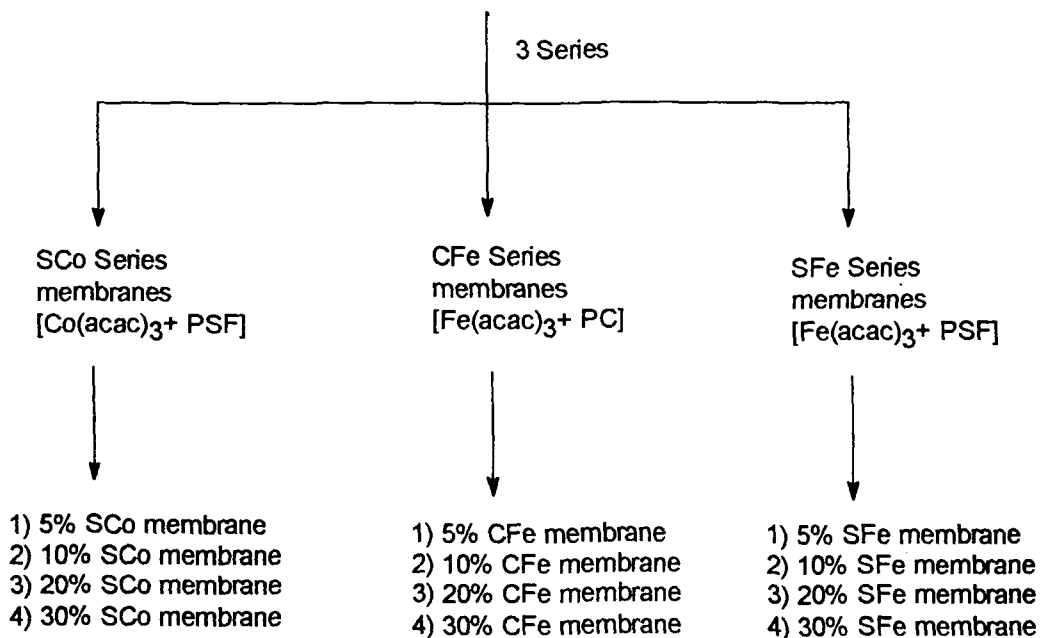
Chapter 7 deals with results and discussion on dispersed systems.

1.2.1 Classification of Additive dispersed polymeric membranes as given in Chart I and Chart II.

LC Dispersed Polymeric Membranes (Chart I)



Metal Complex Dispersed Polymeric Membranes (Chart II)



Chapter 2

Literature Related to Polyarylate Systems

2. Theory of permeation

2.1 Introduction

Gas diffusion through nonporous membrane is a concentration driven process, which follows the Fick's first law [Crank, (1975)];

$$J = -D\nabla c, \quad \text{-----(2.1)}$$

where J is the flux across the membrane, D is the diffusion coefficient and c is gas or penetrant concentration.

In the gas separation process, gas molecules are separated on the basis of difference in their rates of permeation through the membrane. The permeation rate of a penetrant molecule through the polymer matrix depends upon size and shape of the penetrant, free volume in the polymer matrix, the polymer - penetrant interactions and chain flexibility [Norman (1975)].

Permeation through non-porous polymeric membranes is defined as:

$$P = (J \times l) / (p_h - p_l) \quad \text{-----(2.2)}$$

where P is the permeability coefficient of the membrane material, l is its thickness, and $(p_h - p_l)$ is the pressure difference across both sides of the membrane. The intrinsic permeability of a polymer is given as P expressed in "Barrer" i.e. $10^{-10} \text{ cm}^3(\text{STP}).\text{cm}/\text{cm}^2.\text{sec}.\text{cm Hg}$.

Gas permeation through non-porous polymer occurs by a solution-diffusion mechanism [Von Wroblewski et al (1879); Wang et al (1982); Zolanz et al (1992)]. Gas permeability of the membrane can be expressed in terms of solubility and diffusivity as,

$$P = D \times S \quad \text{-----(2.3)}$$

where S is the solubility coefficient which is a thermodynamic quantity and is affected by polymer-penetrant interactions as well as available free volume in the polymer matrix. The average diffusion coefficient D is kinetic in nature and largely determined by polymer-penetrant dynamics. Diffusivity of a gas increases as the diameter of the gas molecule

decreases. As an empirical rule, gases which have higher critical temperatures and / or smaller molecular diameters permeate faster [Hoehn et al (1985); Stern et al (1969)].

When the downstream pressure is negligible compared to the upstream pressure, the separation factor (or selectivity) α for a pair of gases is determined by a ratio of pure gas permeabilities for the individual components i and j

$$\alpha_{ij} = P_i/P_j \quad \text{-----(2.4)}$$

where P_i and P_j are the permeability coefficients of the two gases. The ability of the membrane to separate penetrant gases is expressed in terms of diffusivity and solubility coefficients. Thus selectivity (α) is given as

$$\alpha_{ij} = (D_i / D_j) \times (S_i / S_j) \quad \text{-----(2.5)}$$

$$\text{i.e. } \alpha_{ij} = (\text{mobility selectivity}) \times (\text{solubility selectivity}) \quad \text{-----(2.6)}$$

2.2 Transport in Glassy polymers

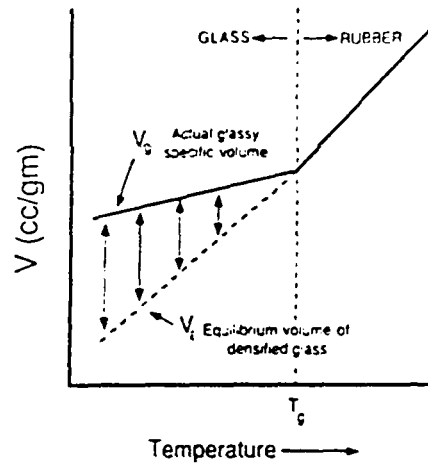
In the glassy polymers due to the more restricted segmental motions an enhanced “diffusivity selectivity” as compared to rubbery polymers [Stannett et al (1979); Koros and Chern (1987)] is observed. As these are inherently size and shape selective than rubbery materials, glassy polymers are more commonly used as the selective layer in gas separation membranes. The solubility selectivity often dominates transport in rubbery polymers. Glassy polymers are able to discriminate effectively between extremely small differences in molecular dimensions of gases in the range 0.2 to 0.5 Å [Zolanz et al (1992)].

Glassy polymers below their glass transition temperature contain “unrelaxed” or “frozen” free volume, as a result of non-equilibrium chain conformations formed in the quenching process below the glass transition, as given in figure 2.1

As shown in the figure 2.1, there is a break in the volume versus temperature plot for a polymer as the temperature is lowered below the glass transition T_g . Below T_g , the excess or “unrelaxed volume” is $(V_g - V_l)$. and this excess volume is thought to be the result of trapped nonequilibrium chain conformations in quenched glasses, resulting from the extraordinarily long relaxation times for segmental motions in glassy state. The excess volume present in glassy polymers permits additional penetrant [Chern et al (1983)].

Gas sorption in glassy polymers is more complex, and transport can be explained by a typical dual sorption isotherm for gases up to moderate pressures (20 to 30 atm) [Koros and Chern (1987)].

Figure 2.1 Polymer specific volume as a function of temperature.



2.2.1 Dual-Mode Sorption Model

The concept of sorption in two idealized environments is inherent in the dual-mode sorption model [Barrer et al (1958), Michaels et al (1963)]. First part is explained by Henry's law where a part of the sorbed population is due to the molecules which are dissolved in the polymer matrix. These are relatively mobile. While the second part of the population follows a Langmuir hole filling process, wherein the sorption is due to unrelaxed volume or "microvoids" present in the polymer matrix. The total sorption is the sum of these two populations and given as:

$$c = c_D + c_H, \quad \text{-----(2.7)}$$

$$c = k_D p + (c'_H b p / 1 + b p) \quad \text{-----(2.8)}$$

where c_D is the Henry's law or dissolution term, c_H is the Langmuir sorption or hole filling term, k_D is Henry's law constant, p is the penetrant pressure, c'_H and b are the Langmuir capacity constant and affinity constant, respectively. The dual-sorption model is illustrated

in Figure 2.2. The dual-mode model successfully describes penetrant sorption in glassy polymers and can be related to model parameters.

The companion transport model to the dual-mode sorption model expresses the local flux J in terms of two contributions [Paul and Koros (1976)] as

$$J = -D_D (dc_D / dx) - D_H (dc_H / dx) \text{ -----(2.9)}$$

where D_D and D_H are the mobility of the dissolved and Langmuir sorbed components respectively. Due to the difference in the energetics of the diffusional jumps in these two environments, D_D is much larger than D_H except for non-condensable gases such as helium or hydrogen.

For the special case in which the downstream pressure is effectively zero, the expression derived from the dual-mode sorption and transport models for steady-state permeability [Koros and Paul (1978)] of a pure gas in a glassy polymer is written as:

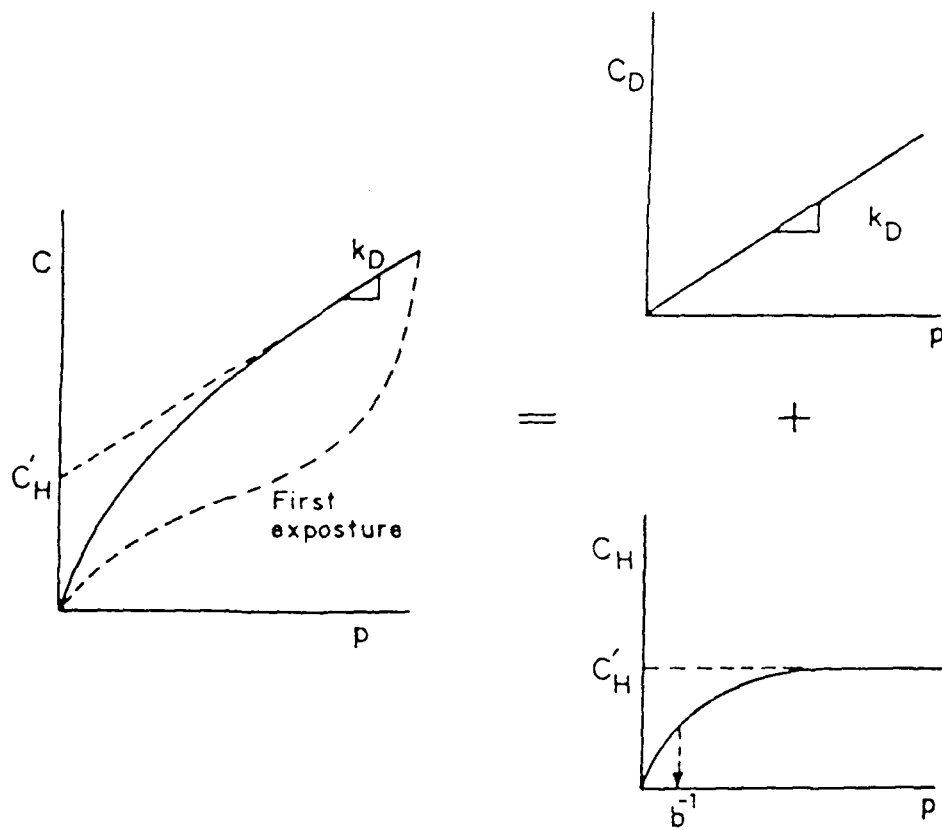
$$P = K_D D_D [1 + (FK / 1 + bp)] \text{ -----(2.10)}$$

where $F = D_H / D_D$ and $K = c'_H b / K_D$ and are convenient dimensionless groups and p is the upstream driving pressure. The first term describes transport in the Henry's law environment, while the second term is related to the Langmuir environment. At high pressure, the permeability approaches a limiting value of $K_D D_D$ (Henry's law term). This trend is related to the saturation of the Langmuir capacity at high pressures.

The above expression for dual-mode transport accounts for two types of diffusion jumps. The terms D_D and D_H represent diffusional jumps in the Henry's law and Langmuir environment, respectively. Barrer (1984) extended the dual-mode transport model to account for the effect of neighboring gas molecules on transport, and it is assumed that a gas molecule can execute four distinct diffusional jumps. If the Henry's law and Langmuir environments are denoted as D and H, respectively, the four possible jumps are depicted by

D → D	(dissolved to dissolved),
H → H	(hole to hole),
D → H	(dissolved to hole),
H → D	(hole to dissolved).

where the four diffusion coefficients are represented by D_{DD} , D_{HH} , D_{DH} , and D_{HD} . The expression for dual-mode transport developed by Barrer is



$$C = C_D + C_H$$

$$C = k_D p + \frac{C'_H b p}{1 + b p}$$

Fig. 2.2 Illustration of the dual-sorption model for glassy polymers.

$$P = K_D D_{DD} + \{[c'_{hb}(D_{HH} + D_{HD}) - k_D D_{DH}] / (1 + bp)\} + \{[2k_D D_{DH} \cdot \ln(1 + bp)] / bp\} \text{-----}(2.11)$$

A prediction technique [Lee (1980)] for gas permeability from polymer structure has been developed on the basis of a specific free volume diffusion theory. In this theory, the free volume available per unit mass in a polymer structure controls the rate of gas diffusion and hence, its rate of permeation.

2.3 Structural correlation with gas permeability in glassy polymers

To optimize the gas permeability, the structure of polymer could be systematically designed to obtain the anticipated permeation properties. Different families of glassy polymers like polysulfones, polycarbonates, polyimides, polyesters, etc. are reported which helps to investigate the effect of structural modification on the gas permeability. Several reviews on these aspects with different polymers are available {Koros and Fleming 1993, Stern 1994, Rebeson et. al. 1994, Ghosal (1994), Paul (1993)}.

In this part, the effect of structural variation in various types of glassy polymers on permeation properties is reviewed. Some of the glassy polymers discussed here are polysulfones, polycarbonates, polyarylates, polyimides and polyphenylene oxides.

2.3.1 Polysulfone (PSF)

Structurally, PSF is composed of two moieties: one containing a sulfone (-SO₂-) moiety and the other a bisphenol. It is widely used as a gas separation membrane material. Membranes based on bisphenolA-PSF are the first commercialized gas separation membranes. The use of PSF ranks second after cellulose acetate as a commercial membrane material with applications in both industrial and laboratory scale [Staude and Breitbach (1991)].

2.3.1.1 Structural modifications in PSF

The phenyl ring and /or the bridge carbon position of the bisphenol-A (bisA) moiety were modified by substituting with different groups [McHattie et al (1991a), (1991b), (1992)]. Symmetric (tetra-) substitution on the bisphenol phenyl rings by methyl groups (TMbisA-PSF) resulted in loose packing, but more rigid structure. This increased permeability of various gases while slightly decreasing selectivities as compared to unsubstituted PSF [McHattie et al (1991a), (1992); Moe et al (1988)].

PSFs obtained from asymmetric (dimethyl) substitution of bisphenol-A (DMbisA-PSF) and bisphenol based on cyclohexanone (DMbisZ-PSF), were tightly packed, i.e. having lower free volume than unsubstituted PSF [McHattie et al (1991a)]. The dimethyl substituted polymers were found to be less permeable and more selective. The changes in permeation characteristics were more pronounced in DMbisZ-PSF than in DMbisA-PSF because cyclohexyl group of DMbisZ-PSF can apparently change conformations to pack closely with other neighbouring molecular groups.

The effect of aryl nitration on gas sorption and permeability in polysulfone was studied by Ghosal K. [Ghosal and Chern (1992), Ghosal et al (1995)]. The degree of nitration was varied from 0 to ~2 nitro groups per repeat units (0-192%). The nitro group substitution on one of the phenyl rings of bisphenol did not change the T_g. The permeability and diffusivity coefficients for all gases decreased with increasing degree of nitro substitution, which is because of the decreased fractional free volume and decreased torsional mobility. The solubility of N₂, O₂, and CH₄ do not show a systematic dependence on degree of substitution. However, CO₂ permeability decreases with increase in degree of substitution. Here nitro group increases the polymer polarity and lowers free volume. CO₂/ CH₄ solubility selectivity increases monotonically as the degree of substitution is increased.

The ring substitution like amino or sulfonate groups offered low selectivity for O₂/N₂ [Staude and Breitbach (1991)].

Substitution at the bisphenol bridge carbon with aliphatic moiety was found to be ineffective in increasing fractional free volume of the polymer. But rigid, aromatic (fluorene) moiety or di-CF₃ groups substituted in place of di-Me of the bridge carbon showed enhancement in free volume of the polymer and lead to two fold increase in gas permeability [McHattie et al (1991a), (1991b); Aguilar-Vega and Paul (1993)]. Replacement of one of the methyl groups of the bridge position by a phenyl ring in PSF-AP (bisphenol derived from acetophenone) lead to a small increase in permeability coefficients with similar or slightly higher selectivity for all gases compared to BisA-PSF [Aguilar-Vega and Paul (1993)]. Incorporation of a phthalide ring at the bridge carbon of bisphenol-A (PPha-PSF) increased permeabilities of various gases by 50-100% with slight improvement in selectivities of various gas pairs [Houde et al (1994)]. Higher solubilities for CO₂ and CH₄ were attributed partly to the presence of an additional ester group in the phthalide ring. Sorption and permeation results were explained by the dual-sorption model.

An enhancement in permeation properties was seen in case of TMPSF6 by McHattie [McHattie et al (1992)] in which bisphenol-A was substituted by tetramethyl groups and both bridge methyl groups replaced by two -CF₃ groups. TMPSF6 showed nearly 10 fold increase in permeability while maintaining selectivity for most of the gas pairs.

Replacement of bisphenol-A by other diols are reported by Aitken et al. [Aitken et al (1992)]. PSFs synthesized from tetramethylbiphenol (TMBIPSF) and hexamethylbiphenol (HMBIPSF) were studied for their gas permeation properties. Out of these, TMBIPSF and HMBIPSF were more permeable and for some gas pairs the selectivities were higher than those of TMbisA-PSF.

PSFs prepared from isomeric naphthalene diols were found to be 27-80% less permeable for different gases than for bisA-PSF [Aitken and Paul (1993)]. In these cases, selectivities for various gas pairs increased by 20-500% at the cost of the

reduction in gas permeability. Gas solubility was unaffected by naphthalene substitution but the diffusivity was drastically reduced.

2.3.2 Polycarbonates (PC)

Bisphenol-A based polycarbonate (bisA-PC) is a glassy, thermoplastic engineering polymer. Extensive study of physical properties of this polymer were done by Immergut et al (Immergut et al 1964). Although, wide information on structure-permeation relation of PC is known, it has not been commercialized as compared to PSF.

An extensive permeability study of bisA-PC was reported by Koros et al (1977). Solubility, diffusivity, time lag and permeability were measured. The data were interpreted by the dual-sorption transport model which postulates that gas sorption results from both a Henry's law mechanism and a Langmuir - type hole filling mechanism. The permeation behavior of pure CO₂ and CH₄ as well as mixtures of these gases were studied at different temperatures [Costello and Koros(1993)]. In the mixed gas system, the activation energy was higher and the rate of permeation was lower than in the pure gas system for both CO₂ and CH₄.

2.3.2.1 Structural modification in PC

Variations in the properties of PCs obtained by chemical modification of bisphenol-A either at the bridge or ring position, and combination of both are known. The substituents were various alkyl or halogen containing groups.

The O₂ permeability of 24 structurally different PCs with various bisphenol substitutions were reported along with their physical properties and T_g [Schmidhauser and Longley (1990)]. In all these polymers 5 to 6 fold increase in O₂ permeability was noted.

PCs obtained from TMbisA and bisF6 were more loosely packed than bisA-PC as reflected from dsp measurements [Hellums et al (1989c)]. This resulted in 3 -5 fold increase in permeability with either improved or similar selectivities. A combination of

these two types of substitutions (ring substitution by methyl and bridge substitution by $-CF_3$) resulted in a large increase (20 fold) in permeability with improved selectivities for He/CH_4 and CO_2/CH_4 . [(Hellums et al (1989d); (1989a) (1989c)]. Permeation characteristics of PC, TMbisA-PC, bisF6PC, TMF6PC were analyzed in terms of segmental mobility, chain rigidity, fractional free volume and carbonyl density.

PCs obtained from bisphenols with symmetric ring substitution by either bromine, chlorine or methyl groups showed decreased subgroup rotational mobility and increased chain rigidity in the following order: bisA-PC < TMbisA-PC < TCibisA-PC < TBrbisA-PC studied by Muruganandam et al. (1987). The observed low permeabilities of halogenated PCs (TBrbisA-PC and TCibisA-PC) in comparison to TMbisA-PC, inspite of the similar size of the halogens and $-CH_3$, was attributed to stronger cohesive forces owing to polarity that might result in denser packing and reduced intersegmental motions. Joginder et al [Joginder et al (1989)] reported for TBrbisA-PC, a separation factor of 7.4 for O_2/N_2 gas pair.

Simultaneous increase in both the permeability and selectivity were obtained in TBrbisF6-PC [Hellums et al (1989b), (1991)] compared to TBrbisA-PC (high diffusivity selectivity) and bisF6-PC [high fractional free volume (FFV)]. In the halogenated polymers studied, both solubility and diffusivity were higher in materials with higher FFV.

The substitution of the bulky spirobiindane (SBI) moiety for bisA in polycarbonates, polyesters, and polyetherimides was studied by Pessan et al (1995) for gas transport. The SBI substitution increases fractional free volume by reducing packing density in polymer and also reduced the intramolecular mobility because of bulk of SBI group. This resulted in high enhancement in the permeabilities for all gases, O_2 by 5.9 folds, CO_2 by 4.8 folds, CH_4 by 4.3 folds. Simultaneously, increase in selectivities for O_2/N_2 gas pair by 13%, while decrease in He/CH_4 and CO_2/CH_4 selectivities for more open SBI containing polymers were noted. SBI containing

polyetherimide material has attractive gas separation properties from the commercial point of view.

The combination of PC with other functionality were also examined for gas separation like polyestercarbonates [Pinnau et al (1991)].

A great deal of similarities were seen in the transport and sorption characteristics of polycarbonate and polysulfone derived from bisphenol-A [Erb and Paul (1981)]. Sorption parameters were similar in magnitude for both polymers. The diffusion coefficient in the Henry's law mode were smaller for each gas in PSF; while Langmuir mode diffusion coefficients were similar for each gas in both polymers.

The permeability coefficients of various gases in PCs were slightly lower than those in polyarylate (PAr) obtained from bisA [Barbari et al (1988)].

A relatively low enhancement in permeability was observed for tetramethyl substitution in TMbisA-PC as compared to the similar substitution in TMbisA-PSF [Moe et al (1988)]. Selectivities in TMbisA-PC were not decreased, while for TMbisA-PSF, a decrease of ~30% was noted in comparison to their respective unsubstituted polymers.

2.3.3 Polyarylates(PAr)

Gas permeation studies of polyarylates have been attempted [Sheu et al (1989); Chern and Provan (1991b); Charati et al (1991); Pessan and Koros (1993)]. However, the potential of using polyarylates obtained from bisphenol-A and an equimolar mixture of iso and terephthalic acid has increased because of its high permeability compared to bisphenol based PC, PSF, polyetherimide and polyhydroxyether. The polyarylate had a reasonably high glass transition temperature and were shown to be non-crystalline. Most of the polyarylates are soluble in common organic solvents. [Wu et al (1983); Charati et al, (1991)]. Further improvements in polyarylate gas permeation properties can be achieved by structural modification of the acid and /or bisphenol monomer.

Tetrahalogenation of bisphenol-A by either chlorine or bromine resulted in polyarylates with higher T_g and crystallinity than bisA-polyarylate [Stackman and Williams (1983)]. Substitution by bromine was more effective in increasing the chain stiffness than chlorine.

Chlorination of bisA-I/T and bromination of poly(phenolphthalein-terephthalate) (i.e. ppha-tere) were found to increase T_g with slight lowering of the packing density [Chern and Provan (1991a)]. CO₂ and CH₄ solubilities were found to be higher in the halogenated polymers. The permeation of the mixed gas (CO₂-CH₄) system was studied by Chern and Provan [(1991a)] for TBrppha-T. Though this polymer had a high T_g, considerable gas induced plasticization was observed.

Bromination at both the bridge as well as ring carbons of bisA in TBrbisF6-T resulted in considerable increase in permeability of (O₂) to 5.25 barrers with O₂/N₂ selectivity of 6.7 [Kawakami et al (1990)]. When bromine was replaced by chlorine, a slight reduction in selectivity and increase in permeability was noted.

Gas permeation properties of polyarylates synthesized with bromine and methyl substituted bisphenols were studied by Kharul et al [(1997), (1998)]. The comparison of polyarylates based on tetrabromobisphenol-A (TBrbisA) and tetramethylbisphenol-A (TMbisA) shows that both substituents increase chain rigidity; however Br-substitution increases packing density and leads to high selectivities. The methyl substitution reduces packing density and increase permeabilities. Further in order to achieve high permeability and high selectivity, both bromine and methyl substitutions were incorporated in the polyarylate in two ways: (1) A copolymer based on TMbisA and TBrbisA and (2) a polyarylate based on Dibromodimethylbisphenol-A (DBrDMbisA). These two hybrid polymers have intermediate permeabilities and higher selectivities than either TMbisA- or TBrbisA- based polyarylates. The copolymer was more selective for CO₂ while the polyarylate based on DBrDMbisA was more selective for He.

The effects of substituent groups of polyarylates based on substituent size, symmetry and polarity on the gas transport properties were examined by Pixton [Pixton and Paul (1995b), Kharul et al (1998)]. The polyarylates were prepared from dimethyl bisphenol-A, tetramethyl bisphenol-A, diisopropyl bisphenol-A condensed with isophthalic acid. Symmetrically placed substituents increased permeability while asymmetrically placed substituents reduced the permeability. Bulky t-Bu- substituent at position 5 on the isophthalate increased permeability by 2-4 folds but lowered selectivity. Mostly the increase in the permeability was due to increase in the diffusion coefficients of the all gases.

Pixton and Paul [(1995a), (1997)] reported gas transport properties of a series of polyarylates based on isophthalic acid and substituted bisphenols. Bisphenols used for synthesis with and without tetrabromo substitution were bisphenol-A, hexafluorobisphenol-A, phenolphthalein, and fluorene bisphenol. The effect of tetrabromination was studied in combination with varying size and shape of connector group of bisphenol. Tetrabromination maintains or increases gas permeability. Particularly, increase in the selectivity for the O₂/N₂ gas pair as compared to non-brominated analog was noted.

Permeability coefficients for various gases in five polyarylates synthesized from different bridge substituents and iso:terephthalic acids (1:1) was reported by Houde et al [Houde et al (1995)]. One of the bridge substituent of bisphenol-A was changed by ethyl, isobutyl, phenyl, and methyl propionate group. These mono substituted bridge substituents of polyarylates showed no effect on intersegmental packing density, but a decrease in the mobility of specific groups in the polymer chain. It showed increased permeability without significant changes in selectivity. This was examined by molecular modelling studies [Charati et al (1992), Kulkarni et al (1994)].

Disubstitution at bisphenol bridge of polyarylates, [Kharul and Kulkarni (1994)] in changing packing density effectively was measured by the d-spacing, and increased chain stiffness. For phenyl disubstituents d-spacing reduces, but decrease in the phenyl

ring mobility resulted in increased permeability and selectivity. For CF_3 - disubstituents, d-spacing increased resulting in increase in permeability and reduced selectivity in comparison with unmodified bisphenol-A polymer.

A coating of poly(tetramethyl) bisphenolA- iso/terephthalate on polysulfone hollow fibers was reported to offer an O_2/N_2 selectivity of 5.8 [Nelson (1989)].

Annealing of the copolyester from 73 mol% hydroxybenzoic acid (HBA) and 27mol% hydroxynaphthoic acid (HNA) increased crystallinity [Weinkauff and Paul (1992a)]. As a result, gas diffusivity decreased. In a separate report, [Weinkauff and Paul (1992b)] gas permeation characteristics of copolymers containing varying compositions of HBA and HNA were correlated with physical properties of the polymer like T_g , sub- T_g transition, density and free volume. Copolymers with the high naphthalene content were found to exhibit very low permeabilities and extremely high O_2/N_2 selectivity (~ 16).

Light and Seymour (1982) prepared polyesters from 2,6-naphthalenedicarboxylic acid, terephthalic and ethylene diol. Increase in the naphthalene acid reduced O_2 permeability in comparison to polyethylene terephthalate.

2.3.4 Polyimides

Aromatic polyimides generally have higher T_g than other glassy polymers like PC, PSF, PAr etc. Polyimides have comparatively higher selectivity for H_2/N_2 and CO_2/CH_4 than other classes of polymers with similar permeabilities [Stern et al (1989)]. Interestingly polyimides are more permeable to N_2 than CH_4 , while the reverse is true for most other polymers [Yamamoto et al (1990)].

Substituted polyimides with number of substituents have also been reported with varying states of efficiency.

2.3.5 Polyphenylene oxides

2,6- Dimethyl polyphenylene oxide (widely known as PPO) has high T_g and low density in comparison to other glassy polymers like PC, PSF. Its high dsp [Story and Koros (1992)] and high free volume [Chern (1990a)] reflect the low packing density of polyphenylene oxide. As a result of this, it has high permeability but low selectivity [Maeda et al (1987a)]. Solubility as well as diffusivity effects were shown to alter the permeation characteristics by modifying the structural variation of PPO. These include substitutions on the phenyl ring as well as on the methyl groups. The changes in the physical and permeation properties brought about by different types of substitutions were attributed to the nature of the substituent groups, i.e., their polarity, rigidity, bulk size etc.

Number of derivatives of PPO effected by halogenation, sulfonation, carboxylation, and nitration are also reported.

Chapter 3
Experimental of Polyarylate

3 EXPERIMENTAL (Polyarylate)

3.1 Materials:

3.1.1 Materials used for the preparation of monomers and polymers

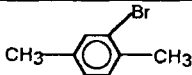
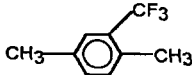
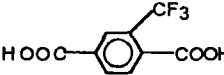
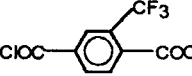
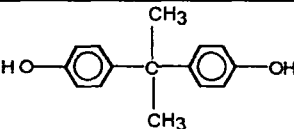
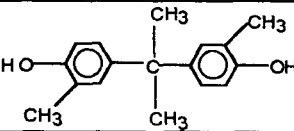
The specifications of materials and monomers procured are given in Table 3.1. The structure of various monomers and polymers are listed in Table 3.2. The solvents and other chemicals, unless otherwise mentioned, were purified by standard procedures [Perrin and Armarego (1988)].

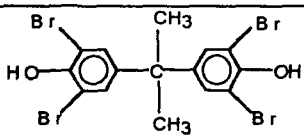
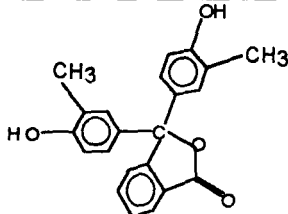
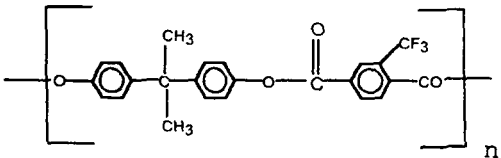
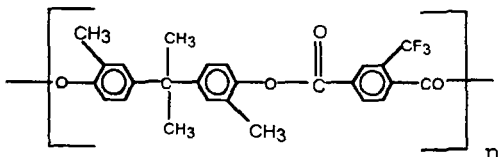
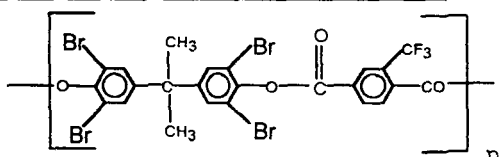
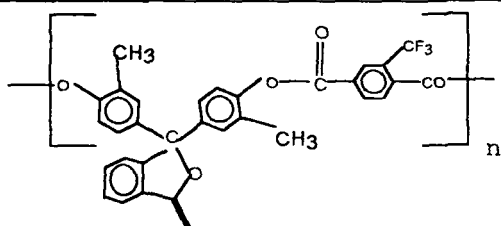
Table 3.1: Sources and purity of materials.

Chemical	Make	Purity / Grade
2-Bromo-1,4-xylene	Aldrich Chemicals, USA.	99%
Copper iodide	Fluka, Switzerland.	99%
Potassium iodide	SD fine chemicals Ltd., India.	LR
Potassium permanganate	SD fine chemicals Ltd., India.	LR
Hydrogen peroxide	SD fine chemicals Ltd., India.	30% aqueous solution.
Calcium chloride	SD fine chemicals Ltd., India.	LR
Trifluoroacetic acid	Aldrich Chemicals, USA.	99%
N-methyl pyrrolidine	SD fine chemicals Ltd., India.	LR
Sodium hydroxide	SD fine chemicals Ltd., India.	LR
Hydrochloric acid	SD fine chemicals Ltd., India.	AR (35.4%)
Thionyl chloride	SD fine chemicals Ltd., India.	AR
Acetyl acetone	Sisco Research Laboratory, India.	Extra pure
Acetone	SD fine chemicals Ltd., India.	AR
Ferric chloride	SD fine chemicals Ltd., India.	AR
Cobalt carbonate	SD fine chemicals Ltd., India.	AR
Bromine	SD fine chemicals Ltd., India.	AR
<i>o</i> -Cresolphthalein (<i>o</i> -Cp)	Aldrich Chemicals, USA.	Indicator grade
N-benzyltriethylammonium chloride (BTEAC)	Aldrich Chemicals, USA.	99%
Bisphenol-A	Aldrich Chemicals, USA.	97%
<i>o</i> -Cresol	SD fine chemicals Ltd., India.	LR
Potassium carbonate	SD fine chemicals Ltd., India.	LR
Zinc chloride	SD fine chemicals Ltd., India.	LR
Sodium sulfate	SD fine chemicals Ltd., India.	LR
Dichloromethane	SD fine chemicals Ltd., India.	AR

1,1,2,2-Tetrachloroethane	SD fine chemicals Ltd., India.	AR
Chloroform	SD fine chemicals Ltd., India.	AR
Acetic acid (glacial)	SD fine chemicals Ltd., India.	AR
Polycarbonate (PC)	Amoco Polymer Products Pvt. Ltd., USA.	M.W. ~35,000
Polysulfone (PSF)	General Electrical Pvt. Ltd., USA.	M.W. ~40,000
Helium (He)	M/s Indian Oxygen Ltd., Bombay, India.	99%
Argon (Ar)	M/s Indian Oxygen Ltd., Bombay, India.	99%
Nitrogen (N ₂)	M/s Indian Oxygen Ltd., Bombay, India.	99%
Oxygen (O ₂)	Industrial Oxygen Company Ltd., Poona, India.	99%
Methane (CH ₄)	M/s Indian Oxygen Ltd., Bombay, India.	99%
Carbon dioxide (CO ₂)	M/s Bombay Carbon Dioxide, Bombay, India.	95%

Table 3.2 Structures and abbreviations of chemicals (monomers/ polymers)

No	Structure of Monomer/ Polymer	Name of Monomer / Polymer	Abbreviation , if any
1.		2-Bromo-1,4-xylene.	-----
2.		2-Trifluoromethyl-1,4-xylene.	-----
3.		Trifluoromethyl terephthalic acid	CF ₃ T
4.		Trifluoromethyl terephthalic acid chloride.	CF ₃ TCl
5.		2,2-Bis(<i>p</i> -hydroxyphenyl)-isopropane (Bisphenol-A)	BisA
6.		Dimethylbisphenol-A	DMbisA

7.		Tetrabromobisphenol-A	TBrbis-A
8.		<i>o</i> -Cresolphthalein (Dimethyl phenolphthalein)	<i>o</i> -Cp
9.		Poly(bisphenol-A-trifluoromethyl-terephthalate)	PA1 (Bis-A-CF ₃ T)
10.		Poly(dimethylbisphenol-A-trifluoromethyl-terephthalate)	PA2 (DMbisA-CF ₃ T)
11.		Poly(tetrabromobisphenol-A-trifluoromethyl-terephthalate)	PA3 (TBrbisA-CF ₃ T)
12.		Poly(<i>o</i> -cresolphthalein-trimethyl-terephthalate)	PA4 (<i>o</i> -Cp-CF ₃ T)

3.1.2 Synthesis / preparation of monomers

3.1.2.1 Tetrabromobisphenol-A (TBrbisA)

10.93 g (0.048 mol) of bisphenol-A, and 38.8 ml of dry methanol were taken in a 100 ml round bottom flask which was equipped with a magnetic needle, dropping funnel and calcium chloride (CaCl₂) guard tube and the contents cooled to ~10°C. Bromine

31.02 g (0.194 mol, 4.05 equivalents) was added dropwise to the reaction mixture over a period of 35 minutes. Stirring was continued for 30 minutes and the reaction mixture kept on reflux for an hour. The reaction mixture was cooled to ambient temperature and water (39 ml) was added, reacted at 60°C for 30 minutes, then cooled to room temperature. The solid obtained was filtered and recrystallized in acetic acid: water mixed solvent (3:1 v/v). The yield was 80.5%. Purity was confirmed by thin layer chromatography (TLC).

Molecular formula: $C_{15}H_{12}Br_4O_2$, Molecular weight: 543.64

Spectral analysis: Figures 3.1, 3.2.

IR (nujol): 3520-3300 cm^{-1} (broad, -OH stretching); 1560-1400 cm^{-1} (m, aromatic C=C stretching); 1250-1150 cm^{-1} (m, C-H in plane bending); 740 cm^{-1} (s, C-H out of plane bending).

1H NMR ($CDCl_3$): δ 1.5 (s, 6H, protons of bridge -CH₃); δ 5.8 (s, 2H, D₂O exchangeable phenolic protons); δ 7.25 (s, 4H, aromatic protons).

The IR and 1H NMR analysis confirmed the structure of the tetrabromobisphenol-A and was consistent with literature report [Kharul, (1995)].

3.1.2.2 Dimethylbisphenol-A (DMbis-A): [2,2-Bis(4-hydroxy-3-methylphenyl)propane]

DMbis-A was prepared by acid catalyzed condensation of *o*-cresol and acetone, using the reported procedure as follows: [Venkateswara et al (1987)].

10.8 g of *o*-cresol (0.1 mol), 2.9 g (0.05 mol) of acetone, 10 ml of concentrated hydrochloric (HCl) and 5 ml of glacial acetic acid were taken in a stoppered conical flask of 100 ml capacity and stirred at ambient temperature for a week. The formed solid was thoroughly washed with distilled water till it was free from acid. The crude product was purified by dissolving in 10% sodium hydroxide (NaOH) and precipitating in cold dilute HCl. The product was filtered, washed with distilled water till it was free from acid and dried at 70°C for 24 hours. The product was recrystallized in acetic acid: water mixture (1:1, v/v). The purity was checked by TLC. The yield was 50%.

Molecular formula : $C_{17}H_{20}O_2$, Molecular weight: 256, Melting Point : 138-139°C.

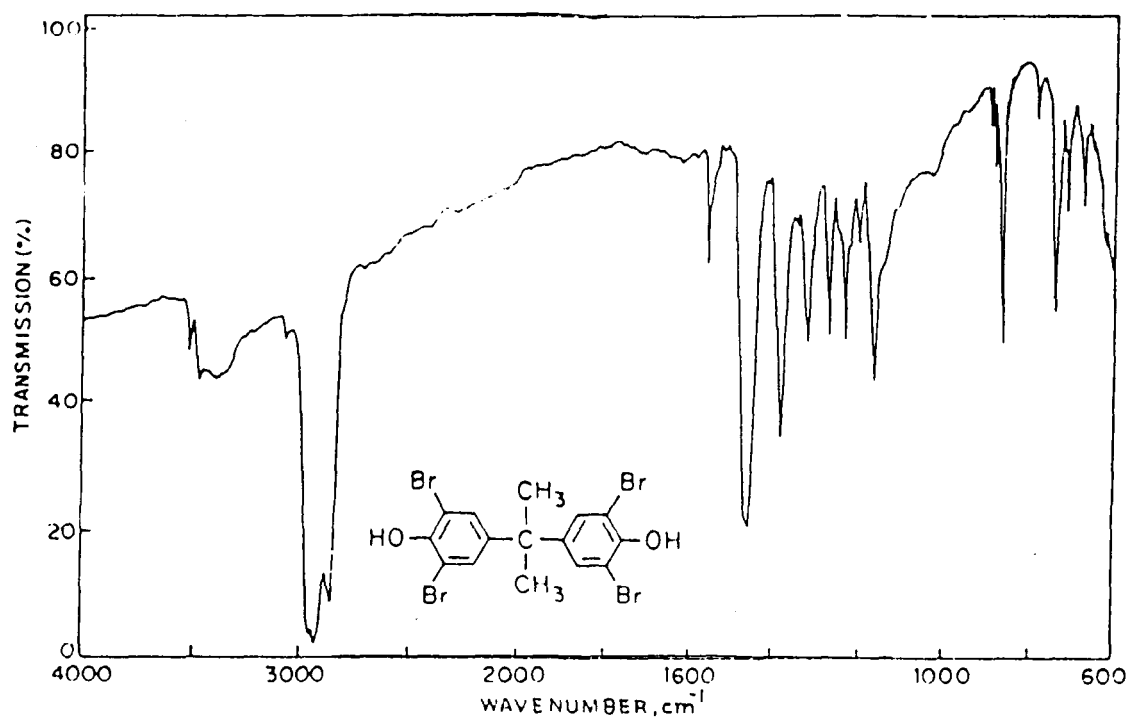


Figure 3.1 IR spectrum of TBrbisA

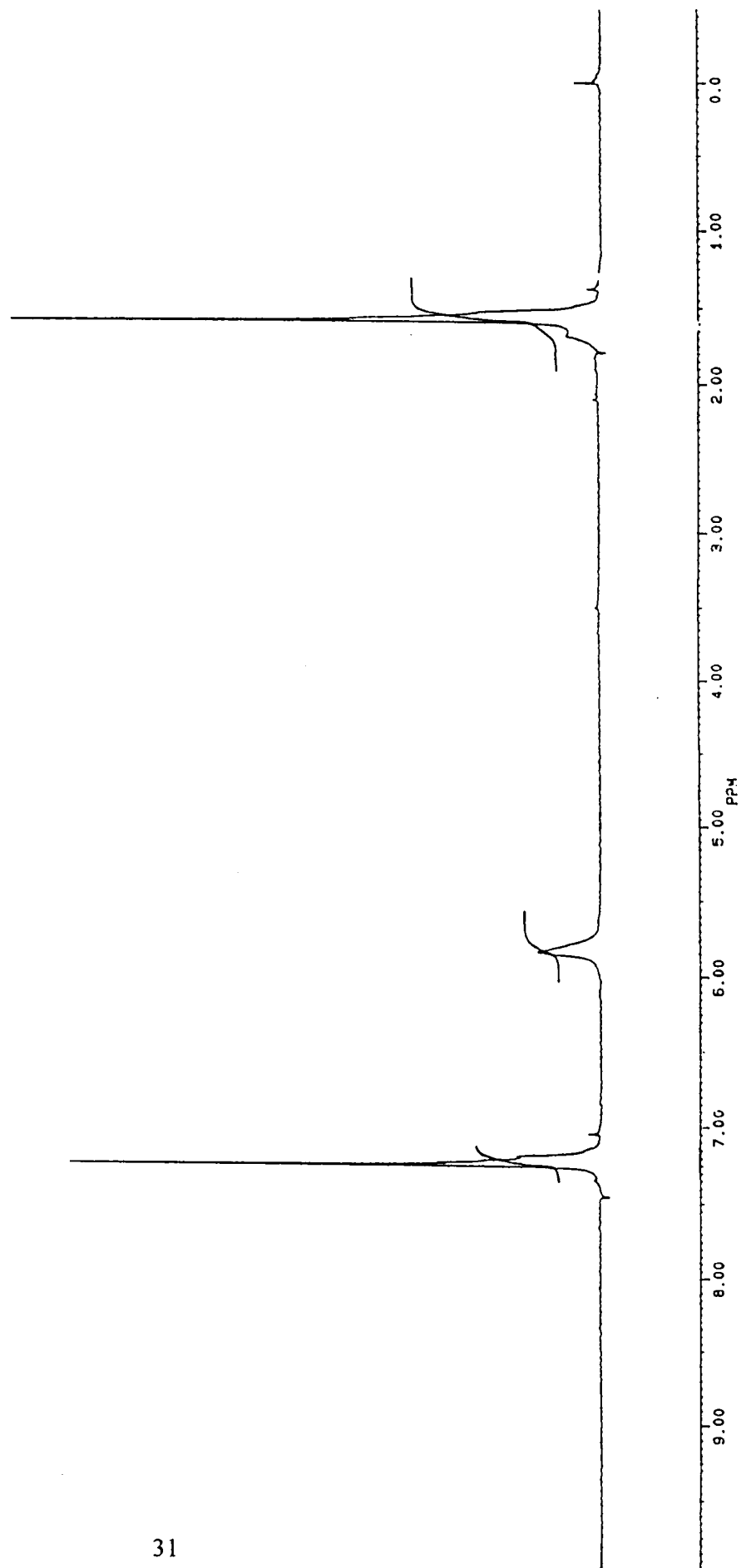


Figure 3.2 NMR spectrum of TBrbis-A monomer

Spectral analysis : Figures 3.3, 3.4.

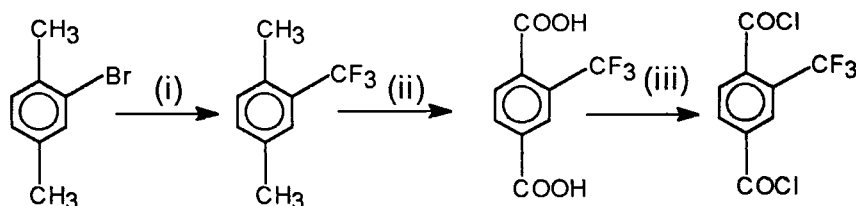
IR (*nujol*) : 3500-3100 cm^{-1} (broad, -OH stretching); 1660-1440 cm^{-1} (m, aromatic C=C stretching); 1260-1120 cm^{-1} (m, C-H in plane bending); 770 cm^{-1} (s, C-H out of plane bending).

$^1\text{H NMR}$ (CDCl_3) : δ 1.5 (s, 6H, protons of bridge - CH_3); δ 2.1 (s, 6H, protons of CH_3 at phenyl ring); δ 4.7 (s, 2H, D_2O exchangeable phenolic protons); δ 6.3-6.9 (s, 6H, aromatic protons).

The IR and $^1\text{H NMR}$ analysis confirmed the structure of dimethylbisphenol-A

3.1.2.3 Synthesis of 2-Trifluoromethyl-1,4-terephthalic acid chloride: It was prepared as shown in the scheme 1.

Scheme 1



Preparation of Sodium trifluoroacetate (CF_3COONa): 57.01 g (0.5 mol) of trifluoroacetic acid (CF_3COOH) was dissolved in 100 ml of water. The solution was neutralised with 100 ml 5N NaOH. The water was evaporated and sodium salt of trifluoroacetate was dried over phosphorus pentaoxide (P_2O_5) in vacuum. The yield was 67g (99%).

3.1.2.3(i) Preparation of 2-trifluoromethyl-1,4-xylene:

38.8 g (0.285 mol) of CF_3COONa , 14.48 g (0.078 mol) of 2-bromo-1,4-xylene and 29.79 g (0.156 mol) of copper iodide (CuI) were taken in a two necked round bottom flask (flame-dried and cooled) under argon atmosphere. After degassing, 450 ml of N-methyl-2-pyrrolidone (NMP) was added. The temperature of the solution was raised to 190°C . As temperature rises, the vigorous evolution of carbon dioxide (CO_2) gas was noticed. Stirring under argon atmosphere was continued for 2.5 hours. The reaction mixture was allowed to cool to room temperature and the product was extracted thrice

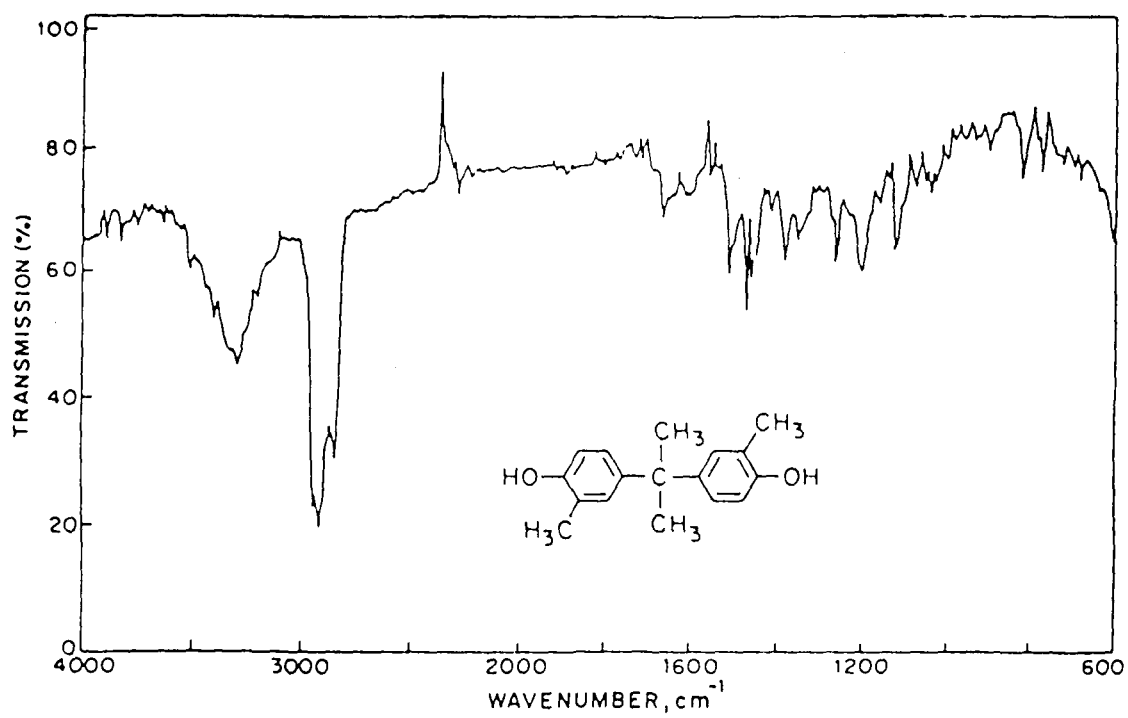


Figure 3.3 IR spectrum of DMbisA

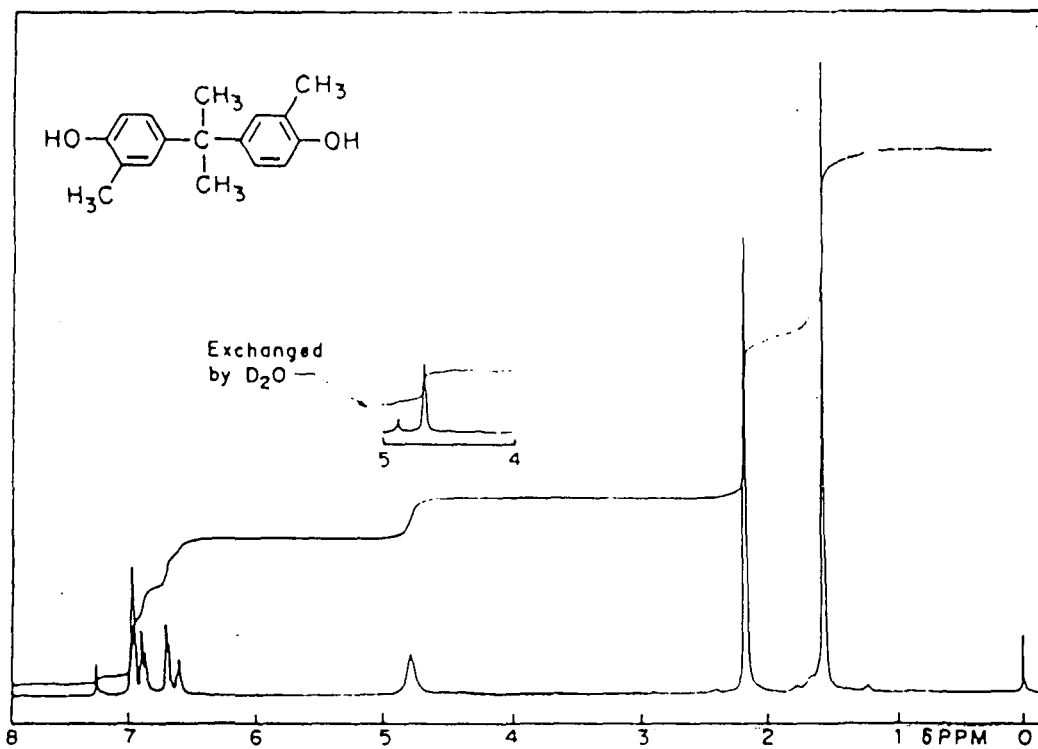


Figure 3.4 NMR spectrum of DMbisA monomer

with 300 ml each of petroleum-ether (total volume 900 ml). The organic layer was washed with 6N HCl, followed by 1N NaOH, and distilled water. It was concentrated and the residue was fractionally distilled in the range 148-185°C. Crude yield was 10.1g (58%).

Molecular formula: C₉H₉F₃; Molecular weight: 174.

Spectral analysis: figures 3.5, 3.6, 3.7.

IR (*nujol*): 2850-2940 cm⁻¹ (C-H bond stretching), 1580 cm⁻¹, 1500-1400 cm⁻¹ (aromatic C=C bending), 1380 cm⁻¹, 1250-1100 cm⁻¹ (C-H in plane bending), 800 cm⁻¹ (C-H out of plane bending).

¹H NMR (CDCl₃): δ 2.35 and 2.5 (2s, 6H, protons of two -CH₃ at phenyl ring); δ 7.1-7.4 (broad, m, 3H, aromatic protons).

MS: 174 (M⁺, 15%), 155 (65%), 105 (65%), 89 (12%), 78 (100%), 69 (40%).

The IR, ¹H NMR and MS analysis confirmed the structure of 2-trifluoromethyl-1,4-xylene.

3.1.2.3(ii) Synthesis of 2-trifluoromethyl-1,4-terephthatic acid : (CF₃T)

It was prepared by oxidation of 2-trifluoromethyl-1,4-xylene. A 500 ml three neck flask was equipped with a mechanical stirrer and a water condenser. 10.1 g (58 mmol) of 2-trifluoromethyl-1,4-xylene, 9 g of potassium permanganate (KMnO₄), 50 mg of 18-Crown-6 and 200 ml of distilled water was refluxed for 2 hrs. The addition of 9g of KMnO₄ was carried out each time till the violet colour of KMnO₄ disappeared. Overall 36.7g (4 equivalents) of KMnO₄ was needed for the completion of reaction. Supernatant liquid was taken from reaction mixture and the precipitate of magnesium dioxide (MnO₂) was twice boiled with distilled water, filtered, and the aqueous layers were mixed. Concentrated H₂SO₄ (20 ml) was added to it followed by the dropwise addition (10 ml) of 30% H₂O₂ till solution became colourless. 50 ml of concentrated HCl was added and kept over-night. The precipitated white compound was filtered, washed, and dried under vacuum. The dissolved acid in the filtrate was recovered by repeated extraction with ethyl acetate (EtOAc), EtOAc layer was washed with brine (saturated NaCl solution), followed by (10 ml) distilled water, and was dried over anhydrous sodium sulfate (Na₂SO₄).

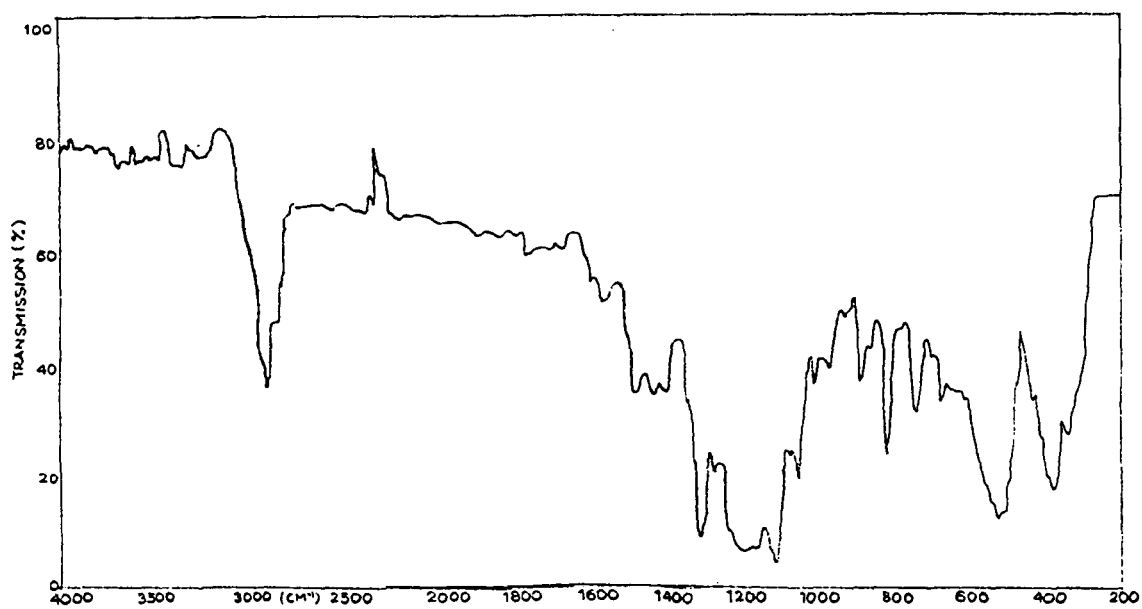


Figure 3.5 IR spectrum of 2-Trifluoromethyl-1,4-xylene

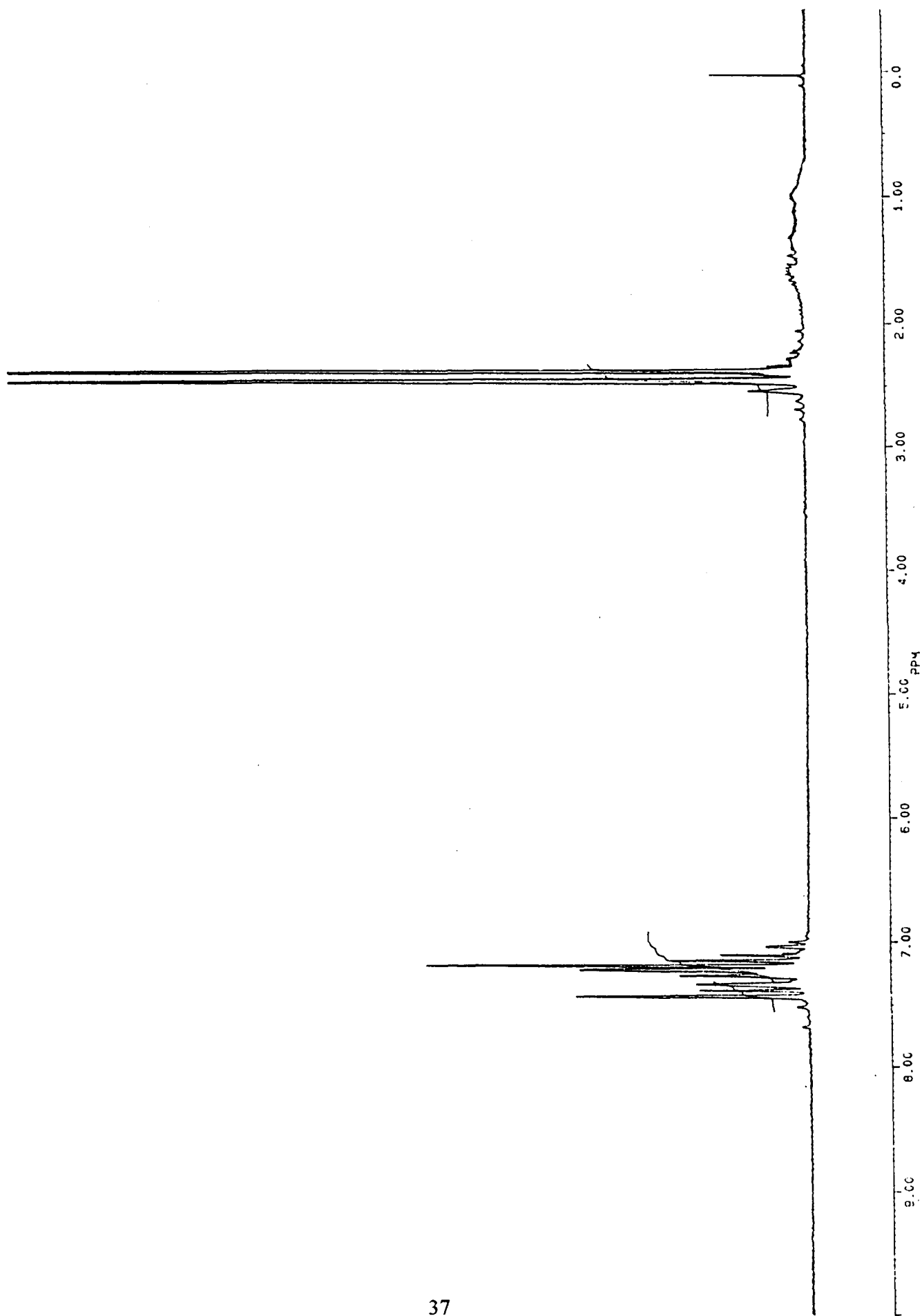


Figure 3.6 NMR spectrum of 2-Trifluoromethyl-1,4-xylene.

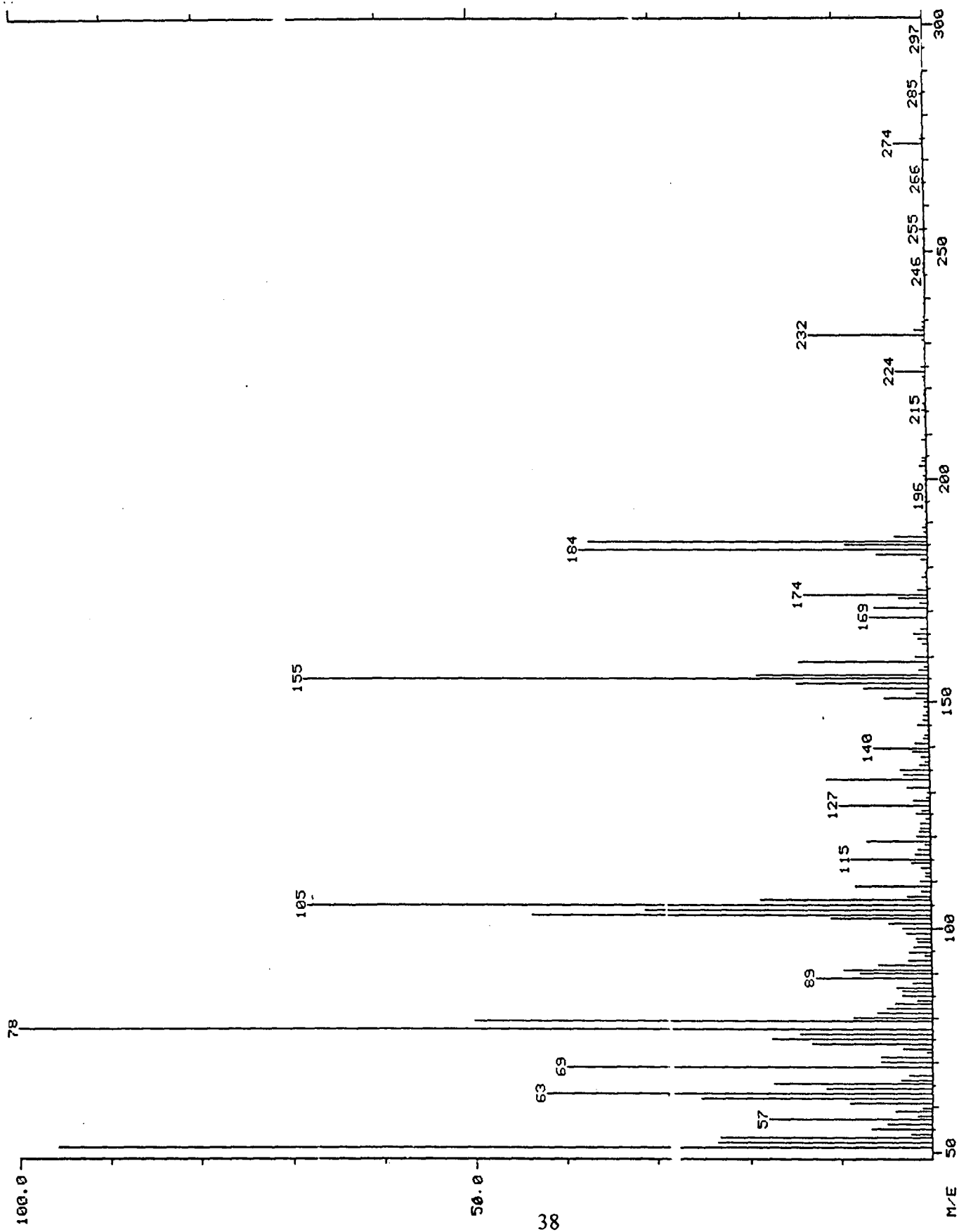


Figure 3.7 Mass spectrum of 2-Trifluoromethyl-1,4-xylene

EtOAc layer was concentrated and white solid (acid) was mixed with the precipitated fraction collected earlier and dried in vacuum at 70°C. Yield was 2.5g (18.4 %).

Molecular formula: C₉H₅F₃O₄; Molecular weight: 234

Spectral analysis: The spectra are shown in Figures 3.8, 3.9.

¹H NMR (CDCl₃): δ 1.6 (s, 2H, protons of carboxylic acid); δ 7.3 (s, 3H, aromatic protons).

MS: 234 (M⁺, 60%), 217 (100%), 189 (25%), 141 (35%), 113 (25%), 75 (45%).

¹H NMR and MS analysis confirmed [Walter et al (1989), (1990)] the structure of the 2-trifluoromethyl-1,4-terephthalic acid.

3.1.2.3(iii) Synthesis of 2-Trifluoromethyl-1,4-terephthalic acid chloride:(CF₃TCl)

2.5g (0.58 mmol) of 2-trifluoromethyl-1,4-terephthalic acid, catalytic amount of DMF and 2.4 ml of thionyl chloride (SOCl₂) were taken in a 25 ml round bottom flask and refluxed for 4 hours. The excess of SOCl₂ was distilled off under vacuum. The traces of SOCl₂ were removed by azeotropic distillation with toluene. The acid chloride flask was flushed with argon and used immediately for the polymerization with various bisphenols as mentioned in the section 3.1.3.

3.1.3 Polymer synthesis:

Polymers based on CF₃TCl (acid chloride) and four different bisphenols (BisA, DMbisA, TBrbisA, and *o*-Cp) were prepared by either solution or interfacial polycondensation.

3.1.3.1 Solution polymerization:

0.93 mmol of bisphenol, 3.96 mmol of triethylamine and 3 ml of dichloromethane were taken in a 25 ml round bottom flask and stirred. The solution of acid chloride (2.03 mmol in 3 ml DCM) was added dropwise over 45 min. through addition funnel equipped with CaCl₂ guard tube. The reaction mixture was stirred overnight and then added to the stirred (250 ml) methanol. The precipitated polymer was filtered and dried at 60°C and purified as mentioned in section 3.1.4. The polymers PA2 (DMbisA-CF₃T) and PA4 (*o*-Cp-CF₃T) were synthesized using this method.

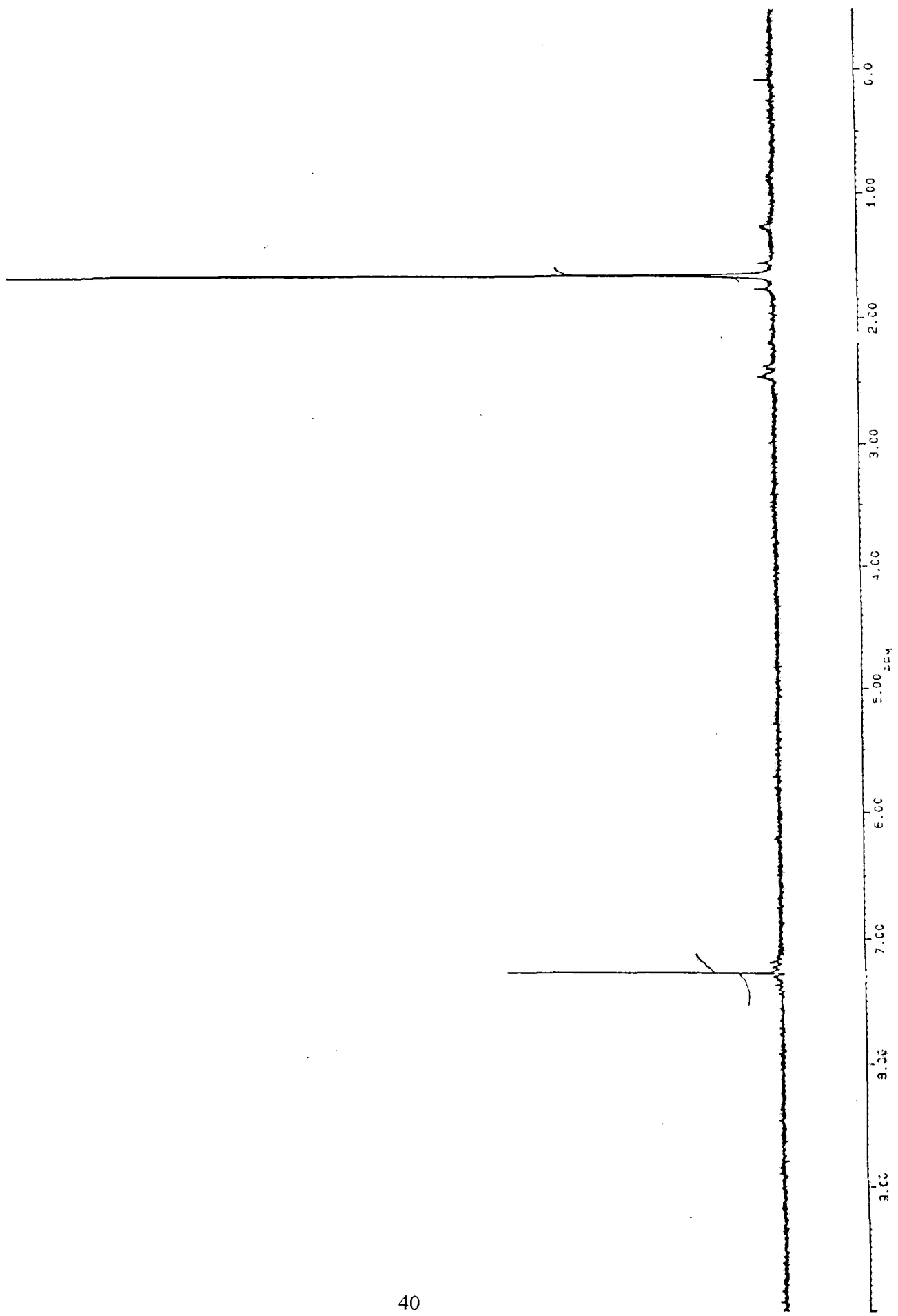


Figure 3.8 NMR spectrum of Trifluoromethyl terephthalic acid

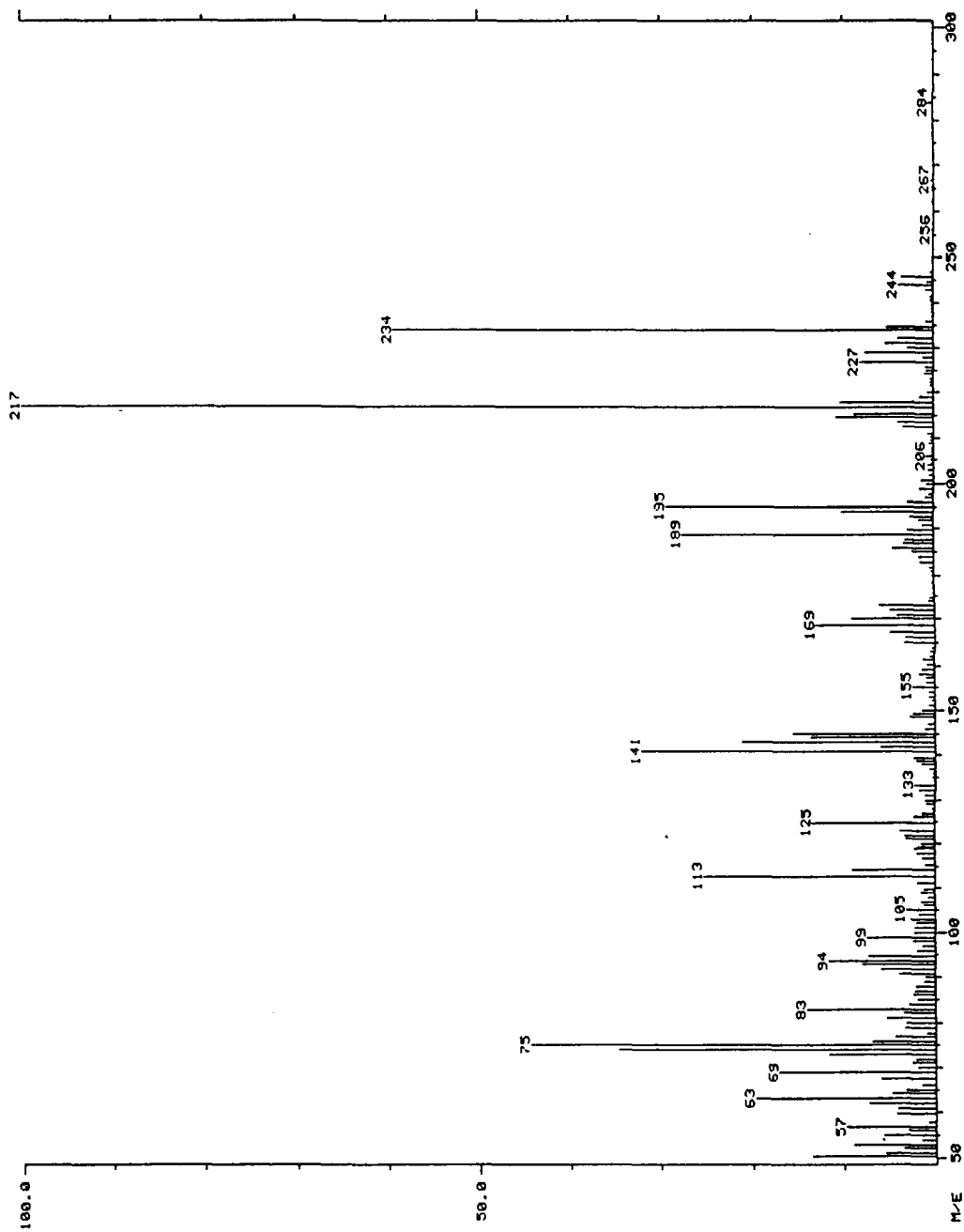


Figure 3.9 Mass spectrum of Trifluoromethyl terephthalic acid

3.1.3.2 Interfacial polymerization:

Dichloromethane was used as the organic phase, water as the second phase and BTEAC (N-benzyltriethylammonium chloride) as a phase transfer catalyst. 5 mmol of bisphenol and 10.5 mmol of NaOH were dissolved in 50 ml of water along with 0.124 mmol of BTEAC. To this, 20 ml of dichloromethane (CH_2Cl_2) was added and the mixture was vigorously stirred at ~1800 rpm. 5.25 mmol of CF_3T acid chloride was dissolved in 5 ml of CH_2Cl_2 and added dropwise to the stirred solution over 10 minutes. The mixture was stirred for an hour after which the phase separation took place. The organic layer was slowly added to stirred (500ml) methanol. The precipitated polymer was filtered and dried at 50°C and purified as given in section 3.1.4. The polymers PA1 (BisA- CF_3T) and PA3 (TBrbisA- CF_3T) were synthesized using this method. Spectral characterization is given in table 3.3. These peaks of IR and NMR spectra correspond to the various functional groups of respective monomers used for the synthesis.

Table 3,3 (IR, NMR spectra for polymers PA1, PA2, PA3, & PA4 are given in the figures 3.10, 3.14; 3.11, 3.15; 3.12, 3.16 and 3.13, 3.17 respectively.)

Polymer	Spectral Analysis
PA1 (BisA- CF_3T)	IR (film): cm^{-1} 2950, 1740, 1590, 1500, 1320 –1050, 810, 750. ^1H NMR (CDCl_3): δ 1.7 (s), δ 7.1-7.4 (m), δ 8.1 (d), δ 8.5 (d), δ 8.6 (s)
PA2 (DMbisA- CF_3T)	IR (film): cm^{-1} 2950, 1740, 1600, 1480, 1330 –1060, 1040, 880, 800, 750. ^1H NMR (CDCl_3): δ 1.7 (s), δ 2.3 (d), δ 7.2 (s), δ 8.2 (q), δ 8.6 (d), δ 8.7 (s)
PA3 (TBrbisA- CF_3T)	IR (film): cm^{-1} 2950, 1760, 1680, 1650, 1450, 1390, 1320, 1280 - 1120, 1070, 1025, 870, 750. ^1H NMR (CDCl_3): δ 1.7 (s), δ 7.5 (s), δ 8.6 (q), δ 8.7 (s)
PA4 (<i>o</i> -Cp- CF_3T)	IR (film): cm^{-1} 3000, 1750, 1600, 1480, 1400, 1320 –1080, 1025, 750. ^1H NMR (CDCl_3): δ 2.3 (d), δ 7.3 (m), δ 7.7 (d), δ 7.8 (d), δ 8.0 (d), δ 8.2 (d), δ 8.6 (d), δ 8.7 (s)

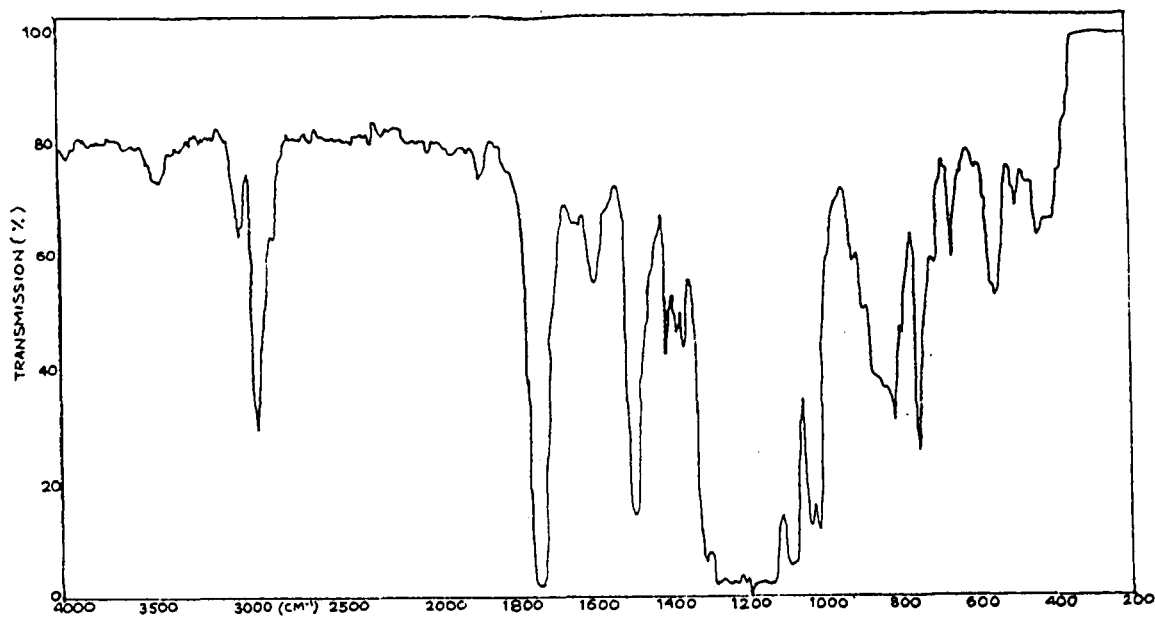


Figure 3.10 IR spectrum of PA1 polymer

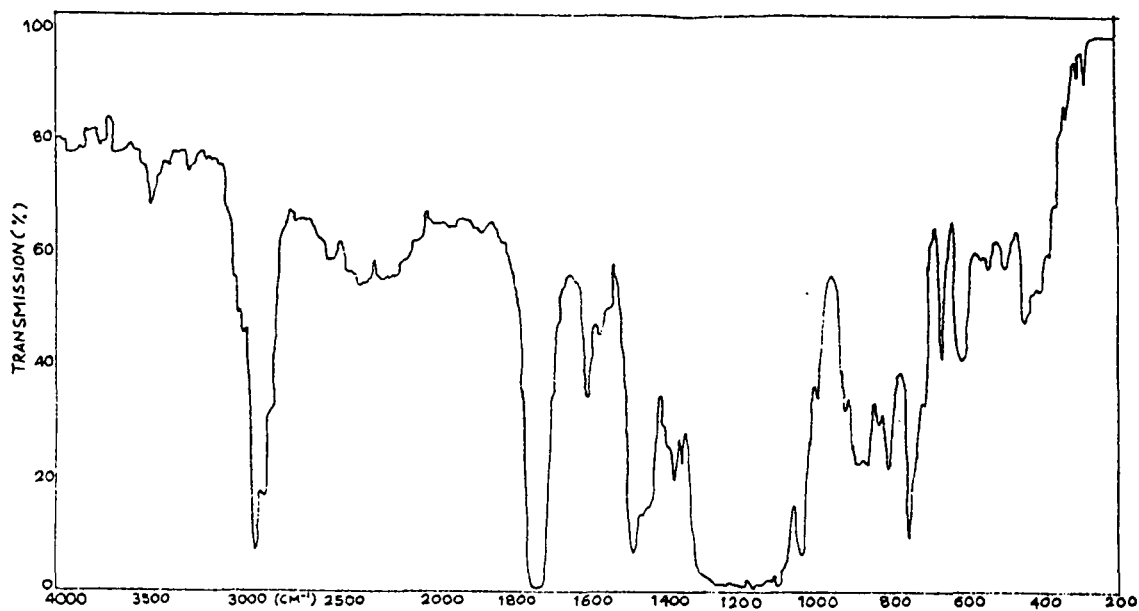


Figure 3.11 IR spectrum of PA2 polymer

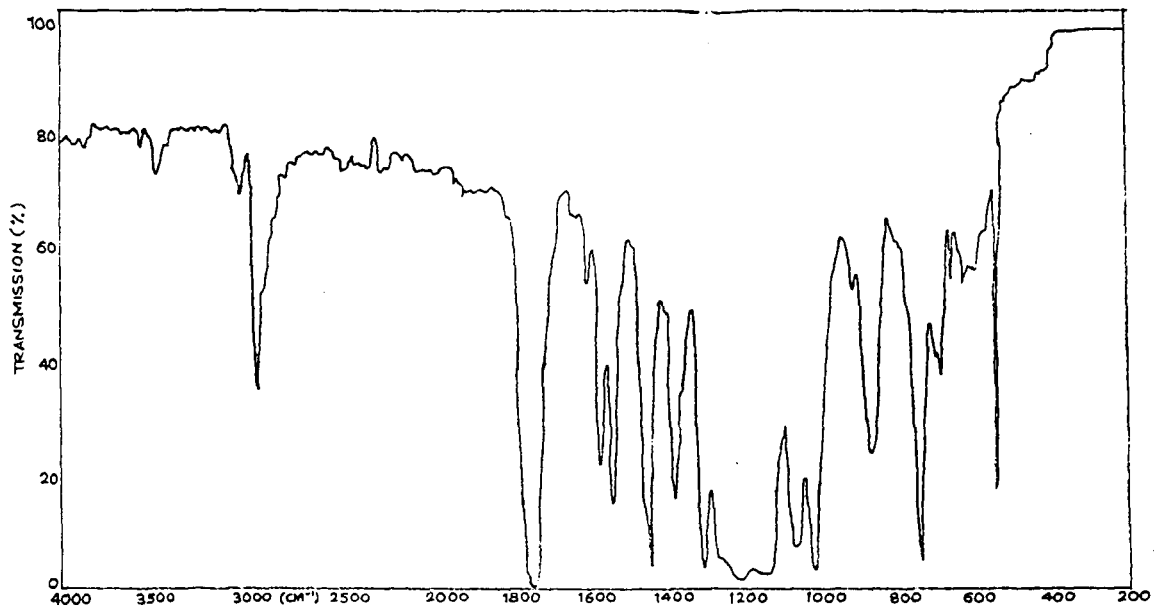


Figure 3.12 IR spectrum of PA3 polymer

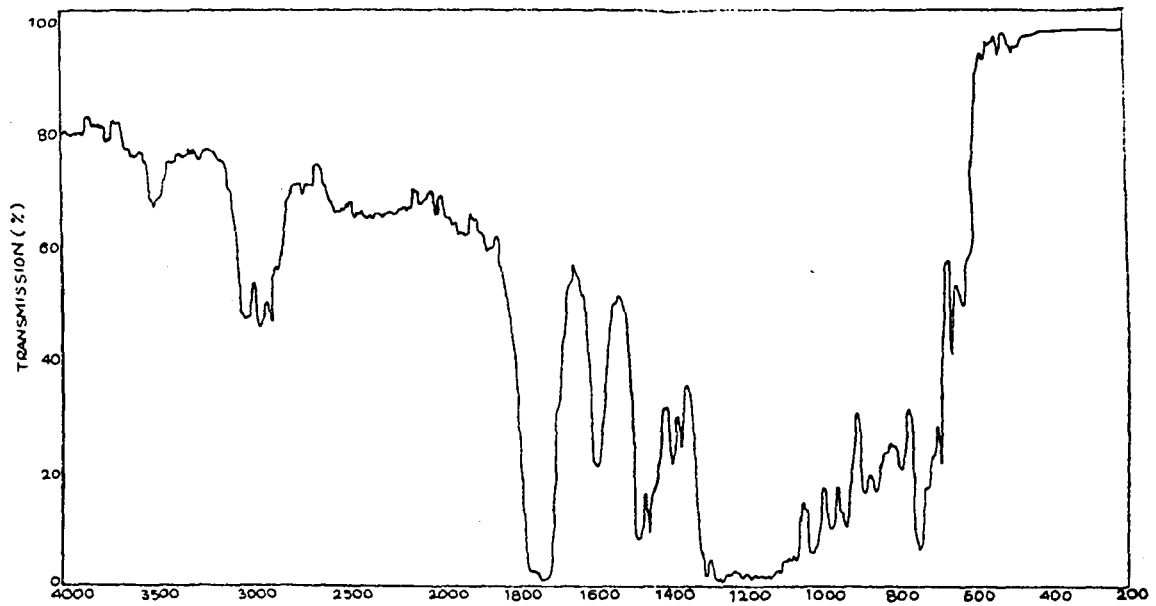


Figure 3.13 IR spectrum of PA4 polymer

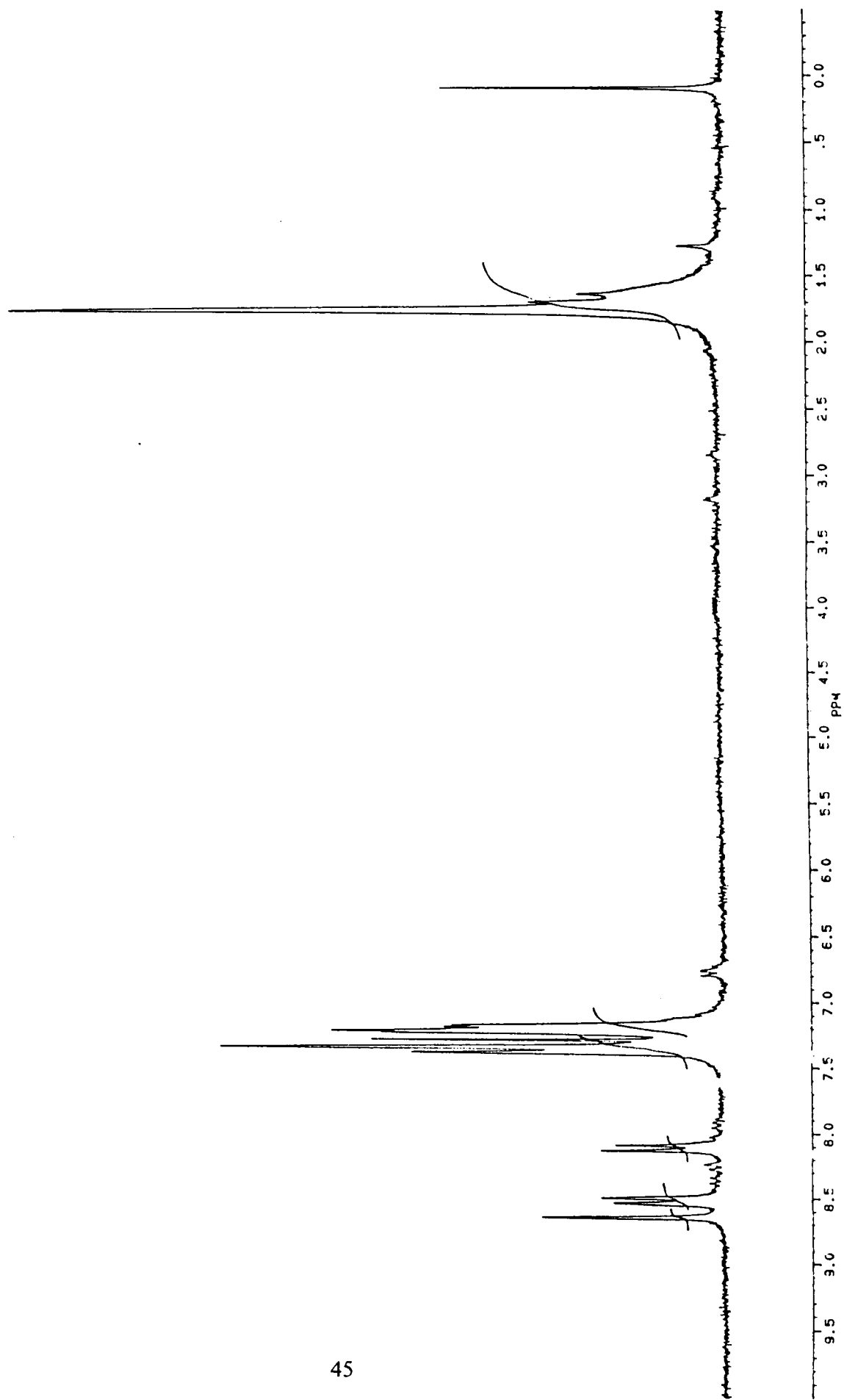


Figure 3.14 NMR spectrum of PA1 polymer

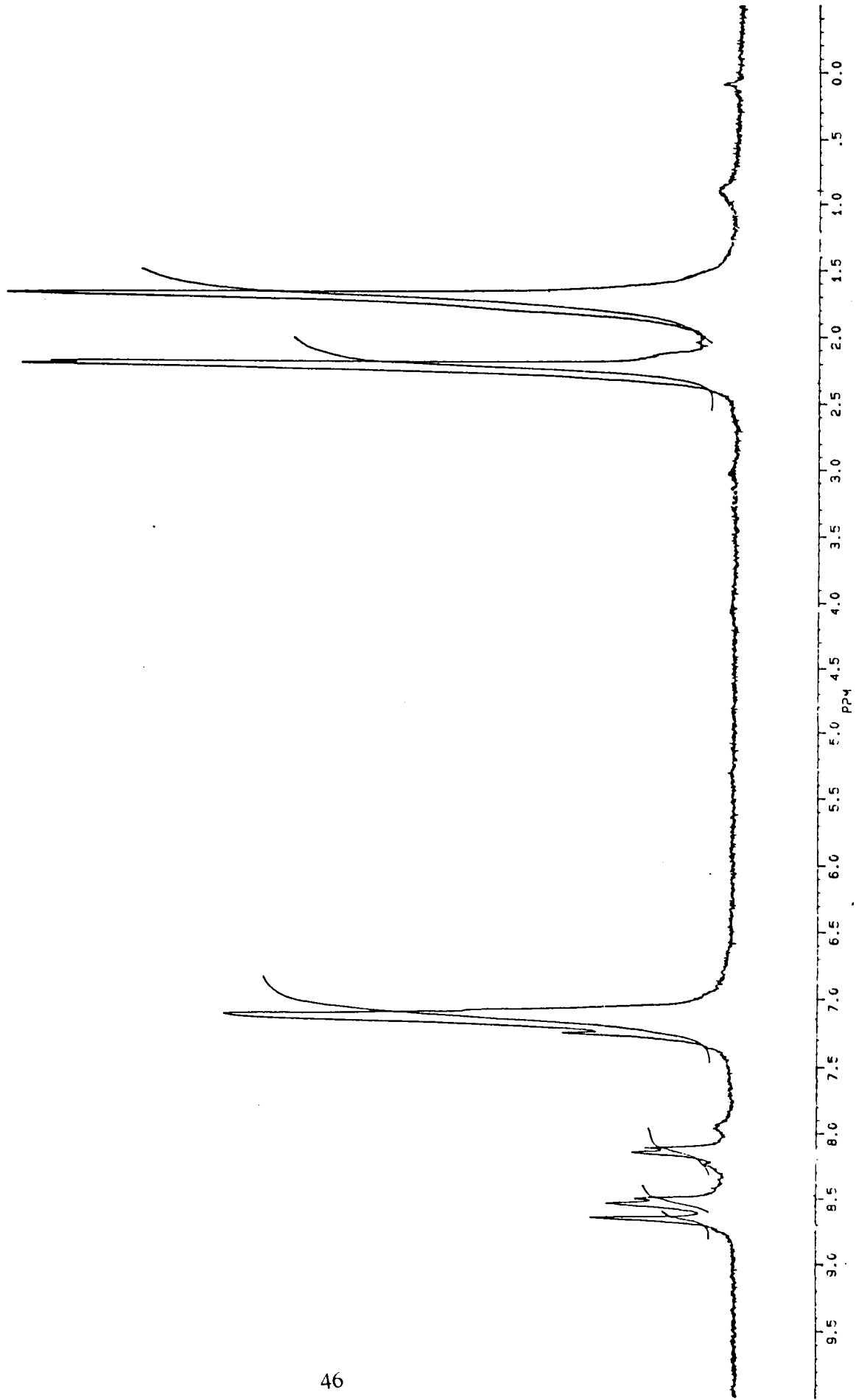


Figure 3.15 NMR spectrum of PA2 polymer

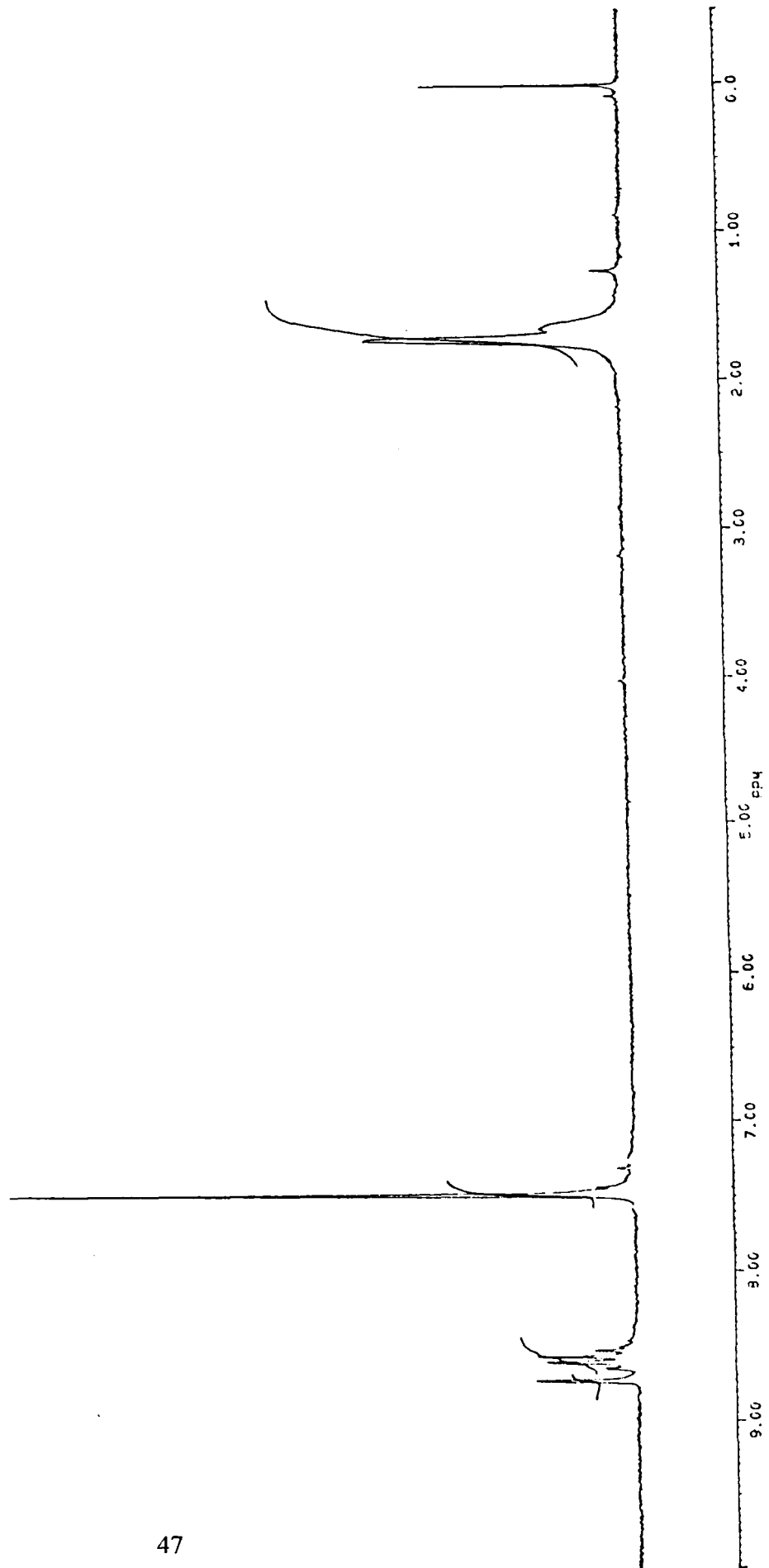


Figure 3.16 NMR spectrum of PA3 polymer

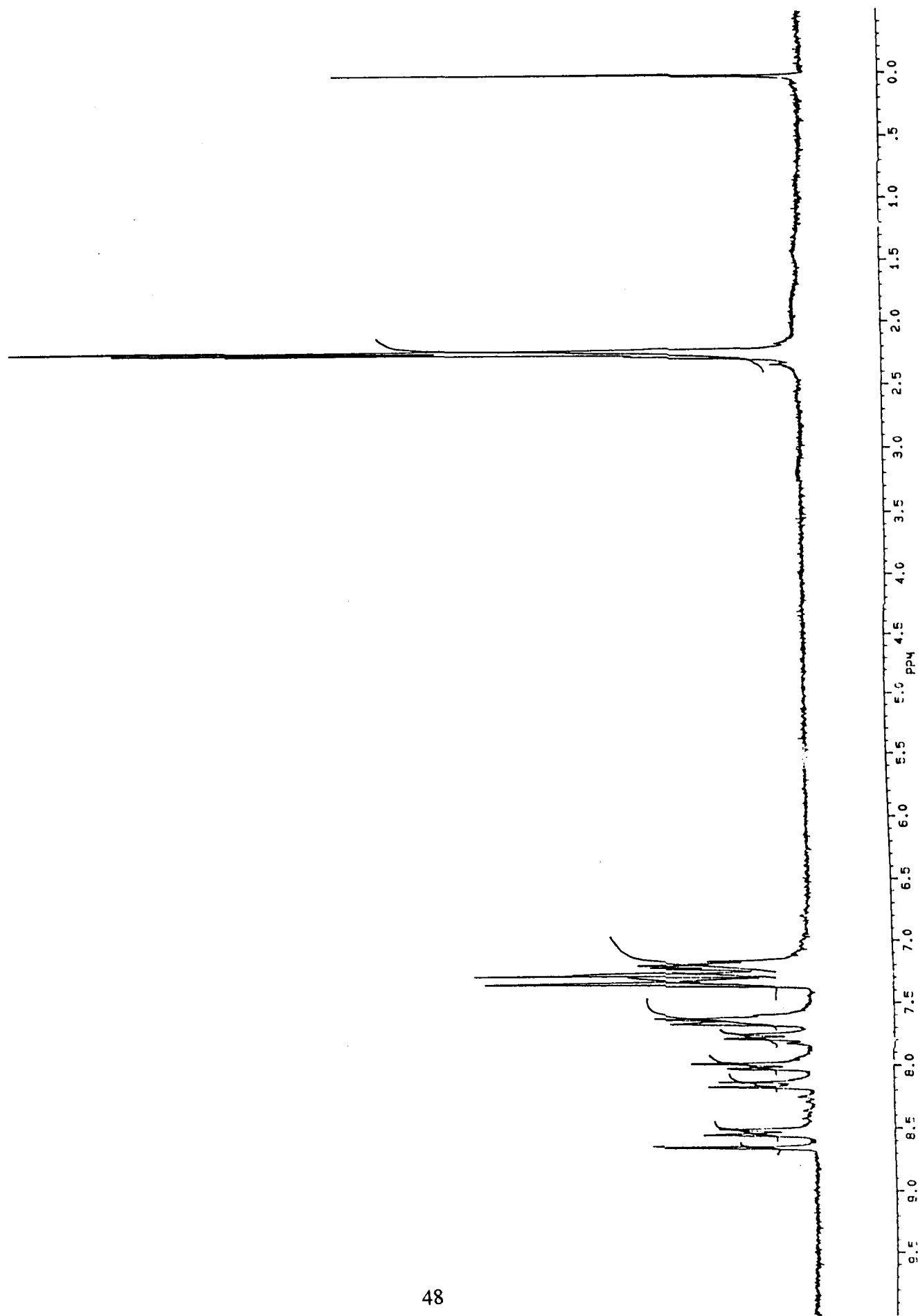


Figure 3.17 NMR spectrum of PA4 polymer

3.1.4 Polymer purification:

All polyarylates thus prepared were purified as follows: 1g polyarylate was dissolved in 12 ml of CHCl_3 , the solution was filtered through sintered glass disc and precipitated by adding it to the stirred methanol as a non-solvent. The precipitated polymer was collected on buchner funnel, dried at 60°C and finally in a vacuum oven at 60°C for 24 hrs to remove traces of solvent.

3.2 Permeation Studies

3.2.1 Casting of membrane

The membranes were prepared by solution casting. Polymer solutions of 2 -2.5% (w/v) concentration were prepared in chloroform (CHCl_3) and filtered through sintered glass discs. The solution was then poured in the petri-dish (having flat bottom surface) which was placed on mercury. Dry atmosphere was maintained using CaCl_2 . The solvent was evaporated at ambient temperature. The films were peeled off and kept in a vacuum oven at 60 - 65°C for 8 days and were stored in a desiccator before using for permeation studies. The thickness of the film thus obtained was 30 - $40\mu\text{m}$.

3.2.2 Gas permeation studies

3.2.2.1 Apparatus

A schematic representation of permeability apparatus is shown in Fig.3.18. The permeation cell diameter was 4.9 cm. All connecting tubes were SS-316 having O. D. of 1/8". The cell was housed in a thermostatic oven at $35 \pm 0.1^\circ\text{C}$. It was equipped with a Heise pressure gauge to measure upstream pressure. More details of the diffusion cell and its specifications are as described by Houde et.al (1991). Valve 1 and valve 2 were used to regulate the desired pressure.

On the permeate side of the diffusion cell, a calibrated borosilicate glass capillary (I.D.= 1.5728mm) containing a small mercury slug (~ 4mm in length) was placed. The displacement of the mercury slug was monitored by a cathetometer (least count = 0.005 mm). Permeate side was connected to the vacuum through valve-4.

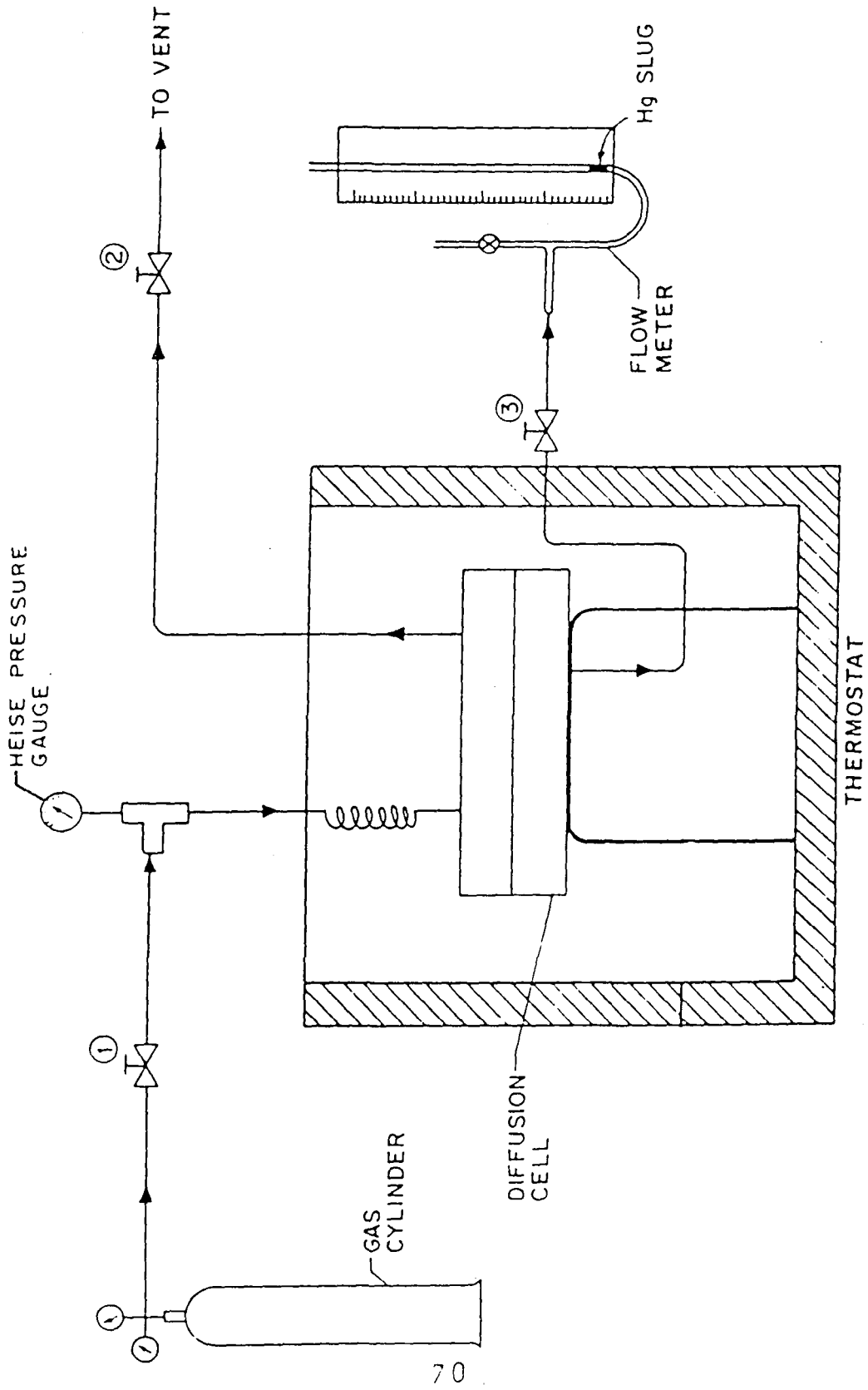


Figure 3.18 Schematic of permeability measurement apparatus.

3.2.2.2 Permeability measurements

1. At the beginning of the experiment, it was confirmed that there was no leakage on either side of the diffusion cell without any membrane mounted in the cell.

2. The membrane was mounted in the diffusion cell. All other valves were kept closed.

3. Through out the following steps, valve-4 was kept closed. The teflon stop-cock, fitted on flow meter X, was initially left open to the atmosphere. This prevented expulsion of the mercury slug from the flow meter in the case of membrane rupture.

4. Valves 1 and 2 were opened. Gas was purged 4-5 times through the upstream side of the membrane and in supply lines with the gas to be tested. This was done in order to eliminate traces of gas impurities.

5. Valve 2 was then closed and a pressure of (p_h) \sim 10 atm. was applied on the upstream side of the membrane with the help of the regulator and valve-1.

6. The teflon stop-cock X was closed slowly.

7. The position of the mercury slug in the capillary was noted at time $t = 0$ using the vertical cathetometer. The mercury slug displacement was a result of the permeating gas.

8. The mercury slug position on the cathetometer was noted after a finite time (t).

9. Several readings were repeated till a constant flow rate was attained. The total time of gas pressurization was between 2 to 24 hours depending on diffusivity of the gas. At least 10 observations were recorded at regular intervals. The rate of displacement of the mercury slug at pressure (p_l) [1 atm. in the present study] and the capillary cross-section area yielded the flow rate of the gas, N [cc (STP)/sec].

The permeability coefficient (P) was calculated using the equation:

$$P = N \cdot l / A \cdot (p_h - p_l)$$

A = effective film area in cm^2 ,

l = thickness of the polymer film in cm,

p_h = feed pressure in mm of Hg and

p_l = pressure at the permeate side in mm of Hg.

The permeation was repeated for 2-3 films and the permeabilities were averaged.

For all membranes, the permeation studies were carried out at 35°C. The upstream pressure was ~10 atm., while permeate side was kept at atmospheric pressure.

Helium (He), argon (Ar), nitrogen (N₂), oxygen (O₂), carbon dioxide (CO₂) and methane (CH₄) were used as received. The purity was >99.5%.

3.3 Polymer Characterization

3.3.1 Viscosity measurements

The intrinsic viscosity [η] of polymer solutions in 1,1,2,2-tetrachloroethane were determined at 35°C using an Oswald viscometer. The concentration of the polymer solution used was 0.1 g/dL. The viscosity [η] was calculated by one point method [Houde (1991)].

3.3.2 Density measurement

The density of polymer films was determined by floatation method at 40°C in aqueous potassium carbonate (K₂CO₃) / zinc chloride (ZnCl₂) solution.

3.3.3 Glass transition temperature, T_g

T_g was determined by differential scanning calorimetry (DSC) on Perkin-Elmer DSC-2C in the temperature range of 30°C to 400°C at a heating rate of 20°C/min.

3.3.4 Determination of d_{sp}

Wide angle X-ray diffraction (WAXD) measurements were carried out on a Phillips PW 1730 and Rigaku Dmax-III X-ray spectrophotometer. The samples cast as given in section 3.2.1 were used having size of 3.0 cm × 2.5 cm and thickness of ~30-35 microns. The measurements were carried out in the range of 4-50° (angle of diffraction, 2 θ) in reflection mode geometry with Cu-K α radiation (λ = 1.5418 Å). The average intersegmental distance, d_{sp} , was estimated from 2 θ value using Bragg's equation.

$$n\lambda = 2 \cdot d_{sp} \cdot \sin \theta_{max}$$

where $2\theta_{\max}$ corresponds to the maximum intensity peak position in the spectra, n is the order of reflection, λ is the wavelength of x-ray and θ is the maximum angle of diffraction [Charati et al (1991), Houde et al (1992)].

3.3.5 Thermogravimetric analysis (TGA)

Thermogravimetric analyses were carried out using Seiko Instruments SSC 5100 model coupled with TG/DTA 32. The analyses were carried out in nitrogen atmosphere. Sample was used either in powder or film form. Thermal study was carried out in temperature range of 30°C to 600°C with a heating rate of 20°C/min.

Chapter 4
Results and Discussion (Polyarylate)

4 Results and Discussion (Polyarylate)

4.1 Results

In this chapter characterization of polyarylates based on CF₃ substituted terephthalate and their permeation properties are discussed.

The physical and permeation properties of polyarylates based on trifluoromethylterephthalic acid (CF₃T) are given in Tables 4.1 and 4.2 respectively. These polyarylates are compared with the polyarylates based on various substituted bisphenols and unsubstituted terephthalic acid.

Table 4.1

Physical properties of CF₃-polyarylates compared with parent polymers.

Polymer	$[\eta]^i$ (dL/g)	d_{sp} (Å)	ρ^{ii} (g/cc)	v_f^{iii} (cc/cc)	T_g (°C)
Asymmetric – Disubstituted					
BisA–T (parent of PA1)	0.83	5.47	1.217	0.351	210
PA1 polymer	0.38	5.47	1.31	0.36	153
Symmetric – Tetrasubstituted					
DMbisA–T	1.28	5.57	1.167	0.355	187
PA2 polymer	0.36	5.54	1.28	0.34	152
Asymmetric – Disubstituted					
o-Cp–T	0.54	5.36	1.251	0.357	314
o-Cp–CF ₃ PA4 polymer	0.35	5.61	-----	----	220

- i. Single point viscosity using 0.1% polymer solution in Tetrachloroethane.
- ii. Density by floatation method at 40°C using aqueous K₂CO₃ or ZnCl₂ solution.
- iii. Fractional free volume calculated according to Sheu et al. (1988).

Table 4.2

Permeation properties of CF₃-polyarylates compared with parent polymers.

Polymer	He	Ar	N ₂	O ₂	CH ₄	CO ₂
Base case-						
BisA-T (parent of PA1)	14	0.84	0.37	1.88	0.4	8.0
PA1 polymer	16.8	0.87	0.38	1.8	0.36	7.4
Asymmetric – Disubstituted						
DMbisA-T (parent of PA2)	18	0.38	0.23	1.1	0.17	5.8
PA2 polymer	14.2	0.38	0.23	0.78	0.23	2.2
Symmetric – Tetrasubstituted						
TBrisA-(I+T) (parent of PA3)	15.3	0.59	0.26	1.6	0.17	5.4
PA3 polymer	24	0.98	0.46	2.1	0.31	7.6
Asymmetric – Disubstituted						
o-Cp-T (Parent of PA4)	13.3	0.4	0.15	1.0	0.18	5.1
PA4 polymer	13.4	0.3	0.19	0.9	0.11	2.9

4.1.1 Physical properties:

The inter-chain spacing (dsp) values estimated from amorphous peak maxima in the WAXD spectra using Bragg's equation. The dsp values are nearly same for PA1, PA2 and PA3. It increased marginally only in case of PA4 polymer. The estimated fractional free volume (using density measurements) is higher for PA1, whereas it is smaller for PA2 and PA3 as compared to the parent polymer based on unsubstituted acid. The glass transition temperature was lowered for all polyarylates with the -CF₃ substitution on the acid moiety [Tanaka et al (1992)]. Intrinsic viscosities are less for all CF₃ substituted polyarylates.

4.1.2 Permeation properties:

In the case of polyarylate PA1, permeabilities were similar to that of unsubstituted polyarylate. This is in accordance with similar dsp value of this polyarylate. A marginal increase in He permeability was noted. Such behavior of increase in gas permeability for smaller gas like He was also noted for DMbisA-T polyarylate [Kharul et al (1998)]. In case of PA2, permeabilities of He, O₂ and CO₂ were decreased, while permeabilities of Ar and N₂ are similar. The permeability of CH₄ found to increase by ~35%. For the polymer PA3, there was 30-80% increase in the permeability for different gases. For polymers PA2 and PA3, permeability data surprisingly showed that, as the size of gas molecule increased, tendency for permeation also increased. For PA4 polymer, He and O₂ permeabilities were similar; Ar, CO₂ and CH₄ permeabilities are decreased while N₂ permeability slightly increased. WAXD analysis of this polymer showed increase in dsp; but the permeability does not increase accordingly for all gases (spectra are shown in figures 4.1 and 4.2). Thermal stability of all -CF₃ group substituted polyarylates increased as given in Table 4.3 (figure 4.3).

4.2 Discussion

4.2.1 Physical properties:

CF₃ substitution in polyarylate is known to increase interchain spacing and fractional free volume of the resulting polymer as compared to the base polymer [Pixton and Paul (1995a)]. The dsp was also investigated and found dependent on the type of substitution on bisphenol. However, PA4 polymer WAXD indicated an increase of dsp. In the case of PA1, dsp remained unchanged. Decrease in T_g indicates increase in overall chain irregularity. Substitution by CF₃ group increases mass; but does not increase volume of the chain segment leading to increase in density. However

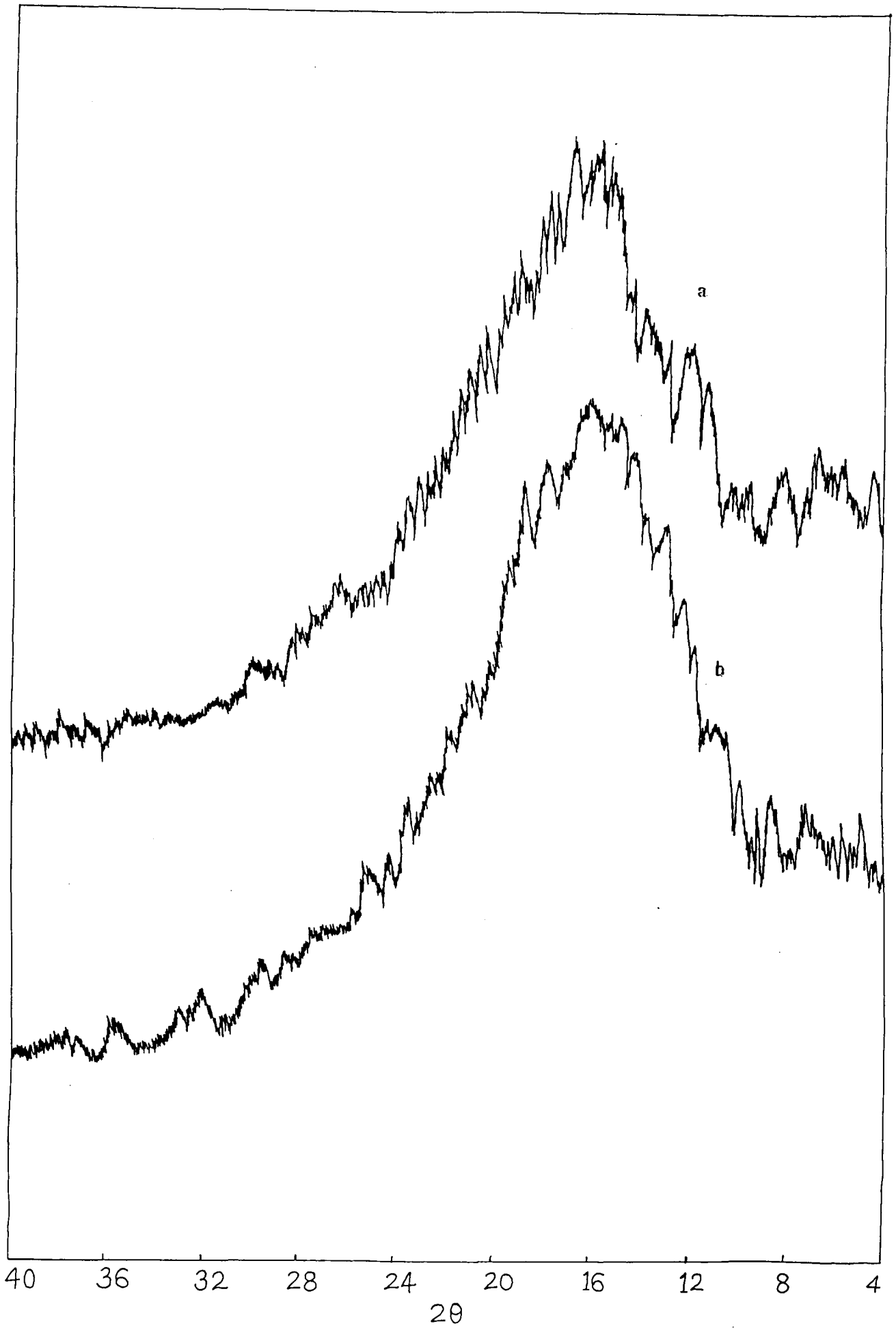


Figure 4.1 WAXD spectra of polyarylates, a) PA1, b) PA2

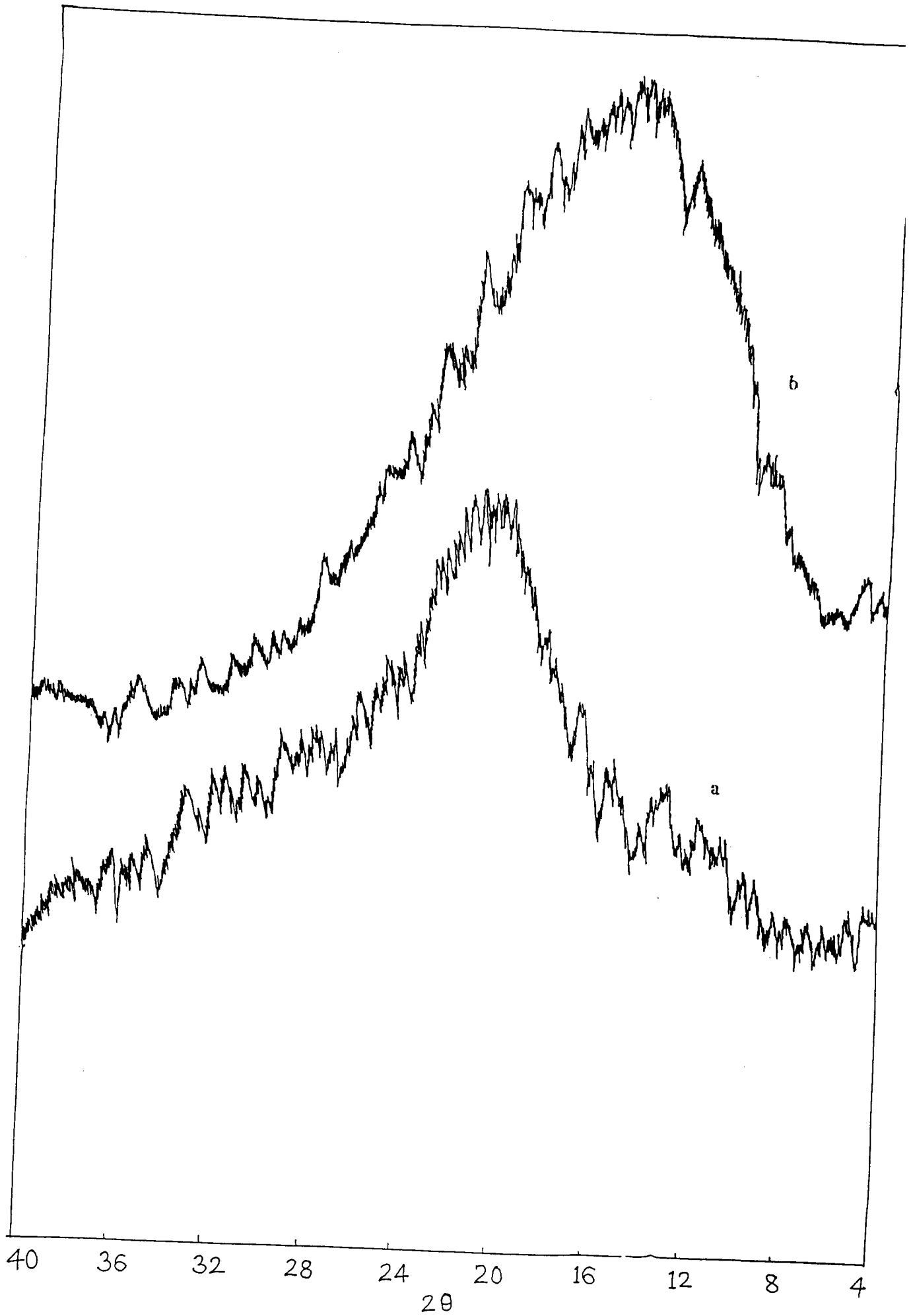


Figure 4.2 WAXD spectra of polyarylates, a) PA3, b) PA4

Table 4.3

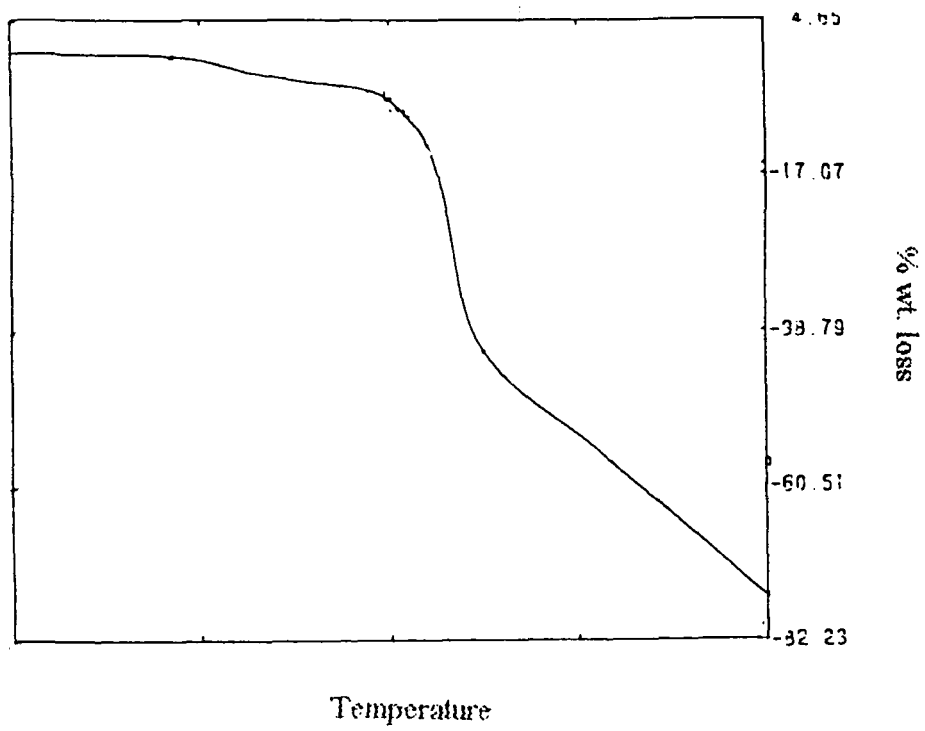
Thermal stability of $-CF_3$ group substituted polyarylates with respective parent polymers in nitrogen atmosphere.

Polymer	Parent of PA1 (BisA-T)	PA1	Parent of PA2 DMbisA-T	PA2	Parent of PA3 [TBrbis-A-(1+T)]	PA3	Parent of PA4 (o-Cp-T)	PA4
Temp.°C	% weight degradation or loss the polymer in nitrogen atmosphere is given.							
200°C	2.0	1.6	1.4	6.7	----	3.0	----	1.7
250°C	2.6	2.16	1.5	10.2	----	4.8	----	3.35
300°C	3.0	2.8	1.9	11.8	----	7.0	3.33	4.42
350°C	4.1	4.2	6.8	12.7	3.0	11.7	11.1	5.5
400°C	9.2	10.0	18.9	17.1	33.7	18.4	28.9	11.1
450°C	32.8	24.2	33.7	19.8	53.5	39.9	41.1	37.5
500°C	54.9	52.1	51.7	52.4	82.5	65.2	64.4	47.2
550°C	86.0	60.3	68.5	64.7	97.6	69.6	88.9	52.6
600°C	100.0	63.1	84.9	66.6	98.2	72.3	98.0	58.5
650°C	-----	64.7	94.0	67.8	98.8	73.0	99.0	64.7
700°C	-----	65.1	98.7	68.4	-----	73.4	-----	71.1

increase in free volume appears to be due to chain irregularity caused by CF_3 moiety and its packing. This structural changes cause increase in permeability for gas with small molecular volume. However, for inert gases like Ar, N_2 with large molecular volume there is marginal increase while for molecules with larger molecular volume for polar gas like O_2 and CO_2 and nonpolar gas like CH_4 , marginal decrease is observed. Overall permeability data of the gases studied indicate that relative increase in free volume is arising from large number of small gaps caused by fluoromethyl moieties and their packing pattern in amorphous state.

For PA2 dsp decreases marginally, density increased indicating better packing which was confirmed by decrease in free volume. Decrease in Tg indicates tendency to

TGA of PA4 polymer in nitrogen.



TGA of PA2 polymer in nitrogen.

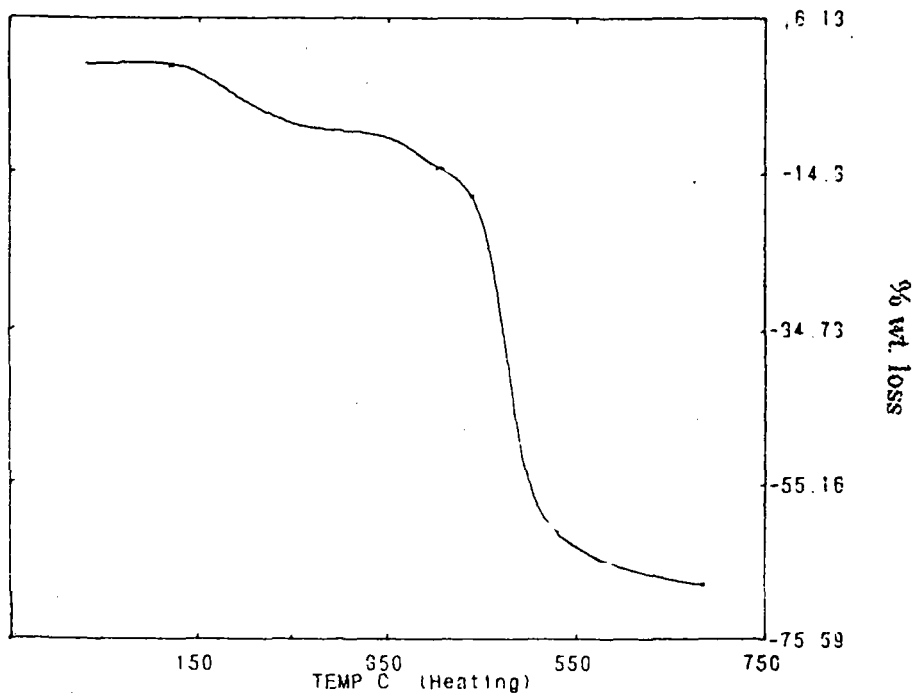


Figure 4.3 TGA of PA4 and PA2 polymers in nitrogen

form more amorphous regions as compared to the base polymer. Gas permeability decreased for very small gases like He and gases with large molecular volume like CO₂. Perhaps CH₄ shows plasticizing effect which showed increase in permeability.

For tetrabromo symmetrically substituted bisphenol-A polymer, PA3, ρ increased with increased density, while free volume decreased. Though these changes are marginal, increase in the permeabilities for all the gases is appreciable.

For PA4, change in T_g was drastic but corresponding change in permeability was marginal. Contribution of CF₃ moiety as compared to the bulky *o*-Cp moiety was marginal as reflected in permeability data.

Thermogravimetric data revealed that changes caused by CF₃ substitution had not affected overall thermal stability of the polymer but with these changes, it is possible to manipulate permeability / selectivity of the gases studied to certain extent. All the synthesised polymers are thermally stable upto 200°C.

Glass transition temperatures is lower than parent polymers in all these polyarylates. Similar behavior was reported by Houde et al [Houde et al (1995), Percec et al (1987)]. This behavior is attributed to the irregularities of the chain structure caused due to CF₃ moiety substitution and disturbance of the packing pattern, which may be responsible for tendency of the polymers to form amorphous regions. For all the polymers synthesized it was possible to cast film/ membranes indicating the DP of the polymers synthesized was sufficient. However the decrease or increase of the intrinsic viscosity was not a major aspect for film/ membrane formation and permeation studies.

4.2.2 Permeation properties

It is reported in the literature that CF₃ substitution on polymer backbone lead to increase in permeability. Such a substitution also generally decreases or maintains the selectivity. In the present investigation, except for the polymer PA3, permeability did not considerably increase. A marginal decrease in selectivity was seen in all the

cases, except for few cases where increased He based selectivity was noted, this may be because of slightly increased diffusivity of inert He gas. (Refer to Tables 4.2 and 4.4).

Table 4.4

Permselectivity (α) of various polyarylates with CF₃ group substitution.

Polymer	He/Ar	He/N ₂	He/CH ₄	Ar/N ₂	O ₂ /N ₂	CO ₂ /N ₂	CO ₂ /CH ₄	N ₂ /CH ₄
Base case-								
BisA+T (parent of PA1)	17.0	38	35	2.25	5.1	22	20	0.93
PA1 polymer	19.3	44	47	2.29	4.7	19.5	20.6	1.0
Asymmetric – Disubstituted								
DMbisA+T (parent of PA2)	47	78	106	1.65	4.9	25	34	1.35
PA2 polymer	36	62	62	1.74	3.4	8.7	8.7	1.0
Symmetric - Tetrasubstituted								
TBrisA+T (parent of PA3)	26	59	90	2.27	6.2	21	32	1.53
PA3 polymer	24	52	77	2.1	4.6	16	24	1.48
Asymmetric – Disubstituted								
o-Cp+T (parent of PA4)	30	89	74	2.9	6.9	34	29	0.82
PA4 polymer	42	71	122	1.7	4.9	15	26	1.72

The polyarylate-PA1 showed marginal increase in He permeability while it remained similar for other gases. As a result, a marginal increase in He based selectivity was observed. The selectivity for other gas pairs were marginally affected. On the other hand, for PA3, 30 to 80% increase in permeability was seen, which could be attributed to the combined effect of tetrasubstitution on the bisphenol and substitution at acid moiety. The increased polarity of this polymer because of the presence of halogen atoms on bisphenol as well as acid moiety effectively may lead to

increase in permeability because of repulsive interaction. A decrease in selectivity for this polyarylate was observed. For PA2 and PA4, the decrease in permeability, (except for P(CH₄) in PA2 and for P(N₂) in PA4) is noted. There is overall decrease in selectivity except for He based selectivity in PA4. Both these polymers have been synthesized using asymmetrically substituted bisphenols. The decrease in permeability and increase in selectivity is known for asymmetric bisphenol substitution type [Kharul et al (1998)]. The reason for lower permeability could be due to the reduction in fractional free volume available for penetrant molecule. The increased permeability for CH₄ in PA2 and for N₂ in PA4 could be an artifact. As against the established trend for polymeric membranes, the lowering of permeability was not associated with an increase in selectivity for the present series of polyarylates. This could be attributed to the CF₃ substituent present on the acid moiety. It is postulated that the CF₃ interacts with the adjacent ester linkage at ortho position and align itself in such a conformation that additional bulk of CF₃ gets accommodated in the bulk of the polymer matrix.

4.3 Effect of CF₃ substitution in combination with the bisphenol substitution

It is seen from the permeability data that for PA1, PA2 and PA4, the permeability was marginally affected. While for PA3, an increase in the permeability for all gases was noted. The selectivity data showed that He based selectivities for PA1 and PA4 were increased, while selectivity for other gas pairs were decreased. This could be because of diffusional gas transport, He was less affected in comparison to other gases. PA2 and PA4 are derived from asymmetrically substituted bisphenols. Polymers based on such bisphenols are known to increase selectivity considerably with some variations in permeability [Kharul et al (1998)]. (In the case of present polyarylates, both permeability and selectivity for PA2 and PA4 are generally reduced, i.e. asymmetric substitution on bisphenol and CF₃ substitution on acid had an adverse

effect on the permeation properties of resulting polyarylate.) For PA3, selectivity for all gas pairs was only slightly reduced (upto 25%). An increase in overall permeability and only marginal reduction in selectivity for this polymer shows that its different behavior than other polymers. This could be related to the polar nature of substituents on acid as well as bisphenol moieties. The bromine substitution on bisphenol and CF_3 substitution on acid may offer optimum polar effects in combination to their bulky nature. This indicates that in case of polyarylates, structural modifications which would impart optimum polarity with bulky substituents may offer attractive permeation properties of the resulting polyarylate.

4.4 Conclusions

The $-\text{CF}_3$ group at bridge carbon of bisphenol-A is known to increase d-spacing, and increase gas permeability of the polymer. It was also expected that substituent on acid moiety should show similar change. This was noted for polyarylate (PA1- 4) polymers.

For all synthesized polyarylates, molecular weights were low. Glass transition temperatures of all polyarylates were low than the parent. This suggested that $-\text{CF}_3$ group substitution decreased interchain cohesive force of the polymers.

Interchain d-spacing values increased as expected for two polymers, PA3 and PA4, while it remained constant for PA1 and marginally decreased for PA2 polymers compared to the respective parent polymer. This increase in d-spacing values is probably because of repulsive force between the polar $-\text{Br}$ and $-\text{CF}_3$ groups.

Fractional free volume of these polymers was not affected drastically by $-\text{CF}_3$ group, but marginal change was observed. Thermal stability of these polymers was observed to increase after $-\text{CF}_3$ group substitution.

The permeability of PA1 polymer increased marginally for He gas only, and decreased for He and CO_2 in PA2 polymer, which showed good agreement with

change in respective FFV. The permeability of PA3 polymer increased for all gases, which was not expected as FFV decreased marginally. This increased permeability might be because of increased solubility of gases in the polymer. For PA4 polymer, d-spacing value was high, but the permeability values showed opposite trend, i.e. permeabilities were either same or decreased for CH₄ and CO₂ gases (as solubility decreased).

All polyarylates showed good performance for He gas selectivity. In case of PA1 polymers, He gas selectivity marginally increased over N₂, Ar, and CH₄ gases, while rest of the gas pairs were showing similar selectivity values. For PA2 polymer He gas selectivity was dropped.

In case of PA3 polymer, permeability values for all gases were doubled with marginal decrease in selectivity. In the case of PA4 polymer, He gas permeability values was nearly same, but selectivity value reached to maximum value among all PA1 to PA4 polymers. The PA4 polymer was efficient in discriminate the gas molecules on their molecular level with good permeability value.

Overall, PA3 and PA4 polymers can be used as helium gas selective membranes.

Chapter 5

Additive dispersed polymer systems (Literature Survey)

5 Additive dispersed polymer system

Generally polymer systems could be tailored for required application by dispersing / mixing additives in polymer to obtain the optimum properties. The prior literature on low molecular weight additive dispersed systems is discussed in this chapter with specific reference to gas transport properties. Various types of low molecular weight additives used are briefly overviewed.

An additive is a compound which may be either miscible or immiscible with the polymer. If it is miscible, then it may act as a plasticizer, antiplasticizer or filler (diluent), depending upon the nature of additive and the polymer (i.e. homogeneous system). If the additive is immiscible, then additive forms discrete domains (i.e. heterogeneous system), which may be either dispersed uniformly through out the polymer matrix or aggregated in the polymer matrix. The morphology of the dispersed polymeric systems depends upon the nature of the additives and that of the polymer and also upon the method used for the preparation.

5.1 Role / Action of additive in dispersed polymer system

The properties of miscible blend systems are dependent on interactions between the polymer and the dispersed additive, (which is dissolved at molecular level with the polymer). The additive may act as a (i) plasticizer, (ii) antiplasticizer, (iii) filler (or diluent) in the polymer matrix. These phenomena are discussed below.

5.1.1 Plasticization

The material which improves flexibility, extensibility and processibility of a polymer is known as plasticizer [Billmeyer, (1984)]. A plasticizer weakens the intermolecular force of attraction between the polymer chains and thus imparts more freedom of movement to the polymer chains. A plasticizer molecule increases the local free volume or the intersegmental chain spacing (dsp) in its vicinity, resulting in decrease in rigidity, strength and chemical resistance of polymer. This increased free volume is responsible for enhancement of permeability through the polymer membrane.

N. Kinjo [Kinjo and Nakagawa (1973)] studied the effect of various plasticizers in PVC by dynamic mechanical moduli. The α -dispersion region (glass transition) lowers on

addition of the plasticizers. It was shown by taking 4 different plasticizers that the extent of plasticization of different polymers will vary with each plasticizer.

It is also known that vapours or liquids sorbed at sufficiently high levels cause significant changes in the polymer state and its behavior. The sorbed vapour tend to swell or plasticize the polymer. Plasticizing species are usually organic vapours or liquids; however, some gases, especially CO₂ which have significant solubility in polymer also show plasticizing effect. Gas solubility is expressed in terms of penetrant pressure (concentration) in plasticized polymer as given by equation below.

$$\ln(p/p^{\circ}) = \ln\phi + (1-\phi) + \chi(1-\phi)^2 \text{ -----(5.1)}$$

p is the penetrant pressure, p^o is the vapour pressure of the penetrant, φ is the volume fraction of the solute and χ is the Flory-Huggins parameter.

For example, exposure of glassy polycarbonate to high pressure CO₂, alters the sorption equilibrium and permeation of CO₂ [Wonder et al (1979)] by plasticization effect. CO₂ gas dilates or separates apart the polymer chains, but upon removal of CO₂ pressure, the glassy polymer does not immediately regain its original volume. This volume expansion gives rise to an increased capacity for the glassy polymer to sorb CO₂ by the Langmuir mechanism.

Wide angle X-ray diffraction (WAXD) is used to investigate the effect of plasticizer in various glassy polymers [Charati et al (1991), Kim et al (1988)]. The change was observed in the polymer films by WAXD in dsp (inter-chain spacing) before and after exposure to gaseous pressure. Polycarbonate and polysulfone show small change in dsp as compared to cellulose acetate [Houde et al (1992)]. This change in dsp can be correlated with the T_g of the polymer prior to plasticization and also with the penetrant solubility in the polymer [Houde et al (1992)].

The effect of plasticization is also observed on diffusion and permeability coefficients. The diffusivity coefficient is given as

$$D = D_0 \exp (\beta' c) \text{ -----(5.2)}$$

where D₀ is the diffusion coefficient (without plasticization) and β' is an empirical parameter, which measures the extent of plasticization by penetrant.

5.1.2 Antiplasticization

The addition of certain types of additives to polymers [Jackson and Caldwell (1967)], like polycarbonate and polyesters result in opposite effects to those seen with plasticizers. The stiffness, hardness and tensile strength of the polymers are increased by antiplasticizers, and the elongation, impact strength, and heat-distortion temperature are decreased.

Antiplasticizers [Jackson and Caldwell (1967)] are typical compounds which are compatible with the polymer which (i) contain polar atoms such as halogen, nitrogen, oxygen or sulfur, (ii) contain at least two nonbridged rings, (iii) have one dimension shorter than about 5.5 Å along at least 65% of the molecule length.

Antiplasticizable polymers are those which have rigid and polar groups, (e.g. bisphenol polyester, polycarbonates, cellulose triacetate). These polymers can be antiplasticized by additives. Polystyrene has stiff chains but no polar groups, and hence cannot be antiplasticized [Jackson and Caldwell (1967)]. Polymers with flexible chains apparently cannot be antiplasticized. In fact, some compounds which are antiplasticizers for stiff polymers are plasticizers for certain flexible polymers. Aroclors and abietic acid esters can plasticize various flexible polymers [Buttrey (1960), Jackson and Caldwell (1967)]. Rigidity and polarity are required in both components, polymer and additive in order to result in antiplasticization.

Jackson, Jr. W. J. (1965) proved the presence of the interaction between the polymer and antiplasticizer by different thermal analysis curves of polycarbonate films containing Aroclors. The DSC curves showed broad endothermic peaks indicating the presence of attractive forces which were broken by thermal energy. These forces were due to interaction between the polar groups of the polymer and the antiplasticizer.

Density measurements [Jackson and Caldwell (1965)] of the polycarbonate films indicated that the densities were significantly higher than those obtained by simple addition of the volume of polymer and Aroclor.

The effect of low molecular weight additives on polymer interchain cohesion was studied by Coran and Anagnostopoulos (1962). The Flory-Huggins interaction parameter χ was determined from the heat of mixing parameter B for the polymer-diluent system. The energy of mixing parameter B was a negative value. As B increases, the stronger interaction between the diluent and polymer is seen.

Anagnostopouls (1962) suggested that the high negative free energy of mixing for tricresyl phosphate (TCP) and polyvinyl chloride (PVC) arises because the cross-interaction energies being greater than the self-interaction energies of the two components. Additives such as TCP are reported to increase the interchain potential in PVC so that more energy is required for a given chain separation. The increased cohesion results in increased activation energy of diffusion, decreased frequencies for gaseous diffusion, and diffusion coefficients.

Maeda and Paul (1987a), (1987d) have found that the addition of 4,4'-dichlorodiphenyl sulfone or tricresyl phosphate to glassy polymers such as polysulfone and poly(phenylene oxide) causes a mechanical antiplasticization, i.e., increased stiffness or strength of the polymers. This antiplasticization also reduces the gas permeability of the polymers. In some cases, this is accompanied by an increased selectivity. This effect is most prominent for gas pairs which significantly differ in molecular size; however, in some cases, selectivity may be lost.

5.1.3 Filler

The term “filler” is usually applied to solid additives incorporated into polymer matrix to modify its physical properties and to reduce the cost of the product. Fillers are divided into two types namely, Reinforcing type and extenders. Reinforcing fillers mainly improve mechanical properties like tensile strength, hardness and toughness, while extender is basically used to reduce the cost of product and to improve properties like hardness, reduce shrinkage, and decrease glass transition temperature. Filler may act to some extent like a plasticizer or an antiplasticizer [Plastics Materials (1989), Engineered Material Handbook, vol. 1, (1989)].

Fillers can be organic, like aramid fibers, carbon fibers, organic compounds and inorganic materials, like metal powders, glass, and minerals etc [Engineered Material Handbook, vol. 1, (1989)]. The filler compounded materials may be transparent or opaque, depending on their refractive indices. When refractive indices of both, filler and polymer are in same range, then it is transparent, and improves coloring effect and gloss (e.g. organic dyes), whereas if indices are in different range, then material is opaque (e.g. pigments).

Fillers are classified in different ways, according to their uses, particle size and shape, composition, density.

Particle size and shape is important from polymer processing point of view, particles in the matrix must be able to roll, slip or tumble past each other. Any nonspherical shape will result in greater viscosity or processing difficulty. Aspect ratios [ratio of length to diameter (thickness) of particle] of particles signifies its resistance to movement and its available bonding area. The flatter the particle for a given mass (i.e. the higher aspect ratio), the larger in available bonding area [Engineered materials handbook, vol. 2, (1989)].

5.2 Theory of permeation in dispersed polymer system

Barrer first proposed diffusion theory in blend system, which consists of a dispersed phase, represented by a lattice of identical rectangular parallelepipeds, embedded in a continuous phase [Barrer (1968)]. Depending on the parallelepiped dimensions, the dispersed molecules / particles may take the form of plates, rods, or fibers, which may be parallel or normal to the direction of flow, or they may even join to create laminated media of type ABAB. The overall flux, J , is related to the overall concentration drop ΔC_B in the continuous phase given by the following equation:

$$J = (a + b)^2 D \Delta C_B / l \quad \text{-----} \quad (5.3)$$

where D is a mean overall diffusion coefficient, $(a + b)$ is the thickness of the tube which surrounds the parallelepipeds, l is the composite thickness and a is the thickness of the parallelepipeds. The total flux is proportional to the sum of the size of the dispersed and continuous phases in the polymeric blend and to the mean overall diffusion coefficient. D can be expressed in terms of the diffusivity of each phase and various geometric parameters as:

$$D = h / (a + b)^2 \{ [a^2 \beta_A k D_A / h_A + (\beta_A h_B k D_A / \beta_B \gamma D_B)] + [b(2a + b) \beta'_A D_B / h_A + (\beta'_A h_B / \beta'_B \gamma')] \} \quad \text{-----} \quad (5.4)$$

If the dispersed phase is impermeable and the thin impermeable plates are oriented normally to the direction of the flow, the equation can be written as:

$$D = [b(2a + b) D_B / (a + b)^2] \gamma' \beta'_B \quad \text{-----} \quad (5.5)$$

Gas diffusion theory combines the molecular models of DiBenedetto (1963) and Brandt (1959). It proposed that the penetrant molecule has to move through the polymer matrix in two distinct ways [Pace and Datyner (1979)]: [1] sliding longitudinally along interchain channels or regions of low local density formed in the disordered glass (DiBenedetto model), or [2] jumping at right angles to the polymer chains whenever adjacent chains are sufficiently separated (Brandt model). The sliding model requires a smaller activation energy than the second, jumping model. Thus, the second process is the rate determining step in diffusion and the activation energy for diffusion is the activation energy for the chain separation.

Gas transport measurements for PVC films containing additives (like TCP (tricresyl phosphate) were carried out by M. D. Sefcik et al (1983), for H₂ and CO gases. The additive TCP is acting as an antiplasticizer upto 15 wt.% loading showing reduction in the gas permeability coefficient and above that it acts as a plasticizer showing enhancement in the gas permeability coefficient. Here M. D. Sefcik quoted the apparent diffusivity coefficient D_a as given by Barrer's method [Barrer (1951)] (which is not the value of the true diffusion coefficients).

$$D_a = l^2/6\theta \text{ -----(5.6)}$$

where *l* is the membrane thickness and *θ* is the time lag.

The apparent diffusion coefficients of both gases show the same dependence on additive concentrations as do the permeability coefficients. The author used the apparent diffusion coefficients only to show the relative change in the diffusivity of gas on addition of TCP into PVC polymer.

These effects can not be explained even qualitatively by the extent of volume contraction on mixing for these mixtures. However, a simple free volume treatment provides an excellent correlation of these effects [Maeda and Paul (1987c)]. Free volume was computed from measured specific volume and an estimate of the specific volume at the absolute zero temperature of the material from a group contribution method.

Specific free volume V_F can be given as,

$$V_F = V - V_o \text{ -----(5.7)}$$

where *V* is the experimentally observed specific volume and *V_o* is the estimated specific volume at the absolute zero of temperature. Lee (1980) has suggested relation between *V_o* the

specific volume and V_w the van der Waals specific volume of polymer from group contributions as suggested by Bondi (1968).

$$V_o = 1.3 V_w, \text{ -----(5.8)}$$

Permeabilities for various polymers for a given gas is given by,

$$P = A e^{-B/(V-V_o)}, \text{ -----(5.9)}$$

where A and B are constants for each gas. This approach implies that the solubility portion of the permeability coefficient does not vary much from polymer to polymer. V_o is an additive function of the polymer and diluent mixture, can be written as,

$$V_o = (V_o)_d w + (V_o)_p (1 - w), \text{ -----(5.10)}$$

where subscript d and p refer to diluent and polymer, respectively, and w is the weight fraction of diluent in the mixture. Since the excess specific volume, ΔV_e is

$$\Delta V_e = V - [V_d w + V_p (1 - w)], \text{ -----(5.11)}$$

thereby, the free volume of the mixture is,

$$V_F = V - V_o = [(V - V_o)_d w + (V - V_o)_p (1 - w)] + \Delta V_e \text{ -----(5.12)}$$

An average effective diffusion coefficient, D, can be written as,

$$D = P \cdot p_2 / c, \text{ -----(5.13)}$$

$p_2 = 10$ atm. pressure driven by the gas (penetrant), c is the amount of gas sorbed by the polymer at 10 atm., P is the permeability of the gas.

Ruoh-Chyu Ruaan (1997) presented dual sorption theory for apparent effect of additive [such as Co(salPr)] addition on the gas transport behavior which cannot be simply explained by the traditional solution-diffusion type of mechanism. The gas sorption was measured and modeled by the dual sorption model which comprised both Langmuir's and Henry's modes of sorption. The overall gas sorption (c) can be described as,

$$c = k_D p + C'_H b p / (1 + b p), \text{ -----(5.14)}$$

where k_D is the Henry's law of dissolution constant, and C'_H and b are the maximum sorption capacity and equilibrium constant, respectively, in Langmuir isotherm.

The solubility S can be described as,

$$S = S_H + S_L = k_D + [C'_H b / (1 + b p)], \text{ -----(5.15)}$$

where S_L is solubility caused by Langmuir sorption and S_H denotes the Henry's mode solubility. The gas permeation through the membrane is determined by both the sorption-

diffusion and the pore diffusion transports [Rangarajan et al (1984)]. Gas permeability (P_m) can be expressed as,

$$P_m = D_L S'_L + D_H S'_H + D_P \text{ -----(5.16)}$$

where D_L represents the diffusivity through Langmuir adsorption layer, D_H is the diffusivity through Henry's sorption mode and D_P is the diffusivity of pore diffusion that relates the part of gas transport independent of gas-polymer interaction. S'_L and S'_H represents Langmuir's and Henry's solubilities at the upstream pressure.

The effective diffusivity of a gas across glassy polymer membrane can be expressed as,

$$D_{eff} = P_m / S = D_L(1 - X'_H) + D_H X'_H + (D_P/S') \text{ -----(5.17)}$$

Where X'_H denotes the fraction of Henry's sorption S'_H / S' .

Shih-Hsiung Chen (1997) has added various amounts of cobalt(III)acetylacetonato, $[Co(acac)_3]$ to polycarbonate (PC) membrane to enhance oxygen enrichment ability. The gas permeability was calculated for homogeneous $Co(acac)_3/PC$ membrane as given by the equation 2.2 in the section 2.1.

There is another theory based on the frozen free volume or microvoids of glassy polymers, for which dual mode of sorption is applied. This is based on Henry's law and Langmuir sorption for condensable gases. This was presented in section 2.3.1(in Polyarylate).

5.3 Mechanism of Transport in Dispersed Polymeric System

The dispersed additive in the polymer matrix may be permeable or impermeable.

5.3.1 Permeation through polymer matrix having impermeable additives

The theory of permeation with dispersed impermeable flakes has been studied by Cussler et al (1988), (1990), (1996). This theory predicts the effect of the flakes on permeability by its volume fraction, the aspect ratio and orientation. The permeability of a composite containing impermeable flakes is given as

$$1/p = J_o/J_n = 1 + \alpha/\sigma\phi + \alpha^2\phi^2/(1-\phi) \text{ -----(5.18)}$$

where α is the flake aspect ratio, σ is the pore aspect ratio, ϕ is the volume fraction of flakes, J_o is the flux of a film without addition of flakes, and J_n is the flux of the composite with n number of flakes. Here the diffusion flux varies with flake loading in two ways. First, if diffusion

through the gaps between the flakes is the rate controlling step, then (J_o/J_n) varies with ϕ . Second, if wiggles (resistance due to tortuous diffusion path because of the impermeable phase) through the flakes are paramount in determining transport resistance, then (J_o/J_n) is proportional to $\phi^2/(1-\phi)$.

The diffusion data for oxygen, water or CO₂ permeation through films of polycarbonate, polyester containing mica or polyamide flakes was studied by Cussler et al. It shows that the diffusion through the tortuous path (wiggles) was controlling factor for solute permeation or transport in dispersed system.

The theory was not consistent in predicting the effect of flake aspect ratio on the reduction in permeability. When diffusion around a single flake was considered, each point on the edge of the flake represents a possible pathway for diffusion. These pathways are in parallel, and the shortest path will be preferred.

The theory assumes that all particles are aligned with the largest dimensions perpendicular to the flow direction. Eitzman et al (1996) extended the theory to impermeable flakes tipped at an angle within the flat polymer film. The authors considered silicone-polycarbonate membranes with mica flakes, wherein the flakes may be arranged in three different patterns viz. the flakes a) are regularly spaced and perpendicular to the direction of the diffusion, b) are randomly oriented, c) are all at a fixed angle not perpendicular to the diffusion direction. In the first case, when the impermeable flakes are perpendicular to the direction of the diffusion, the permeability of the composite depends strongly on the microstructure of the flakes, and on the location of the slit between adjacent flakes. When the slits are oriented on top of each other, diffusion takes place quickly across the flake-filled film. When the flakes are oriented parallel to the direction of the diffusion, the slits between the flakes are staggered. The diffusion was greatly retarded by three factors: the tortuous wiggles to get around the flakes, the tight slits between the flakes, and the uncertain resistance of turning at the corner to go from the wiggle into the slit. Diffusion of carbon dioxide through silicon-polycarbonate membranes containing perpendicularly arranged mica flakes was proportional to the volume fraction of the flakes, to the square of the aspect ratio, and to the square of the cosine of the angle at which the flakes are oriented. Considering permeation through the tortuous path through which the permeate has to pass, the flux can be expressed as:

$$J_o/J_n = \alpha^2 \phi^2 \cos^2 \theta / 1-\phi \quad \text{-----(5.19)}$$

where θ is the angle at which the flakes are oriented.

5.3.2 Two phase systems with both phases permeable to different extents

Polymer membranes containing selectively permeable flakes show modified selectivities. Cussler (1990) has modelled the permeability and selectivity through membranes containing permeable selective flakes. The membrane filled with semipermeable flakes was idealized as a continuous matrix filled with multiple lamellae. Each lamella contains two layers, one of polymer and one containing polymer and flakes. Diffusion first occurs through the layer of polymer. It then occurs through the second, mixed layer, either by going through a flake or by wiggles around the flakes. As a result, each lamella contains three resistances: a resistance due to the pure polymer layer in series with the two parallel resistances due to the flakes and wiggles in the second mixed layer. When the flakes are highly selective, the relative fluxes are proportional to the square root of the inherent selectivity. If the flakes are moderately selective, the relative flux approaches this moderate value. Achieving this selectivity requires carefully adjusting the diffusion coefficient in the polymer continuum to the geometric average of the diffusion coefficient in the flakes times the aspect ratio of the flakes. When the flakes are too permeable, the diffusing species can easily pass across the flakes and the polymer controls the mass transfer resistance of the composite. The flux of the film containing highly permeable flakes can be given as

$$J_o / J = 1 - \phi + \alpha^2 \phi^2 / 1 - \phi \quad \text{-----} \quad (5.20)$$

where ϕ is the volume fraction of the flakes. In this case, the selectivity is controlled by the selectivity in the polymer.

5.4 Transport of Penetrant in Dispersed Polymer System

In this section the literature survey is summarized with respect to the transport properties of dispersed polymer systems in this section. The discussion is divided according to nature of the additives.

- 1) Organic low molecular weight compounds,
- 2) Inorganic compounds,
- 3) Organometallic compounds,
- 4) Low molecular weight polymeric materials (oligomers).

5.4.1 Organic low molecular weight Compounds as an additives

Various types of low molecular weight organic compounds are used as additives, for examples liquid crystals, different phthalates, compounds having ketone, ether, amide, imide, azo functions and also some solvents. These additives may contain polar groups or atoms. These additives behave in different ways with different polymers, depending upon the interactions between the additive and polymer matrix. These interactions are responsible for changing morphology and thereby the properties of the dispersed polymer system.

Huh [Huh et al (1983)] studied thermotropic LC materials, p-ethoxybenzylidene-bis-4-n-butylaniline (EBBA) and terephthal-bis-4-n-butylaniline (TBBA), which behave as plasticizers for polystyrene (PS). EBBA and TBBA are miscible in PS upto 20% and 11% of LC concentration respectively. Plasticization effect was observed from reduced glass transition temperature. It was also seen that above the solubility limit, the LC separated out and there was no further decrease in T_g or viscosity. In contrast, a composite membrane prepared from sulfonic perfluorinated ionomer and Nafion with LC compound (4-cyano-4'-n-hexylbiphenyl) is an example of an immiscible system [Ratto et al (1993)]. The LC compound separates out in the form of the droplets in polymer matrix.

Kajiyama et al [(1982), (1984)] have shown that LC-polymer blends have unique transport properties. The EBBA was molecularly dispersed upto 30% in PVC or PC polymers, But at 60% EBBA addition, composite shows 3D network of polymer fibrils in an LC continuous phase. The permeability values were enhanced in the vicinity of the crystalline to nematic transition of EBBA (T_{KN}) through 60% EBBA composite membrane because of the increased pore formation. The observed enhanced permeability below T_{KN} and above T_{KN} was by diffusivity and solubility coefficients respectively. It is also known to increase permeability of LC-polymer blend after applying electrical field [Kajiyama et al (1985)].

McIntyre and Soane (1988) have prepared a system in which LC compound, EBBA, in PMMA is partially soluble, which is used as reversible optical storage medium.

West (1988) has shown that the three general ways to prepare polymer dispersed liquid crystalline PDLC materials : 1) The LC is dissolved in a polymer precursor and the dispersed LC phase forms during polymerization, 2) The LC is dissolved in a polymer melt and phase separation of the droplets occurs during cooling of the melt, or 3) The LC and the polymer are

dissolved in a common solvent and then evaporation of the solvent, during which the LC precipitates as a microphase.

Pant et al (1994) have modified the gas separation properties of polystyrene polymer by addition of liquid crystalline compound, [2,3-dimethyl-4-n-butyl-4-(4'-methoxybenzoyl) azobenzene] (BMA). They observed that 2-3% addition of BMA reduces the permeability by 30-40%, but further addition of BMA does not decrease the permeability further. At low BMA concentration, molecules act as an antiplasticizer in polystyrene matrix by occupying the space between the polymer chains and reducing the free volume available for solute transport, thus decreasing the permeability.

In another case, addition of certain low molecular weight diluents to glassy polymers causes antiplasticization, i.e. increased stiffness also reduces the permeability of gases. For few pairs, the selectivity increased because of the difference in molecular size. Also, there is a loss in selectivity in many cases [Maeda and Paul (1987a)].

The effect of low molecular weight photosensitizer and UV irradiation on gas permeability and selectivity of polyimide membrane was studied [Matsui et al (1998), Liu et al (1995)]. Here, the changes in the gas permeation were attributed to the densification of the membrane rather than cross-linking.

Gas permeation studies through cis-polybutadiene/ LC [LC like ABECA, ABEOA, and ABMA] composite membrane was done by C. Zhou et al (1998). The oxygen elements in composite enhance the O₂ permeability as well as selectivity. These membranes can be used in the oxygen enrich application.

The effect of additive on gas diffusivity of PVC polymer was studied by M. D. Sefcik (1983). The additive like TCP (Tricresyl Phosphate) is acting as an antiplasticizer below 15 wt% concentration and above that it is playing a role of plasticizer. WAXD does not show any change in intersegmental chain distance. When TCP is acting as an antiplasticizer, it reduces gas permeability of H₂ and CO, while at high concentration it increases permeability. Here the diffusivity coefficient was changed with additive concentration, but solubility coefficient was not affected much.

The addition of TCP causes the change in free volume of PVC, compared to specific volume of the mixture. It is observed from the density measurements that PVC containing TCP upto 50 wt% [Jacobson U., (1973)] have monotonical decrease in the free volume, with the

addition of TCP over the entire range of additive concentration. Regardless of this, the change in free volume with plasticizer content neither correlates with diffusivity measurements nor with mechanism. Many researchers have correlated mobility of gas with changes in polymer packing or polymer chain mobility. When additive is dispersed in polymer, it alters the molecular motion of the polymer which was responsible for observed change in the diffusivity. Robeson (1969) suggested that the addition of antiplasticizers to polymers restricted the molecular flexibility of chains, thereby restricting diffusion of penetrants.

Sefcik (1983) suggested that the addition of low levels of TCP increase the average interchain potential in PVC, i.e. restriction in main-chain motion, so that more energy is required for chain separation. The increased cohesion results in higher activation energy for diffusion, and results in lowering diffusion coefficients (i.e. as the penetrant diameter increases diffusion coefficient decreases).

Liquid crystalline materials are known to be used in applications, such as electro-optical display technology [Dutta et al (1993)], light valve, temperature sensors, variable transmission windows, optical recording media, stationary phases [Panse et al (1984)] in gas chromatographic technique below their crystal to nematic transition temperatures, light scattering in the films which depends upon its nematic and isotropic phase transitions, microdroplet size and on applied electrical field.

5.4.2 An inorganic compound as an additive

Many inorganic compounds are used as additives by dispersing in polymer matrix for modifying certain properties and to reduce the cost of material [Cussler et al (1988), (1990); Ward et al (1991)]. Inorganic additives used are mica, talc, glass fibers, metal oxides and its salts etc. The properties of the dispersed polymer depends upon the additive loading, size, shape (dimensions) of additive, and its compatibility with polymer matrix.

Zhong et al (1988) added inorganic salts to water-swollen poly(vinyl alcohol) (PVA) membranes and measured the effect on O₂ and N₂ permeability. The effect of addition of 5 wt.% of each CsCl, thiourea, and LiCl on the permeability, diffusivity, and solubility of O₂ and N₂ in the water swollen PVA membranes was studied. The O₂ / N₂ selectivity was unchanged at 3.5 with the addition of 5 wt.% CsCl, whereas it increased to 8.2 with the addition of 5% thiourea and to 13.8 with LiCl. The permeability of N₂ in thiourea and LiCl containing

membranes decreased while the O₂ permeability did not change appreciably. This decrease in N₂ permeability was caused mainly by decreased diffusivity. The selectivity of these membranes originate from the increase in solubility of O₂ as a result of specific interactions between the polymer chains, additive and water. This increased solubility compensates for the decreased gas diffusivity in the case of O₂. Thus, additives which have a high affinity for the polymer were found to improve the selectivity of O₂ over N₂ in swollen PVA membranes by 50%.

A toluene solution of linear polystyrene-aluminium copper(I) chloride complex [Hirai et al (1994)] was prepared for separation of carbon monoxide from a gaseous mixture containing N₂, O₂, H₂, CO₂ and H₂O by selective adsorption. The aluminium copper(I) chloride is deactivated by water, but polystyrene protects metal-complex from deactivation and prolongs its life.

Separation coefficient of polyimide [Yingyong et al (1993)] was increased by the additives such as Co(NO₃)₂, MnCl₂, Cr(OAc)₃, but permeability coefficient was decreased. However, use of organometallic compounds such as Cr-bis(di-Bu-Phthalate) increased the gas permeability without changing selectivity.

Juin-Yih Lai and coworkers [Juin- Yih Lai et al (1993)] have studied the effect of casting solution composition and solvent evaporation time on morphology, gas permeability, and selectivity of O₂/N₂ of PC membranes. The PC/DMF/Metal salt (CuCl₂) membranes significantly improved the gas permeabilities compared to the pure PC membrane.

Many other inorganic compounds [Lai et al (1992)], like titanium dioxide, copper chloride, metal sulfide etc. are used as an additive in various polymers for gas separation studies [Lai et al (1992), (1993), Hu et al (1997), Fritsch et al (1994)]. Similarly, various types of zeolites [Paul (1973)] are used for gas separation in dispersed form. [Suer et al (1994), Guer et al (1994), Duval et al (1992)].

5.4.3 Organometallic compounds as an additive

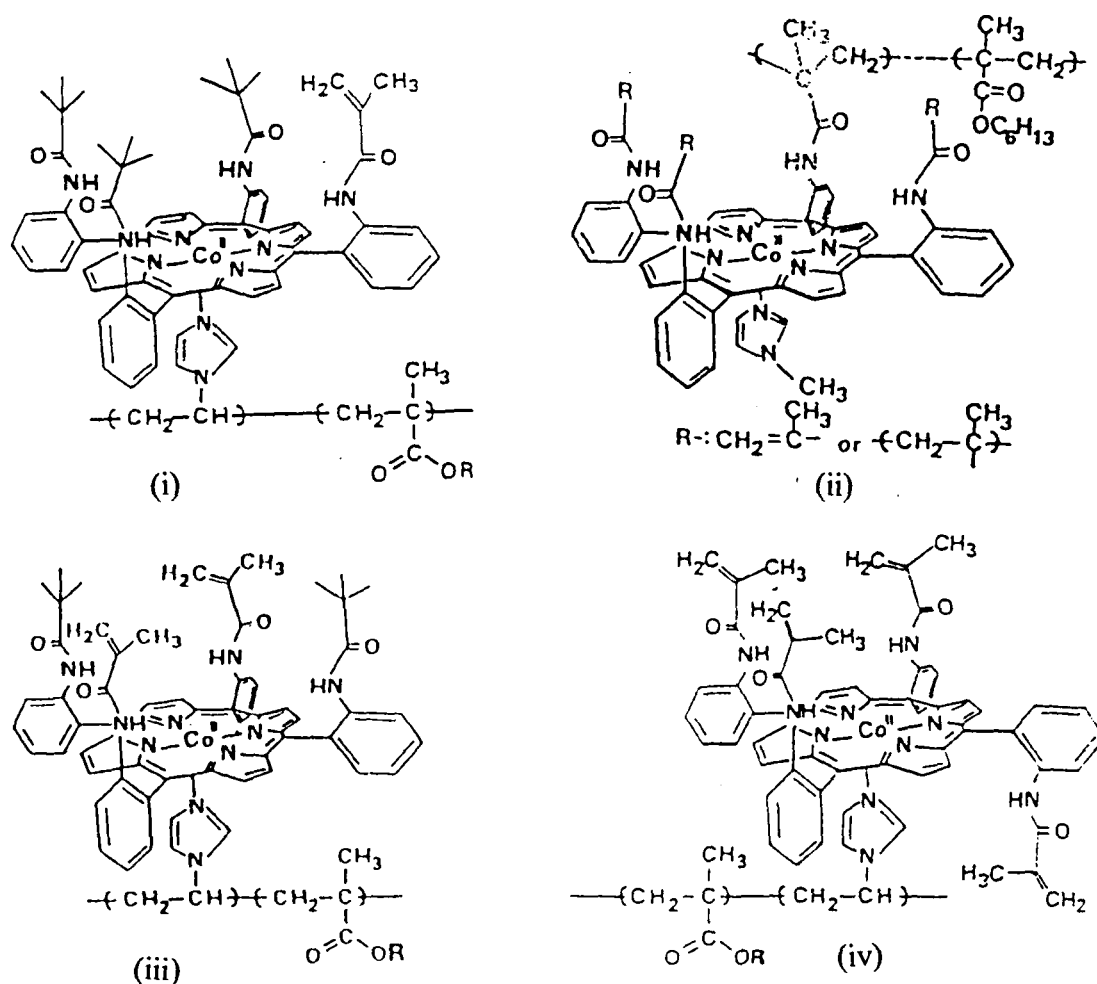
The organometallic chelate compounds play important role in biological oxidation-reduction systems. In 1946, M. Calvin and group [Calvin et al (1946)] have prepared some compounds which show behavior similar to hemoglobin molecule as an oxygen-carriers.

These compounds are mainly used as the gas carriers in liquid and glassy membranes.

A polymer-metal complex membrane is composed of a synthetic polymer with transition-metal ions [Tsuchida and Nishide (1977)], which can be represented as an organic polymer phase and inorganic functional group. Metal ions and their complexes have specific and reversible binding with gaseous molecules. In living cells, hemoglobin and myoglobin are conjugated proteins containing iron porphyrin(s), of which central iron (II) selectively binds to molecular oxygen in coordinate manner.

A series of modified Co- and Fe-porphyrin complexes [Nishide et al (1986), (1987), (1988), (1990), (1991)] and tetrakis(alkylamidophenyl)porphinatometals (figure 5.1) were dispersed or fixed on the polymer, to give a flexible, transparent membrane, that binds the oxygen selectively and reversibly. The modified complexes were coordinated or covalently bonded on polymer matrices poly(1-vinylimidazole- or 4-vinylpyridine-copolymer), which keeps steric pocket, like vacant cavity on the porphyrin plane to coordinate with molecular oxygen.

Figure 5.1 Modified Cobalt-porphyrin polymer complexes.



H. Nishide, et al. [Nishide, et al. (1990), (1991)] showed that the membrane containing 30% cobaltporphyrin (CoP) complex, sorbs oxygen 500 times larger than that of physically dissolved nitrogen. The oxygen sorption is in response to an atmospheric oxygen pressure. Here the Henry's law is for the physical sorption and Langmuir isotherm is for the chemical dissolution to the complex, and an equilibrium constant K for the binding interaction.



CoP = cobaltporphyrin, Im = imidazolyl residue.

K value indicate the oxygen binding affinity of the CoP which inturn depend upon its chemical structure.

Polycarbonate membrane shows an improvement in the permeability when nonsolvent like DMF is used but it reduces its selectivity [Chen et al (1997), Chen Shih-Hsiung and Lai (1996)], while oxygen-carrier [as a N,N'-disalicylidene ethylene diamine cobalt (II)(Cosalen)] improved selectivity. After optimization of combination of DMF and oxygen-carrier (Cosalen) resulted in an improvement in both permeability and seletivity of the PC blend membrane. A dual mode sorption mechanism was used to explain the permeability through the cobalt complexed membrane.

Many polymer-metal complex membranes are reviewed in literature [Nishide and Tsuchida (1992), Lehmann et al (1998), Ruoh-Chyu Ruaan et al (1997)] which show the specific and reversible binding to the particular gas with the help of metal-complex. The permeability of the polymer was improved drastically by addition of metal-phthalocyanines with appropriately chosen substituents. It is seen that bulky, fluorinated substituents gave high permeate flux. Metals used were Fe, Ni, Co in the metal-phthalocyanines. A solution-diffusion mechanism was used to understand gas transport behavior.

Shih-Hsiung Chen et al (1997) have studied gas permeation in the polycarbonate PC/Co⁺³acetylacetonate [Co(acac)₃] blend membranes. They observed that 20%[Co(acac)₃]/PC membrane showed improvement in oxygen selectivity mainly by diffusivity selectivity factor. The O₂/N₂ selectivity was 8.4 at 25°C and at 1 atm. The selectivity was expected to be higher at a lower pressure. Similarly it was observed that solubility selectivity was slightly improved. They noticed that the carbonyl peak of PC absorbs at 1782 cm⁻¹ which splits after the addition of [Co(acac)₃]. The absorbance of the second split peak is at 1775 cm⁻¹ and increases with the

addition of $[\text{Co}(\text{acac})_3]$. The splitting of the carbonyl peak implied that there is an interaction between polycarbonate and $\text{Co}(\text{acac})_3$. This interactions might be responsible for the improving solubility selectivity.

Incorporation of transition metal complexes into cellulose acetate (CA) membranes reduce the permeation flux, since they act like cross-linking agents, resulting in decrease in the free volume. CA membranes containing $\text{RuCl}_3 \cdot 3\text{H}_2\text{O}$ and $\text{RhCl} [\text{P}(\text{C}_6\text{H}_5)_3]_3$ were prepared by Lee et al (1991). There was no permeation of CO gas through these membranes. During the permeation process, the carbon monoxide molecule interacts with CA polymer molecule and exist in a ketone type structure, which causes the slow permeation of CO. However the permeation of other gas molecules, such as H_2 , N_2 , and O_2 through the same membrane was reduced slightly, probably due to the crosslinking effect of the transition metal complexes on CA. It was found that pure H_2 gas could be recovered from a 1:1 mixture of H_2 and CO using ruthenium-containing CA membranes.

5.4.4 Low molecular weight polymer as an additive

The polymer blending or dispersion with the help of other polymers is carried out to achieve unique properties or to lower cost of the membrane material. These polymer blends are used for gas permeation studies. They may be miscible or immiscible blends. Few examples are highlighted below.

Low density polyethylene (LDPE), Linear low density polyethylene (LLDPE), and high density polyethylene (HDPE) blended with various nylon resins: like nylon-6, nylon-6,6, and modified nylon-6,6 were studied by Kamal et al (1984). Similarly membranes prepared from various weight ratios of poly(vinylchloride) PVC and oligo (dimethyl siloxane) (ODMS) were studied by Lerma et al (1987).

Semi-crystalline homopolymers can be described as dispersions of a well-defined and ordered polymer within a continuous matrix of an amorphous polymer [Lerma et al (1987)]. Normally [exception of poly(4-methylpentene)] the amorphous regions of a semi-crystalline polymer are less dense and more permeable than crystalline regions which are dispersed within the matrix of a permeable polymer. Crystallites reduce the polymer permeability by acting as an impermeable flakes for penetrant transport and by compelling the transport along irregular tortuous paths.

A successful packaging material is prepared by coextrusion of a five-layer film of PE-EVA-PVDC-EVA-PE. The gas barrier is given by PVDC core film, while the PE skin layers provides good heat sealability. The EVA layer bonds the PVDC and PE layers. These films are used in packaging food, which provide excellent gas barrier properties (meat, cheese, nuts, snacks, fruits, drinks, etc.) and in some medical applications [Schrenk and Alfrey (1987)].

Chapter 6

Experimental: Additive dispersed polymeric membranes

Chapter 6

Experimental: Additive dispersed polymeric membranes

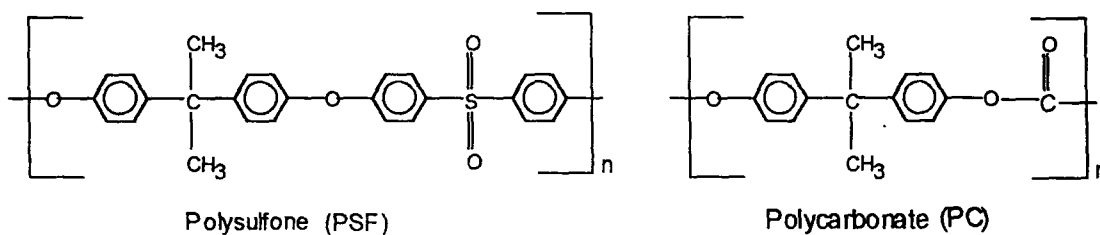
6.1 LC-Dispersed polymeric membranes

The methods used for membrane preparation containing liquid crystalline compound (LC), characterization and permeability studies are described in this section. Section 6.1.1 gives the information about the materials used. Details about membrane prepared by dispersing liquid crystalline compounds [(LC1 or LC2) as the additives] in polycarbonate (PC) and polysulfone (PSF) are given. The section 6.1.2 describes the film preparation and permeation studies, whereas, section 6.1.3 deals with membrane characterization.

6.1.1 Materials

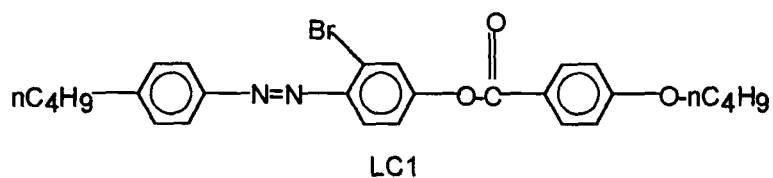
6.1.1.1 Polymers

The virgin polysulfone (PSF) was used as received from General Electric Pvt. Ltd. USA. The mol. wt. was ~40,000. Polycarbonate (PC) was used as received from Amoco Polymer Products Pvt. Ltd. USA. The mol. wt. was ~35,000. The structures of PC and PSF polymers are given below:

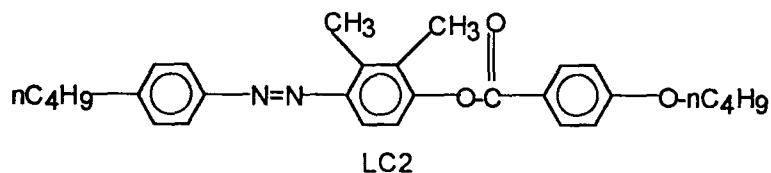


6.1.1.2 Liquid Crystalline Compounds: (LC1 and LC2)

These were synthesized in-house and were purified before use. The structures of LC1 and LC2 are shown below [Panse et al (1982)].



For LC1 [2-Bromo-4-n-butyl-4'-(4''-butyloxybenzoyloxy)azobenzene], the crystalline to nematic transition temperature T_{C-N} was 78°C and the nematic to isotropic transition temperature T_{N-I} was 160°C.



For LC2 [2,3-Dimethyl-4-n-butyl-4'-(4''-butyloxybenzoyloxy)azobenzene], the crystalline to nematic transition temperature T_{C-N} was 112°C and the nematic to isotropic transition temperature T_{N-I} was 216°C. The respective IR, NMR and Mass spectra for LC1 and LC2 are shown in figures 6.1, 6.3, 6.5 and 6.2, 6.4, 6.6 respectively.

6.1.2 Film preparation

The film was prepared by dissolving LC material and polymer in dichloromethane. The resulting solution was used for casting as mentioned in the section 3.2.1. The concentrations of the LC component were varied from 0-12%.

There were 4 different combinations obtained by using 2 different LC materials (i.e. LC1 and LC2) and 2 different polymers (i.e. PC and PSF). These combinations are designated as below:

- 1) CL1 series: LC1 material dispersed in PC.
- 2) CL2 series: LC2 material dispersed in PC.
- 3) SL1 series: LC1 material dispersed in PSF.
- 4) SL2 series: LC2 material dispersed in PSF.

Each series comprised of 5 different concentrations: 1%, 3%, 6%, 9% and 12% (w/w)

The specific amount of LC material, polymer and solvent (in ml.) used for the casting of different membranes are given in tables 6.1–6.4. The thickness of films obtained were ~30µm.

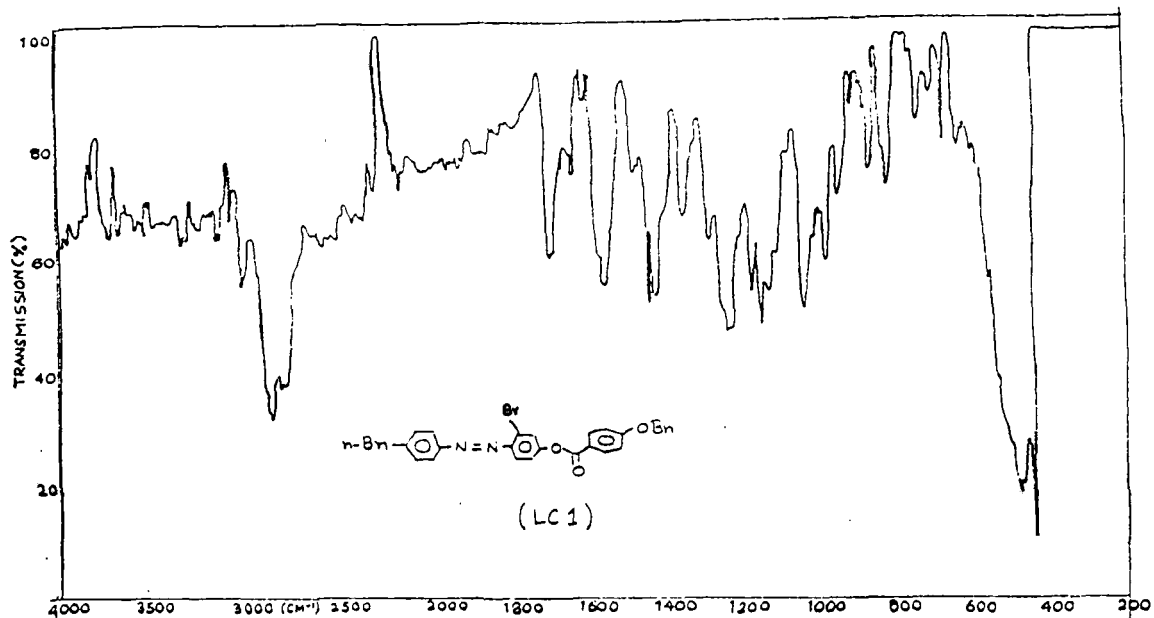


Figure 6.1 IR spectrum of LC1

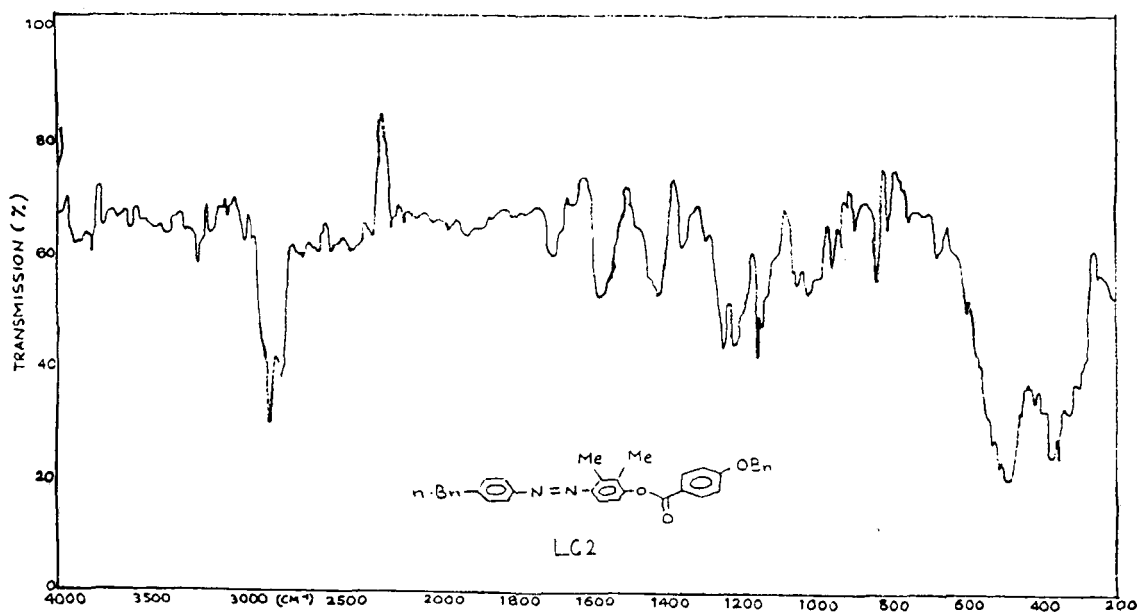


Figure 6.2 IR spectrum of LC2

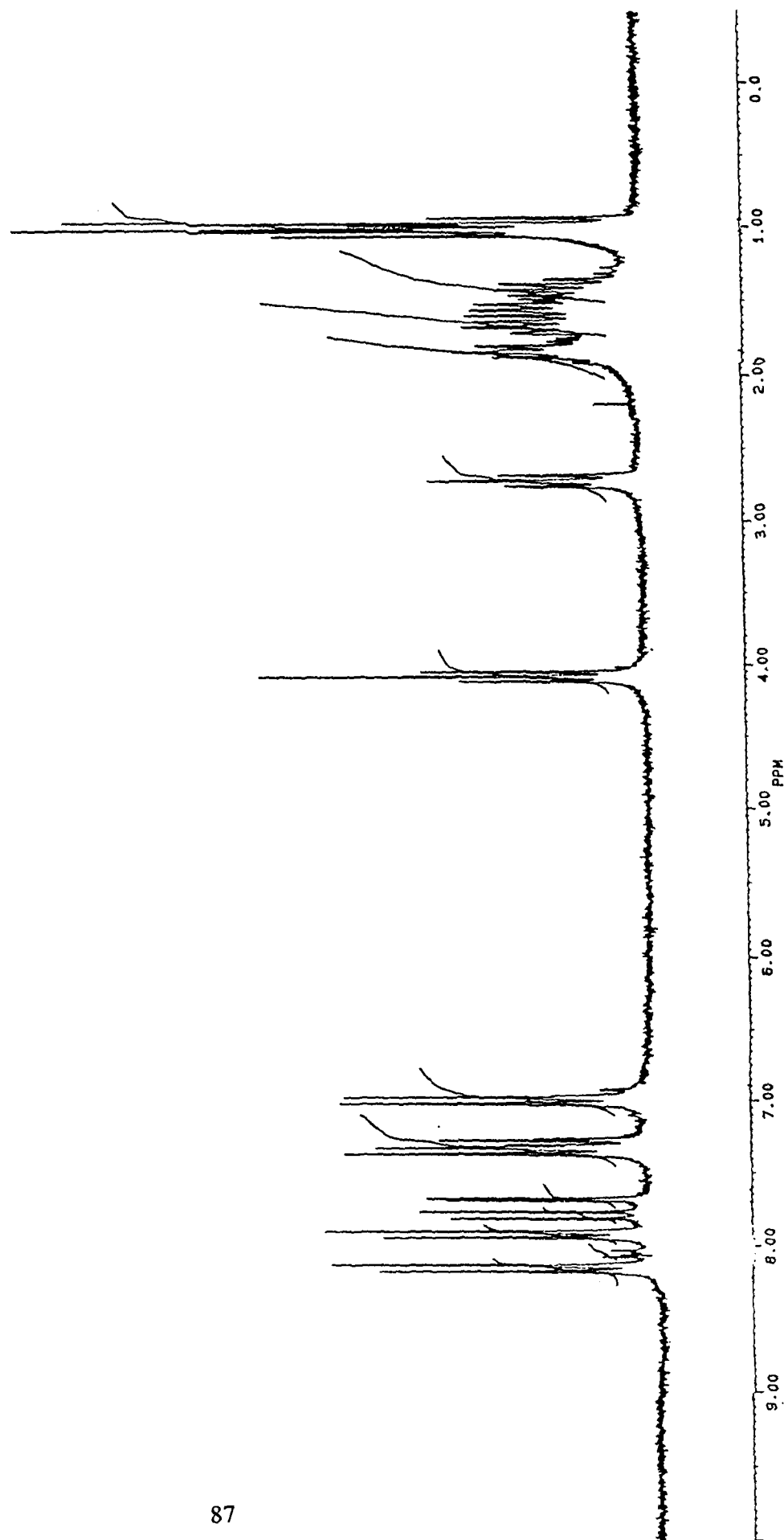
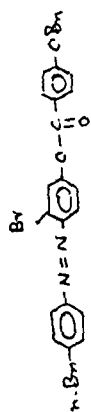


Figure 6.3 NMR spectrum of LC1

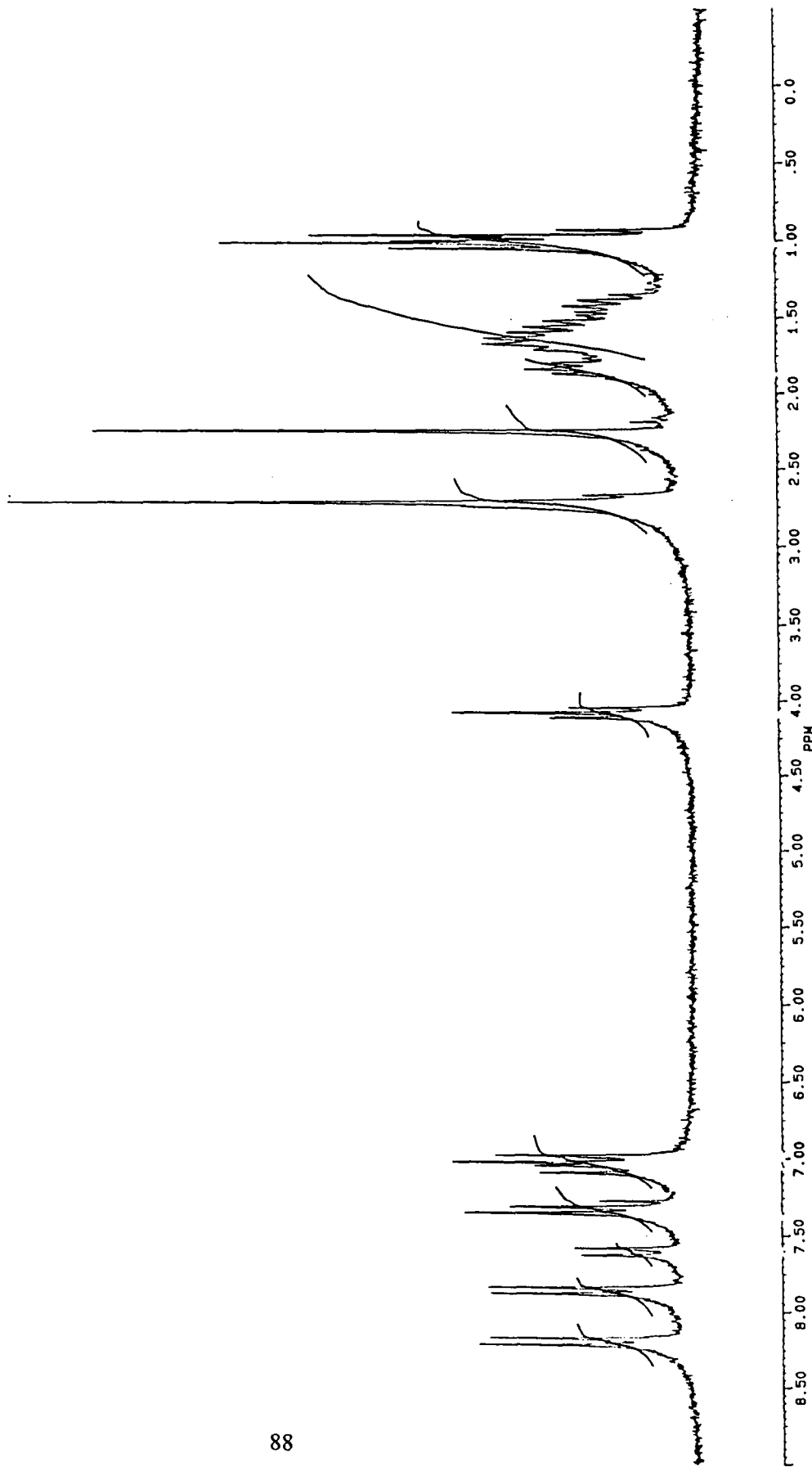
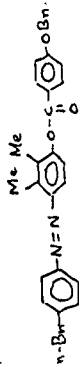


Figure 6.4 NMR spectrum of LC2

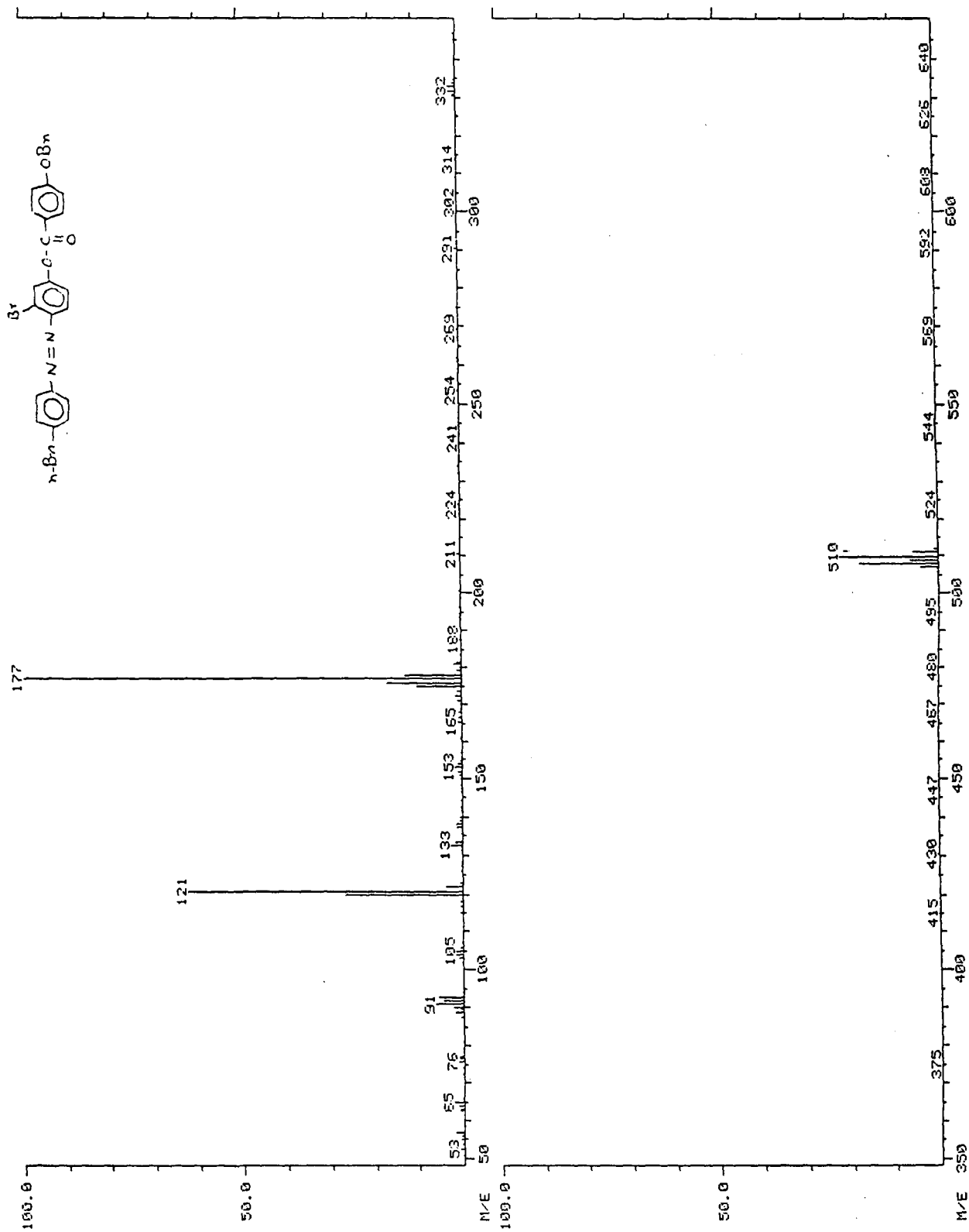


Figure 6.5 Mass spectrum of LC1

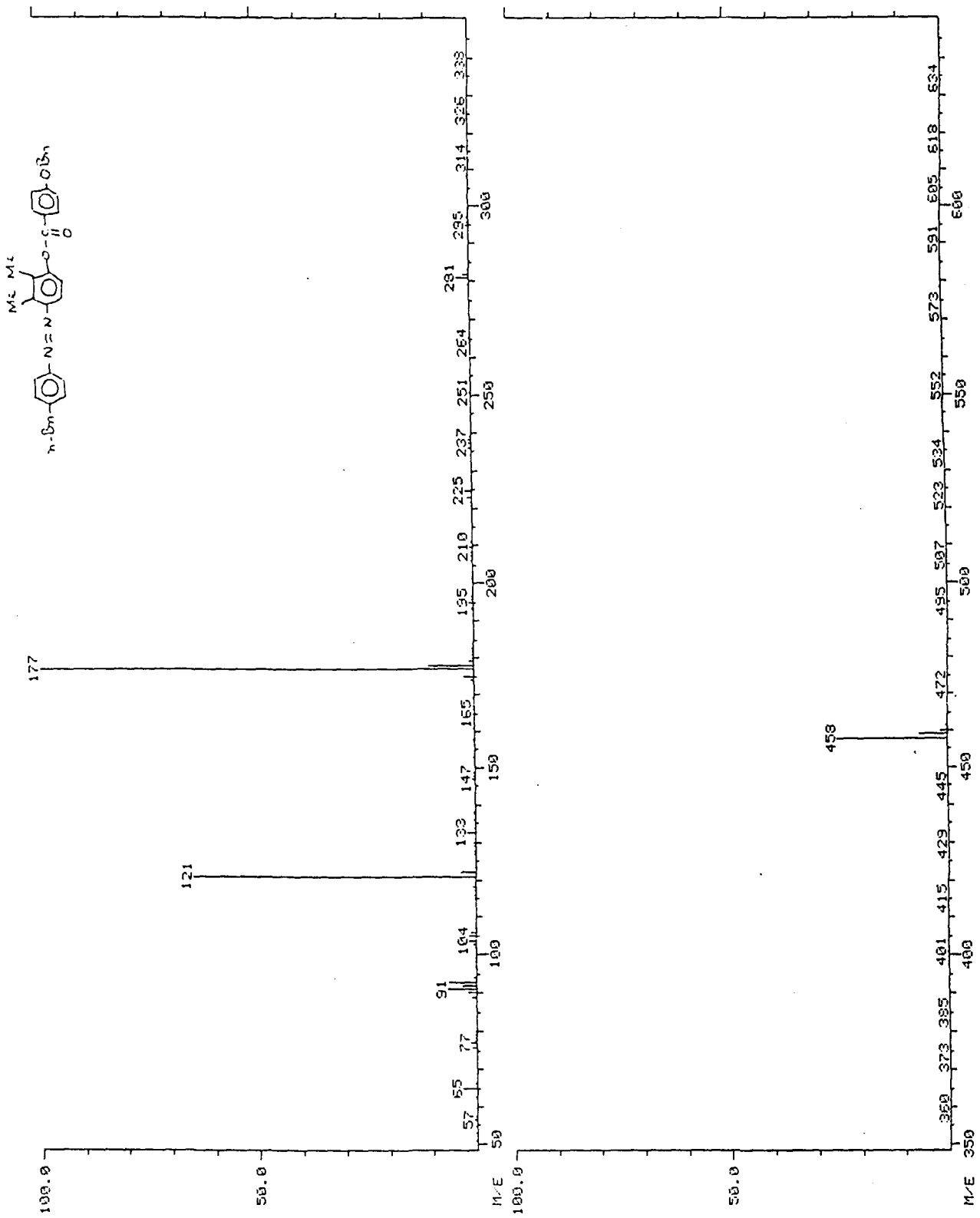


Figure 6.6 Mass spectrum of LC2

Table 6.1

Composition of membranes belonging to CL1 series

Membrane designation	Amount of LC1 dispersed (mg)	Polymer (PC) (mg)	Amount of solvent (ml)
Pure PC	0	300	15
1% CL1 membrane	3	300	15
3% CL1 membrane	9	300	15
6% CL1 membrane	18	300	15
9% CL1 membrane	27	300	15
12% CL1 membrane	36	300	15

Table 6.2

Composition of membranes belonging to CL2 series

Membrane designation	Amount of LC2 dispersed (mg)	Polymer (PC) (mg)	Amount of solvent (ml)
Pure PC membrane	0	300	15
1% CL2 membrane	3	300	15
3% CL2 membrane	9	300	15
6% CL2 membrane	18	300	15
9% CL2 membrane	27	300	15
12% CL2 membrane	36	300	15

Table 6.3

Composition of membranes belonging to SL1 series

Membrane designation	Amount of LC1 dispersed (mg)	Polymer (PSF) (mg)	Amount of solvent (ml)
Pure PSF membrane	0	300	15
1% SL1 membrane	3	300	15
3% SL1 membrane	9	300	15
6% SL1 membrane	18	300	15
9% SL1 membrane	27	300	15
12% SL1 membrane	36	300	15

Table 6.4

Composition of membranes belonging to SL2 series

Membrane designation	Amount of LC2 dispersed (mg)	Polymer (PSF) (mg)	Amount of solvent (ml)
Pure PSF membrane	0	300	15
1% SL2 membrane	3	300	15
6% SL2 membrane	18	300	15
12% SL2 membrane	36	300	15

6.1.2.2 Measurement of gas permeability

Using these LC-dispersed polymeric membranes, the gas permeation measurements were carried out as given in the section 3.2.2. Gases used were He, N₂, O₂, and CO₂.

6.1.3 Membrane Characterization

The membranes (preparation given in section 6.1.2) were characterized by using different techniques such as differential scanning calorimetry (DSC), wide angle x-ray diffraction (WAXD), thermal gravimetric analysis (TGA). TGA analysis was carried out in two different environments, nitrogen (N₂) as well as static air. Same procedures were followed for these techniques as given in section 3.3

6.2 Metal complex dispersed polymeric systems

The methods used for membrane preparation, characterization and permeability studies of metal complex dispersed polymeric membranes are described in this section. Section 6.2.1 describes the details of the materials used: metal complexes Fe(acac)₃ and Co(acac)₃. The section 6.2.2 describes film preparation and permeation studies while section 6.2.3 deals with membrane characterization.

6.2.1 Preparation of Metal Complexes

6.2.1.1 Synthesis of Tris(2,4-pentanediono)iron(III), [Chaudhuri and Ghosh (1983)].

Additive [Fe(acac)₃] designated as MX1

Anhydrous iron (III) chloride (4.0g, 24.7 mmol) was dissolved in water (6 ml) with gentle warming. To this ammonia solution (specific gravity 0.88, 12 ml) was added slowly with constant stirring. The mixture was heated on a steam-bath for 15-20 min., and the precipitate of iron (III) hydroxide was then filtered off and washed with water until free from chloride. The moist iron (III) hydroxide and acetylacetone (12.0g, 120mmol) were placed in a small conical flask, plugged with cotton wool, and the whole mixture was heated on a steam-bath for 35 min. On cooling, large red crystals of Fe(acac)₃ were obtained which were filtered and dried on filter paper. Recrystallized from ethanol. Yield was 7.3g (84%), M.P. 190°C.

Molecular formula: C₁₅H₂₁FeO₆, Molecular Weight: 353

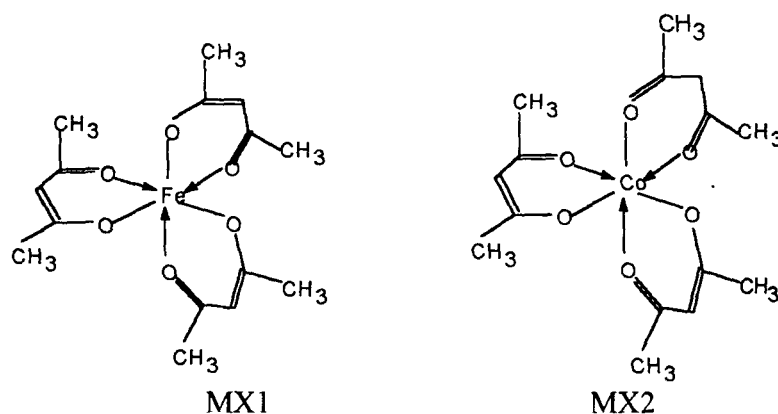
Spectral analysis: Figures 6.7, 6.9.

IR (CHCl₃): cm⁻¹ 2950, 1570-1480, 1350, 1260, 1200, 1000, 920, 770-720.

¹H NMR (CDCl₃): δ 2.2 (s, 18H, protons of six methyl); δ 5.5 (s, 3H, olefinic protons)

Elemental analysis: Theoretical values: C, 50.99; H, 5.95, Found: C, 51.24; H, 6.24

The structures of MX1 i.e. Fe(acac)₃, and MX2 i.e. Co(acac)₃ are given below.



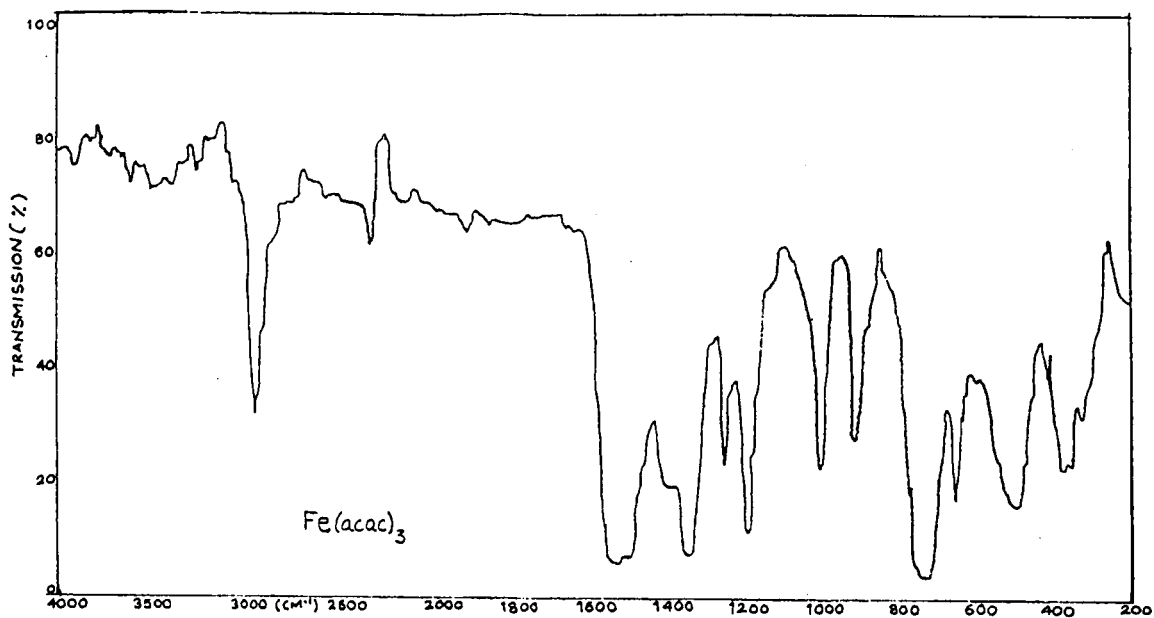


Figure 6.7 IR spectrum of $\text{Fe}(\text{acac})_3$

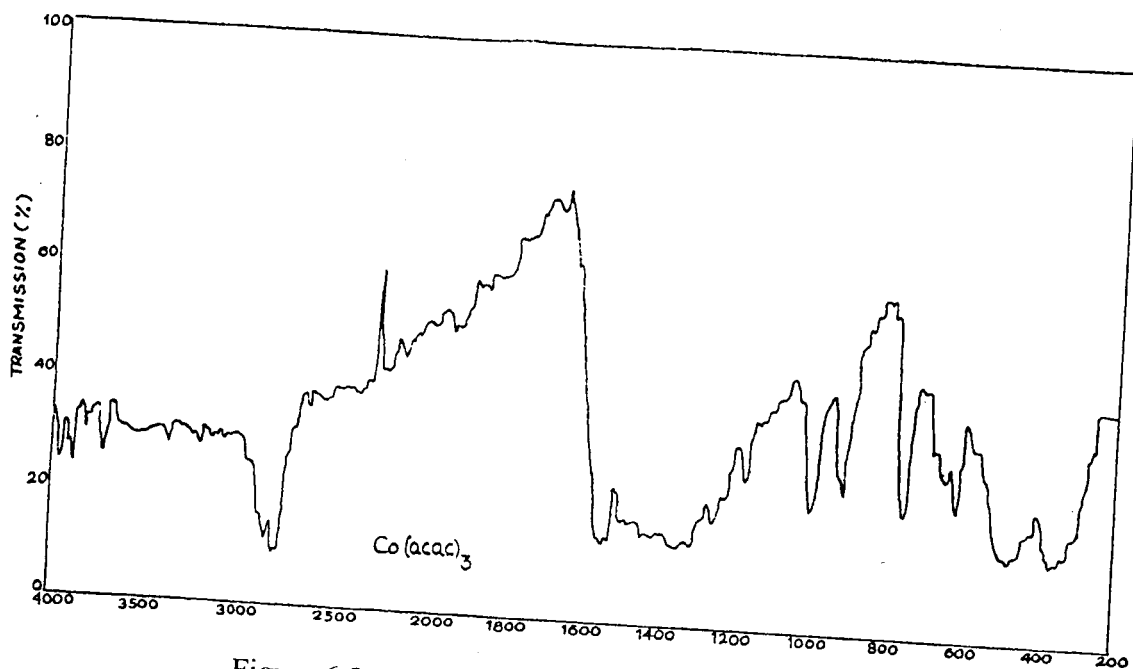


Figure 6.8 IR spectrum of $\text{Co}(\text{acac})_3$

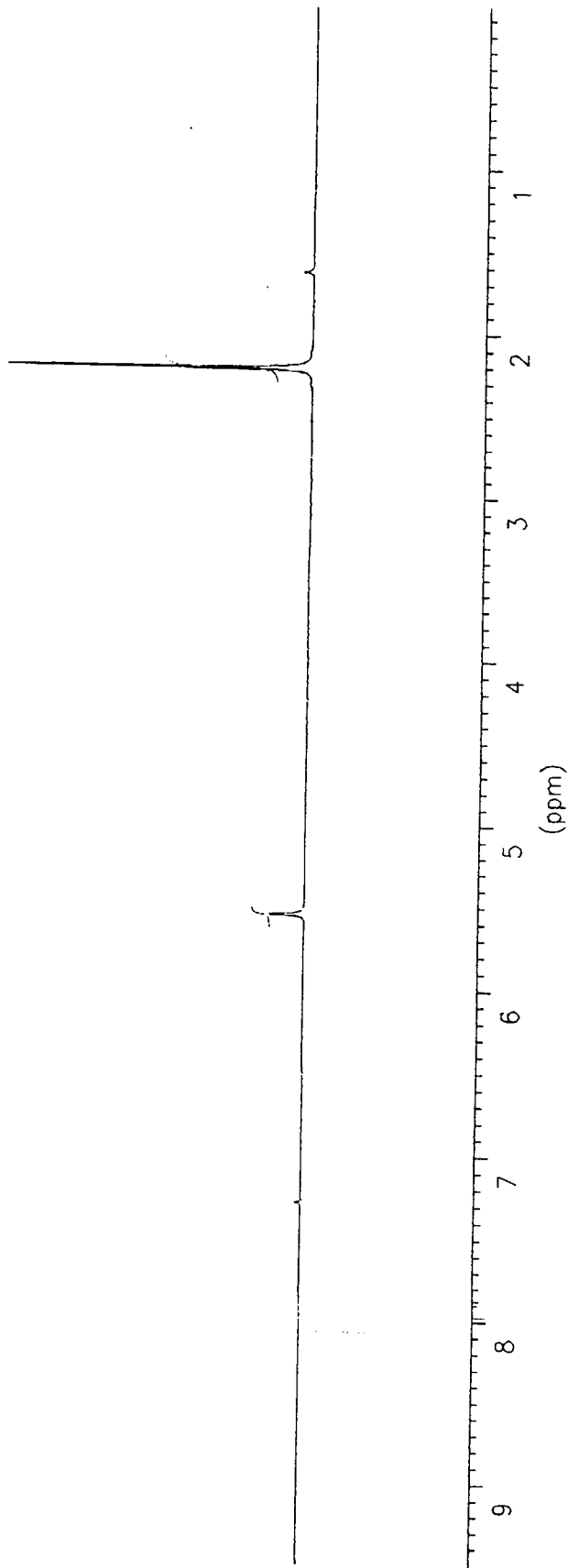


Figure 6.9 NMR spectrum of $\text{Fe}(\text{acac})_3$

6.2.1.2 Synthesis of Tris(2,4-pentanediono)cobalt(III), [Co(acac)₃], designated as MX2 [Burl and Conard Fernelius].

5g of cobalt (II) carbonate (0.042 mol) and 40 ml of acetylacetonate (0.4 mol) were taken in a 250ml conical flask and was heated to 90°C. The mixture was rapidly stirred and 60 ml of 10% hydrogen peroxide (H₂O₂) was added dropwise. The addition of H₂O₂ was completed in 45-50 min. At the end of reaction, the intense green liquid layer with small amount of green crystalline solid was observed. The mixture was chilled to 0-5°C and filtered. The crystals were dried at 110°C and crystallized from benzene: petroleum ether mixture (60:400 v/v) and the mixture cooled in an ice-salt bath. The product was removed by filtration and air-dried. The yield of dark green crystals was 10.5g (69%), M.P. 216°C.

Molecular formula: C₁₅H₂₁CoO₆, Molecular Weight: 358

Spectral analysis: Figures 6.8, 6.10.

IR (CHCl₃): cm⁻¹ 2850, 1550, 1510-1200, 1000, 980,760.

¹H NMR (CDCl₃): δ 2.2 (s, 18H, protons of six methyl); δ 5.5 (s, 3H, olefinic protons)

Elemental analysis: Theoretical values: C, 50.57; H, 5.94, Found: C, 51.12; H, 6.07.

6.2.2 Casting of Membrane (Film):

The casting method of MX_n-dispersed polymeric membrane was similar to that of LC-dispersed polymeric membrane. Membranes were prepared using metal complexes [Fe(acac)₃, Co(acac)₃] and polymer matrix (PC, PSF) by dissolving in dichloromethane. These membranes were designated as below.

- 1) SFe system: Fe(acac)₃ dispersed in PSF.
- 2) SCo system: Co(acac)₃ dispersed in PSF.
- 3) CFe system: Fe(acac)₃ dispersed in PC.

Metal complex concentration in polymer matrix was varied at 5%, 10%, 20% and 30% (w/w).

The details of metal complex, polymer and solvent used for various membrane preparation in each series is given in the tables 6.5-6.7. The thickness of films obtained were ~30μm.

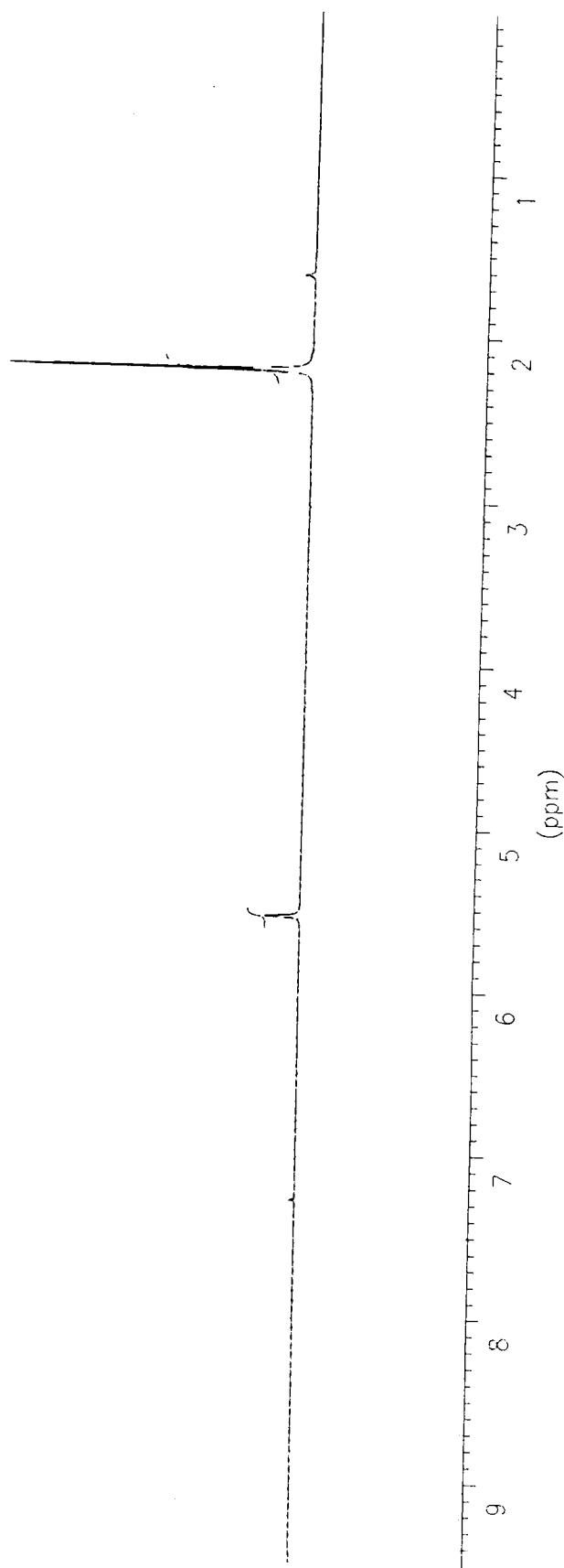


Figure 6.10 NMR spectrum of $\text{Co}(\text{acac})_3$

Table 6.5

Composition of membranes belonging to CFe series

Membrane designation	Amount of Fe(acac) ₃ dispersed (mg)	Polymer (PC) (mg)	Amount of solvent (ml)
Pure PC membrane	0	300	15
5% CFe membrane	15	300	15
10% CFe membrane	30	300	15
20% CFe membrane	60	300	15
30% CFe membrane	90	300	15

Table 6.6

Composition of membranes belonging to SFe series

Membrane designation	Amount of Fe(acac) ₃ dispersed (mg)	Polymer (PSF) mg	Amount of solvent (ml)
Pure PSF membrane	0	300	15
5% SFe membrane	15	300	15
10% SFe membrane	30	300	15
20% SFe membrane	60	300	15
30% SFe membrane	90	300	15

Table 6.7

Composition of membranes belonging to SCo series

Membrane designation	Amount of Co(acac) ₃ dispersed (mg)	Polymer (PSF) (mg)	Amount of solvent (ml)
Pure PSF membrane	0	300	15
5% SCo membrane	15	300	15
10% SCo membrane	30	300	15
20% SCo membrane	60	300	15
30% SCo membrane	90	300	15

Same method was used for the permeability studies as given in the section 3.2.2 for MXn-dispersed polymeric membranes. Gases used were He, N₂, O₂, and CO₂.

6.2.3 Membrane / polymer Characterization

The membranes (as per preparation in section 6.2.2) were characterized by using different techniques such as, wide angle x-ray diffraction (WAXD), thermogravimetric analysis (TGA). TGA technique was carried out in two different environments, N₂ and air. These techniques are used for both metal complex materials MX1 and MX2. The same procedures were followed as given in section 3.3.

CHAPTER 7

Results And Discussion

7 Results and Discussion

This chapter presents results of characterization of additives dispersed in polymers namely polycarbonates and polysulfone. The additives dispersed in these polymers were of two types. One type of additive was liquid crystalline in nature designated as SL1, SL2, CL1 and CL2. This is presented in part 7.1. The other type of additive dispersed were iron and cobalt complexes designated as SFe, SCo and CFe. This is presented in part 7.2. Permeation properties of the films/ membranes made by these dispersions are also discussed.

7.1 LC-dispersed polymeric systems

PSF and PC membranes have moderate permeabilities for various gases which limits its use as barrier packaging [Zolanz and Fleming (1992); Maeda and Paul (1987a); Ward et al (1991); Schrenk and Alfrey (1987)]. LC material was incorporated in these polymers to overcome this limitation. The effect of nature and concentration of LC as additive with PC and PSF were studied in relation to physical properties and gas permeabilities [Maeda and Paul (1987a), (1987d); Ruiz-Trevino and Paul (1997)].

In the present investigations, the LC-dispersed polymeric films were studied as membranes in their glassy form. The films were characterized by known techniques. The gas permeability results were correlated with the results from the physical properties of LC-dispersed polymers.

7.1.1 Results

WAXD spectral data of all four series for different LC concentrations are given in Tables 7.1, 7.2, 7.3, and 7.4 (figures 7.1 to 7.4). All the LC-dispersed series showed resemblance in the WAXD spectra to their respective PC or PSF polymer, suggesting formation of a homogenous composite material. Similar behavior was observed by

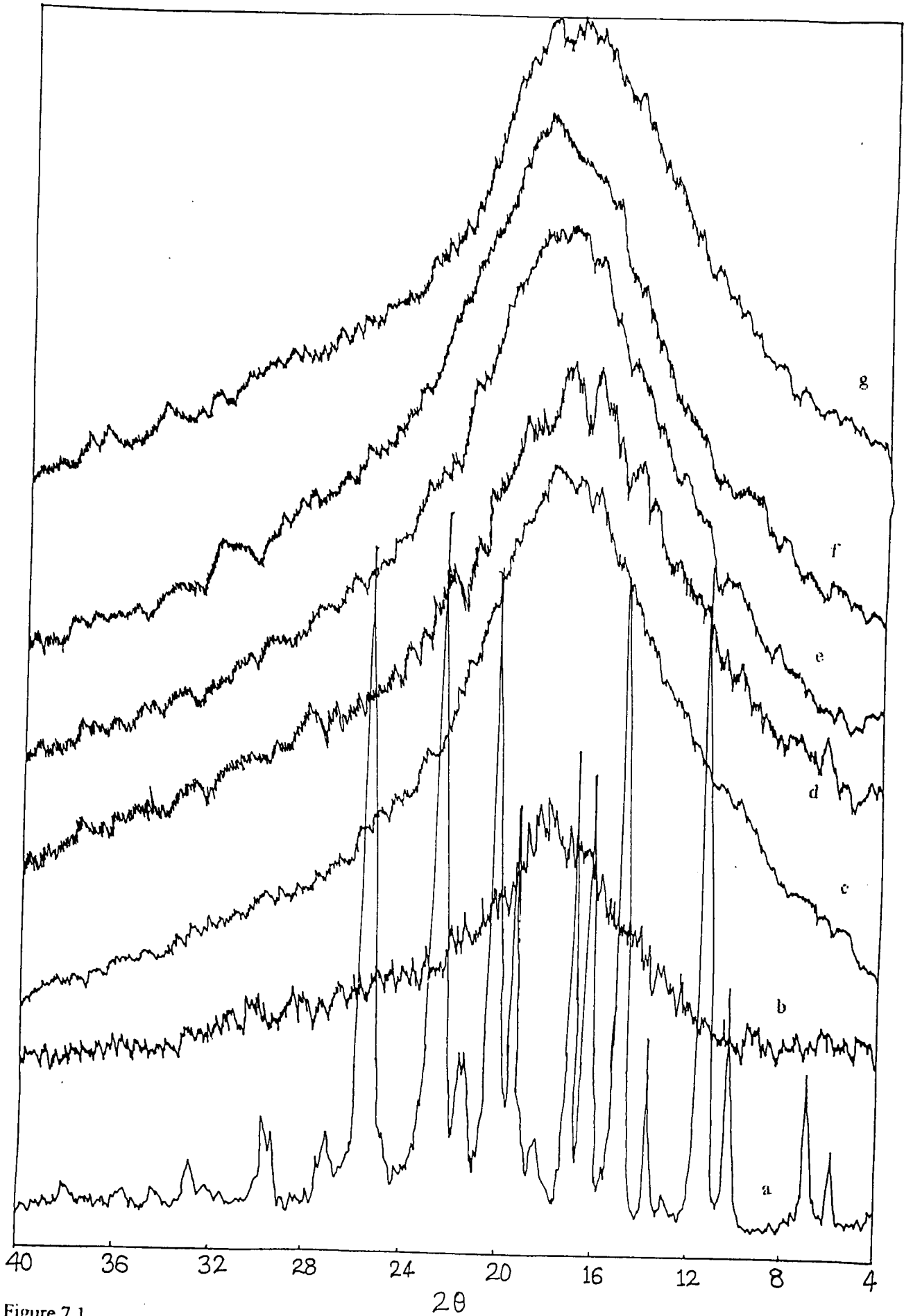


Figure 7.1

WAXD spectra of SL1 series polymers, a) LC1, b) 0%, c) 1%, d) 3%, e) 6%, f) 9% and g) 12% series polymer.

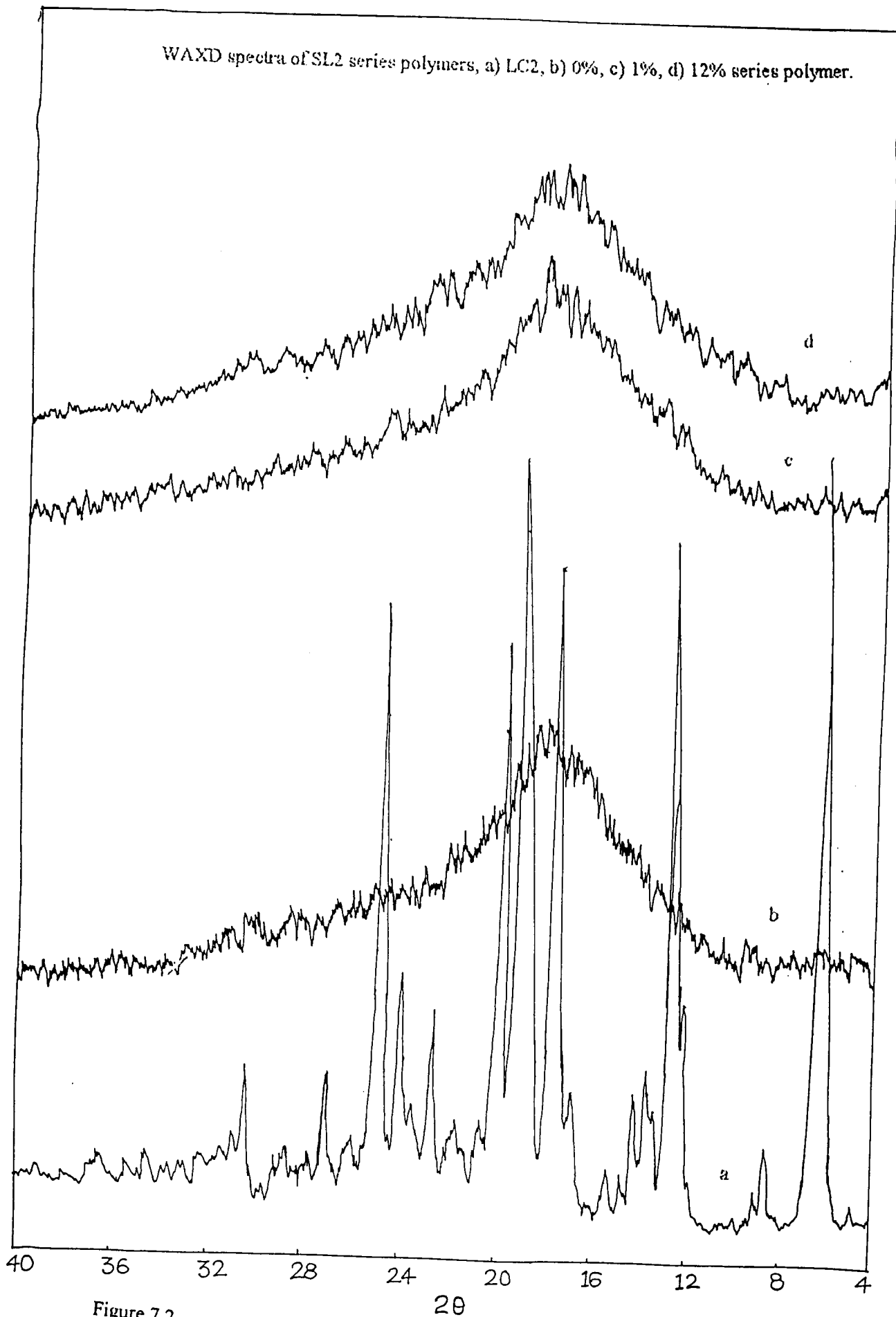


Figure 7.2

WAXD spectra of CLI-series polymers, a) LC1, b) 0%, c) 1%, d) 6%, e) 9% and f) 12% series polymer.

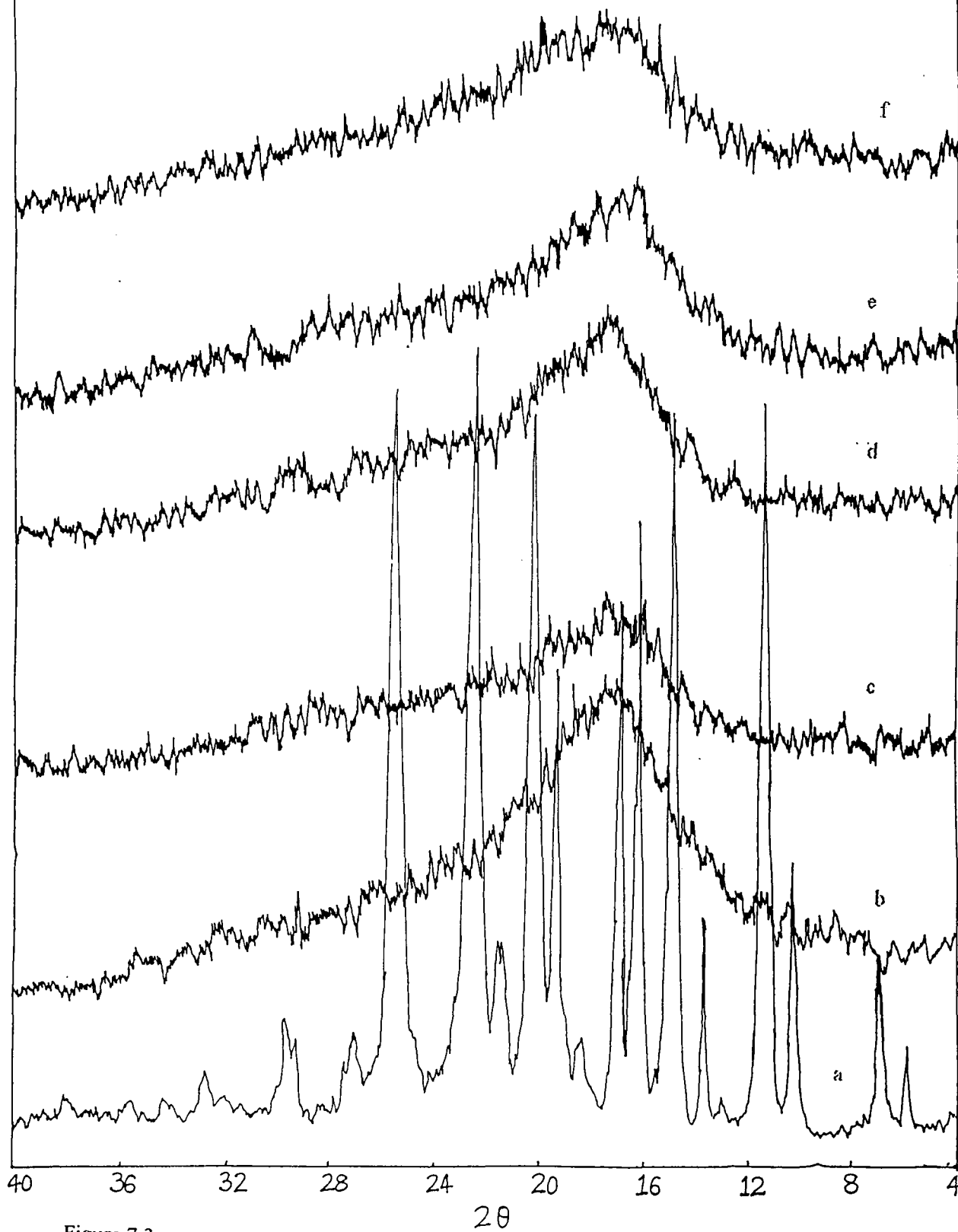


Figure 7.3

WAXD spectra of CL2 series polymers, a) LC2, b) 0%, c) 1%, d) 6%, e) 9% and f) 12% series polymer.

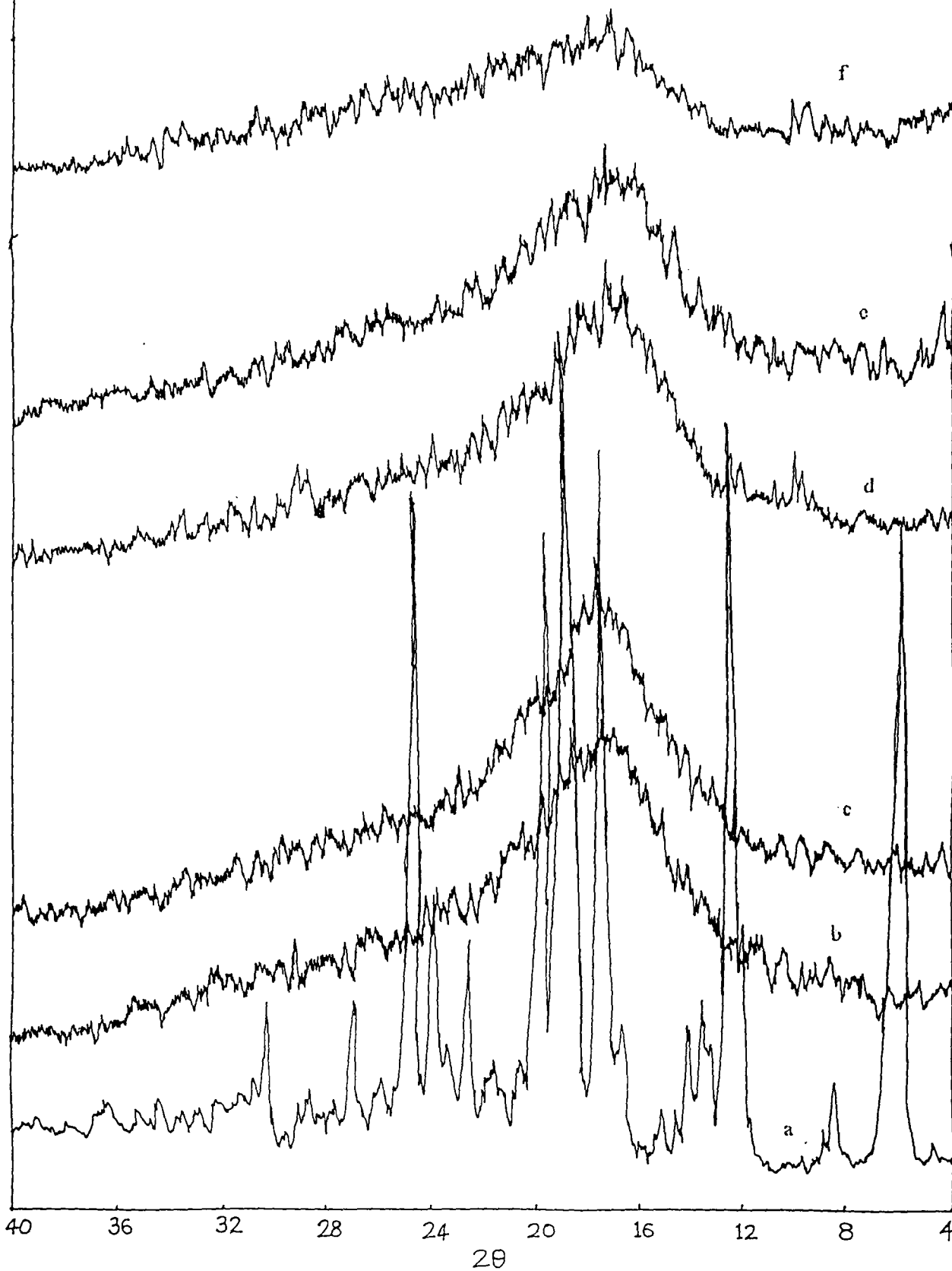


Figure 7.4

Sefcik et al (1983) for a different system. The inter-chain spacing (dsp) was not altered after addition of LC in respective PC or PSF matrix as shown in Tables. These results are in agreement with those reported by Pant (1997) [Sefcik et al (1983)].

There are no sharp peaks in the spectra suggesting that no discrete domains were observed for LC compounds in all 4 series investigated suggesting that LC material was very well dispersed in the polymers used. The LC compounds in powder form showed several sharp peaks for its crystalline nature.

Table 7.1

Inter-segmental spacing of SL1 series membranes

% of LC1 in SL1 series membranes	0%	1%	3%	6%	9%	12%
dsp in Å	4.92	4.98	4.92	4.96	4.96	4.96

Table 7.2

Inter-segmental spacing of SL2 series membranes

% of LC2 in SL2 series membranes	0%	1%	6%	12%
dsp in Å	4.92	4.99	----	4.95

Table 7.3

Inter-segmental spacing of CL1 series membranes.

% of LC1 in CL1 series membranes	0%	1%	3%	6%	9%	12%
dsp in Å	5.15	5.15	----	5.15	5.27	5.22

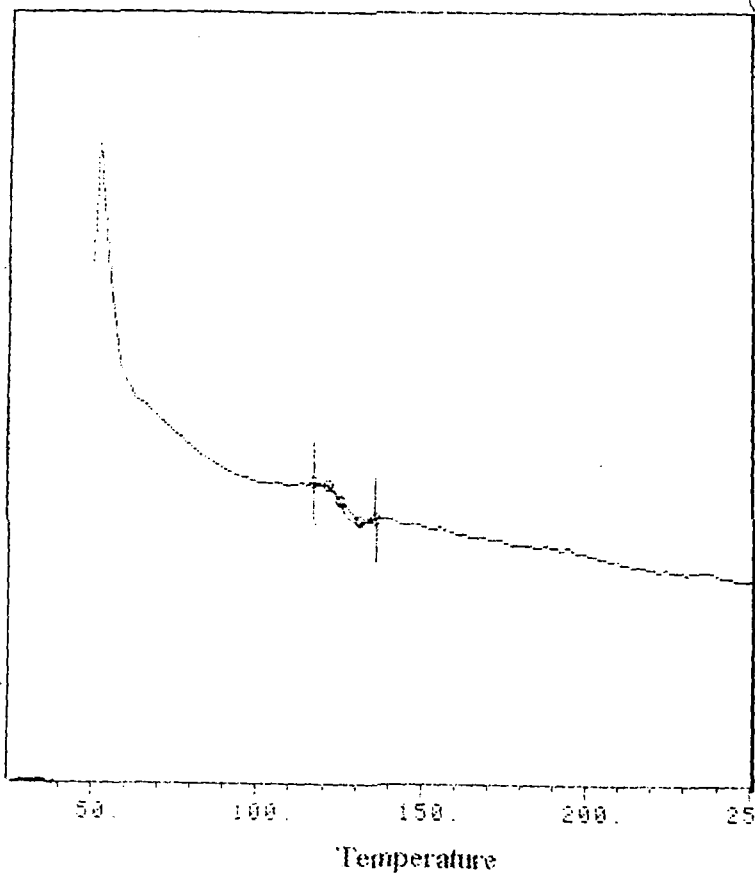
Table 7.4

Inter-segmental spacing of CL2 series membranes.

% of LC2 in C21 series membranes	0%	1%	3%	6%	9%	12%
dsp in Å	5.15	5.15	----	5.22	5.22	5.15

DSC data for all four series are summarized in Tables 7.5 and 7.6 (figures 7.5 to 7.7). After addition of LC compound in polymer matrix, the glass transition temperatures decreased for all LC-dispersed polymers. This trend was also noticed by [Huh et al (1983)]. This decrease in T_g for LC-dispersed polymeric system was in accordance with LC loading in polymer matrix [Maeda and Paul (1987b)]. Both base LC compounds showed two endothermic peaks in DSC spectra (Table 7.7, Figure 7.8), for crystalline to nematic and nematic to isotropic transitions respectively. These LC transitions were not observed separately in DSC spectra of these LC-dispersed polymers. There was a single transition supporting molecular dispersion of each LC in PC or PSF matrix. However, lowering of T_g with increase in LC concentration in all 4 series, suggests that LC addition leads to reduction in the inter-chain cohesive force of attraction and increased segmental motion of polymer chains.

DSC of 12% S1.2 series polymer.



DSC of PSF polymer.

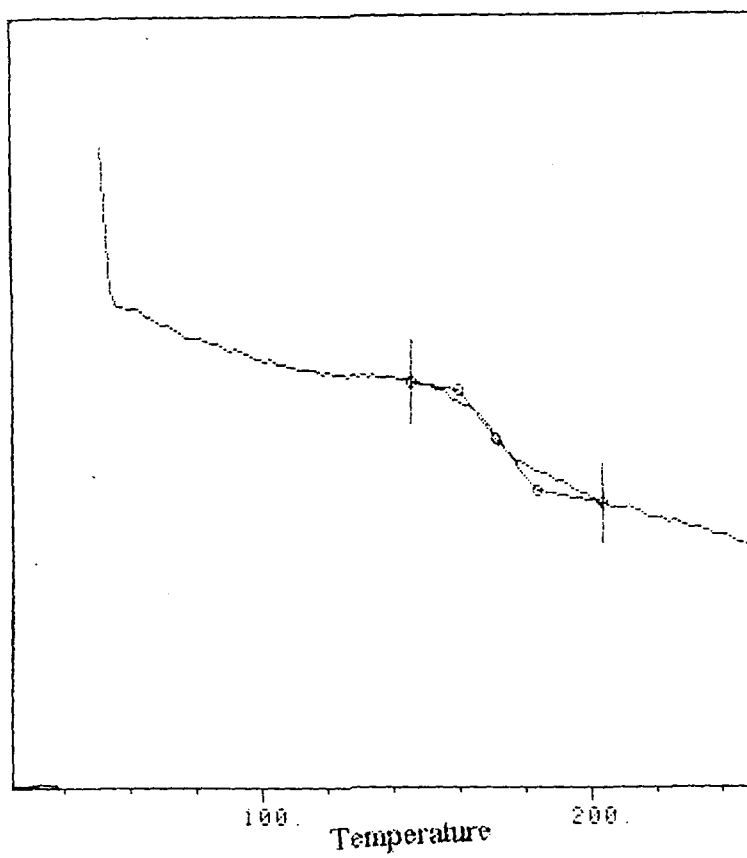


Figure 7.5 DSC of 12% and PSF polymers

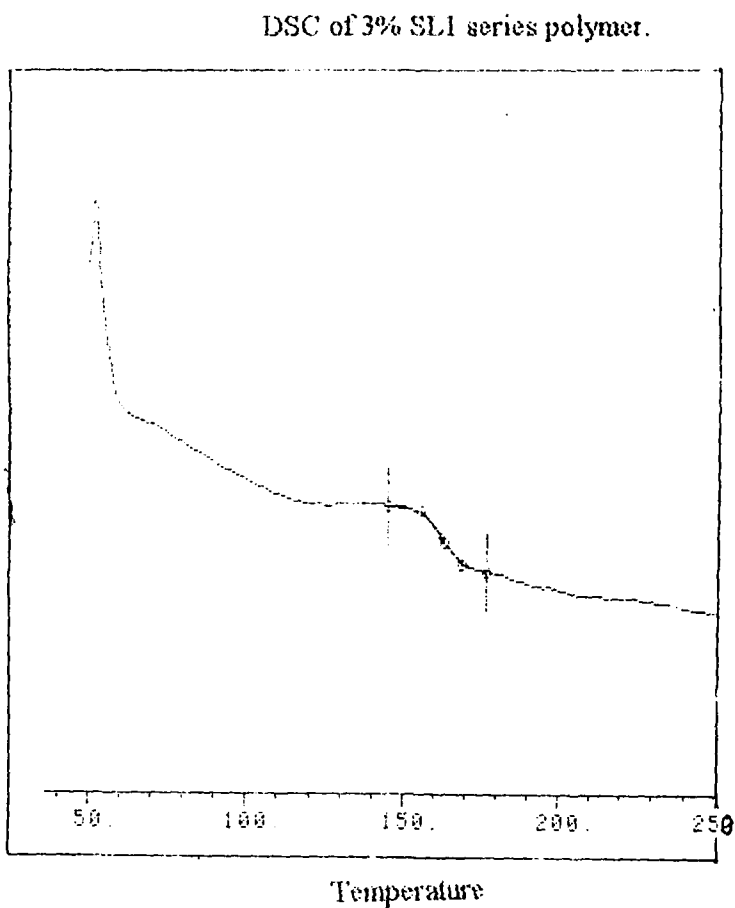
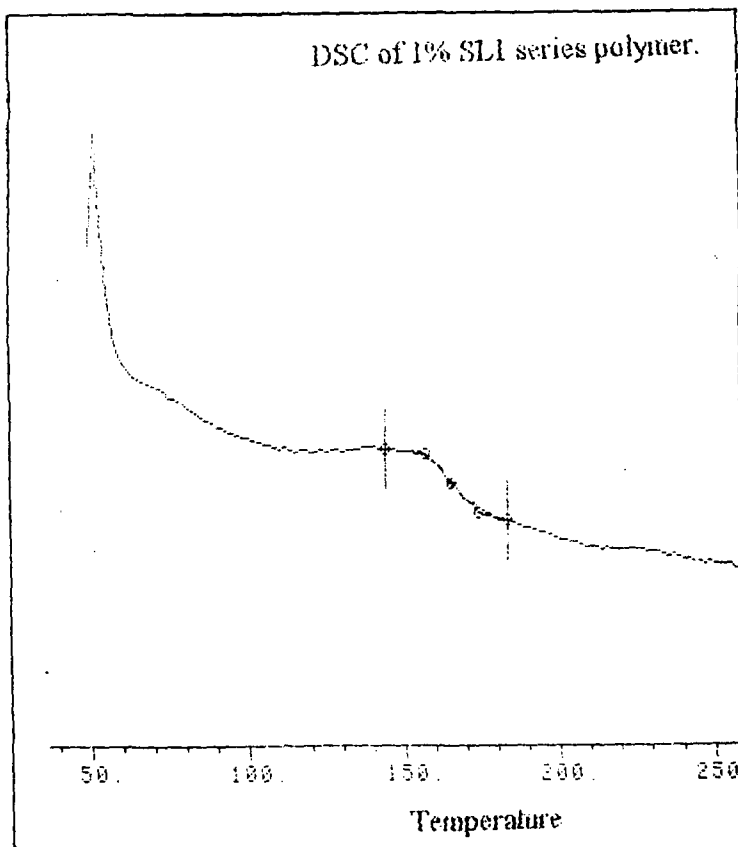


Figure 7.6 DSC of 1% and 3% SL1 series polymers

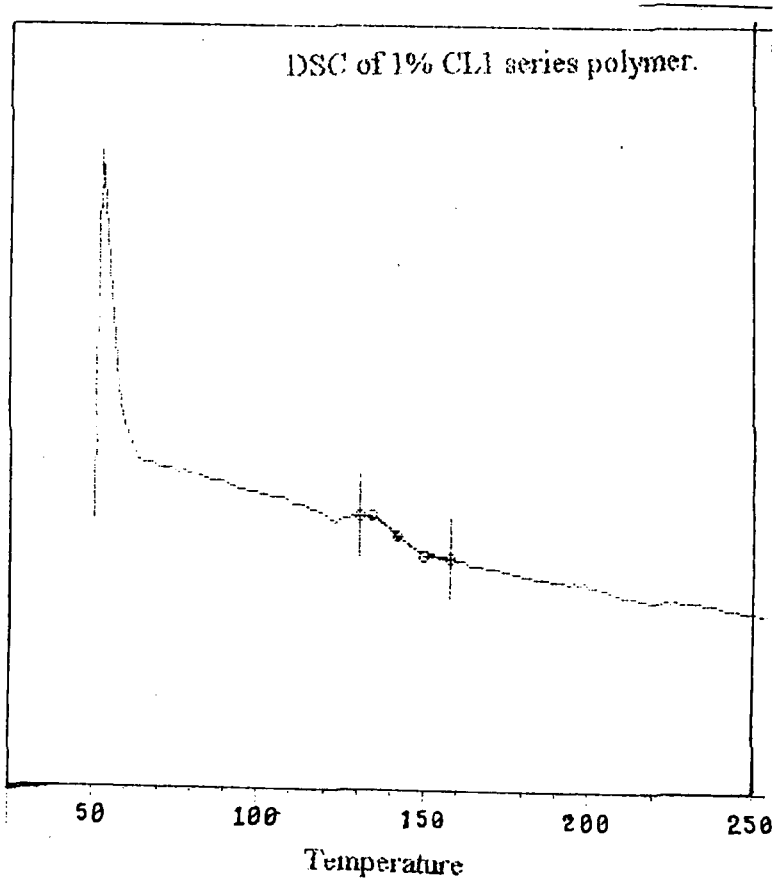
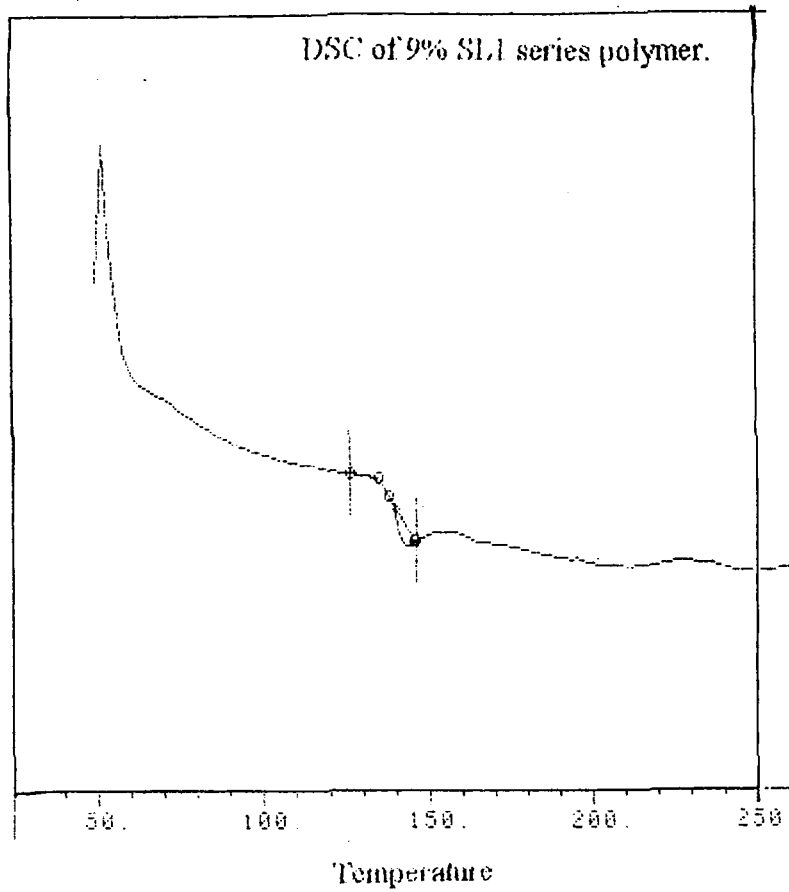


Figure 7.7 DSC of 9% SL1 and 1% CL1 series polymers

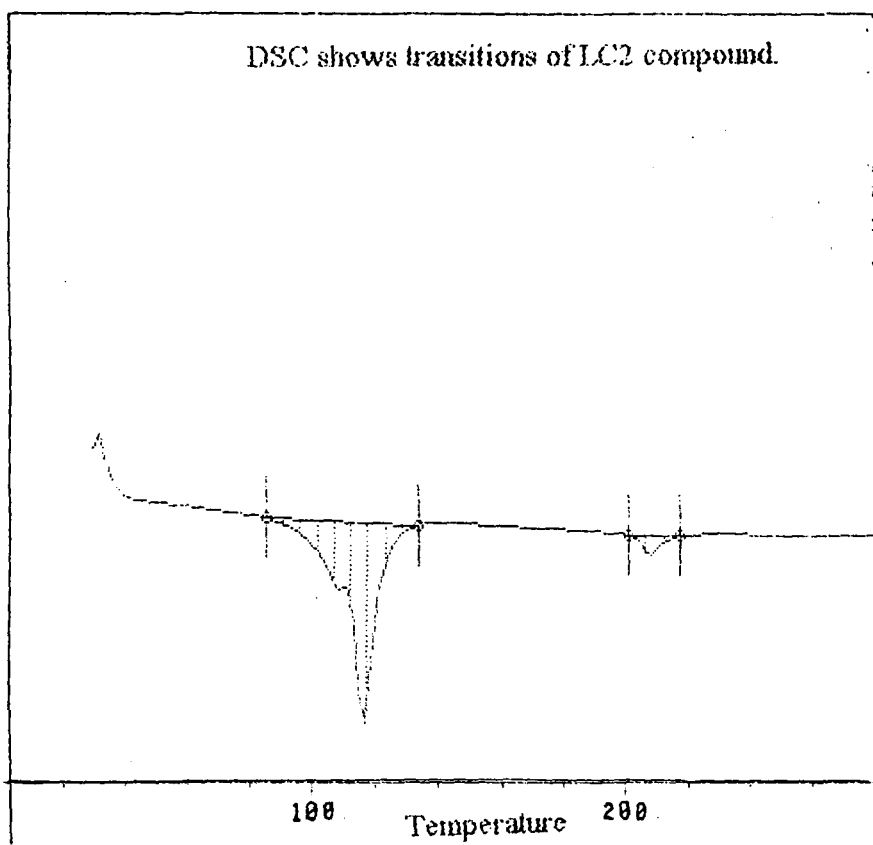
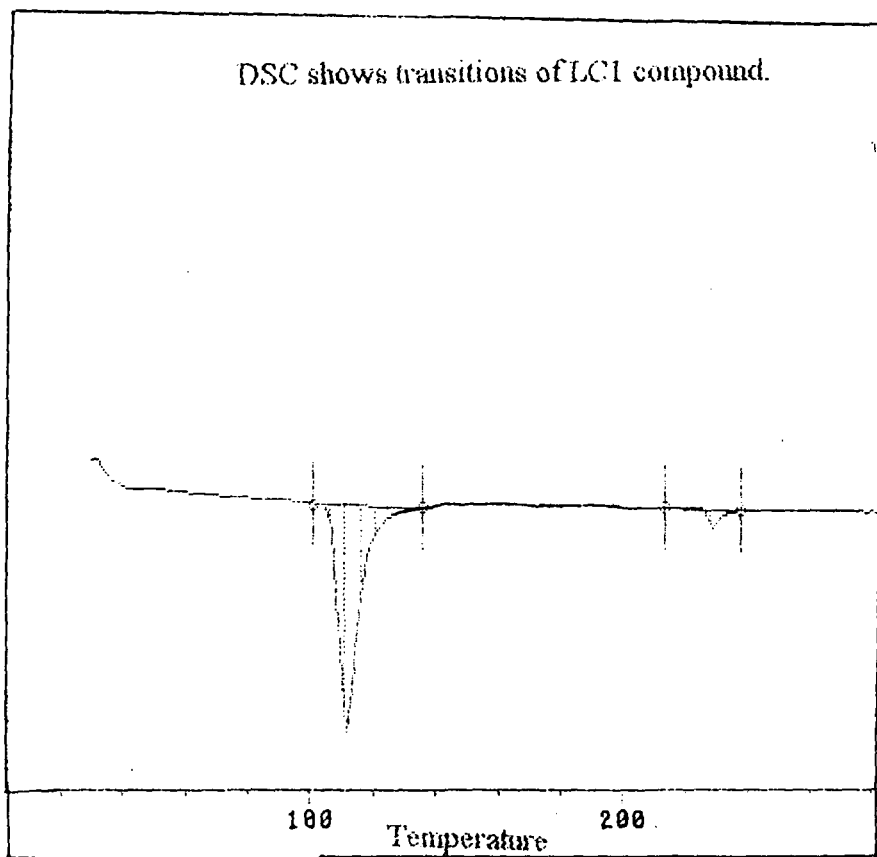


Figure 7.8 DSC of LC1 and LC2 show transitions

Table 7.5

Glass transition temperatures of SL1 and SL2 series as a function of LC.

SL1 series	Glass transition temperature (°C)	SL2 series	Glass transition temperature (°C)
PSF membrane (0%)	171	PSF membrane (0%)	171
1% SL1 membrane	165	1% SL2 membrane	172
3% SL1 membrane	161	-----	-----
6% SL1 membrane	148	6% SL2 membrane	160
9% SL1 membrane	140	-----	-----
12% SL1 membrane	---	12% SL2 membrane	128

Table 7.6

Glass transition temperatures of CL1 and CL2 series as a function of LC.

CL1 series	Glass transition temperature (°C)	CL2 series	Glass transition temperature (°C)
PC membrane (0%)	144	PC membrane (0%)	144
1% CL1 membrane	142	1% CL2 membrane	---
3% CL1 membrane	131	3% CL2 membrane	---
6% CL1 membrane	113	6% CL2 membrane	118
9% CL1 membrane	---	9% CL2 membrane	---
12% CL1 membrane	---	12% CL2 membrane	104

Table 7.7

Transition temperatures of LC1 and LC2

Liquid Crystalline material	Tranision (T_{K-N}) °C	Tranision (T_{N-I}) °C
LC1	107	227
LC2	114	207

TGA data is given in the Tables 7.8 to 7.12 for all 4 series and for LC additives. The effect of LC on thermal stability of LC-dispersed polymer was investigated by this technique. Thermal stability was examined in static air and nitrogen atmosphere. Thermal degradation is reported as the percentage weight loss of LC-dispersed polymers against temperature, (Figures 7.9 to 7.12).

LC dispersed PSF SL1 and SL2 series polymers

SL1, SL2 series polymers and pure PSF were thermally stable below 200°C only. Thermal behavior in both the environments was almost same for both the series.

Table 7.8

Thermogravimetric data for SL1 series polymers

Polymer	PSF		1% SL1 polymer		6% SL1 polymer		12% SL1 polymer	
	% weight loss		% weight loss		% weight loss		% weight loss	
Temp.°C	Air	N ₂	Air	N ₂	Air	N ₂	Air	N ₂
200°C	0.6	0.0	1.2	1.4	1.9	1.9	1.9	1.3
250°C	1.8	2.4	2.5	2.4	2.4	2.3	2.8	1.7
300°C	1.3	2.5	2.8	2.9	2.5	2.3	4.2	2.1
350°C	1.3	2.5	3.1	4.0	3.7	3.5	9.1	2.9
400°C	1.4	2.7	3.5	4.5	6.1	6.2	11.1	8.2
450°C	1.9	3.0	4.2	4.7	7.1	6.9	12.2	9.6
500°C	5.0	7.7	7.4	6.4	10.8	8.8	15.5	11.3
550°C	38.1	55.2	43.2	45.5	42.1	46.5	48.9	27.0
585°C	54.6	60.0	57.6	59.7	56.7	60.0	57.8	57.6

Table 7.9

Thermogravimetric data for SL2 series polymers

Polymer	PSF membrane % weight loss		1% SL2 polymer % weight loss		6% SL2 polymer % weight loss		12% SL2 polymer % weight loss	
	Air	N ₂	Air	N ₂	Air	N ₂	Air	N ₂
200°C	0.6	0.1	0.9	1.4	0.7	0.9	2.3	2.9
250°C	1.8	2.4	1.5	2.1	1.4	1.2	2.5	3.4
300°C	1.3	2.5	1.6	2.4	1.3	1.0	2.5	3.6
350°C	1.3	2.5	1.8	3.0	2.8	1.9	4.6	5.7
400°C	1.4	2.7	2.1	3.5	4.8	3.5	8.1	10.1
450°C	1.9	3.0	2.6	3.8	5.7	4.9	10.0	12.2
500°C	5.0	7.7	5.6	5.3	8.1	8.03	14.0	15.1
550°C	38.1	55.2	37.6	44.4	47.6	34.2	42.6	49.6
585°C	54.6	60.0	55.7	57.1	61.3	53.0	60.1	64.8

Table 7.10

Thermogravimetric data for CL1 series polymers

Polymer	PC polymer % weight loss		1% CL1 polymer % weight loss		6% CL1 polymer % weight loss		12% CL1 polymer % weight loss	
	Air	N ₂	Air	N ₂	Air	N ₂	Air	N ₂
200°C	1.6	1.1	0.6	0.4	0.1	0.7	1.4	1.4
250°C	2.0	1.7	0.9	0.9	0.2	0.8	1.5	1.5
300°C	2.3	1.8	1.3	1.2	0.6	1.2	2.1	0.9
350°C	2.4	2.0	1.8	1.6	2.1	3.1	6.2	4.3
400°C	2.9	2.4	3.9	2.7	5.0	6.3	10.7	9.8
450°C	5.5	3.6	12.7	5.3	15.2	12.9	21.6	19.9
500°C	25.7	17.2	54.1	28.2	51.2	47.5	51.1	60.7
550°C	69.6	71.7	76.4	73.2	73.4	76.4	76.1	76.4
585°C	75.4	74.1	87.3	74.8	92.2	78.2	94.0	77.9

CL1 and CL2 series polymers:

PC system is thermally more unstable compared to PSF system. CL1 and CL2 series polymers showed less degradation in nitrogen environment compared to that in static air, as expected.

Table 7.11

Thermogravimetric data for CL2 series polymers.

Polymer	PC polymer		1% CL2 polymer		6% CL2 polymer		12%CL2 polymer	
	% weight loss		% weight loss		% weight loss		% weight loss	
Temp.°C	Air	N ₂	Air	N ₂	Air	N ₂	Air	N ₂
200°C	1.6	1.1	0.4	0.8	0.2	0.3	1.3	0.1
250°C	2.0	1.7	0.3	1.2	1.1	0.3	2.0	0.9
300°C	2.2	1.9	0.5	1.6	1.6	0.9	3.2	2.2
350°C	2.5	2.0	1.2	2.4	3.0	2.7	6.6	6.0
400°C	2.9	2.4	3.4	4.7	6.8	5.6	16.8	12.1
450°C	5.5	3.6	22.0	12.2	22.9	11.2	51.4	21.0
500°C	25.7	17.2	70.2	5.6	69.4	39.1	74.8	51.9
550°C	69.6	71.6	76.2	75.8	79.6	70.0	81.2	79.7
585°C	75.4	74.1	83.8	77.7	90.7	71.4	96.1	81.2

The thermal studies of LC dispersed PC and LC dispersed PSF was undertaken firstly as a tool of polymer characterisation and as a valuable data for the future work that may be undertaken. One can study these systems below and above transition temperatures of the liquid crystals upto which the membrane materials are thermally stable.

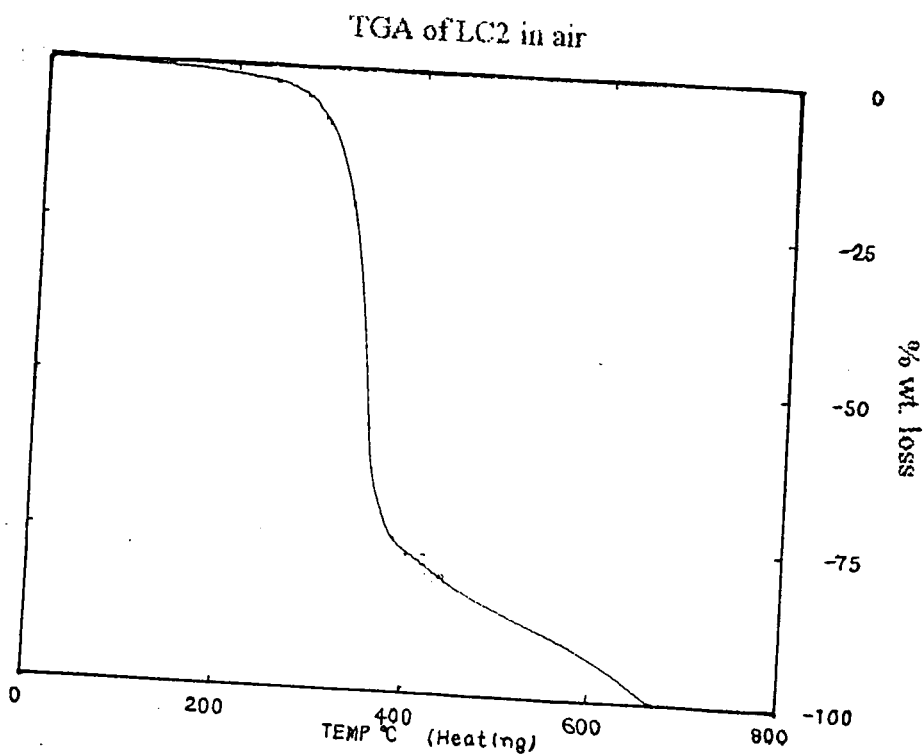
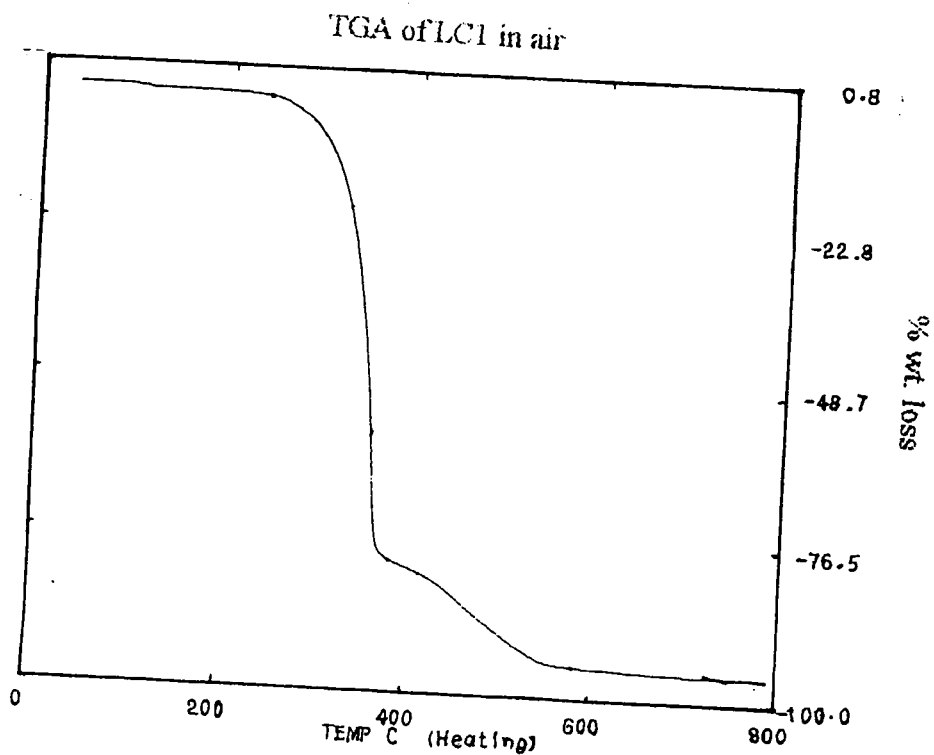
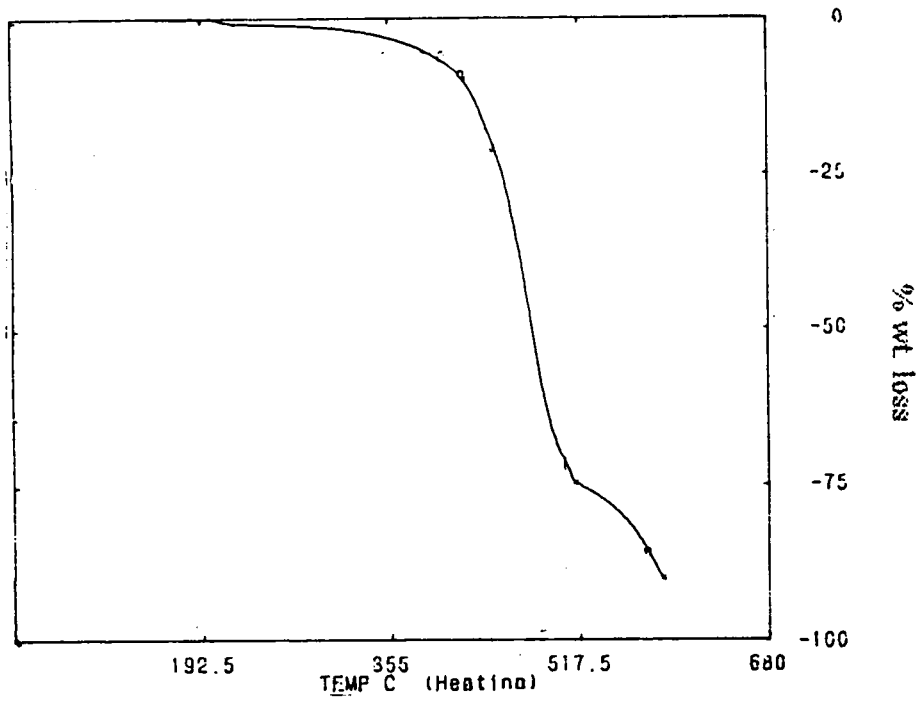


Figure 7.9 TGA of LC1 and LC2 compounds in air

TGA of 6% CL2 series polymer in air.



TGA of PC polymer in air.

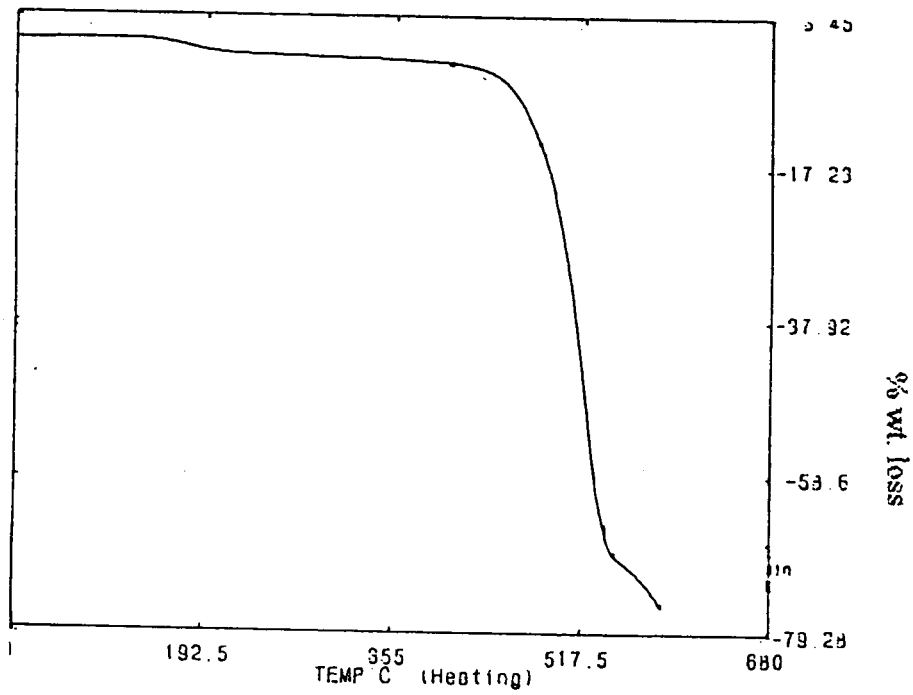
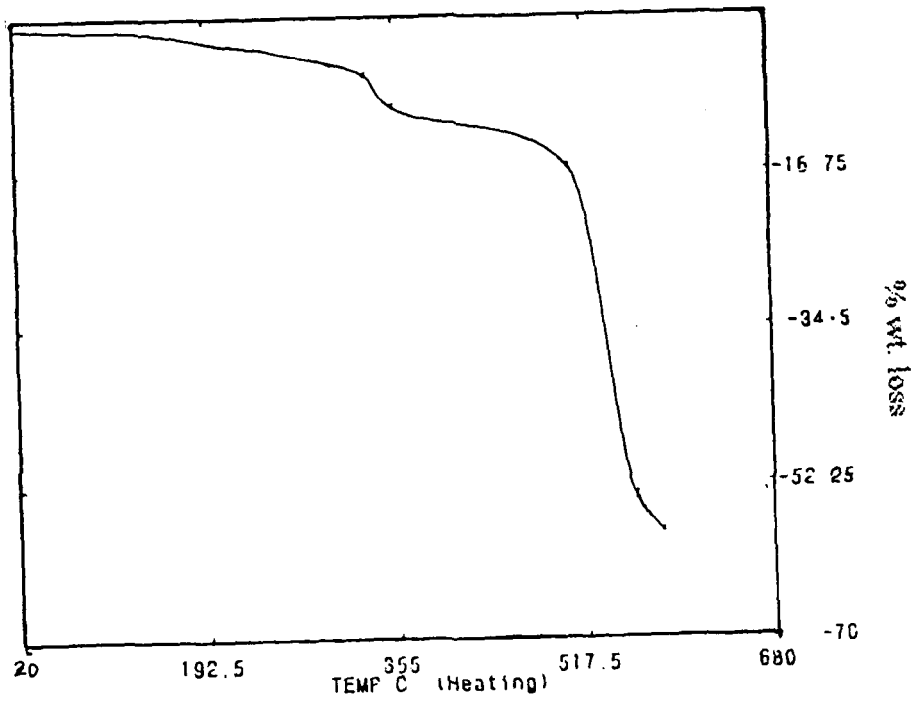


Figure 7.10 TGA of 6%CL2 and PC polymers in air

TGA of 12% SL2 series polymer in air.



TGA of 12% CL1 series polymer in air.

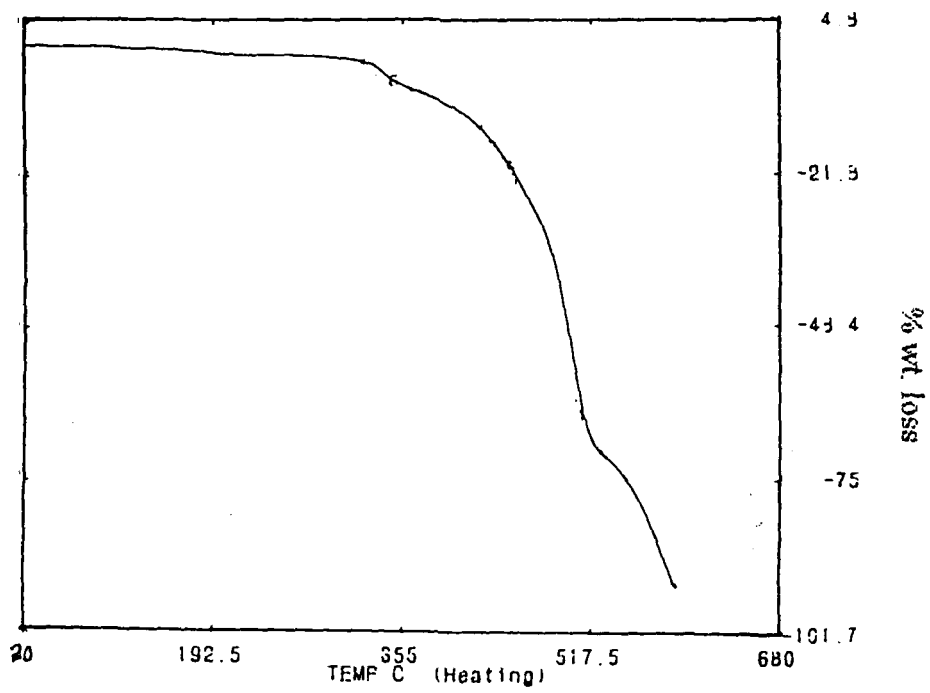


Figure 7.11 TGA of 12% SL2 and 12% CL1 series polymers

TGA of 12% SL1 series polymer in air.

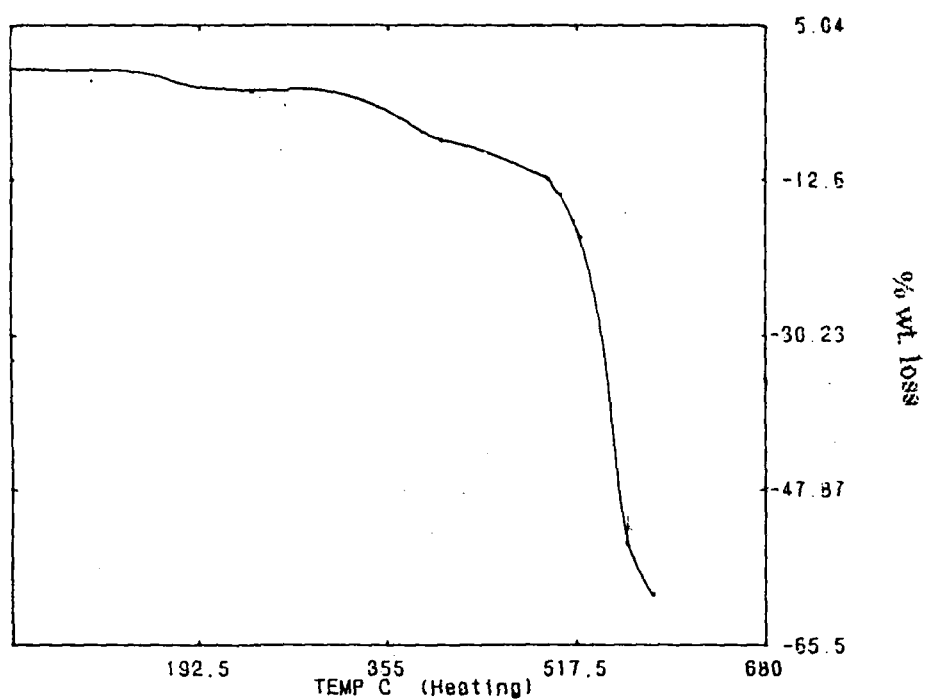


Figure 7.12 TGA of 12% SL1 series polymer in air

Table 7.12

Thermogravimetric data for LC1 and LC2.

Sample	LC1	LC2
Temp. °C	% weight loss N ₂	% weight loss N ₂
200°C	0.6	1.4
250°C	1.6	2.5
300°C	8.4	8.8
350°C	45.2	51.0
400°C	81.4	77.3
450°C	85.6	82.3
500°C	91.8	86.5
550°C	96.6	89.3
600°C	97.5	93.1
650°C	97.8	98.1
700°C	98.1	100.0
750°C	-----	-----

Density was determined for different series by floating experiments using K₂CO₃ solutions.

SL1 series:

All polymers of SL1 series showed enhancement in the density than parent polymer PSF. As LC1 concentration was increased in SL1 series the density increased from 1.240 to 1.254 [Jackson and Caldwell (1965), Jacobson (1973)]. This increased density might be because of electrostatic force of attraction between -Br atom of LC1 and -S- atom of PSF polymer and the gradual enhancement in density might be because of number of -Br atoms which are heavier.

SL2 and CL2 series:

In both series polymers, as LC2 concentration was increased, the density decreased. Dimethyl groups of LC2 additive might be reducing packing density of SL2 and CL2 series polymers. In SL2 series, density changes from 1.240 to 1.224

CL1 series:

It was observed that after addition of LC1 material in PC matrix, the density for all CL1 series polymers were lowered from 1.20 to 1.16 compared to PC. At lowest LC1 concentration (i.e. 1% LC1), density was lowest and as LC1 concentration was increased, density was gradually increased. (which were less than density of PC). This increase in density was probably because of -Br substituent of LC1 additive which was denser, hence changes from 1.16 to 1.17. Hence LC1 is denser than LC2 but lighter than PC. The LC1 when dispersed at lower concentration (1%) allowed to form more population of smaller free volume making the material lightest and further increase in LC1 concentration reduce the free volume resulting in an increase in density which is lower than parent polymer.

Gas permeation

Permeation data for all four series as a function of respective LC concentration is summarized in Tables 7.13, 7.15, 7.17 and 7.19 for He, N₂, O₂ and CO₂ (Figures 7.13 to 7.16). The permeability and selectivity data of LC-dispersed polymeric membranes were compared with their respective parent polymeric membrane. All four series showed decrease in the permeability for all gases. This decrease in permeability was gradual with respective LC loading [Maeda and Paul (1987a), (1987d); Kamal et al (1984); Lee et al (1991); Ruiz-Trevino and Paul (1997)]. Selectivity data for all four series was summarized in Tables 7.14, 7.16, 7.18 and 7.20.

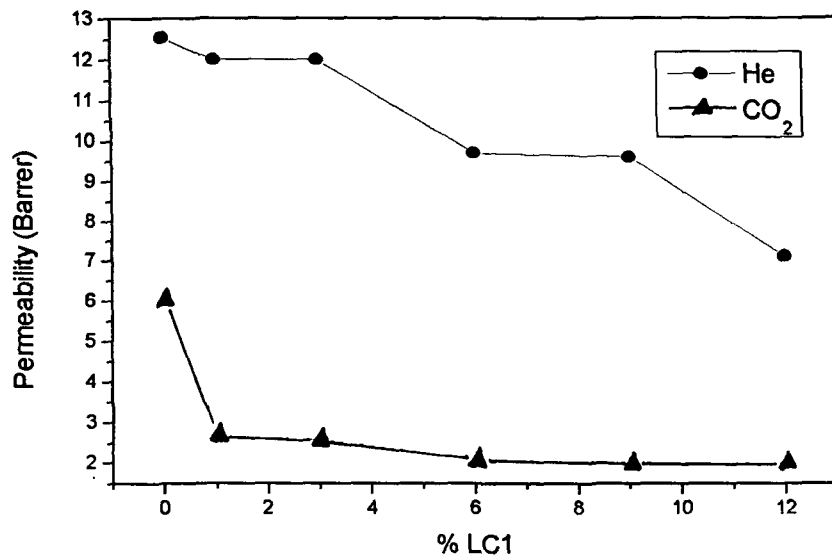
SL1 series

In this series, as LC1 concentration increased from 1% to 12%, there was a gradual decrease in permeability in the range [Maeda and Paul (1987a), (1987b)] 5-44% for helium, 13-54% for N₂, 24-55% for O₂, and 57-68% for CO₂ (Table 7.13). The selectivities were different for different gas pairs as compared to pure PSF membrane (Table 7.14). The selectivity for He/N₂ increased for all SL1 series, in which 6% and 9% loading showed maximum (53-55%) enhancement in the selectivity. The selectivity for He/CO₂ was increased for all SL1 series, in the range 70% to 130% compared to PSF membrane. Maximum increase is seen for 6% and 9% SL1 loading. The selectivity for O₂/N₂ was marginally decreased (upto 13%) for 1%, 6% and 9% of SL1 loading and other showed same selectivity. The selectivity for CO₂/N₂ was decreased remarkably in the range 31-50%, which was more or less independent of LC1 concentration.

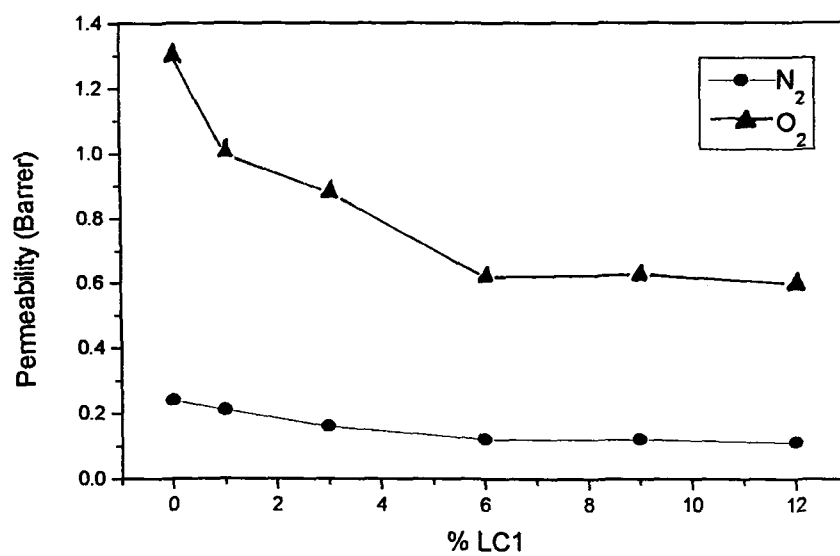
Table 7.13

Permeability of SL1 series as function of LC1 concentration.

% of LC1 in SL1 series membrane at 35°C	He (in barrer)	N ₂ (in barrer)	O ₂ (in barrer)	CO ₂ (in barrer)
0%	12.54	0.24	1.29	5.98
1%	12.0	0.21	0.99	2.6
3%	12.0	0.16	0.87	2.5
6%	9.7	0.12	0.61	2.0
9%	9.6	0.12	0.62	1.94
12%	7.1	0.11	0.59	1.9



Permeability for He and CO₂ measured at 35°C and 10 atm. as a function of % LC1 loading in SL1 series membranes.



Permeability for N₂ and O₂ measured at 35°C and 10 atm. as a function of % LC1 loading in SL1 series membranes.

Figure 7.13

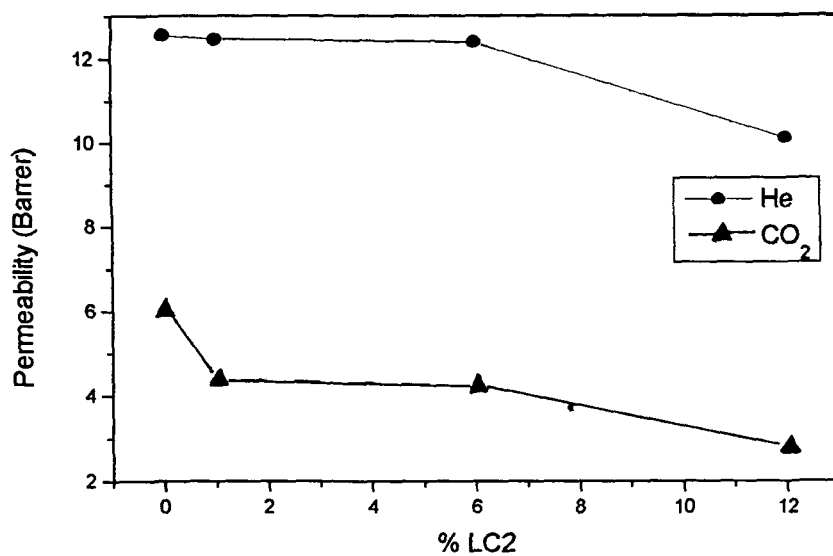
Table 7.14

Selectivity of SL1 series as a function of LC1 concentration

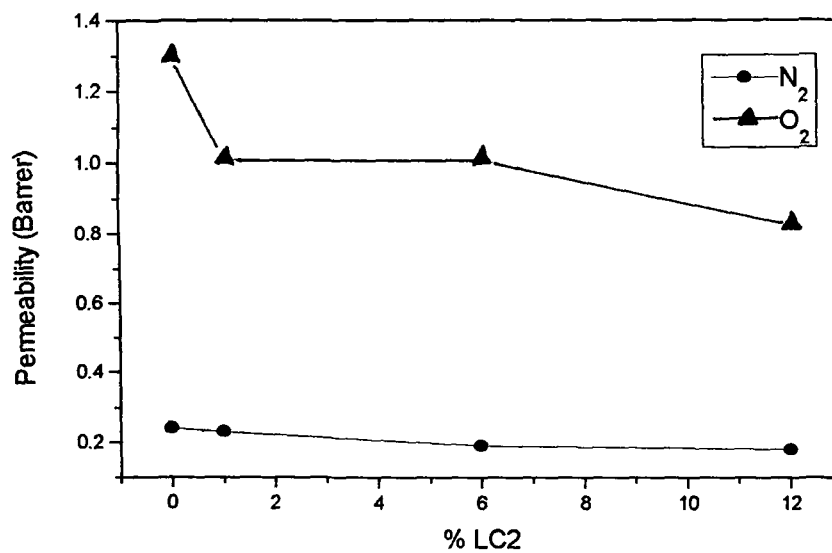
% of LC1 in SL1 series membrane at 35°C	α He/N ₂	α He/CO ₂	α O ₂ /N ₂	α CO ₂ /N ₂
0%	52.3	2.1	5.4	24.9
1%	57	4.6	4.7	12.4
3%	75	4.8	5.4	15.6
6%	81	4.85	5.1	16.7
9%	80	4.95	5.1	16.2
12%	65	3.7	5.4	17.3

SL2 series:

In this series, as LC2 concentration was increased from 1% to 12%, permeability gradually decreased [Maeda and Paul (1987b)] in the range, 1-20% for helium, 5-25% for N₂, 27-38% for O₂ and 28-58% for CO₂ (Table 7.15). The selectivity trends were different for different gas pairs as compared to pure PSF membrane (Table 7.16). The selectivity for He/N₂ was increased marginally for 1% and 12% membranes of SL2 series, while for 6% SL2, enhancement was upto 25%. The selectivity for He/CO₂ increased gradually for all SL2 series membranes, from 38% to 70% with LC loading compared to PSF membrane. Maximum increase was seen for 12% SL2 series [Maeda and Paul (1987a)]. The selectivity for O₂/N₂ was decreased marginally for all films of SL2 series in the range 2-22%. There was a considerable decrease in CO₂/N₂ selectivity for all SL2 series membranes in the range 12-38%.



Permeability for He and CO₂ measured at 35°C and 10 atm. as a function of % LC2 loading in SL2 series membranes.



Permeability for N₂ and O₂ measured at 35°C and 10 atm. as a function of % LC2 loading in SL2 series membranes.

Figure 7.14

Table 7.15

Permeability of SL2 series as function of LC2 concentration

% of LC2 in SL2 series membrane at 35°C	He (in barrer)	N ₂ (in barrer)	O ₂ (in barrer)	CO ₂ (in barrer)
0%	12.54	0.24	1.29	5.98
1%	12.45	0.23	1.0	4.34
6%	12.4	0.19	1.0	4.19
12%	10.1	0.18	0.81	2.77

Table 7.16

Selectivity of SL2 series as a function of LC2 concentration

% of LC2 in SL2 series membrane at 35°C	α He/N ₂	α He/CO ₂	α O ₂ /N ₂	α CO ₂ /N ₂
0%	52.3	2.1	5.4	24.9
1%	54	2.9	4.2	18.9
6%	65	3.0	5.3	22
12%	56	3.6	4.5	15.4

CL1 series

In this series, as LC1 concentration was increased from 1% to 12%, there was a gradual decrease in permeability in the range, 6-38% for helium, 7-49% for N₂, 26-56% for O₂ and 51-75% for CO₂ (Table 7.17). The selectivity trends were different for different gas pairs compared to pure PC membrane as given in Table 7.18. The selectivity for He/N₂ was nearly same for 1% and 3% CL1 membranes, while for 6%, 9% and 12% CL1 series membranes He/N₂ selectivity values were increased marginally upto 20% only. The selectivity for He/CO₂ increased gradually for all CL1 series membranes, from 90% to 140% compared to PSF membrane. Maximum

increase for He/CO₂ was observed for 9% and 12% CL1 series membranes. The selectivity for O₂/N₂ was decreased slightly in the range 13-20% for all CL1 series membranes. The selectivity for CO₂/N₂ was decreased remarkably in the range 53-48% for all CL1 series.

Table 7.17

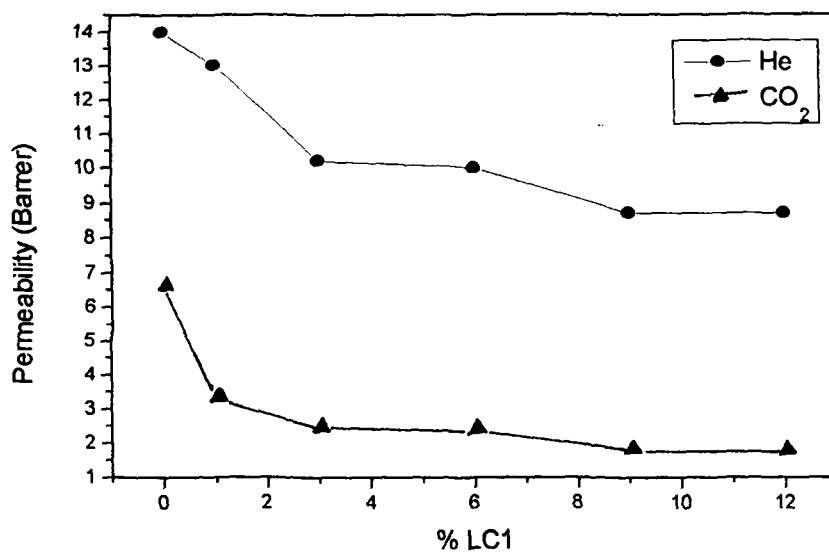
Permeability of CL1 series as function of LC1 concentration

% of LC1 in CL1 series at 35°C	He (in barrer)	N ₂ (in barrer)	O ₂ (in barrer)	CO ₂ (in barrer)
0%	14	0.289	1.48	6.5
1%	13	0.27	1.1	3.2
3%	10.2	0.22	0.99	2.35
6%	10.0	0.20	0.88	2.3
9%	8.7	0.16	0.7	1.7
12%	8.7	0.15	0.65	1.66

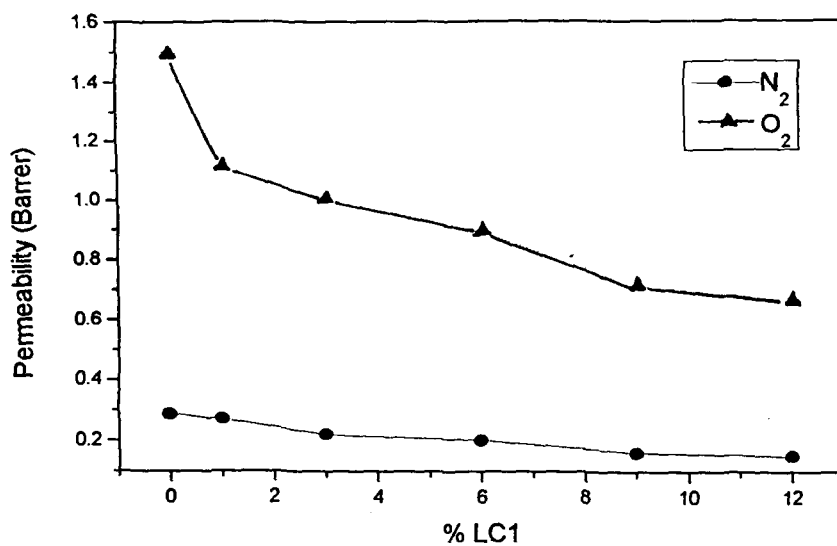
Table 7.18

Selectivity of CL1 series as a function of concentration

% of LC1 in CL1 series at 35°C	α He/N ₂	α He/CO ₂	α O ₂ /N ₂	α CO ₂ /N ₂
0%	48.4	2.15	5.12	22.5
1%	48	4.1	4.1	11.8
3%	46	4.3	4.5	10.7
6%	50	4.3	4.4	11.5
9%	54	5.1	4.4	10.6
12%	58	5.2	4.3	11.0



Permeability for He and CO₂ measured at 35°C and 10 atm. as a function of % LC1 loading in CL1 series membranes.



Permeability for N₂ and O₂ measured at 35°C and 10 atm. as a function of % LC1 loading in CL1 series membranes.
Figure 7.15

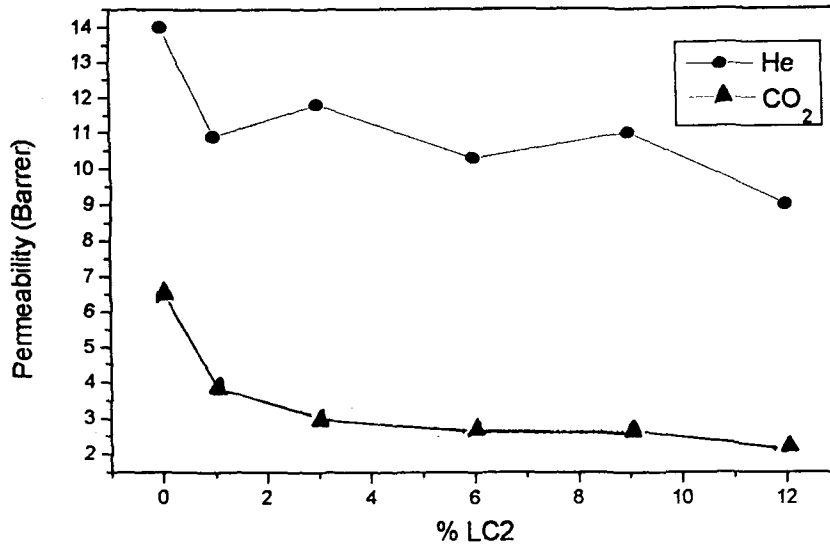
CL2 series

In this series, as LC2 concentration was varied from 1% to 12%, there was a decrease in permeability in the range, 16-36% for helium, 10-35% for N₂, 26-49% for O₂ and 42-68% for CO₂ (Table 7.19). The selectivity for He/N₂ showed marginal decrease for 1%, 6% and 12% CL2 membranes, while 3% and 9% CL2 membranes showed slight increase in selectivity as compared to PC membrane. The selectivity for He/CO₂ was increased gradually for all CL2 series membranes, in the range 35% to 100% compared to PC membrane (Table 7.20). Maximum increase was observed for 12% CL2 series membrane. The selectivity for O₂/N₂ was decreased marginally in the range 11-22% for all CL2 series membranes. The selectivity for CO₂/N₂ was decreased remarkably in the range 36-52% for all CL2 series membranes.

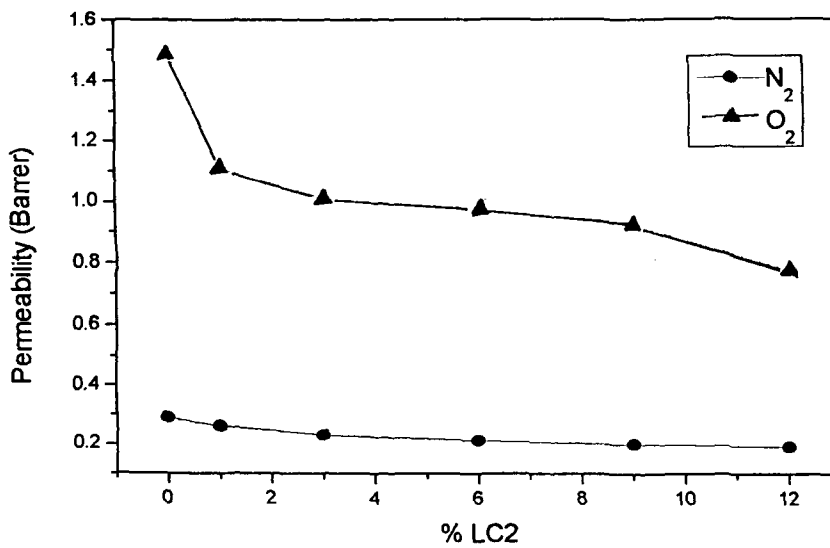
Table 7.19

Permeability of CL2 series as function of LC2 concentration.

% of LC2 in CL2 series at 35°C	He (in barrer)	N ₂ (in barrer)	O ₂ (in barrer)	CO ₂ (in barrer)
0%	14	0.289	1.48	6.5
1%	10.9	0.26	1.1	3.8
3%	11.8	0.23	1.0	2.9
6%	10.3	0.21	0.96	2.6
9%	11.0	0.20	0.91	2.6
12%	9.0	0.19	0.76	2.1



Permeability for He and CO₂ measured at 35°C and 10 atm. as a function of % LC2 loading in CL2 series membranes.



Permeability for N₂ and O₂ measured at 35°C and 10 atm. as a function of % LC2 loading in CL2 series membranes.

Figure 7.16

Table 7.20

Selectivity of CL2 series as a function of LC2 concentration

% of LC2 in CL2 series at 35°C	α He/N ₂	α He/CO ₂	α O ₂ /N ₂	α CO ₂ /N ₂
0%	48.4	2.15	5.12	22.5
1%	42	2.9	4.2	14.6
3%	51	4.1	4.3	12.6
6%	49	4.0	4.6	12.4
9%	55	4.2	4.6	13.0
12%	47	4.3	4.0	11.0

7.1.2 Discussion

7.1.2.1 SL1 series

Relation between physical properties and permeability of polymers

WAXD spectra of SL1 series membranes showed resemblance with parent PSF membrane. These spectra did not show presence of any distinct sharp peak for LC1 material and the inter-chain spacing (dsp) is of the same order as compared to PSF. While DSC data showed a single peak for films of SL1 series, all T_{gs} gradually decreased with increasing LC1 concentration in the series. This reduction indicates that inter-chain interactions of polymer PSF are reduced. It favours processibility at lower temperature. On the other hand, thermal stability was not affected by addition of LC1 material, as observed from the TGA data. Transition temperatures corresponding to LC1 were not detected in TGA and DSC, The polymer density of SL1 series increased gradually with LC1 concentration in the PSF matrix. This could be attributed to more pronounced interactions of polar bromine on LC and S on PSF. The SL1 series showed gradual decrease in the permeabilities with LC1 concentration for all gases used (He, N₂, O₂ and CO₂).

Possible mechanism for permeability reduction in SL1 series

It is possible to explain the probable mechanisms of the permeability reduction in the SL1 series with LC1 addition by (1) antiplasticization, or (2) stiffening of the polymer chains.

(1) Antiplasticization : The addition of certain low molecular weight additive in polymer, enhances modulus and tensile strength, while reduces the elongation, and impact strength of the polymer. This phenomena is called antiplasticization and additive is called as antiplasticizer [Jackson and Caldwell (1967a)]. In the SL1 series polymers, WAXD data showed that d-spacing was not altered, while density gradually increased with LC1 addition. This increase in density was either by interactions between polymer and additive or because of heavier -Br atom present in LC1 compound, whereas the permeability reduction in the SL1 series membranes was because of either (1) antiplasticization, or (2) by stiffening in PSF polymer chains.

LC1 might be acting as an antiplasticizer by interacting with PSF polymer chains, which decreased fractional free volume without changing the interchain distance. This resulted in decreased gas permeability. Similar situation was observed by Sefcik et al (1983) wherein TCP additive was antiplasticizing PVC polymer below 15% concentration with same d-spacing values and resulted in decrease in the gas permeability. In case of SL1 series polymers, T_g gradually decreased with LC1 addition. Normally, T_g was decreased with plasticization effect and in very few cases by antiplasticization as well [Maeda and Paul (1987a), (1987b)].

(2) Stiffening of PSF polymer chains: In case of SL1 series polymers, the density increased because of the heavier -Br atom of LC1 additive, with similar interchain distance of PSF polymer. In this case, LC1 additive stiffened the polymer chains by hindering the inter-segmental motions. This resulted in reduction in the free volume of

the polymer [Maeda and Paul (1987a), (1987d)]. Thus, the gradual reduction in the gas permeability was observed for SL1 series membranes.

7.1.2.2 SL2, CL1 and CL2 series

Relation between physical properties and permeability of polymers

WAXD spectra of polymers of these three series showed similarities with PC or PSF. There was no change in the inter-chain spacing of these three series polymers. T_g of all polymers of three series, decreased with increase in LC concentration. This indicates interruption of polymer- polymer interaction due to the presence of LC component. SL2 series of PSF showed thermal stability upto reasonably high temperature. Thus the addition of LC materials did not affect thermal stability of the PSF to any extent, especially in the range applications for gas separations. Thermal stability of PC is relatively low as compared to PSF. Addition of LC materials in PC matrix though has lowered the thermal stability. However, this lowering has not hampered the use of these dispersed system as a membrane material significantly. In DSC, absence of transition temperature peaks corresponding to LC1 or LC2 in PC or PSF indicate homogeneous dispersion of the liquid crystalline moieties in polymer matrix. The miscibility of LC in the polymer was supported by WAXD (which showed absence of sharp peak). In the case of SL2 and CL2 series polymers, density decreased with increase in LC2. For CL1 series polymers, density decreased for all LC1 concentration, as LC1 concentration decreased density decreased. The d-spacing values were unaltered to that of the parent polymer. The permeability of all gases used (He, N₂, O₂ and CO₂) decreased with respective LC concentration, indicating that LC was acting as a barrier.

Probable mechanism for reduction in permeability in SL2, CL1 and CL2 series

In these three series, the density of the polymers decreased compared to PC or PSF, but inter-chain spacing remained constant. Permeability decreased with LC concentration. This means that addition of LC causes disorder in chain configuration of the polymeric matrix. It acts as a gas barrier or obstacle for the gas molecules. [Pace and Datyner (1979)] and occupy the channel passage and decreasing the free volume available for the gas molecules. This simultaneously screens up for the gas molecules on the basis of their size, shape, diffusivity and solubility in the polymer matrix. Thus, the reduction in permeability for each gas was different in the three series membranes (i.e. the percentage permeability reduction was different for each gas). This behavior of LC may be due to that of impermeable flake (or lamelle) [Cussler et al (1988), (1990); Eitzman et al (1996)]

7.1.3 Investigation of permeation of LC-dispersed polymeric systems

In all the four series, overall permeabilities decreased with increase in LC concentration for all gases used compared to PC and PSF. Helium is small and inert, diffuses faster than other gases. It showed small reduction in permeability compared to other gases. Nitrogen is a large molecule compared to He molecule, therefore, there was a large decrease in permeability, while O₂ molecule has slightly smaller kinetic diameter than N₂. It was observed from permeability of O₂ and N₂, that the % permeability reduction remained nearly similar at all LC concentrations in all four series membranes.

In LC-dispersed polymer membranes, permeability of CO₂ decreased. This reduction in permeability was probably because of the arrangement or orientation of LC in respective polymer matrix [Eitzman et al (1996)], which acts as a gas barrier. Thus, lowering in permeability was seen.

In all four series, the selectivity for He/N₂ was increased compared to parent polymer in PSF based polymers (i.e. for SL1 and SL2 series membranes) and remained same for CL1 and CL2 series. This was due to the large decrease in N₂ permeability compared to He permeability with increased LC concentration. The selectivities of He/CO₂ increased with increase in LC concentrations in all the four series. This was because of the small decrease in permeability of He and dramatic lowering in permeability of CO₂ [Maeda and Paul (1987b), Ruiz-Trevino and Paul (1997)]. In case of O₂/N₂ selectivity, there was a marginal change compared to parent polymer, as both gases showed similar decrease in their permeabilities, whereas, the decreased selectivity for CO₂/N₂, was mainly because of the dramatic reduction in permeability of CO₂ gas.

By careful analysis of permeability selectivity data, for polysulfone based membranes SL1 series, about 6% and 3% concentration of LC1 appears to be optimum for better selectivity and permeability. These membranes may find applications as helium selective membrane and probably for H₂/CO₂ separation.

7.1.4 LC compounds as the membrane materials in PSF and PC matrices.

TGA showed that basically pure PSF is more thermally stable than PC polymer. After addition of LC1 and LC2 in PSF matrix, thermal stability of LC-dispersed PSF matrices were not altered at any concentration (used), whereas, in the dispersed PC membranes, the complete degradation (>90% at 600°C) with increased LC concentration was observed, which was independent of type of LC material.

Film density after LC dispersion in PC matrix were observed to be decreased. While PSF matrix distinguishes between LC1 and LC2 additives and interacts in different ways, SL1 series membranes have higher density than pure PSF and SL2

series membranes density lower compared to PSF. This indicate that SL1 series membranes have better packing arrangement of PSF and LC1 material compared to SL2 series membranes.

WAXD spectra of all four series membranes showed resemblance with their parent polymer spectrum, which showed that LC compounds were not changing inter-chain spacing of the polymer, and which indirectly reduced the free volume available.

In PC matrix, after addition of LC, the permeability was lower as compared to PSF matrix. Enhancement in selectivities does not compensate the reduced permeabilities of different gases. Thus, LC dispersed PC membranes can act as better barrier material than PSF.

7.2 Metal Complex -Dispersed Polymeric Membranes

In this section, three series of MX_n -dispersed polymer membrane systems are discussed. There are:

- 1) SFe series: $\text{Fe}(\text{acac})_3$ dispersed in PSF.
- 2) SCo series: $\text{Co}(\text{acac})_3$ dispersed in PSF.
- 3) CFe series: $\text{Fe}(\text{acac})_3$ dispersed in PC.

7.2.1 Results

WAXD spectra of the MX_n -dispersed series of membranes showed resemblance to PC and PSF as noted by [Pant (1997); Sefcik et al (1983)]. However, there were some marginal changes in the intensity of the peaks. No separate peak corresponding to the crystalline metal complex was observed indicating absence of microcrystalline domain. The broad diffused peaks indicated the amorphous nature of polymer. Intensity maxima of these broad peaks indicated that there was hardly any change in the d-spacing of the polymer for concentrations upto 30% w/w. The d-spacing data of the systems is presented in Tables 7.21 to 7.23, (figures 7.17 to 7.19).

Table 7.21

Intersegmental spacing for SCo series membranes.

% of $\text{Co}(\text{acac})_3$ (w/w)	0%	5%	10%	20%	30%
dsp in Å for SCo films	5.04	5.01	4.98	4.96	5.01

Table 7.22

Intersegmental spacing for SFe series membranes.

% of $\text{Fe}(\text{acac})_3$ (w/w)	0%	5%	10%	20%	30%
dsp in Å for SFe membranes	5.04	4.95	4.92	4.95	4.92

WAXD spectra of SCo series polymers, a) $\text{Co}(\text{acac})_3$, b) 0%, c) 5%, d) 10%, e) 20% and f) 30% series polymer.

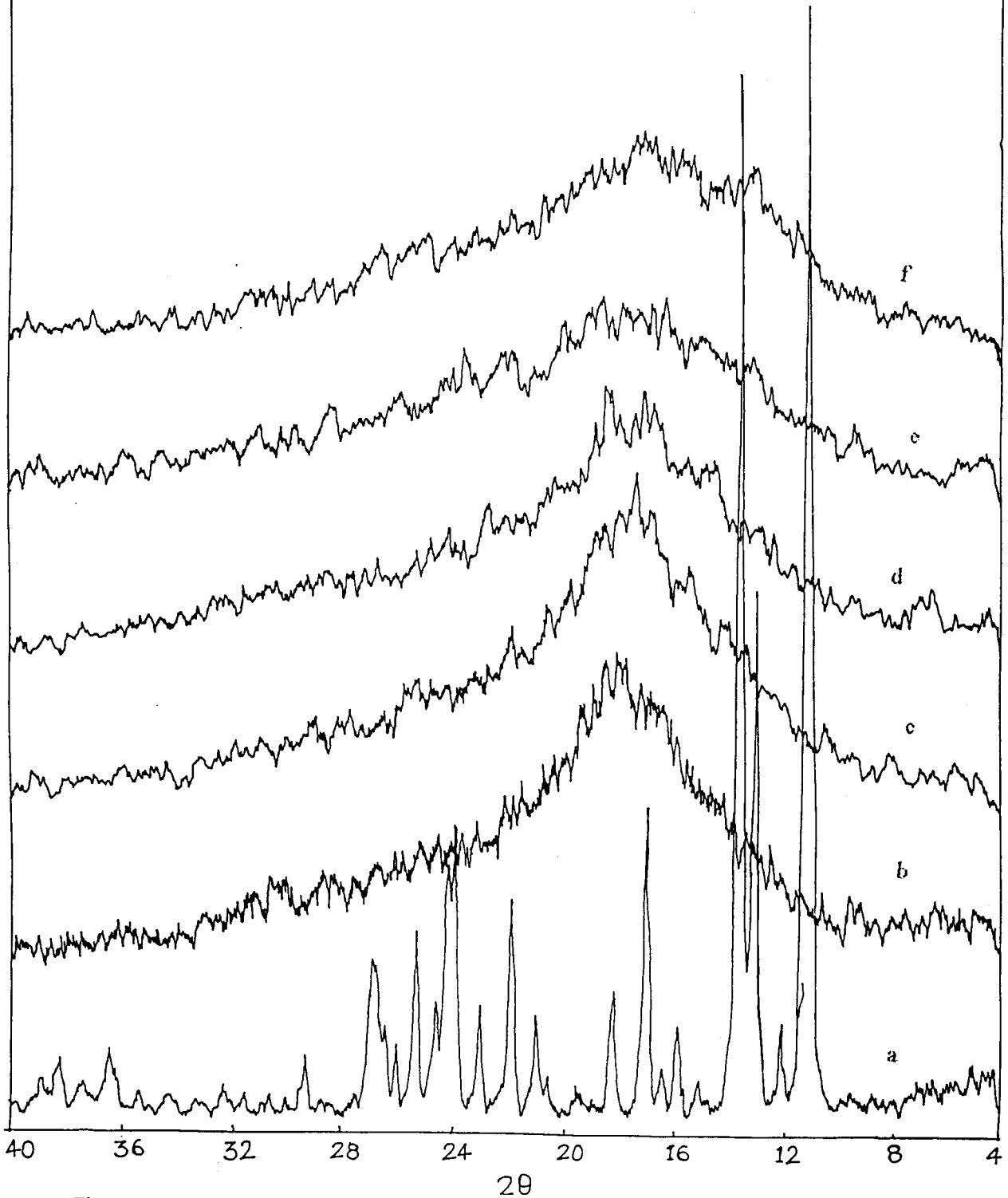


Figure 7.17 WAXD spectra of SCo series polymers, a) $\text{Co}(\text{acac})_3$, b) 0% (PSF), c) 5%, d) 10%, e) 20%, f) 30% series polymer.

WAXD spectra of SFe series polymers, a) $\text{Fe}(\text{acac})_3$, b) 0%, c) 5%, d) 10%, e) 20% and f) 30% series polymer.

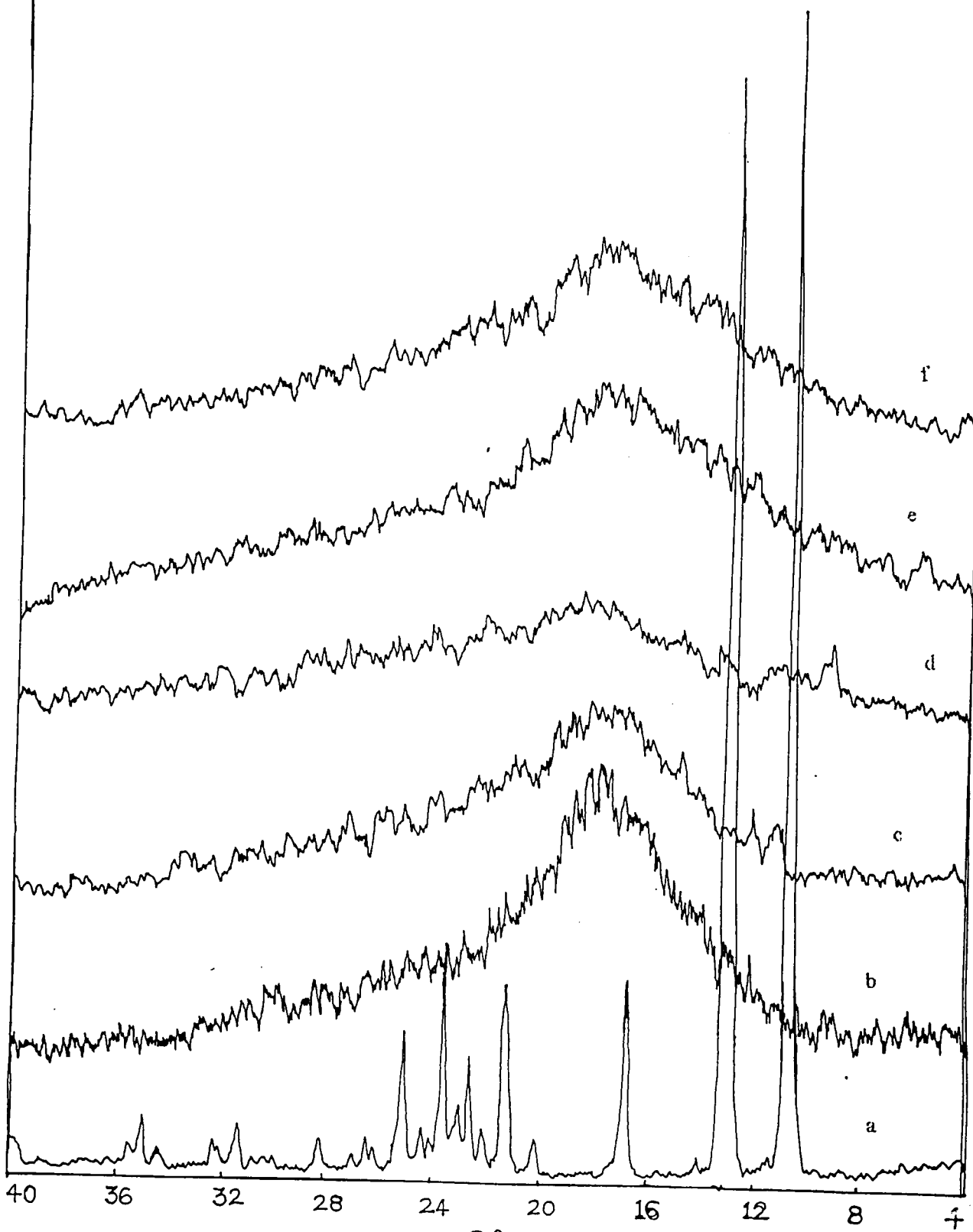


Figure 7.18 WAXD spectra of SFe series polymers, a) $\text{Fe}(\text{acac})_3$, b) 0% (PSF), c) 5%, d) 10%, e) 20%, f) 30% series polymer.

WAXD spectra of CFe series polymers, a) $\text{Fe}(\text{acac})_3$, b) 0%, c) 5%, d) 10%, e) 20% and f) 30% series polymer.

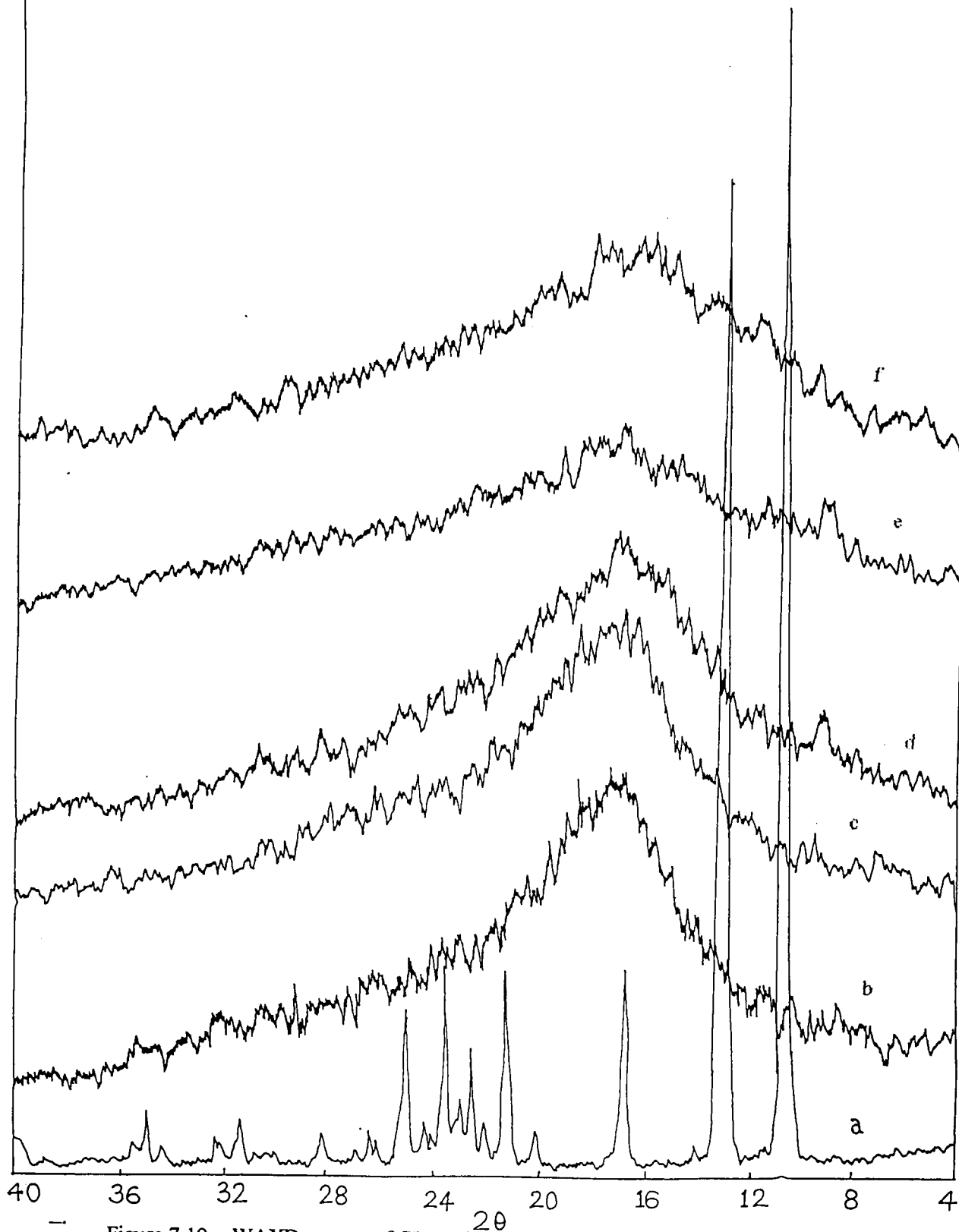


Figure 7.19 WAXD spectra of CFe series polymers, a) $\text{Fe}(\text{acac})_3$, b) 0% (PC), c) 5%, d) 10%, e) 20%, f) 30% series polymer.

Table 7.23

Intersegmental spacing for CFe series membranes.

% of Fe(acac) ₃ (w/w)	0%	5%	10%	20%	30%
dsp in Å for CFe membranes	5.15	5.15	5.27	5.19	5.27

TGA data of all three series (SCo, SFe and CFe) of polymers and the pure metal complexes are presented in Tables 7.24 to 7.27 (figures 7.20, 7.21). The thermal stability of polymer matrix after addition of MX_n was investigated in air and nitrogen using TGA. The thermal stability of SFe and SCo series membrane materials were low but did not affect permeation properties, as the studies were conducted at much lower temperature. The thermal stability of these systems decreased with increasing concentration of metal complex in air and N₂ compared to PSF.

Table 7.24

Thermal degradation of SCo series as a function of temperature

Polymer	PSF (% wt. loss)		5% SCo (% wt. loss)		10% SCo (% wt. loss)		20% SCo (% wt. loss)	
	Air	N ₂	Air	N ₂	Air	N ₂	Air	N ₂
200° C	0.62	0.0	4.3	2.1	3.5	3.0	6.7	7.7
250° C	1.79	2.4	4.7	5.4	7.1	9.9	12.9	16.1
300° C	1.3	2.5	5.2	6.2	8.1	10.2	14.2	16.8
350° C	1.3	2.5	5.7	6.4	9.4	10.5	15.8	17.4
400° C	1.4	2.7	6.0	6.9	11.0	10.7	17.5	18.0

Table 7.25

Thermal degradation of SFe series as a function of temperature

Polymer	PSF (% wt. loss)		5% SFe (% wt. loss)		10% SFe (% wt. loss)		20% SFe (% wt. loss)	
	Air	N ₂	Air	N ₂	Air	N ₂	Air	N ₂
200°C	0.62	0.0	0.95	1.9	1.2	12.8	1.5	1.4
250°C	1.79	2.4	2.72	4.6	3.9	12.1	6.0	5.3
300°C	1.3	2.5	3.51	5.1	5.5	4.5	8.0	6.6
350°C	1.3	2.5	4.2	5.5	6.7	5.6	10.1	8.5
400°C	1.4	2.7	4.8	5.8	7.5	6.0	11.2	9.4

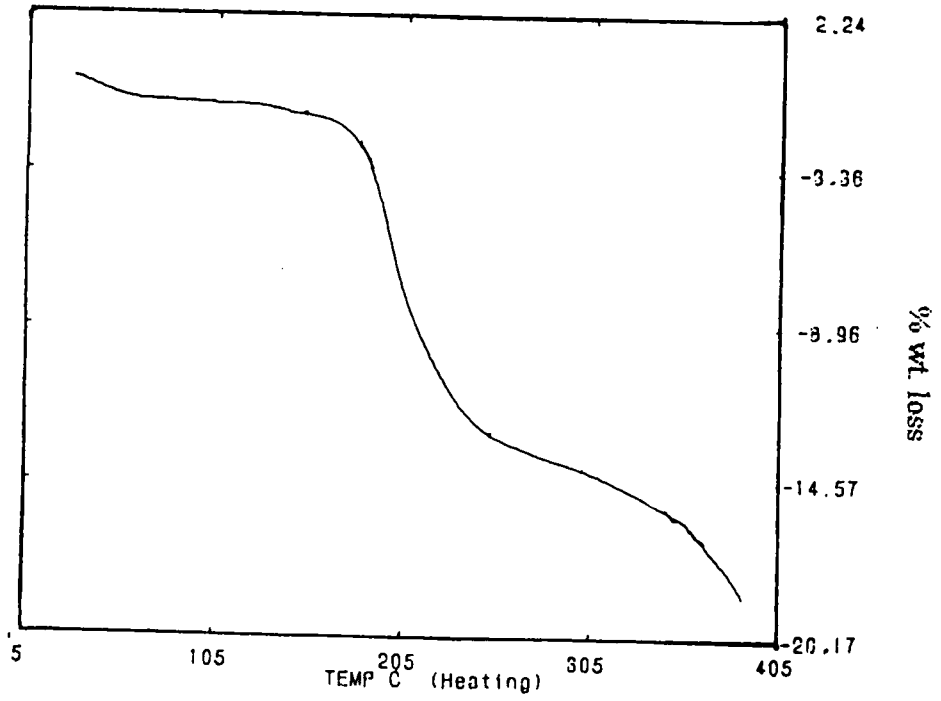
Table 7.26

Thermal degradation of CFe series as a function of temperature.

Polymer	PC (% wt. loss)		5% CFe (% wt. loss)		10% CFe (% wt. loss)		20% CFe (% wt. loss)	
	Air	N ₂	Air	N ₂	Air	N ₂	Air	N ₂
200°C	1.64	1.06	0.8	0.9	4.2	16.9	4.8	3.7
250°C	2.02	1.66	4.9	3.5	8.8	6.4	11.3	8.9
300°C	2.25	1.86	12.9	8.4	21.1	10.7	31.6	23.9
350°C	2.45	2.03	29.5	28.0	42.1	34.7	45.4	55.6
400°C	2.90	2.36	38.5	53.7	58.0	56.6	63.3	63.7

TGA data indicated that thermal stability of MX_n-dispersed polymers based on PSF based composites was better as compared to PC probably because of the intrinsic thermal stability of the base polymer.

TGA of 20% SCo series polymer in air.



TGA of 20% CFe series polymer in air.

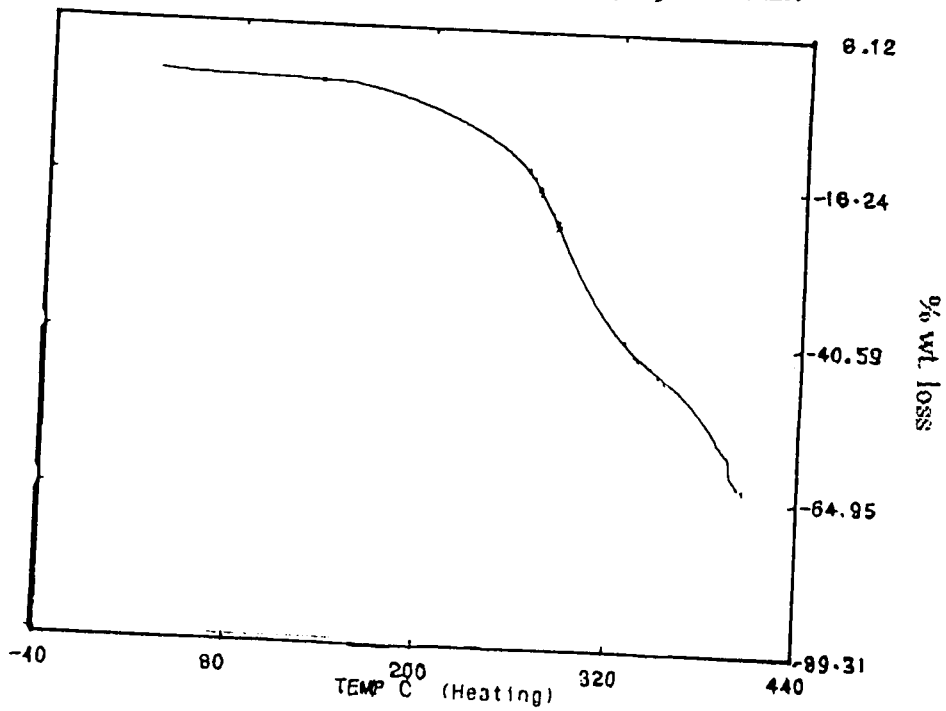
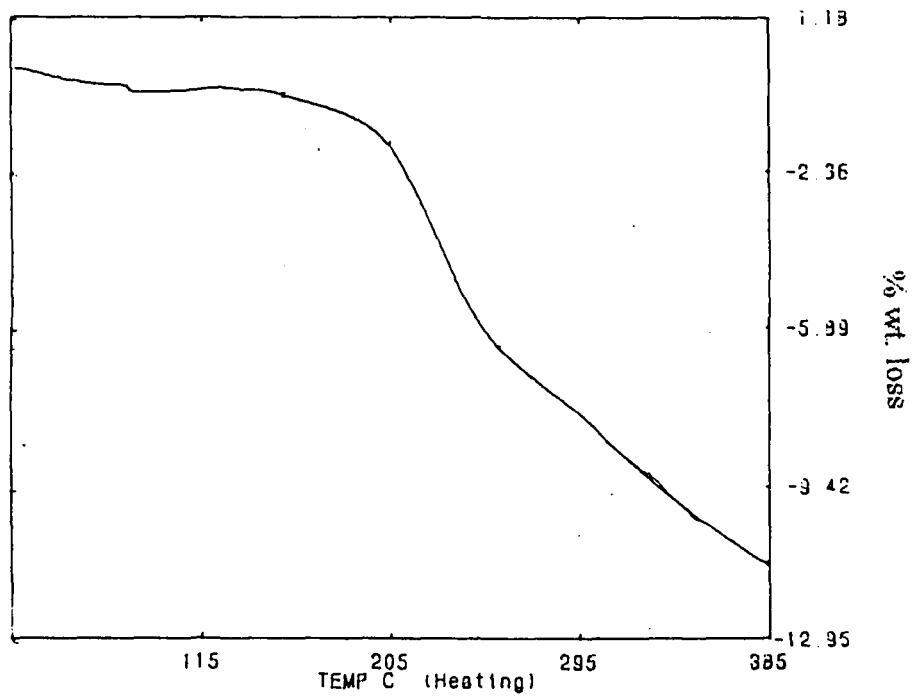


Figure 7.20 TGA of 20% SCo and 20% CFe series polymers in air

TGA of 20% SFe series polymer in air.



TGA of PSF polymer in air.

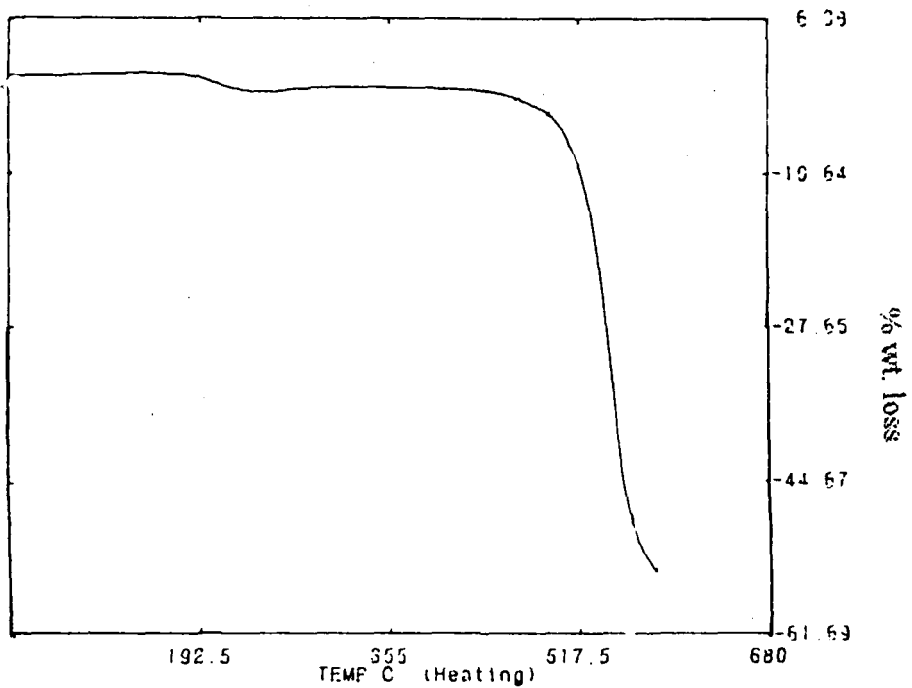


Figure 7.21

Table 7.27

Thermogravimetric data for Fe(acac)₃ and Co(acac)₃

Sample	Fe(acac) ₃	Co(acac) ₃
Temp. °C	% weight loss	% weight loss
	N ₂	N ₂
200°C	23.9	6.2
250°C	71.8	68.9
300°C	75.6	73.9
350°C	79.8	77.9
400°C	83.3	79.7
450°C	85.3	82.3
500°C	85.9	84.2
550°C	86.2	85.9
600°C	86.3	87.7
650°C	-----	89.8
700°C	-----	92.0
750°C	-----	93.6

Increase in density indicated two possible phenomena, one could be interchain interaction due to co-ordination of metal ion in the additive, other density of the filler (MX_n). In this system, additive and polymer arranged in such a way that it reduced the fractional free volume of the polymer for the gas transport. Lee [Lee et al (1991)] observed that additives get arranged in such a way that it reduces fractional free volume. Density varied from 1.240 to 1.253 for SCo, 1.240 to 1.248 for SFe and 1.20 to 1.21 for CFe.

Membranes of the three MX_n-dispersed series were examined under polarized light microscopy (PLM) and also the membranes of highest MX_n concentration were carried out under scanning electron microscopy (SEM). There was no discrete

domain for metal complex in the MX_n -dispersed membranes. This suggested that the metal complex was molecularly dispersed in polymer matrix [Maeda and Paul (1987b)]. This was also supported by WAXD technique.

Gas Permeation studies

Permeation data for all three SCo, SFe and CFe series as a function of metal complex concentration for He, N₂, O₂ and CO₂ is presented in Table 7.28 to 7.30. The permeation data for MX_n -dispersed polymer membranes were compared with PC and PSF [Zolandz and Fleming (1992b)]. In all series, there was a decrease in permeabilities of all gases with increasing MX_n concentration from 5% to 30% [Maeda and Paul (1987a), (1987b), (1987c); Ruiz-Trevino and Paul (1997)].

Table 7.28

Gas permeability of SCo series as a function of Co(acac)₃ loading.

% of Co(acac) ₃ in SCo series	He (in Barrer)	N ₂ (in Barrer)	O ₂ (in Barrer)	CO ₂ (in Barrer)
0%	12.54	0.24	1.29	5.98
5%	10.6	0.17	0.84	2.65
10%	9.8	0.12	0.75	2.1
20%	10.1	0.10	0.63	1.84
30%	8.6	0.09	0.44	0.9

For SFe (PSF-Fe metal complex) series membranes, as Fe(acac)₃ concentration was increased, there was a decrease in permeability in the range, 17-23% for He, 34-63% for N₂, 40-65% for O₂ and 59-79% for CO₂ (figure 7.22).

For SCo (PSF -Co metal complex) series membranes, as Co(acac)₃ concentration was increased, there was a lowering in permeation range, 16-32% for He, 30-63% for N₂, 35-66% for O₂ and 56-85% for CO₂ (figure 7.23).

For CFe (PC - Fe metal complex) series membranes, as Fe(acac)₃ loading was increased, there was a reduction in permeability in the range, 20-47% for He, 35-66% for N₂, 40-76% for O₂ and 62-81% for CO₂ (figure 7.24).

Table 7.29

Gas permeability of SFe series as a function of Fe(acac)₃ loading.

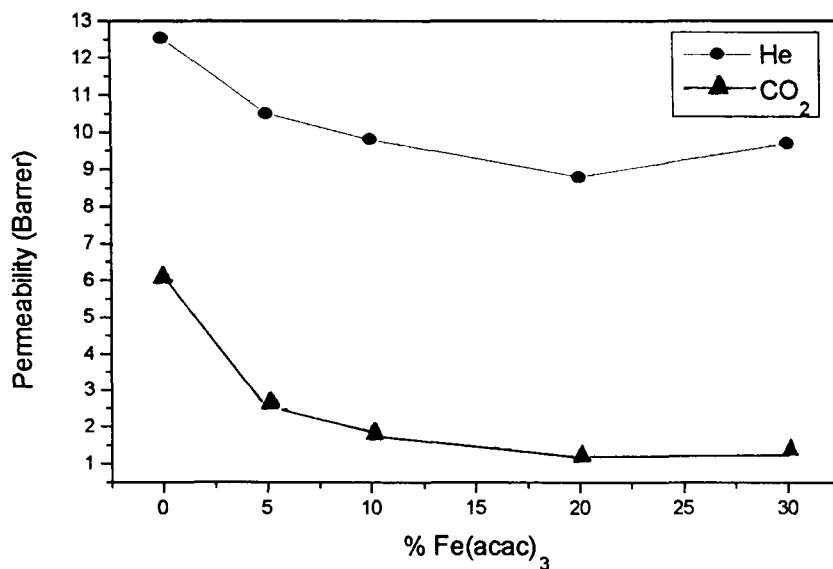
% of Fe(acac) ₃ in SFe series	He (in Barrer)	N ₂ (in Barrer)	O ₂ (in Barrer)	CO ₂ (in Barrer)
0%	12.54	0.24	1.29	5.98
5%	10.5	0.16	0.78	2.51
10%	9.8	0.12	0.64	1.73
20%	8.8	0.08	0.48	1.16
30%	9.7	0.09	0.46	1.28

Table 7.30

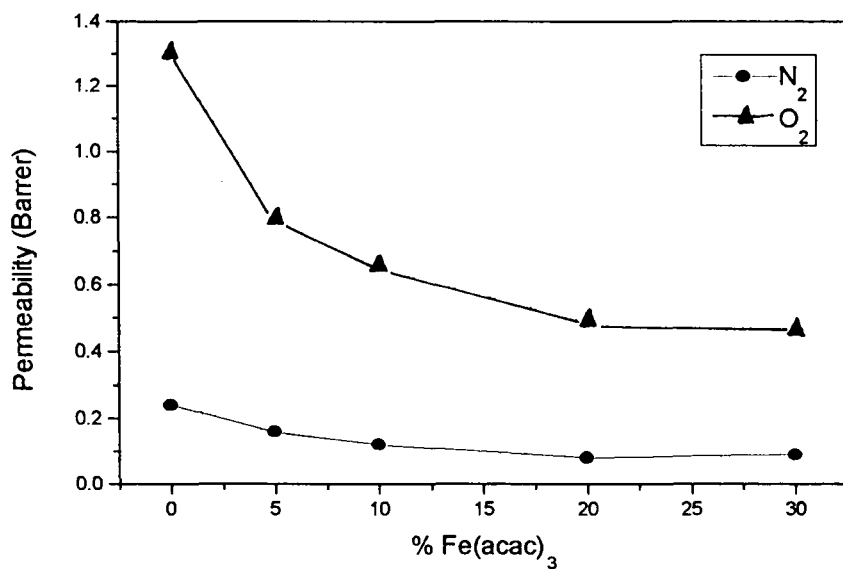
Gas permeability of CFe series as a function of Fe(acac)₃ loading.

% of Fe(acac) ₃ in CFe series	He (in Barrer)	N ₂ (in Barrer)	O ₂ (in Barrer)	CO ₂ (in Barrer)
0%	14	0.29	1.48	6.5
5%	11.3	0.19	0.89	2.5
10%	9.3	0.16	0.70	---
20%	10.6	0.13	0.66	1.56
30%	7.47	0.1	0.36	1.26

The selectivity trends of the three series were similar to each other which were compared to their parent polymer as given in Tables 7.31 to 7.33. The overall selectivity of He/N₂ was increased because of the higher rate of reduction for N₂ permeability than for He. The O₂/N₂ selectivity was marginally affected, as percentage decrease in the permeability was similar for O₂ and N₂. For He/CO₂ pair selectivity

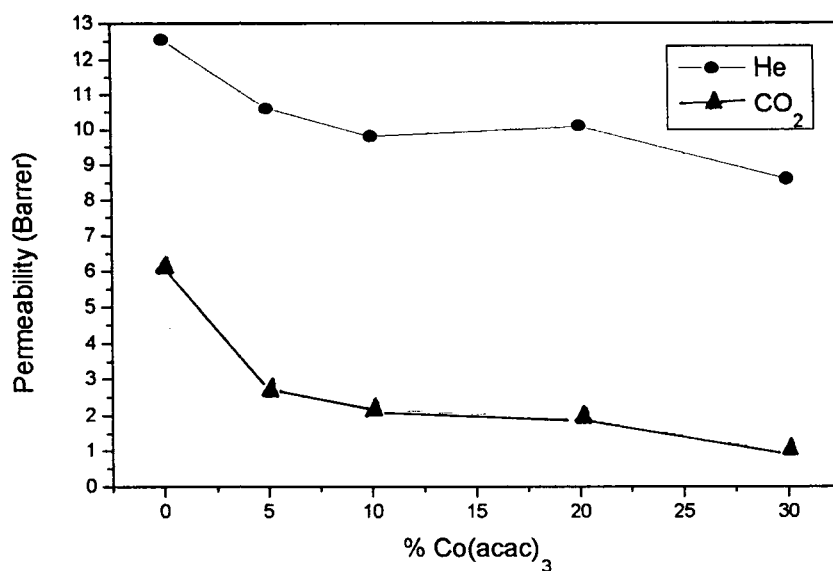


Permeability for He and CO₂ measured at 35°C and 10 atm. as a function of % Fe(acac)₃ loading in SFe series membranes.

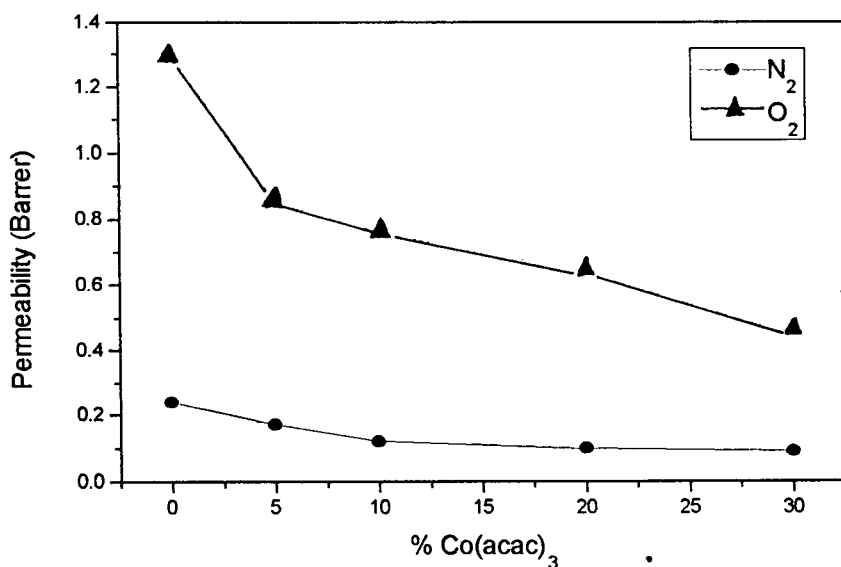


Permeability for N₂ and O₂ measured at 35°C and 10 atm. as a function of % Fe(acac)₃ loading in SFe series membranes.

Figure 7.22

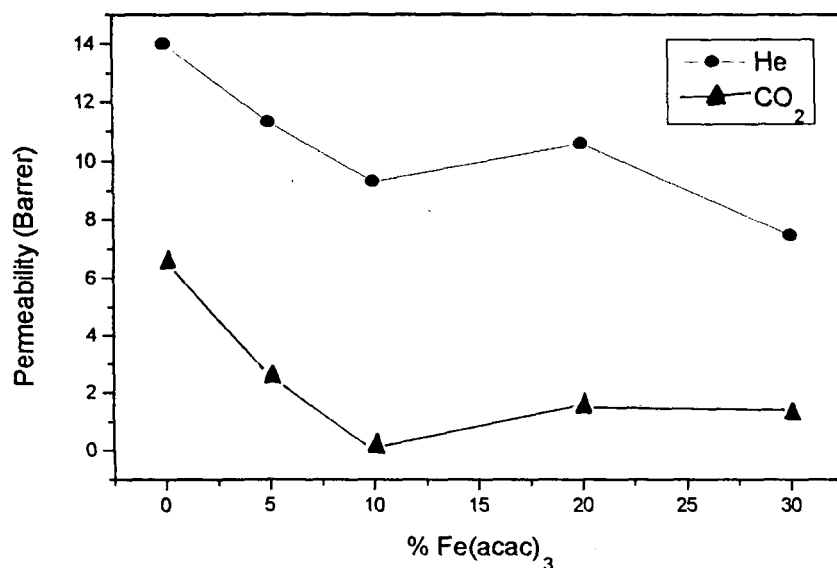


Permeability for He and CO₂ measured at 35°C and 10 atm. as a function of % Co(acac)₃ loading in SCo series membranes.

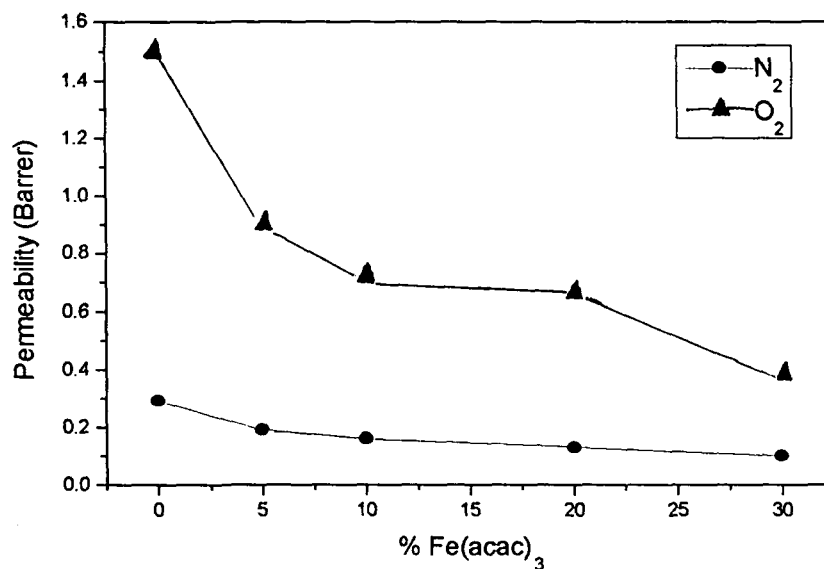


Permeability for N₂ and O₂ measured at 35°C and 10 atm. as a function of % Co(acac)₃ loading in SCo series membranes.

Figure 7.23



Permeability for He and CO₂ measured at 35°C and 10 atm. as a function of % Fe(acac)₃ loading in CFe series membranes.



Permeability for N₂ and O₂ measured at 35°C and 10 atm. as a function of % Fe(acac)₃ loading in CFe series membranes.

Figure 7.24

increased in multiples, as there was a slow decrease in He permeability whereas a sudden decrease in CO₂ permeability. The CO₂/ N₂ selectivity decreased at all MX_n loadings, as CO₂ permeability decreased dramatically in comparison to N₂ as observed from the selectivity data [Maeda and Paul (1987a), (1987b), (1987c); Sefcik et al (1983); Ruiz-Trevino and Paul (1997)].

Table 7.31

Permselectivity of gases for SCo series as a function of Co(acac)₃ loading.

% Co(acac) ₃ in SCo series	α He/N ₂	α He/CO ₂	α O ₂ /N ₂	α CO ₂ /N ₂
0%	52.3	2.1	5.4	24.9
5%	62.4	4.0	4.9	15.6
10%	81.7	4.7	6.2	17.5
20%	105.2	5.5	6.3	18.8
30%	96.6	9.6	4.9	10.1

Table 7.32

Permselectivity of gases for SFe series as a function of Fe(acac)₃ loading.

% Fe(acac) ₃ in SFe series	α He/N ₂	α He/CO ₂	α O ₂ /N ₂	α CO ₂ /N ₂
0%	52.3	2.1	5.4	24.9
5%	65.6	4.2	4.9	15.7
10%	81.7	5.7	5.3	14.4
20%	104.8	7.6	5.7	14.0
30%	103.2	7.6	4.9	13.6

Table 7.33

Permselectivity of gases for CFe series as a function of Fe(acac)₃ loading.

% Fe(acac) ₃ in CFe series	α He/N ₂	α He/CO ₂	α O ₂ /N ₂	α CO ₂ /N ₂
0%	48.4	2.15	5.12	22.5
5%	59.5	4.52	4.7	13
10%	58.1	----	4.4	---
20%	81.5	6.79	5.1	12
30%	74.7	5.93	3.6	12.6

In the case of SFe series, the selectivity for He/N₂ increased in the range of 25-100%. For the lowest Fe(acac)₃ loading 5%, the increase in selectivity was minimum, it increased upto 20% loading, followed by marginal decreased at 30% loading. The selectivity for O₂/N₂ gas pair increased at 10% and 20% Fe(acac)₃ loading, while for other concentrations, slight decrease in selectivity was observed. The selectivity for He/CO₂ was increased with Fe(acac)₃ loading in the range of 100-350%. The selectivity for CO₂/N₂, was decreased remarkably in the range 24-60% with Fe(acac)₃ addition because of sudden decrease in CO₂ permeability, which was not highly dependent on additive concentration.

For membranes belonging to the SCo series, the selectivity for He/N₂ increased in the range of 19-100 % for 5 - 20% Co(acac)₃ concentration, which was slightly dropped down for 30% Co(acac)₃ loading. The selectivity for He/CO₂ increased with Co(acac)₃ loading in the range of 100-260 %. The selectivity for O₂/N₂ was increased at 10% and 20% Co(acac)₃ concentrations, while it decreased at 5% and 30% Co(acac)₃ loading. The selectivity for CO₂/N₂ also decreased noticeably in the range (35-45%) by the addition of Co(acac)₃. This selectivity trend decreased with Co(acac)₃ concentration.

In case of CFe series membranes, the selectivity for He/N₂ increased in a range (20-68%) from 5% Fe(acac)₃ loading and reached the highest value at Fe(acac)₃ concentration, then slightly lowered to 54% for 30% Fe(acac)₃ loading. The selectivity for He/CO₂ increased from 5% to 20% Fe(acac)₃ concentrations in the range of 110-210 %, after that slightly decreased to 175% for 30% Fe(acac)₃ loading. The selectivity for O₂/N₂ reduced for all concentrations of Fe(acac)₃. Similarly, the selectivity of CO₂/N₂ remarkably decreased for all Fe(acac)₃ concentrations in the range (42-47%). This decreasing trend of selectivity for CO₂/N₂ was not in accordance with change in Fe(acac)₃ concentration.

7.2.2 Discussion

7.2.2.1 Correlation between physical and permeation properties

Density measurements showed a gradual increase in density with MX_n loading as anticipated. There might be some kind of interactions between MX_n and polymer functional groups, as observed by Shih-Hsiung Chen et al (1997) in Co(acac)₃ / PC polymer blends. Such bonding was not evident in these three MX_n dispersed series IR spectra.

All WAXD spectra of MX_n dispersed polymers showed similar pattern compared to parent polymer. No distinct crystalline peak was observed after addition of MX_n. This indicates the homogeneous dispersion of MX_n in respective polymer matrix with some interactions, polarized light microscopy and SEM techniques suggested that MX_n was molecularly dispersed in the respective polymer matrix, which needs to be studied further in details. TGA showed that thermal stability was good for SFe and SCo series as compared to PSF polymer after addition of Fe(acac)₃ and Co(acac)₃ metal complex respectively. In the case of CFe series, the thermal stability

was decreased with $\text{Fe}(\text{acac})_3$ concentration. It can be easily seen from TGA data that thermal degradation of PC is faster than PSF.

Gas permeation results showed that there was an overall decrease in permeability for all gases. This permeability decrease with increasing MX_n concentration can be correlated to the compactly arranged structure of MX_n -dispersed polymer matrix resulted after the addition of MX_n in respective parent polymer.

Helium diffuses faster than rest of the gases, which showed smaller reduction in permeability values compared to the other gases. Nitrogen showed a large decrease in permeability compared to He. While O_2 molecule has slightly smaller kinetic diameter than N_2 , which was transported preferably by sorption. This behavior can be attributed to paramagnetic nature of oxygen and magnetically active metal complexes. It was seen from permeability data of O_2 and N_2 , that the decreases in permeability remain nearly same at all MX_n concentrations in all three series membranes.

In general, CO_2 gas has a tendency to sorb in polymer matrix and diffuse through it, which results in an increase in its permeability. In the MX_n -dispersed polymer membranes, permeability of CO_2 decreased remarkably. This reduced permeability is because of reduced CO_2 sorption in MX_n -dispersed polymer matrix [Maeda and Paul (1987b); Ruiz-Trevino and Paul (1997)], or due smoke rejecting property of Fe and Co complexes [Bert et al (1978)].

In all three series membranes, the selectivity for He/N_2 increased compared to parent polymer. This was mainly due to the comparatively larger decrease in N_2 permeability than for He with increased additive (MX_n) concentration. The selectivity of He/CO_2 , increased with MX_n concentration. It was because of small decrease in He permeability and the dramatic drop in CO_2 permeability. While O_2/N_2 selectivity was marginally changed because of the similar decrease in % permeabilities of both O_2 and N_2 . There was dramatic decrease in permeability of CO_2 , which results in decreasing selectivity of CO_2/N_2 gas pair.

Overall, 20 % SFe and 20 % SCo membranes showed better performance in comparison to the membranes with other additive concentrations. These membranes can probably find application as helium selective membranes and barrier materials for CO₂.

7.2.2.2 Possible mechanism for permeability Reduction:

Explanation for the reduction in permeability of MX_n-dispersed membranes can be given by two mechanisms, (i) MX_n may act as an antiplasticizer, (ii) MX_n may act as a filler.

(i) Antiplasticizer: Generally, additives containing polar group or functionality in polymer matrix like PC, PVC, PPO and PSF are known to have antiplasticising effect. [Jackson and Caldwell (1967a); Maeda and Paul (1987d); Steger et al (1980)]. These additives generally increased mechanical strength, modulus and tensile strength of the polymer and decreased elongation. It reduces interchain spacing of polymer matrix and decreases free volume available for the penetrant transport, thus reducing the gas permeability.

WAXD scans indicate that Fe(acac)₃ and Co(acac)₃ are molecularly dispersed in PC and PSF matrices. Sefcik et al (1983) showed that TCP (Tricresyl phosphate) antiplasticizes PVC below 15% concentration without changing d-spacing. The antiplasticization was responsible for the decreased permeation rate.

In the present series, there was no direct evidence for antiplasticising action of the additives. These membranes showed resemblance in WAXD spectra with parent polymer, that is in d-spacing, and decrease in permeation values with additive (MX_n) concentrations. This behaviour is similar to that reported by Sefcik et al (1983).

Antiplasticizer reduces free volume of the polymer matrix, This is attributed to the interaction between the additive and the polymer chains [Maeda and Paul (1987d), Shih-Hsiung Chen et al (1997)] This affects chain flexibilities [Robeson (1969)]. Thus, it reduced permeability of gas. Presently, the observed permeability decreased in all the

three series for all the gases, and does not change the d_{sp} value. This suggested that reduction in permeability was probably caused by decreased free volume of polymer matrix.

Thus, MX_n might be acting as an antiplasticizer in PC and PSF polymers.

2) Additive as a filler: Fillers are mainly used for filling the free volume of polymer matrix of the plastic product and to reduce its production cost. Some fillers improve some of the properties. In the present study, when MX_n was mixed with polymer (PC or PSF) matrix, the density of each polymer was increased.

The filler may be soluble or insoluble in the polymer which depends on the nature of the filler and polymer. In the three series, MX_n either acts as an antiplasticizer or as an impermeable filler. [Eitzman et al (1996)]. The filler acts as the barrier for penetrant molecule while diffusing through the membrane. Hence, molecule has to pass through the tortuous path.

When the penetrant diffuses through the membrane (Diffusion model) DiBenedetto (1963), [Brandt, (1959)], it passes through two distinct ways : (a) along the axis of a "tube" formed by adjacent parallel chains (DiBenedetto model); (b) perpendicular to this axis through two polymer chains separating sufficiently apart to permit passage for the gas molecule (Brandt model). The first motion does not require significant activation energy and is a fast process, whereas second path motion is a slow step, it involves when there are impermeable flakes in the polymer matrix. At this step, when penetrant molecule comes across any type of impermeable body / crystallite, it has to undergo through second step, which involves jumps across two polymer chains when those are sufficiently separated. In this process, high activation energy is required and is a rate determining step. At this step, there will be discrimination of gas molecules on the basis of size, shape, diffusivity and solubility. First discrimination is done at the surface of polymer membrane only. Thereby permeability reduction is observed because of reduced free volume, which was because of impermeable fillers and reason for the permeability reduction of each gas. The selectivity

change is observed because of this permeability reduction [Pace and Datyner (1979); Maeda and Paul (1987a); Ruiz-Trevino and Paul (1997)]. Similar kind of mechanism takes place in this MX_n -dispersed polymer membranes.

7.2.3 MX_n compounds as the additive in PSF and PC matrices

In the three series, the membranes obtained from 20% MX_n concentration showed ~100% and ~70% enhancement in helium gas selectivity for PSF and PC respectively. These membranes can be used as a barrier for CO_2 gas as drastic decrease in permeability after MX_n addition was observed.

7.3 Conclusions (Additive dispersed polymer system)

Both types of additives (liquid crystals and metal complexes) acted as the gas barriers.

Both the types of additive were molecularly dispersed in polymer matrices at all concentrations used. The decrease in T_g with LC loading in polymers (PC, PSF) in LC-dispersed polymer systems favours processability at lower temperature. Thermal stability of PSF polymer was not affected by addition and equally with its concentration compared to PC.

In both additive dispersed systems, gas permeability decreased with additive concentration for all gases. For He gas permeability reduction was less compared to other gases. In case of N_2 and O_2 , reduction in permeability were nearly similar, whereas CO_2 gas permeability dramatically decreased by addition of additive irrespective of its concentration. From permeability data, it can be established that additive acts as a gas barrier, decreasing gas permeability according to their molecular nature.

In case of additive dispersed polymer systems, trends were observed to be different for different gas pairs under consideration. In the case of He/N₂, selectivity based on PSF polymer showed increase, while for PC based polymers were maintaining selectivity compared to respective parent polymer. The selectivity for He/CO₂, the trend showed increase in multiples compared to respective parent polymer for all additive dispersed systems. In case of O₂/N₂ selectivity, the trend was maintained. For CO₂/N₂ selectivity decreased for all additive dispersed polymer systems.

In case of He/N₂ and He/CO₂ selectivities, enhancement was probably because of increased diffusivity selectivity, while CO₂/N₂ selectivity decreased because of decreased solubility selectivity.

Better performance for He/N₂ selectivity was shown by 6% SL2, 3% SL1, 20% SCo, 20% SFe and 30% SFe membranes, while for He/CO₂ selectivity, 3% SL1, 30% SCo, 20% SFe, 30% SFe and 20% CFe membranes were observed to be good in performance in comparison with other membranes. These membranes compensate reduction in permeability by selectivity in their performance.

In this part of the studies relevant to additive dispersed homogeneously in polymer matrix as membrane material. With the dispersion of additives, it has been found that there was hardly any change in d-spacing. But the permeability of all the gases under the study decreased. This decrease in permeability of gases is probably due to increase in path length of transport. So one of the reasons could be reduction in the available free volume by additive addition and increasing tortuous path of the penetrant. The another probable reason could be the hindrance caused by impermeable additive species along the passage. If we consider mass effects only, the lighter gas like helium permeates relatively faster in spite of tortuosity of the path or hindrance. So the overall permeability of helium in all the systems studied is not significantly reduced while for the bulkier gases like carbon dioxide, oxygen and nitrogen this reduction in permeability was significant. Further complication in interpreting the permeability

behavior arises from the polar nature of permeating species (CO_2 , O_2 and their bulkier nature) and also polar nature of sulfonyl and carbonyl groups of PSF and PC and similar groups present in LC as well as metal complexes. It is very difficult to analyse these complex and complicated interactions between permeating species and membrane matrix.

References

- Aguilar-Vega M. and Paul D. R., *J. Polym. Sci., Part B: Polym. Phys.*, **31**, 1599, (1993).
- Aitken C. L. and Paul D. R., *J. Polym. Sci., Part B: Polym. Phys.*, **31**, 1061, (1993).
- Aitken C. L., Koros W. J. and Paul D. R., *Macromolecules*, **25**, 3651, (1992).
- Asahi Garasu, Zaidan Josei, *Kenkyu Seika Hokoku*, 43-9, (1994).
- Barbari T. A., Koros W. J. and Paul D. R., *J. Polym. Sci., Part B: Polym. Phys.*, **26**, 709, (1988).
- Barrer R. M., "*Diffusion in and through Solids*", Cambridge, 18, (1951).
- Barrer R. M., Barrie J. A. and Slater, J., *J. Polym. Sci.*, **27**, 177, (1958).
- Barrer R. M., *J. Memb. Sci.*, **18**, 25, (1984).
- Barrer R.M., "*Diffusion in Polymers*", Chapter 6, Crank and Park, (1968).
- Billmeyer F. W., *Textbook of Polymer Science, 2nd ed.* New York: Wiley-Interscience, (1984). Chapter 12
- Bondi, A., "*Physical properties of molecular crystals, liquids, and glasses*", John Wiley and sons, New York, (1968).
- Brandt W. W., *J. Phys. Chem.*, **63**, 1080, (1959).
- Brydson J. A., "*Plastics Materials*", 5th Ed., 120, (1989).
- Burl E. Bryant and W. Conard Fernelius, *Inorganic synthesis: Vol.5*, pg188.
- Buttrey D. N., "*Plasticizers*", 2nd Ed., Franklin, Palisades, N. J., **110**, 89, (1960).
- Calvin R. H., Bailes W. K., Wilmarth., *J. Org. Chem.*, **68**, 2254, (1946).
- Charati S. G., Houde A. Y., Kulkarni S. S. and Kulkarni M. G., *J. Polym. Sci., Part B: Polym. Phys.*, **29**, 921, (1991).
- Charati S.G., Vetrivel R., Kulkarni M. G. and Kulkarni S. S., *Macromolecules*, **25**, 2215, (1992).
- Chaudhuri M. K., Ghosh S. K., *J. Chem. Soc. Dalton Trans.*, **4**, 839, (1983).
- Chen Shih-Hsiung and Lai J.Y., *J. Appl. Polym. Sci.*, **59**(7), 1129-35, (1996).
- Chen Shih-Hsiung, Ruaan Ruoh-Chyu, Lai Juin-Yih., *Sep. Sci. Technol.*, **32**(5), 925-37, (1997).
- Chern R. T. and Provan C. N., *J. Memb. Sci.*, **59**, 293, (1991b).
- Chern R. T. and Provan C. N., *Macromolecules*, **24**, 2203, (1991a).
- Chern R. T., Jia L., Shimoda S. and Hopfenberg H. B., *J. Memb. Sci.*, **48**, 333, (1990).
- Chern R. T., Koros W. J., Sanders E. S., Chen S. H. and Hopfenberg H. B., *ACS Symp. Ser. No. 233, Industrial Gas Separations*, ed. Whyte. T. E., Yon C. M. and Wagener E. H. Washington, DC: American Chemical Society, pp. 47-73, (1983).
- Chern R. T., *Sep. Sci. Technol.*, **25**, 1325, (1990).
- Chern R. T., Sheu F. R., Jia L., Stannett V. T. and Hopfenberg H. B., *J. Memb. Sci.*, **35**, 103, (1987).
- Coran A. Y., Anagnostopoulos, C. E., *J. Polym. Sci.*, **57**, 13, (1962).
- Costello L. M. and Koros W. J., *Ind. Eng. Chem. Res.*, **32**, 2277, (1993).

- Crank J., *The Mathematics of Diffusion*. 2nd ed. Clarendon: Oxford., (1975).
- Cussler E. L., Hughes S. E., Ward W. J. and Rutherford A., *J. Memb. Sci.*, **38**, 161, (1988).
- Cussler E. L., *J. Memb. Sci.*, **52**, 275, (1990).
- DiBenedetto A. T., *J. Polym. Sci.A*, **1**, 3477, (1963).
- Dutta D., Fruitwala H., Kohli A. and Weiss R. A., *Polym. Eng. and Sci.*, **30**, 1005, (1993).
- Duval J. M., Folkers B., Mulder M. H. V., Smolders C. A., Desgrandchamps G., *Recent Prog. Genie Procedes*, **6**, 337, (1992).
- Eitzman D. M., Melkote R. R. and Cussler E. L., *AIChE Journal*, **42**, 2, (1996).
- Engineered Material Handbook, Vol. 1, *Composites*, pp. 11, Ed. ASM International Handbook Committee, USA, (1987).
- Engineered materials handbook, Vol. 2, "*Engineering plastics*", pp. 497, Ed. ASM International Handbook Committee, (1988).
- Erb A. J. and Paul D. R., *J. Memb. Sci.*, **8**, 11, (1981).
- Fritsch D., Peinemann K. V., Behling R. D., *Ger. Offen.* DE 4232496 A1 31 Mar (1994).
- Fu H., Jia L. and Xu J., *J. Appl. Polym. Sci.*, **51**, 1399, (1994a).
- Fu H., Jia L. and Xu J., *J. Appl. Polym. Sci.*, **51**, 1405, (1994b).
- Ghosal K. and Chern R. T., *J. Memb. Sci.*, **72**, 91, (1992).
- Ghosal K., Chern, R. T., Freeman B. D., Savariar R., *J. Polym. Sci., Part B: Polym. Phys.*, **33**, 657, (1995).
- Ghosal, K., *Polym. Adv. Technol.*, **5**, 673-97, (1994).
- Guer Turgut M., *J. Memb. Sci.*, **93**, 283, (1994).
- Hammer C. F., *Polymer Blends*, vol. 2, Chapter 17, Ed. by Paul and Newman Academic press, (1978).
- Hellums M. W., Koros W. J., and Husk G. R., *Polym. Mater. Sci. Engg.*, **61**, 378, (1989a).
- Hellums M. W., Koros W. J., and Husk G. R. *Polym Mater. Sci. Engg.*, **61**, 639, (1989b).
- Hellums M. W., Koros W. J., Husk G. R., and Paul D. R., *J. Memb. Sci.*, **46**, 93, (1989c).
- Hellums M. W., Koros W. J., Husk G. R., and Paul D. R., *J. Appl. Polym. Sci.*, **43**, 1977, (1991).
- Hellums M. W., Koros W. J., Paul D. R., and Husk G. R., *AIChE Symp. Ser. No. 272*, **85**, 6, (1989d).
- Hoehn, H. H., *ACS Symp. Ser.*, **269**, 81, (1985).
- Houde A. Y., Kulkarni S. S. and Kulkarni M. G., *J. Memb. Sci.*, **95**, 147, (1994).
- Houde A. Y., Kulkarni S. S., Kharul U. K., Charati S. G., Kulkarni M. G., *J. Memb. Sci.*, **103**, 167, (1995).
- Houde A.Y., Kulkarni S. S. and Kulkarni M.G., *J. Memb. Sci.*, **71**, 117, (1992).

- Houde A.Y., Ph.D. dissertation, University of Poona, India, (1991).
- Hu Q., Marand E., Dhingra S., Fritsch D., Wen J., Wilkes G., *J. Memb. Sci.*, **135**(1), 65, (1997)
- Huh W., Weiss R. A. and Nicolais L., *Polym. Eng. Sci.*, **23**, 779, (1983).
- Immergut E. H., Mark H. F., Schnell H., "Chemistry and Physics of polycarbonates", John Wiley and Sons Inc., New York, (1964).
- Jackson W. J. JR, and Caldwell J. R., *J. Appl. Polym.Sci.*, **11**, 211, (1967a).
- Jackson W. J. JR, Caldwell J. R., *Advan. Chem. Scr.*, **8**, 185, (1965).
- Jackson W. J. JR., and Caldwell J. F., *J. Appl. Poly. Sci.*, **11**, 227, (1967b).
- Jacobson U., *Br. Plast.*, **32**, 152, (1959).
- Jacobson U., *Br. Plast.*, **7**, 6, (1973).
- Jogider A. N., Stephen B. E., Darrell F. C. and Thomas J. O., *U. S. patent 4,840,646*; CA : 112-9441h.
- Lai J., Chen S., Lee M., Shyu S., *J. Appl. Polym. Sci.*, **47**, 1513, (1993).
- Kajiyama T., Washizu S., Kumano A., Terada I., Takayanagi M., Shinkai S., *J. Appl. Polym. Sci., Appl. Polym. Symp.*, **41**, 327, (1985).
- Kajiyama T., Washizu S., Takayanagi M., *J. Appl. Polym. Sci.*, **29**, 3955, (1984b).
- Kajiyama T., Nagata Y., Washizu S., Takayanagi M., *J. Memb. Sci.*, **11**, 39, (1982).
- Kamal M. R., Jinnah I. A., and Utraki L. A., *Polym. Eng. and Sci.*, **24**, 1337, (1984a),
- Kawakami J. H., Muruganandam M., Brode G. L., *Eur. Pat. Appl.*, EP 376,234(1990), CA : 114-63781y (1990).
- Kharul U. K., Kulkarni S. S., *Bull. Mater. Sci.*, **17**, 1071, (1994).
- Kharul U. K., Kulkarni S. S., Kulkarni M. G., Houde A. Y., Charati S. G., and Joshi S. G., *Polymer*, **39**, 2011, (1998).
- Kharul U. K., Kulkarni S. S., *Macromol. Chem. Phys.*, **198**, 1909, (1997).
- Kharul U.K., Ph.D. dissertation, University of Poona, (1995).
- Khulbe K. C., Matsuura T., Lamarche G., Kim H. J., *J. Memb. Sci.*, **135**, 211, (1997).
- Kim T. H., Koros W. J., Husk G. R. and O'Brien K. C., *J. Memb. Sci.*, **37**, 45, (1988).
- Kinjo N., Nakagawa T., *Polymer*, **4**, 143, (1973).
- Koros W. J. and Chern R. T., "Handbook of Separation Process Technology", ed., Rousseau R. W., New York: John Wiley & Sons., pp. 862- 953, (1987).
- Koros W. J. and Fleming G. K., *J. Memb. Sci.*, **83**, 1, (1993).
- Koros W. J., and Paul D. R., *J. Polym. Sci. Polym. Phys.* **16**, 2171, (1978).
- Koros W. J., Chan A. H., and Paul D. R., *J. Memb. Sci.*, **2**, 165, (1977).
- Kulkarni S. S., *Bull. Mater. Sci.*, **17**, 1307, (1994).
- Lai J., Chen S., Mei H., Shyu S. S., *J. Appl. Polym. Sci.*, **47**, 1513, (1993).
- Lai J., Huang S. and Chen S., *J. Memb. Sci.*, **74**, 71, (1992).
- Lai J., Huang S., Huang S., Shyu S. S., *Sep. Sci. Technol.*, **30**, 461, (1995).

- Langsam M., *Plast. Eng.*, **36**, 697, (1996).
- Lee K., Shim I., and Hwang S., *J. Memb. Sci.*, **60**, 207, (1991).
- Lee W. M., *Polym. Eng. Sci.*, **20**, 65, (1980).
- Lehmann H. D., Eberhardt W., Hanack M., *J. Memb. Sci.*, **147**, 49, (1998).
- Lerma M. S., Iwamoto K. and Seno M., *J. Appl. Polym. Sci.*, **33**, 625, (1987).
- LeRoux J. D., Paul D. R., Kampa J. and Lagow R. J., *J. Memb. Sci.*, **90**, 21, (1994).
- Light R. R. and Seymour R. W., *Polym. Engg. Sci.*, **22**, 857, (1982).
- Liu Y., Ding M., Xu J., *J. Appl. Polym. Sci.*, **58**, 485, (1995).
- Maeda Y. and Paul D. R., *J. Memb. Sci.*, **30**, 1, (1987a).
- Maeda Y. and Paul D. R., *J. Polym. Sci., Part B: Polym. Phys.*, **25**, 957, (1987b).
- Maeda Y. and Paul D. R., *J. Polym. Sci., Part B: Polym. Phys.*, **25**, 981, (1987c).
- Maeda Y. and Paul D. R., *J. Polym. Sci., Part B: Polym. Phys.*, **25**, 1005, (1987d).
- Matsui S., Sato H., Nakagawa T., *J. Memb.Sci.*, **141**, 31, (1998).
- Matsumoto K., Xu P. and Nishikimi T., *J. Memb. Sci.*, **81**, 15, (1993).
- McHattie J. S., Koros W. J. and Paul D. R., *Polymer*, **32**, 2618, (1991).
- McHattie J. S., Koros W. J. and Paul D. R., *Polymer*, **32**, 840, (1991).
- McHattie J. S., Koros W. J. and Paul D. R., *Polymer*, **33**, 1701, (1992).
- McIntyre W. D. and Soane D. S., *Am. Chem. Soc., Div. Polym. Chem., Polym. Prepr.*, **29**, 197, (1988).
- Michaels A. S., Vieth W. R. and Barrie J. A., *J. Appl. Phys.*, **34**, 13, (1963).
- Moe M. B., Koros W. J., and Paul D. R., *J. Polym. Sci., Part B: Polym. Phys.*, **26**, 1931, (1988).
- Muruganandam N., *J. Polym. Sci., Part B: Polym. Phys.*, **25**, 1999, (1987).
- Nakagawa T., Nakono H., Enomoto K. and Higuchi A., *AIChE Symp. Ser. No. 272*, **85**, 1, (1989).
- Nakanish S., Ito K., Kusuki Y., *Eur. Pat. Appl. EP 747418 A1* 11 (1996).
- Nelson J. K., *U.S. Pat. 4,822,382*, CA : **111**:600095e, (1989).
- Nishide H., Dawakami H., Toda S., Tsuchida E., and Kamiya Y., *Macromolecules*, **24**, 5851, (1991).
- Nishide H., Kawakami H., Suzuki T., Azechi T., and Tsuchida E., *Macromolcule*, **23**, 3714, (1990).
- Nishide H., Ohyanagi M., Okada O., and Tsuchida E., *Macromolecules*, **20**, 417, (1987).
- Nishide H., Ohyanagi M., Okada O., and Tsuchida T., *Macromolecules*, **19**, 494, (1986).
- Nishide H., Ohyanagi M., Okada O., and Tsuchida T., *Macromolecules*, **21**, 2910, (1988).
- Nishide H., Tsuchida E., *Polym. Gas. Sep.*, 183-219, (1992).
- Norman N. Li, *Recent developments in separation science*, vol. II, CRC Press, (1975).

- O'Brien K. C. and Koros W. J., *J. Memb. Sci.*, **35**, 217, (1988).
- Pace R. J., Datyner A., *J. Polym. Sci. Polym. Phys. Ed.*, **17**, 437, (1979).
- Panse D. G., Bapat B. V., Ghatge B. B., *J. Chromato.*, **284**, 242, (1984).
- Panse D.G., Ph.D. dissertation, University of Poona, (1982).
- Pant B. G., Kulkarni S. S., Panse D. G., Joshi S.G., *Polymer*, **35**, 2549, (1994).
- Pant B. G., Ph. D. dissertation, Pune University, (1997).
- Paul D. R. and Koros W. J., *J. Poly. Sci., Polym. Phys.*, **14**, 674, (1976).
- Paul D. R., *Adv. Filtr. Sep. Technol.*, **7**, 408-11, (1993).
- Percec S., *J. Appl. Polym. Sci.*, **33**, 191, (1987).
- Perego G., Roggero A., Sisto R. and Valentini C., *J. Memb. Sci.*, **55**, 325, (1991).
- Perrin D.D. and Armarego W.L.F., "Purification of laboratory chemicals", 3rd Edn., Pergamon Press, London, (1988).
- Pessan L. A. and Koros W. J., *J. Polym. Sci., Part B: Polym. Phys.*, **31**, 1245, (1993).
- Pessan L. A., *J. Polym. Sci. Part B: Polym. Phys.*, **33**, 487, (1995).
- Petersen J., Pienemann K.-V., *J. Appl. Polym. Sci.*, **63**, 1557, (1997).
- Petropoulos J. H., *J. Polym. Sci., Polym. Phys.*, **8**, 1797, (1970).
- Pinnau I., Hellums M. W. and Koros W. J., *Polymer*, **32**, 2612, (1991)
- Pixton M. R., and Paul D. R., *J. Polym. Sci., Part B: Polym. Phys.*, **33**, 1353, (1995a).
- Pixton M. R., Paul D. R., *J. Polym. Sci. Part B: Polym. Phys.*, **33**, 1135, (1997).
- Pixton M. R., Paul D. R., *Maccormoleculs*, **28**, 8277, (1995b).
- Rangarajan R., Mazid M. A., Matsuura T., Sourirajan S., *Ind. Eng. Chem. Process Desalination. Development.*, **23**, 79, (1984).
- Ratto J. A., Ristori S., Volino F., Pineri M., Thomas M., Escoubes M. and Blumstein R. B., *Chem. Mater.*, **10**, 1570, (1993).
- Robeson L. M., Burgoyne W. F., Langsam M., Savoca A. C. and Tien C. F., *Polymer*, **35**, 4970, (1994).
- Robeson L. M., *Polym. Eng. Sci.*, **9**, 277, (1969).
- Robeson L. M., Smith C. D., Langsam M., *J. Memb. Sci.*, **132**, 33, (1997).
- Ruiz-Trevino F. A., Paul D. R., *J. Appl. Polym. Sci.*, **66**, 1925, (1997).
- Ruaan R., Chen S., Lai J., *J. Memb. Sci.*, **135**, 9, (1997).
- Schmidhauser J. C. and Longley K. L., *J. Appl. Polym. Sci.*, **39**, 2083, (1990).
- Schrenk E. J. and Alfrey T., *Polymer Blends*, vol 2, Chapter 15, Ed. by Paul and Newman, Academic press (1987).
- Sefcik M. D., Schaefer J., May F. L., Raucher D. and Dub S. M., *J. Polym. Sci: Polym. Phys.*, **21**, 1041, (1983).
- Sheu F. E., Chern R. T., Stannett V. T. and Hopfenberg H. B., *J. Polym. Sci., Part B: Polym. Phys.*, **26**, 883, (1988).

- Sheu F. R. and Chern R. T., *J. Polym. Sci., Part B: Polym. Phys.*, **27**, 1121, (1989).
- Chen S., Lai J., Ruan R., Wang A. A., *J. Memb. Sci.*, **123**, 197, (1997).
- Sisto R., Bonfanti C. and Valentini C., *J. Memb. Sci.*, **95**, 135, (1994).
- Stackman R. W. and Williams A. G., *Polym. Sci. Technol.*, **21**, 321, (1983).
- Stannett V. T., Koros W. J., Paul D. R., Lonsdale K. K. and Baker R. W., *Adv. Polym. Sci.*, **32**, 69, (1979).
- Staude E. and Breitbach L., *J. Appl. Polym. Sci.*, **43**, 559, (1991).
- Steger T. R., Schacfer J., Stejskal E. O. and McKay R. A., *Macromolecules*, **13**, 1127, (1980).
- Stern S. A., *J. Memb. Sci.*, **94**, 1, (1994).
- Stern S. A., Malhaupt J. T. and Gareis P. J., *AIChE Journal*, **15**, 64, (1969).
- Stern S. A., Mi Y., and Yamamoto H., and St. Clair A. K., *J. Polym. Sci., Part B: Polym. Phys.*, **27**, 1887, (1989).
- Story B. J. and Koros W. J., *J. Memb. Sci.*, **67**, 191, (1992).
- Suer M. G., Bac N., Yilmaz L., Gurkan T. and Sacco A. Jr., *Process Technol. Proc.*, **11**, 661, (1994).
- Surface T. M., Kwon A. H., Lew B. M. and Kaner R. B., *Polym. Prepr. (Am. Chem. Soc., Div. Polym. Chem.)*, **37**, 670, (1996).
- Takada K., Matsuya H., Masuda T. and Higashimura T., *J. Appl. Polym. Sci.*, **30**, 1605, (1985).
- Tanaka K., Kita H., Okano M. and Okamoto Ken-ichi, *Polymer*, **33 (3)**, 585. (1992).
- The DOE Industrial Energy Program: Research and Development in Separation Technology, DOE Publication number DOE / NB M—8002773, (1987).
- Toshima N., “*Polymer for gas separation*”, Chapter 3, pg 127, (1991a).
- Toshima N., “*Polymer for gas separation*”, Chapter 4, pg 137, (1991b).
- Tsuchida E. and Nishide H., *Adv. Polym. Sci.*, **24**, 1, (1977).
- Venkateswara R.M., Rojivadiya A.J., Parsania P.H. and Parekh H.H., *J. Indian Chem. Soc.*, **LXIV**, 758-759, (1987).
- Von Wroblewski, Wiedemanns S., *Ann. Physik*, **8**, 29, (1879).
- Vrentas J. S., Jarzebski C. M. and Duda J. L., *AIChE J.*, **21**, 894, (1975).
- Walter Heitz, *Makromol. Chem.*, **190**, 1561-1572 (1989).
- Walter Heitz, *Makromol. Chem.*, **191**, 225-235 (1990).
- Wang C. H., Kramer E. J., and Sachse W. H., *J. Polym. Sci., Part B: Polym. Phys.*, **20**, 1371, (1982).
- Ward W. J., Gaines G. L., Alger M. M., and Stanley T. J., *J. Memb. Sci.*, **55**, 173, (1991).
- Weinkauff D. H. and Paul D. R., *J. Polym. Sci., Part B: Polym. Phys.*, **30**, 819, (1992a).

- Weinkauff D. H. and Paul D. R., *J. Polym. Sci., Part B: Polym. Phys.*, **30**, 837, (1992b)
- West J. L., *Molec. Cryst. Liq. Cryst.*, **157**, 427, (1988).
- Winston Ho W. S. and Sirkar K. K., “*Membrane Handbook*”, Van Nostrand Reinhold, Chapter I, (1992).
- Wonder A. G. and Paul D. R., *J. Poly. Sci.*, **5**, 63, (1979).
- Wu H., Wang B., Liu H. and Li S., *Huadong Huagong Xuebao*, **543**, (1983).
- Yamada Y., Furukawa N., Tujita Y., *High Perform. Polym.*, **9**, 145, (1997).
- Yamamoto H., Mi Y., and Stern S. A., *J. Polym. Sci., Part B: Polym. Phys.*, **28**, 2291, (1990).
- Zhang W., Nodera A., Satoh M., Komiyam J., *J. Memb. Sci.*, **35**, 311, (1988).
- Zhou C. and Lin S., *Eur. Polym. J.*, **34**, 1663, (1998).
- Zolandz R. R. and Fleming G. K., “*Membrane Handbook*”, Van Nostrand Reinhold, Ed. by Winston and Sirkar, Chapter, **2**, (1992a).
- Zolandz R. R., and Fleming G. K., “*Membrane Handbook*”, Van Nostrand Reinhold, Ed. by Winston and Sirkar, Chapter, **3**, (1992b).